Characterising the Role of Canonical Wnt Signalling in Adult Hippocampal Stem Cells

Sophie Hannah Luxon Austin

Imperial College London

and

The Francis Crick Institute

PhD Supervisor: François Guillemot

A thesis submitted for the degree of

Doctor of Philosophy

Imperial College London

March 2020

Declaration

I Sophie Hannah Luxon Austin confirm that the work presented in this thesis is my own. Where information has been derived from other sources, I confirm that this has been indicated in the thesis.

Copyright Declaration

The copyright of this thesis rests with the author. Unless otherwise indicated, its contents are licensed under a Creative Commons Attribution Non-Commercial 4.0 International Licence (CC BY-NC)

Under this licence, you may copy and redistribute the material in any medium or format. You may also create and distribute modified versions of the work. This is on the condition that: you credit the author and do not use it, or any derivative works, for a commercial purpose.

When reusing or sharing this work, ensure you make the licence terms clear to others by naming the licence and linking to the licence text. Where a work has been adapted, you should indicate that the work has been changed and describe those changes.

Please seek permission from the copyright holder for uses of this work that are not included in this licence or permitted under UK Copyright Law.

Abstract

Adult neurogenesis is the continuous process of generating new neurons from neural precursors in the adult mammalian brain. Adult hippocampal neurogenesis plays a role in modulating mood and memory and its dysregulation during ageing and disease highlights important clinical and therapeutic implications in understanding how it is regulated. Adult hippocampal neurogenesis begins with a multipotent population of adult hippocampal stem cells (AHSCs) that are largely quiescent to ensure the long-term maintenance of the AHSC pool. AHSCs' activation is tightly regulated by signals from the surrounding niche to ensure correct initiation of adult hippocampal neurogenesis. Canonical Wnt signalling is present within the hippocampal neurogenic niche, however its' role during adult hippocampal neurogenesis still remains unclear. Within the current literature Wnt has been postulated to play contradictory roles in promoting neural precursor self-renewal whilst also instructing neuronal commitment and differentiation. It is also unclear if and how Wnt signalling directly affects both quiescent and active AHSCs and whether it plays a role in regulating the switch between these two AHSC states. As such, the aim of this project is to characterise the role of canonical Wnt signalling in quiescent and active AHSCs.

Using BATGAL Wnt reporter mice and an *in vitro* model of active and quiescent adult hippocampal stem and progenitor cells (AHSPCs), I found that AHSCs in both states respond to canonical Wnt in a heterogeneous manner. This suggests that AHSCs' response to Wnt signalling is independent of their activation state *in vivo* and *in vitro*. I found that inhibiting AHSCs' response to canonical Wnt signalling, by deleting β-catenin, did not affect AHSC maintenance and function *in vitro* or *in vivo*. This indicates that intact canonical Wnt signalling is not required to maintain AHSC homeostasis, which contrasts published reports showing that loss of intact canonical Wnt signalling impairs AHSC maintenance and proliferation.

I also found that stimulating canonical Wnt signalling in active AHSPCs initiates neuronal differentiation, whereas the same level of Wnt stimulation in quiescent AHSPCs promotes proliferation. This indicates that AHSPCs respond in a state-specific manner to the same level of canonical Wnt simulation. In addition, a higher level of Wnt stimulation promotes neuronal differentiation of quiescent AHSPCs, indicating that quiescent AHSPCs respond to stimulated canonical Wnt signalling in a dose-dependent manner. This state-specific and dose-dependent response to stimulated canonical Wnt signalling could reconcile the contradictions in the current literature as to the role of canonical Wnt signalling in AHSCs. It could also provide a possible

mechanism describing how active and quiescent AHSCs coordinate their response to a niche-derived signal to meet the neurogenic demands of the hippocampus.

Finally, I used an *in vivo* model to stimulate canonical Wnt signalling in AHSCs by stabilising β-catenin. However, I found that stabilising β-catenin in AHSCs *in vivo* promotes their displacement from their correct niche location and impairs adult hippocampal neurogenesis. This displacement could be due to β-catenin's role in cell-cell adhesion and highlights the importance of maintaining cell adhesion properties to ensure correct adult hippocampal neurogenesis.

Acknowledgements

First and foremost, I must thank my supervisor Dr. François Guillemot and co-supervisor Dr. Noelia Urbán for their continued support and guidance throughout this PhD project. Thank you for sharing your knowledge with me and thank you for your patience in answering my many questions. A special thank you to Noelia for her continued positivity in light of my pessimism both inside and outside of the lab.

A special thank you to Lachlan, Mar and Isabelle for their help with experiments, discussions and support throughout this project. I must also thank Lachlan, Stefy and Zachary for their analysis of the RNA sequencing datasets. My thanks also go to Lan for her assistance in sectioning throughout this project. A huge thank you to all members of the Guillemot lab for making these past 4.5 years a hugely enjoyable journey. Thank you for your discussions, advice and the many happy memories made. Past and present members include Noelia, Mar, Isabelle, Lachlan, Lan, Michael, Marco, Clementina, Oana, Cristina, Berta, Ale, Stefy, Siew-Lan, Zachary, Debbie, Alice, Piero, Koji, Mary and Yu Xuan.

Thank you to my thesis committee, Simona Parrinello, Tristan Rodriguez, Stephan Beck and Axel Behrens for their support, discussions and guidance throughout my PhD.

My thanks go to all the BRF staff in HR6 and HR5 who diligently looked after the mice for this project with particular thanks to Nic, Michael, Rekha and Hannah. My thanks also go to the staff of the FACS STP and Sequencing STP. I must also thank Gavin Kelly for his advice on statistical analysis.

I must also thank other 5th floor members for their encouragement, support and laughs since moving to the Crick especially Illaria and Izzie for their constant positivity. My thanks also go to my PhD colleagues and friends in particular Nagisa, Kayleigh and Sang Eun for their encouragement and support. Attending the Crick Running Club gave me the opportunity to take a step back from the bench on Thursday lunch times and to meet a fantastic group of people from across the Crick. I thank all Crick Running Club members for their advice and encouragement regarding matters of science and running! Special thanks to David for organising the Crick Running Club and for his help in fixing Word.

To my friends outside of the Crick, thank you for your support and the breaks away from the lab. For the last time I'm not working with *Drosophila*!

To John, Jo, Roger and especially Joyce. You have been constant pillars of strength, encouragement and common sense since I first walked through those classroom doors in Year 1. Thank you for cheering me on throughout my PhD, dispelling my pessimism and reminding me of the important things in life.

Finally, to my mum Elaine. I don't have enough words to fully express my gratitude for your unwavering support and encouragement throughout this PhD. I honestly don't know how you have put up with me for so long but I am so glad that you have. Thank you!

Table of Contents

Abstract **4**
Acknowledgements **6**
Table of Contents **8**
Table of Figures **11**
List of Tables **14**
Abbreviations **15**
Chapter 1. Introduction **19**
1.1 Adult Neurogenesis **19**
1.1.1 History of Adult Neurogenesis 19
1.1.2 Adult Neurogenesis in Humans 21
1.1.3 Regions of Adult Neurogenesis in the Rodent Brain 23
1.1.4 The Ventricular-Subventricular Zone Neurogenic Niche in the Rodent Brain 25
1.1.5 The Hippocampal Neurogenic Niche in the Rodent Brain 26
1.1.6 Comparison Between Ventricular-Subventricular Zone and Dentate Gyrus Adult Neurogenesis 30
1.1.7 Functions of Adult Neurogenesis 34
1.1.8 Adult Neurogenesis in Ageing and Disease 36
1.2 Adult Hippocampal Stem Cell Activation States **37**
1.2.1 AHSC Origin and Heterogeneity 37
1.2.2 Quiescent and Active AHSCs 38
1.2.3 AHSC Behaviours 40
1.3 Regulation of Adult Hippocampal Stem Cell States and Adult Hippocampal Neurogenesis **42**
1.3.1 Extrinsic Factors Regulating AHSCs and Adult Hippocampal Neurogenesis 42
1.3.2 Niche-Derived Signals Regulating AHSCs and Adult Hippocampal Neurogenesis 44
1.3.3 Intrinsic Mechanisms Regulating AHSC Activation States 52
1.4 Wnt Signalling **56**
1.4.1 Production of Wnt Ligands 57
1.4.2 Wnt Cell Surface Receptors 58
1.4.3 Natural Wnt Agonists and Antagonists 59
1.4.4 Canonical β-catenin Dependent Wnt Signalling Pathway 61
1.4.5 Structure and Functions of β-catenin 64
1.4.6 Non-canonical β-catenin independent Wnt signalling pathways: Wnt/PCP pathway and Wnt/Ca^{2+} pathway 66
1.5 Role of Wnt Signalling During Neurogenesis **68**
1.5.1 Role of Wnt Signalling in Neurogenesis During Development 68
1.5.2 Role of Non-Canonical Wnt Signalling During Adult Hippocampal Neurogenesis 71
1.5.3 Role of Canonical Wnt Signalling During Adult Hippocampal Neurogenesis 72
1.6 Project Aims **77**
Chapter 2. Materials and Methods **79**
2.1 Experimental Models **79**
2.1.1 Mouse Models 79
2.1.2 Generation and Maintenance of Primary Cell Cultures 80
2.1.3 *in vitro* Model of Active and Quiescent AHSPCs 81
2.2 Method Details **81**
2.2.1 Tamoxifen and EdU Administration *in vivo* 81
2.2.2 Tissue Preparation and Immunofluorescence 82
2.2.3 RNA *in situ* Probe Preparation 84

2.2.4 Tissue Preparation and *in situ* hybridisation....85
2.2.5 Microscopic Analysis and Quantifications....86
2.2.6 Dentate Gyrus Dissections and Fluorescence-activated Cell Sorting (FACS)....86
2.2.7 RNA Extraction, Complementary DNA synthesis and Quantitative PCR....87
2.2.8 RNA Sequencing and Analysis with Seurat....88
2.2.9 Constructs, Plasmid Transfection and Viral Transduction....89
2.2.10 Cell Treatments....91
2.2.11 Protein Purification and Western Blots....94
2.3 Quantifications and Statistical Analysis....95
2.3.1 Quantification of Immunofluorescence....95
2.3.2 Statistical Analysis....96
Chapter 3. Results 1: Adult Hippocampal Stem Cells Respond to Canonical Wnt Signalling Independent of their Activation State....97
3.1 Adult Hippocampal Stem Cells Express Components of the Canonical Wnt Signalling Pathway *in vivo* and *in vitro*....97
3.1.1 Adult Hippocampal Stem Cells *in vivo* Express the Machinery to Respond to Canonical Wnt Signalling....97
3.1.2 Active and Quiescent AHSPC Cultures Recapitulate the Gene Expression Patterns of Wnt Pathway Components Observed *in vivo*....106
3.2 AHSCs *in vivo* Respond to Canonical Wnt Signalling Independently of their Activation State....109
3.3 Active and Quiescent AHSPC Cultures Respond to Canonical Wnt Signalling in a Heterogeneous Manner....119
Chapter 4. Results 2: Adult Hippocampal Stem Cells are Unaffected by Deletion of β-catenin....124
4.1 Small Molecule Wnt Inhibitors Do Not Inhibit Baseline Canonical Wnt Signalling in Active AHSPC Cultures....124
4.2 *in vitro* AHSPC Cultures are Unaffected by Loss of β-catenin....129
4.2.1 β-catenin is Robustly Deleted in Active β-cat$^{fl/fl\ ex3-6}$ AHSPCs, Which Prevents Their Response to a Canonical Wnt Stimulus, But Fails to Inhibit Baseline Canonical Wnt Signalling....129
4.2.2 Active AHSPCs Do Not Require Intact β-catenin Signalling to Maintain Their Stemness or Their Activation State....134
4.2.3 Under Normal Culture Conditions, β-catenin Deletion Does Not Affect Quiescent AHSPC Activation....137
4.2.4 Chronic Loss of β-catenin Does Not Affect AHSPCs' Stemness, Their Ability to Enter a Quiescent State or Their Ability to Differentiate into Astrocytes and Neurons....143
4.3 *in vivo* Model Fails to Reliably Delete β-catenin and Inhibit Canonical Wnt Signalling in AHSCs....151
4.3.1 Unsuccessful β-catenin Deletion in AHSCs *in vivo*, Means That Canonical Wnt Signalling Remains Intact in the AHSCs of β-cat$^{del\ ex3-6}$ Mice....152
4.3.2 Adult Neurogenesis is Unaffected in β-cat$^{del\ ex3-6}$ Mice Due to Failed Recombination....158
4.4 Deletion of β-catenin in AHSCs from a Second β-catenin$^{fl/fl}$ Mouse Model Does Not Affect AHSCs But Does Impair Adult Neurogenesis....162
4.4.1 β-catenin is Successfully Deleted in YFP+ Cells from The DG of β-cat$^{del\ ex2-6}$ Mice....162
4.4.2 AHSCs are Largely Unaffected by Deletion of β-catenin in β-cat$^{del\ ex2-6}$ Mice 30 Days After Tamoxifen Induced Cre-Mediated Recombination of the *β-cat$^{fl/fl\ ex2-6}$* Allele....166
4.4.3 Normal Progression Along the Neurogenic Lineage is Impaired by the Loss of β-catenin in AHSCs....168
Chapter 5. Results 3: Levels of Canonical Wnt Stimulation are Important for Determining a Proliferation or Neuronal Differentiation Response in Quiescent AHSCs....171

5.1 Stimulating Canonical Wnt Signalling in Active AHSPCs Initiates Neuronal Differentiation 171
5.2 Stimulating Canonical Wnt Signalling in Quiescent AHSPCs Promotes Differential Effects Depending on the Levels of Wnt Stimulation 176
5.2.1 Over-stimulating Canonical Wnt Signalling in Quiescent AHSCs Induces Neuronal Differentiation Whereas Lower Levels of Wnt Stimulation Promotes Proliferation 176
5.2.2 Wnt Induced Proliferation of Quiescent AHSPCs is Sustained Over Time But Could Promote Lineage Progression Towards a Progenitor Fate 182
5.2.3 Stimulating Canonical Wnt Signalling in Quiescent AHSPCs With Recombinant Wnt3a Also Promotes Proliferation and Activation But With Mechanistic Differences 192
5.3 Stabilising β-catenin in AHSCs *in vivo* Causes Their Displacement from Their Correct Niche Location 197
5.3.1 AHSCs are Lost from the Dentate Gyrus 30 days After β-catenin Stabilisation 197
5.3.2 AHSC Homeostasis is Unaffected by Short-Term Stabilisation of β-catenin 201
5.3.3 β-catenin Stabilisation Causes the Displacement of AHSCs from the SGZ, Which Induces Their Activation 207
5.3.4 Adult Neurogenesis is Disrupted by the Displacement of AHSCs Induced by β-catenin Stabilisation 213
Chapter 6. Discussion 219
6.1 AHSCs Respond Heterogeneously to Canonical Wnt Signalling Independent of their Activation State 221
6.2 Limitations of Canonical Wnt Reporters 223
6.3 Baseline Canonical Wnt Signalling Persists in AHSCs Despite Various Attempts to Inhibit Canonical Wnt Signalling 224
6.4 Different Efficiencies of Deleting β-catenin in AHSCs *in vitro* and *in vivo* 225
6.5 AHSC Homeostasis is Unaffected by Inhibition of Canonical Wnt Signalling 226
6.6 Neurogenic Lineage Progression is Affected by Loss of β-catenin signalling *in vivo* 227
6.7 Levels of Stimulating Canonical Wnt Signalling Are Important for Determining a Proliferative vs Neuronal Differentiation Response in Quiescent AHSPCs 228
6.7.1 Active and Quiescent AHSPCs Display Different Sensitivities to Levels of Canonical Wnt Stimulation 228
6.7.2 Potential Mechanisms Responsible for Inducing the Dose-Dependent Effects of Canonical Wnt Signalling in Quiescent AHSPCs 229
6.8 Dose-Dependent Effects of Stimulating Canonical Wnt Signalling in AHSPCs Could Reconcile Current Contradictions in the Literature 232
6.9 Adult Hippocampal Neurogenesis is Impaired by AHSC Displacement Induced by Stabilised β-catenin 233
6.9.1 Displacement of AHSCs Promotes their Loss from the Hippocampal Neurogenic Niche 233
6.9.2 Correct Niche organisation Influences Adult Hippocampal Neurogenesis 234
6.9.3 Role of β-catenin at Adherens Junctions Could Mediate the Displacement Phenotype 235
6.9.4 Different Models are Required to Fine Tune the Activation of Canonical Wnt Signalling in AHSCs *in vivo* 237
6.10 Canonical Wnt Signalling in AHSCs Could be Required to Facilitate their Response to External Stimuli 238
6.11 Conclusions and Future Perspectives 239
Reference List 241
Appendix 283

Table of Figures

Figure 1.1: Adult neurogenic niches in the rodent brain. 24
Figure 1.2: Schematic of the V-SVZ neurogenic niche. 26
Figure 1.3: Schematic of the neurogenic niche in the dentate gyrus of the hippocampus. 28
Figure 1.4: Expression of cell specific markers across the hippocampal neurogenic lineage.. 30
Figure 1.5: Characteristics of quiescent and active AHSCs. 40
Figure 1.6: Intrinsic mechanisms regulating quiescent and active AHSCs. 56
Figure 1.7: Schematic of Wnt secretion from the cell. 58
Figure 1.8: The canonical Wnt signalling pathway. 63
Figure 1.9: Genomic structure of *CTNNB1* and structure of β-catenin 65
Figure 1.10: Schematic of the non-canonical β-catenin independent Wnt signalling pathways: the Wnt/PCP pathway and the Wnt/Ca^{2+} pathway. 68
Figure 3.1: *in vivo* single cell RNA sequencing data showing the expression of Wnt receptors in Nestin-GFP+ AHSCs and IPCs. 100
Figure 3.2: *in vivo* single cell RNA sequencing data showing the expression of Wnt pathway components in Nestin-GFP+ AHSCs and IPCs. 102
Figure 3.3: *in vivo* single cell RNA sequencing data showing the expression of Wnt ligands and Wnt inhibitors in Nestin-GFP+ AHSCs and IPCs. 104
Figure 3.4: AHSCs express β-catenin at the protein level. 105
Figure 3.5: Bulk RNA sequencing and Western blot analysis of Wnt pathway components in active (10ng/ml FGF2) and quiescent (10ng/ml FGF2 + 20ng/ml BMP4) AHSPC cultures. .. 108
Figure 3.6: Wnt responding AHSCs in the Dentate Gyrus of 2-month-old and 7-month-old BATGAL Wnt reporter mice. 112
Figure 3.7: Wnt Responding IPCs and neuroblasts in the dentate gyrus of 2-month-old BATGAL Wnt reporter mice. 114
Figure 3.8: Response to canonical Wnt signalling does not enrich for AHSC proliferation in 2-month-old BATGAL Wnt reporter mice. 116
Figure 3.9: Characterisation of Wnt responding AHSCs using TCF/LEF:H2B:mCherry and Axin2-mTurQ Wnt reporter mice. 118
Figure 3.10: Analysis of active and quiescent AHSPCs nucleofected with the 7TGC Wnt reporter plasmid. 121
Figure 3.11: Active AHSPC cultures derived from BATGAL mice respond to endogenous canonical Wnt signalling. 123

Figure 4.1: Expression of the Wnt target gene *Axin2* and activity of the Wnt reporter plasmid 7TGC is unaffected in active AHSPCs treated with small molecule Wnt inhibitors. 127
Figure 4.2: Robust deletion of β-catenin in active AHSPCs fails to inhibit baseline canonical Wnt signalling but prevents their response to an external Wnt stimulus. 132
Figure 4.3: Loss of β-catenin signalling does not affect AHSPCs' ability to maintain an active state or retain their stem-like properties. 136
Figure 4.4: Quiescent β-cat$^{del\ ex4-5}$ AHSPCs re-activate and proliferate similarly to quiescent Control AHSPCs when returned to active culture conditions. 139
Figure 4.5: Loss of β-catenin signalling does not alter the mechanism of quiescent AHSPC activation nor does it affect quiescent AHSPC maintenance. 142
Figure 4.6: Maintenance of AHSPCs' active state and stem-like characteristics are unaffected by chronic loss of β-catenin. 144
Figure 4.7: Chronic loss of β-catenin signalling does not affect AHSPCs ability to enter quiescence. 147
Figure 4.8: Chronic loss of β-catenin signalling does not impair AHSPCs ability to differentiate into neurons and astrocytes *in vitro*. 150
Figure 4.9: Canonical Wnt signalling is not inhibited in YFP+ AHSCs of β-cat$^{del\ ex3-6}$ mice 30 days after tamoxifen 153
Figure 4.10: β-catenin immunolabelling and *in situ* analysis in the DG of Control and β-cat$^{del\ ex3-6}$ mice 30 days after the first tamoxifen injection. 155
Figure 4.11: Recombination of the floxed region of *β-catenin* is inefficient in FAC Sorted YFP+ cells from β-cat$^{del\ ex3-6}$ mice. 157
Figure 4.12: Adult neurogenesis is unaffected in β-cat$^{del\ ex3-6}$ mice 30 days after tamoxifen.. 160
Figure 4.13: *β-cat$^{fl/flex\ 2-6}$* allele is successfully recombined in FAC Sorted YFP+ cells from β-cat$^{del\ ex2-6}$ mice. 163
Figure 4.14: β-catenin protein levels are decreased in the DG of β-cat$^{del\ ex2-6}$ mice 30 days after tamoxifen induced Cre-mediated recombination of the *β-cat$^{fl/fl\ ex2-6}$* allele in Glast+ cells..... 165
Figure 4.15: Immunostaining for AHSCs, IPCs and proliferation in the DG of Control and β-cat$^{del\ ex2-6}$ mice 30 days after tamoxifen administration. 167
Figure 4.16: Progression along the neurogenic lineage is impaired in the DG of adult β-cat$^{del\ ex2-6}$ mice 30 days after the first tamoxifen injection. 169
Figure 5.1: Treatment of active AHSPCs with the Wnt agonist CHIR99021 promotes neuronal differentiation. 174

Figure 5.2: Over-stimulating canonical Wnt signalling using CHIR99021 in quiescent AHSPCs initiates neuronal differentiation. 178
Figure 5.3: Lower Wnt stimulation using 5μM CHIR99021 in quiescent AHSPCs, promotes quiescent AHSPC activation and proliferation. 181
Figure 5.4: 5μM CHIR99021 induced quiescent AHSPC proliferation is sustained over time. 183
Figure 5.5: MitoTracker™ Deep Red staining in Control quiescent AHSPCs and quiescent AHSPCs treated with 5μM CHIR99021 over time..... 185
Figure 5.6: qPCR analysis of the gene expression changes induced by 5μM CHIR99021 treatment in quiescent AHSPCs over time. 187
Figure 5.7: Immunostaining of proliferation markers in quiescent AHSPCs treated with 1μM, 2.5μM and 5μM CHIR99021 for 6hrs, 12hrs and 24hrs..... 189
Figure 5.8: qPCR analysis of quiescent AHSPCs treated with 1μM, 2.5μM and 5μM CHIR99021 for 6hrs, 12hrs and 24hrs..... 191
Figure 5.9: Recombinant Wnt3a promotes proliferation of quiescent AHSPCs..... 193
Figure 5.10: Mechanistic differences between recombinant Wnt3a and CHIR99021 induced quiescent AHSPC activation. 196
Figure 5.11: AHSCs are lost from the DG 30 days after β-catenin stabilisation in AHSCs. ... 200
Figure 5.12: AHSCs are unaffected by short-term stabilisation of β-catenin. 203
Figure 5.13: β-catenin stabilisation does not affect AHSCs' ability to return to quiescence... 206
Figure 5.14: Immunofluorescence of AHSCs and proliferation markers in the DG of Control, Cat-ca^{Het} and Cat-ca^{Hom} mice 10 days after β-catenin stabilisation..... 209
Figure 5.15: AHSCs are displaced from the SGZ 10 days after stabilisation of β-catenin which induces their activation. 212
Figure 5.16: Tbr2+ progenitors are displaced in the DG of Cat-ca^{Het} and Cat-ca^{Hom} mice compared to Control..... 215
Figure 5.17: DCX+ neuroblasts are disrupted in the DG of Cat-ca^{Het} and Cat-ca^{Hom} mice compared to Control..... 217

List of Tables

Table 1: Antibodes. 84
Table 2: List of TaqMan probes from Applied Biosystems used for qPCR gene expression assays. 88
Table 3: Summary Evaluation of Results 220
Table 4: Permissions summary for third party copyright works. 283

Abbreviations

ACVR1	Activin receptor type 1 A
A.U.	Arbitrary units
AHSC	Adult Hippocampal Stem Cell
AHSPCs	Adult Hippocampal Stem and Progenitor Cells
AMPA	α-Amino-3-hydroxy-5-methyl-4-isoxazolepropionic acid
APC	Adenomatous polyposis coli
ARM	Armadillo repeats
Ascl1	Achaete-scute like 1; Mash1
ATAC-Seq	Assay for transposase-accessible chromatin sequencing
BDNF	Brain-Derived Neurotrophic Factor
bHLH	Basic helix-loop-helix
BMP	Bone Morphogenetic Protein
BMPRIA	BMP type I receptor A
BMPRIB	BMP type I receptor B
BMPRII	BMP type II receptor
BrdU	5-bromo-3'-deoxyuridine
CA	Cornu Ammonis
Ca^{2+}	Calcium ion
CamKII	Calcium calmodulin-dependent kinase II
cdk	Cyclin dependent kinase
cDNA	Complementary Deoxyribonucleic Acid
ChIP-Seq	Chromatin immunoprecipitation sequencing
CK1γ	Casein Kinase 1γ
CNS	Central Nervous System
CRD	Cysteine rich domain
CTD	C-Terminal Domain
Daam1	Dishevelled associated activator of morphogenesis 1
DAPI	4' 6-diamidino-2-phenylindole
DBI	Diazepam Binding Inhibitor
ddCt	delta delta cycle threshold
DG	Dentate Gyrus
DISC1	Disrupted In Schizophrenia 1

Dkk	Dickkopf
DMSO	Dimethyl sulfoxide
DNA	Deoxyribonucleic Acid
dpi	Days post injection
Dvl	Dishevelled
E	Embryonic day
ECS	Electroconvulsive stimulation
EdU	5-ethynyl-2'-deoxyuridine
EGF	Epidermal Growth Factor
ER	Endoplasmic reticulum
FAC Sorted	Fluorescence activated cell sorted
FACS	Fluorescence activated cell sorting
FGF2	Fibroblast Growth Factor-2
FGFR1	FGF receptor 1
FPKM	Fragments per Kilobase of transcript per Million mapped reads
Fzd	Frizzled
GABA	γ-aminobutyric acid
GCL	Granule Cell Layer
GFAP	Glial Fibrillary Acidic Protein
GFP	Green Fluorescent Protein
Glast	Glutamate aspartate transporter
Grg	Groucho-related-gene Proteins
GSK3β	Glycogen Synthase Kinase 3 β
hrs	Hours
Id	Inhibitor of differentiation
IGF1	Insulin Growth Factor-1
IL-1β	Interleukin-1β
ip	Intraperitoneal
IP3	Inositol 1, 4, 5-triphosphate
IPC	Intermediate Progenitor Cell
kDa	Kilodalton
LGR	leucine-rich repeat-containing G-protein coupled receptor
LRP5/6	LDL-Receptor-related Protein 5/6
MAP	Microtubule Associated Protein
mGluR	G-protein coupled glutamate receptors

min	Minutes
ML	Molecular Layer
MMP	Matrix metalloproteinases
moi	Multiplicity of infection
mRNA	Messenger RNA
NB	Neuroblast
NDS	Normal donkey serum
NeuN	Neuronal nuclear protein
NGF	Nerve Growth Factor
Ngn2	Neurogenin 2
NICD	Notch intracellular domain
NLK	Nemo-like kinase
NMDA	N-methyl-D-aspartate
NSC	Neural Stem Cell
NT3	Neurotrophin 3
NT4	Neurotrophin 4
NTD	N-Terminal Domain
P	Postnatal day
$p75^{NTR}$	p75 Neurotrophin Receptor
PBS	Phosphate buffered saline
PCR	Polymerase chain reaction
PCP	Planar cell polarity
PFA	Paraformaldehyde
PI3k	Phosphoinositide 3-kinase
PKC	Protein kinase C
PLC	Phospholipase C
Porc	Porcupine
PP2A	Protein phosphatase 2A
PSA-NCAM	Polysialylated neural-cell-adhesion molecule
PSD-95	post-synaptic density protein-95
qPCR	quantitative PCR
RGL	Radial Glial Like
RMS	Rostral Migratory Stream
RNA	Ribonucleic Acid
ROCK	Rho-associated kinase

Rspo	R-spondin
RYFP	Rosa Yellow Fluorescence Protein
SSC	Saline-sodium citrate buffer
SEM	Standard Error of the Mean
sFRP	Secreted-frizzled related proteins
SGZ	Subgranular Zone
Shh	Sonic hedgehog
STP	Science Technology Platform
SVZ	Subventricular Zone
TAK	TGFβ activated kinase
Tbr2	T-box brain gene 2 or Eomes
TCF/LEF	T-cell factor/ Lymphoid enhancer-binding factor
TGFβ	Transforming Growth Factor β
TLE	Transducin-Like Enhancer of split Protein
Trk	Tyrosine Kinase Receptor
Tuj1	β-III-tubulin
UMAP	Uniform Manifold Approximation and Projection
V-SVZ	Ventricular-Subventricular Zone
VCAM1	Vascular cell adhesion molecule-1
VEGF	Vascular Endothelial Growth Factor
Wg	Wingless
WIF	Wnt-Inhibitory protein
Wls	Wntless
WT	Wild Type
X-gal	5-bromo-4-chloro-3-indolyl-b-D-galactopyranoside
YFP	Yellow Fluorescent Protein

Chapter 1. Introduction

Neurogenesis is the developmental process of generating new neurons from neural precursors or stem cells. The majority of neurons are generated during early embryonic development up until early postnatal stages and this was thought to be the only point of neurogenesis throughout an organisms' lifespan. However, in the 1960s Altman and Das published the first evidence of adult born neurons in the rat hippocampus, thus overturning Cajal's accepted doctrine of, *"once development was ended…everything may die, nothing may be regenerated".* Since then, regions of adult neurogenesis have been characterised across multiple species, such as rodents, song birds and humans. In the rodent brain the best characterised regions of adult neurogenesis include the subventricular zone (SVZ) of the lateral ventricles and the subgranular zone (SGZ) of the dentate gyrus (DG) in the hippocampus. Within these neurogenic regions, newborn neurons are generated from a population of neural stem cells, which are regulated by a combination of intrinsic mechanisms and extrinsic signals from the surrounding niche microenvironment. Canonical Wnt signalling is one such signal that has been implicated in adult neurogenesis, however its precise role in adult hippocampal neurogenesis still remains unclear. Canonical Wnt signalling has been shown to promote proliferation and neuronal differentiation, however whether it regulates quiescent AHSC activation is still unknown.

In this chapter, I will summarise the current knowledge within the adult neurogenesis field with a focus on the current understanding of the role of canonical Wnt signalling during adult hippocampal neurogenesis. I will start with a brief history of the field of adult neurogenesis before focussing on the importance and regulation of adult hippocampal neurogenesis. I will then explore the adult hippocampal stem cells (AHSCs) in more detail and describe the importance and regulation of AHSC activation states. I will next describe the canonical Wnt signalling pathway before exploring the current knowledge on the role of canonical Wnt signalling during adult hippocampal neurogenesis.

1.1 Adult Neurogenesis

1.1.1 History of Adult Neurogenesis

Adult neurogenesis is the continuous process of generating new neurons from neural precursors in the adult brain. Until the 1980s, this was largely dismissed by neuroscientists who universally retained the central dogma established by Ramon y Cajal in the late 19th to early 20th century,

that no new neurons were generated in the adult mammalian brain; *"Once the development was ended, the founts of growth and regeneration of the axons and dendrites dried up irrevocably. In the adult centres, the nerve paths are something fixed, ended, and immutable. Everything may die, nothing may be regenerated. It is for the science of the future to change, if possible, this harsh decree"* (Ramón y Cajal. 1928). This conclusion was based on the evidence that the adult brain is comprised primarily of post-mitotic neurons that require stable neuronal connections to maintain memories (Gross. 2000). This "harsh decree" was challenged by work from Joseph Altman in 1963. Altman used [^{3}H]-thymidine autoradiography, whereby [^{3}H]-thymidine is incorporated into the DNA (deoxyribonucleic acid) of dividing cells and is maintained in their progeny, thus allowing the identification of newborn neurons. Altman detected [^{3}H]-thymidine labelled cells in the neocortex (Altman. 1963; Altman. 1966), dentate gyrus (DG) of the hippocampus (Altman. 1963; Altman et al., 1965) and olfactory bulb (Altman. 1969) of young and adult rats. This was the first evidence of the generation of newborn neurons in the adult mammalian brain and Altman postulated that these "micro-neurons" were important for learning and memory. These results were corroborated by work from Michael Kaplan, who used electron microscopy to show that [^{3}H]-thymidine labelled cells in the DG and olfactory bulb of adult rats have structural characteristics of neurons such as dendrites and synapses (Kaplan et al., 1977; Kaplan et al., 1984). Furthermore, work from Fernando Nottebohm and colleagues provided functional relevance to the process of adult neurogenesis by showing that new neurons generated in the adult canary forebrain are incorporated into functional circuits involved in auditory response (Goldman et al., 1983; Paton et al., 1984; Burd et al., 1985). However, these results were largely met with scepticism due to technical limitations and studies showing that adult neurogenesis is not present in the adult primate brain (Rakic. 1985a; Rakic. 1985b; Eckenhoff et al., 1988).

It wasn't until the 1990's, with the introduction of new experimental techniques, that adult neurogenesis in the mammalian brain became an established phenomenon. The generation of cells *in vitro* from the adult mouse forebrain with stem-like properties marked an important milestone in the adult neurogenesis field, by showing that multipotent neuronal precursor cells exist in the adult rodent brain (Reynolds et al., 1992; Richards et al., 1992). The introduction of the synthetic thymidine analogue 5-bromo-3'-deoxyuridine (BrdU), which is incorporated into the DNA of dividing cells during S-phase of the cell cycle, allowed the visualisation of proliferating cells and their progeny using immunohistochemical techniques (Nowakowski et al., 1989). Using BrdU labelling in adult rats, Kuhn and colleagues showed that neuronal progenitor cells divide in the subgranular zone (SGZ) of the DG, thus providing robust evidence of adult neurogenesis

in rodents (Kuhn et al., 1996). BrdU incorporation has since been used to show the presence of adult neurogenesis across a variety of species including, but not limited to; teleost fish (Zupanc et al., 1995), reptiles (Pérez-Cañellas et al., 1997; Font et al., 2001), guinea pigs (Guidi et al., 2005), non-human primates (Kornack et al., 1999; Gould et al., 1999) and humans (Eriksson et al., 1998). However, it should be noted that the presence of adult neurogenesis in humans is still debated due to the recent publication of studies arguing both for and against the presence of adult neurogenesis in humans (Boldrini et al., 2018; Sorrells et al., 2018).

1.1.2 Adult Neurogenesis in Humans

In 1998 Eriksson and colleagues published the first evidence of adult neurogenesis in humans (Eriksson et al., 1998). They identified cancer patients who had received diagnostic infusions of BrdU, and analysed the brains post mortem (Eriksson et al., 1998). They found BrdU labelled newborn neurons, derived from dividing progenitor cells in the DG and proliferating progenitors in the subventricular zone (SVZ) of the adult human brain (Eriksson et al., 1998). Adult neural progenitor cells have since been isolated from the hippocampus and SVZ and have been shown to be able to differentiate into neurons *in vitro*, highlighting the presence of mitotically competent neural progenitor cells in the adult human brain (Kukekov et al., 1999; Roy et al., 2000). The extent of adult human neurogenesis in the SVZ and hippocampus has been evaluated by performing immunohistochemistry for the neuroblast marker doublecortin (DCX) on human post-mortem brain tissue (Knoth et al., 2010; Sanai et al., 2011; Wang et al., 2011). Whilst these studies show that newborn neurons are generated in the SVZ and hippocampus of the human brain, it was the work from Spalding and Ernst and colleagues who provided evidence for the integration of newborn neurons in the striatum (Ernst et al., 2014) and hippocampus (Spalding et al., 2013). To assess the generation of newborn neurons in humans, they took advantage of the elevated atmospheric carbon-14 (^{14}C) levels caused by nuclear bomb testing during the Cold War (1955-1963) (Spalding et al., 2005). The authors measured the concentration of ^{14}C in the genomic DNA of cells isolated from the striatum and hippocampus of human post-mortem brain tissues and applied retrospective ^{14}C birth-dating techniques to assess the levels of adult neurogenesis (Spalding et al., 2013; Ernst et al., 2014). From this the authors determined that the annual turnover rate of human striatal neurogenesis is 2.7% (Ernst et al., 2014) and approximately 700 new neurons are incorporated daily into the adult human hippocampus (Spalding et al., 2013). These results show the presence of quite robust neurogenesis in the adult human hippocampus and striatum, which contrasts with the very limited adult neurogenesis reported in the human olfactory bulb (Wang et al., 2011; Sanai et al., 2004).

The persistence of human adult hippocampal neurogenesis throughout life remains a controversial subject of debate, as published studies have provided evidence both for and against the continued production of newborn hippocampal neurons throughout the human lifespan (Knoth et al., 2010; Kempermann. 2011b; Spalding et al., 2013; Dennis et al., 2016; Mathews et al., 2017). Recently in 2018, two studies were published that directly contradict each other in regards to the persistence of adult human hippocampal neurogenesis throughout life (Sorrells et al., 2018; Boldrini et al., 2018). Sorrells and colleagues used immunohistochemical techniques to label progenitor cells and young neurons in post-mortem and intraoperative samples of the human hippocampus from foetal to adult stages (Sorrells et al., 2018). They found that the recruitment of newborn neurons declines rapidly within the first few years of life and does not continue in the adult hippocampus (Sorrells et al., 2018). On the other hand, Boldrini and colleagues used stereological quantification of immunohistochemical labelled post-mortem hippocampal samples from women and men aged 14-79 years old, to show that the number of newborn neurons was stable throughout life (Boldrini et al., 2018). Both studies base their conclusions on the expression of the neuronal lineage marker proteins polysialylated neural-cell-adhesion molecule (PSA-NCAM) and/or DCX, which label intermediate progenitors and neuroblasts respectively (Seki. 2002; Brown et al., 2003). Technical differences such as post-mortem delay and fixation times, may provide one explanation for the different conclusions between these studies and highlights an important need in developing new techniques to study adult neurogenesis in humans (Kempermann et al., 2018). Indeed, Moreno-Jiménez and colleagues have recently optimised a tissue processing protocol to address the issue of fixation and improve immunofluorescence detection in human post-mortem brain tissue (Moreno-Jiménez et al., 2019). Using these optimised techniques, the authors identified thousands of DCX+ neuroblasts in the DG of 13 neurologically healthy patients between 43 and 87 years of age, indicating that adult hippocampal neurogenesis robustly persists throughout physiological ageing in humans until the ninth decade of life (Moreno-Jiménez et al., 2019). The presence of neural stem cells within the adult human brain still remains unresolved, however the development and optimisation of tissue processing and immunofluorescence techniques may allow for the identification of these cells and could have profound ramifications for human health and disease.

1.1.3 Regions of Adult Neurogenesis in the Rodent Brain

Adult neurogenesis occurs within specialised regions of the adult rodent brain known as neurogenic niches. These neurogenic niches consist of a complex microenvironment that provide the necessary physical and molecular signals to balance the maintenance of adult neural precursor cells and the progression of adult neurogenesis throughout life. In the rodent, adult neurogenesis is mostly restricted to the ventricular-subventricular zone (V-SVZ or SVZ) of the lateral ventricles and the subgranular zone (SGZ) of the dentate gyrus (DG) in the hippocampus (Altman et al., 1965; Altman. 1969) (Figure 1.1). The adult neurogenesis in the V-SVZ produces granule layer neurons and interneurons that integrate into the olfactory bulb, following the migration and maturation of precursor sub-types, along the rostral migratory stream (RMS), as well as some oligodendrocytes (Lois et al., 1994; Lois et al., 1996). In the DG of the hippocampus, multipotent adult hippocampal stem cells (AHSCs) are responsible for producing astrocytes and mature granule neurons that displace locally into the granule cell layer (GCL) of the hippocampus and integrate into existing neural networks (Espósito et al., 2005). Subsequent studies have identified other possible neurogenic niches in the neocortex, hypothalamus, amygdala and striatum in the rodent brain, however further characterisation of these areas is required (reviewed by (Gould. 2007)) (Figure 1.1).

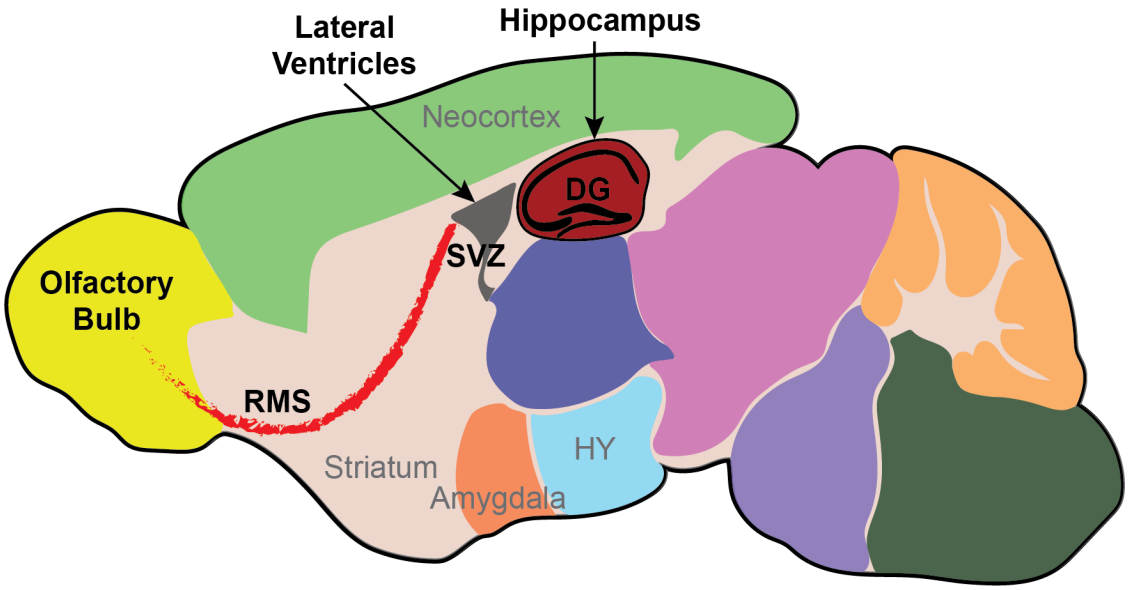


Figure 1.1: Adult neurogenic niches in the rodent brain.
Schematic highlighting the regions of adult neurogenesis in the rodent brain. The ventricular subventricular zone (V-SVZ) of the lateral ventricles and subgranular zone (SGZ) of the dentate gyrus (DG) in the hippocampus are two regions of adult neurogenesis that have been extensively characterised in the rodent brain. Adult neurogenesis in the V-SVZ generates new neurons that migrate along the rostral migratory stream (RMS) and integrate into the olfactory bulb. Adult hippocampal neurogenesis in the DG produces granule neurons that integrate locally into existing hippocampal neural networks. Adult neurogenesis has also been described in the neocortex, striatum, amygdala and hypothalamus in the rodent brain, however these regions are less characterised. SVZ, Subventricular Zone. SGZ, Subgranular zone. DG, Dentate Gyrus. RMS, Rostral Migratory Stream. HY, Hypothalamus. As not all of these brain regions are present within the same sagittal plane, their approximate locations are represented on this schematic.

The stem cell niche is not only the physical location of stem cells *in vivo*, but is a specialised microenvironment responsible for coordinating the development and maintenance of stem cells. It facilitates this through the integration and interaction of extrinsic stimuli including cell-cell interactions and signals from various signalling pathways (Ferraro et al., 2010). Regulating these interactions is key for balancing quiescent stem cell maintenance vs their activation and maturation towards a differentiated fate (Ferraro et al., 2010). The stem cell niche was first hypothesised by R. Schofield in 1978, who postulated that removing hematopoietic stem cells from their specialised niche location would result in their differentiation (Schofield. 1978). The first studies characterising niche components were performed in *Drosophila melanogaster* (Xie et al., 1998) and *Caenorhabditis elegans* (Kimble et al., 1981) gonads and has led to the identification of common niche components at the cellular, molecular and functional level, across

multiple species and biological systems including the skin, muscle and intestine (reviewed by (Li et al., 2005; Ferraro et al., 2010; Morrison et al., 2008)).

As stated above, adult neurogenesis predominately occurs within two germinal regions of the rodent brain; the V-SVZ of the lateral ventricles and the DG of the hippocampus. The importance of these neurogenic niches in maintaining the undifferentiated state of neural precursor cells, whilst regulating their differentiation, is highlighted by the transplantation of neural precursor cells into neurogenic and non-neurogenic regions of the mammalian brain (Herrera et al., 1999). SVZ derived neural precursors exhibit limited survival and poor neuronal differentiation when transplanted into non-neurogenic regions, but were able to differentiate correctly when transplanted into neurogenic regions (Herrera et al., 1999). Interestingly, SVZ neural precursor cells transplanted into the DG generate hippocampal neurons and DG neural precursors transplanted into the RMS generate olfactory neurons (Suhonen et al., 1996). This indicates that whilst there are common features shared between these neurogenic niches, some molecular signals regulating neuronal differentiation may be niche specific.

1.1.4 The Ventricular-Subventricular Zone Neurogenic Niche in the Rodent Brain

The ventricular-subventricular zone (V-SVZ) lines the lateral wall of the ventricle and houses neural stem cells (NSC), which generate neuroblasts. These neuroblasts migrate anteriorly along the rostral migratory stream (RMS) towards the olfactory bulb, where they mature into local olfactory neurons. The NSCs are separated from the ventricular space by a layer of ependymal cells (E) and are arranged in a “pinwheel” architecture where the NSC apical surface is surrounded by ependymal cells (Mirzadeh et al., 2008) (Figure 1.2). NSCs retain astroglial properties, such as the expression of the astrocyte marker glial fibrillary acidic protein (GFAP) and were identified based on retroviral labelling and their ability to generate multipotent neurospheres *in vitro* (Doetsch et al., 1999). NSCs project a thin apical process through the ependymal layer to contact the ventricular space and also project a basal process that directly contacts the vasculature (Mirzadeh et al., 2008) (Figure 1.2). This apical-basal polarity allows NSCs to receive signals from the cerebral spinal fluid, circulated blood and surrounding supporting cells to coordinate their behaviour in response to current demands (Fuentealba et al., 2012). Once activated, NSCs will divide to generate a proliferating intermediate progenitor cell (IPC) which undergoes a number of symmetrical divisions before differentiating into a neuroblast (NB, Figure 1.2). These neuroblasts then enter the RMS and migrate towards the olfactory bulb by forming a chain along a tube of astrocytes (Lois et al., 1996) (Figure 1.2). Upon

reaching the olfactory bulb, the neuroblasts detach from the RMS and migrate and differentiate into different subtypes of interneurons (reviewed by (Lledo et al., 2006)) (Figure 1.2).

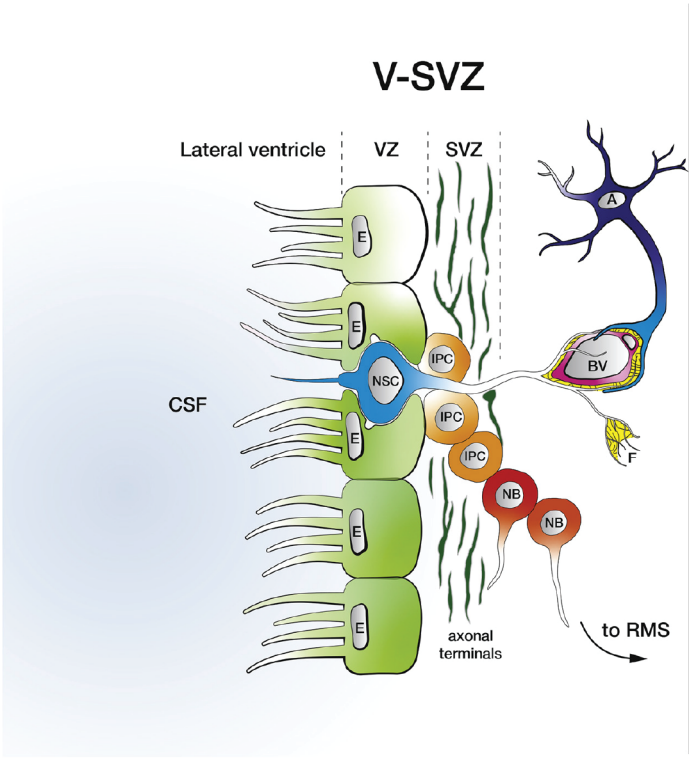


Figure 1.2: Schematic of the V-SVZ neurogenic niche.
The ventricular-subventricular zone (V-SVZ) is located along the wall of the lateral ventricle. Neural stem cells (NSCs) reside within the SVZ above a layer of ependymal cells (E) occupying the ventricular zone (VZ). NSCs have an apical-basal morphology which allows them to send processes towards the cerebral spinal fluid (CSF) in the ventricular space and blood vessels (BV). NSCs divide to generate intermediate precursor cells (IPCs). IPCs divide a number of times before differentiating into neuroblasts (NBs), which migrate to the olfactory bulb via the rostral migratory stream (RMS) where they terminally differentiate into subtypes of interneurons. A, astrocyte; F, fractone. Image reproduced from (Urbán et al., 2019) with permission from the rights holder, Elsevier.

1.1.5 The Hippocampal Neurogenic Niche in the Rodent Brain

The hippocampal neurogenic niche resides within the dentate gyrus (DG) and the adult hippocampal neural stem cells (AHSCs) are located in the subgranular zone (SGZ), which marks the interface between the hilus and DG (Figure 1.3). AHSCs retain many astrocytic characteristics and are commonly referred to as radial glial-like cells (RGL) due to their radial

morphology (Bonaguidi et al., 2011; Bonaguidi et al., 2012; Seri et al., 2001). AHSCs are polarised with their cell body located in the SGZ and a radial process that projects through the granule cell layer (GCL), which either branches into the inner molecular layer (ML) (76% of RGL AHSCs) or terminates at the GCL/ML interface (24% of RGL AHSCs) (Gebara et al., 2016). This radial morphology allows AHSCs to coordinate signals from a variety of sources including neighbouring cells (e.g. astrocytes and IPCs), blood vessels and neurons (reviewed by (Fuentealba et al., 2012; Gebara et al., 2016; Moss et al., 2016; Licht et al., 2016)). AHSCs are multipotent and are able to differentiate into granule neurons via the neurogenic lineage as well as astrocytes (Steiner et al., 2004). AHSCs give rise to intermediate progenitor cells (IPCs), which are small cells with short processes that cluster in close proximity to the AHSCs in the SGZ (Figure 1.3). IPCs are highly proliferative and are responsible for the amplification of the neurogenic lineage (Kronenberg et al., 2003). As IPCs differentiate into neuroblasts (NB) they migrate a short distance into the GCL (Figure 1.3) (Fuentealba et al., 2012). As they mature, neuroblasts adopt a rounded cell body with an apical dendrite and become post-mitotic as they begin to lose their proliferative capacity. As neuroblasts differentiate into granule neurons they begin to establish connections to the hippocampal network, which is essential for their long-term survival (Kempermann et al., 2004). Approximately 4 weeks after the first AHSC division, mature newborn granule neurons integrate into the tri-synaptic hippocampal circuit, that links the entorhinal cortex, the DG and cornu ammonis (CA) regions, by extending dendrites towards the ML and axons through the hilus towards CA3 (reviewed by (Li et al., 2009)).

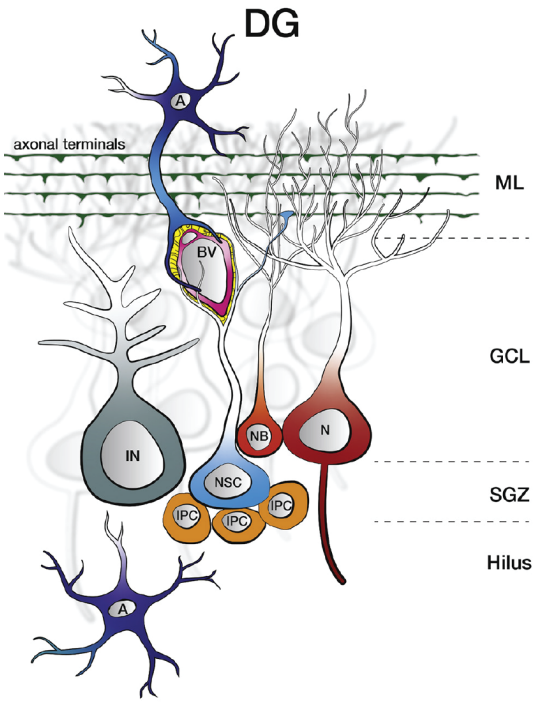


Figure 1.3: Schematic of the neurogenic niche in the dentate gyrus of the hippocampus. Adult hippocampal stem cells (AHSCs or NSCs) are located in the subgranular zone (SGZ) at the interface between the hilus and the dentate gyrus (DG). AHSCs have a radial glial-like morphology that allows them to coordinate signals from across the neurogenic niche to regulate their behaviour. AHSCs give rise to intermediate progenitor cells (IPCs), which in turn differentiate into neuroblasts (NBs) that migrate into the granule cell layer (GCL). In the GCL, neuroblasts mature further and differentiate into granule neurons (N) that integrate into existing hippocampal neural networks. A, astrocyte; IN, interneuron. Image reproduced from (Urbán et al., 2019) with permission from the rights holder, Elsevier.

As cells progress along the hippocampal neurogenic lineage, they undergo gene expression and physiological changes that can be used to characterise their cellular identity (Figure 1.4). In addition to their niche location and radial morphology, AHSCs can be identified based on their expression of neural stem cell markers, such as Sox2 and Nestin (Filippov et al., 2003; Suh et al., 2007). Due to their astrocytic nature, AHSCs also co-express the astrocytic markers glial fibrillary protein (GFAP) and glutamate aspartate transporter (Glast), however they can be distinguished from mature astrocytes by the lack of expression of the mature astrocyte marker S100β (Seri et al., 2001; Brunne et al., 2010; Steiner et al., 2004).The majority of AHSCs are maintained in a quiescent state, however a small proportion (1-5%) are able to re-enter the cell cycle and become activated in response to extrinsic stimuli (Kronenberg et al., 2003; Seri et al.,

2001; Andersen et al., 2014). Currently there are no unique quiescence markers however, quiescent and active AHSCs can be differentiated based on their gene expression patterns, expression of cell cycle markers and metabolic differences, which will be discussed further in Section 1.2.2 (Urbán et al., 2019). Active AHSCs retain the classical RGL morphology, express cell cycle markers and express the basic helix-loop-helix transcription factor Ascl1 at the protein level (Andersen et al., 2014; Urbán et al., 2016). Like active AHSCs, IPCs exhibit a proliferation signature and can be distinguished from active AHSCs based on their rounded compact morphology (Figure 1.4). Early IPCs (Type IIa) share the expression of many AHSC associated markers including Ascl1, Nestin and Sox2 (Figure 1.4). As IPCs progress along the neurogenic lineage, these later stage IPCs (Type IIb) lose their expression of AHSC associated genes and begin to express markers associated with neuronal commitment such as T-box brain gene 2 (Tbr2 or Eomes) and Neurogenin2 (Ngn2) (Hodge et al., 2008; Roybon et al., 2009). As Tbr2+ IPCs differentiate into neuroblasts, they start to express the neuroblast marker doublecortin (DCX) (Brown et al., 2003). The overlapping expression of Tbr2 and DCX can be used to identify early neuroblasts vs more mature neuroblasts that express DCX, lose Tbr2 expression and develop an apical dendrite. Differentiating neuroblasts begin to express β-III-tubulin (antibody called Tuj1) before terminally differentiating as mature granule neurons expressing the neuronal nuclear protein NeuN (Ambrogini et al., 2004).

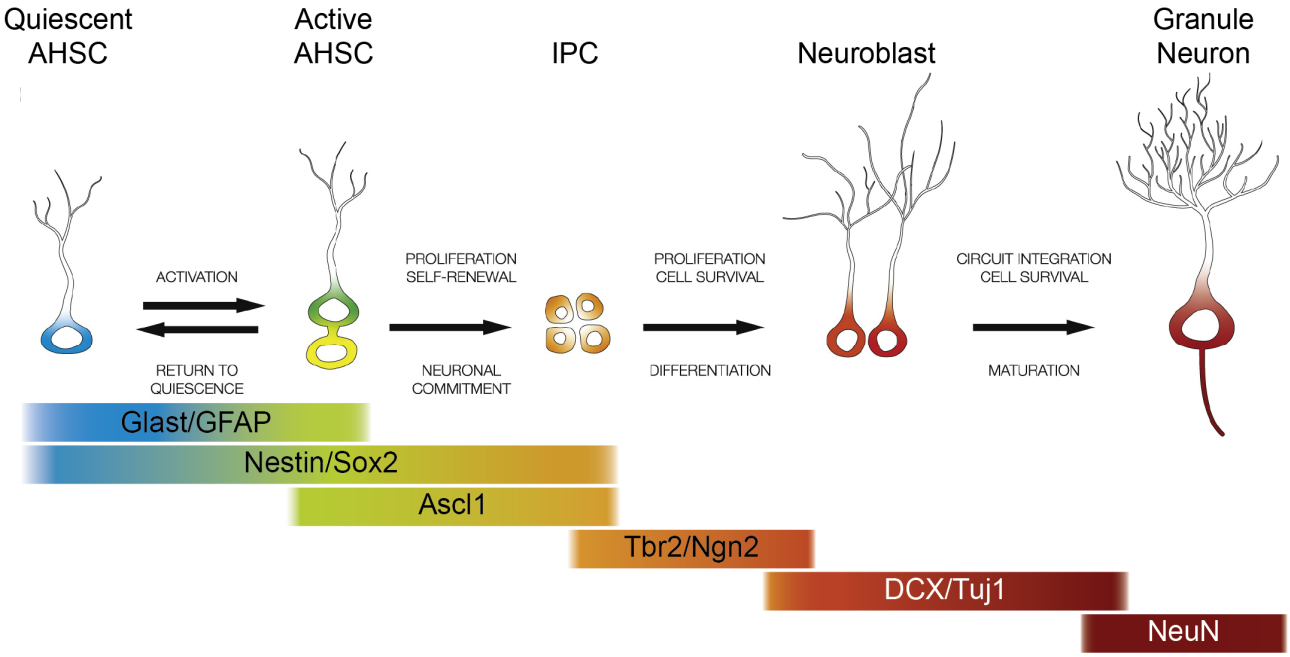


Figure 1.4: Expression of cell specific markers across the hippocampal neurogenic lineage.

The cells of the hippocampal neurogenic lineage can be identified based on the expression of stage-specific markers. Quiescent and active AHSCs can be identified by their expression of Glast, glial fibrillary protein (GFAP) Nestin and Sox2. Active AHSCs and intermediate progenitor cells (IPCs) express high levels of the transcription factor Ascl1. IPCs also express Nestin and Sox2. Differentiating IPCs express Tbr2 and Ngn2 before differentiating into DCX+ neuroblasts. Maturing neuroblasts express β-III-tubulin (Tuj1) before terminally differentiating as a mature NeuN+ granule neuron. Image adapted from (Urbán et al., 2019) with permission from the rights holder, Elsevier.

1.1.6 Comparison Between Ventricular-Subventricular Zone and Dentate Gyrus Adult Neurogenesis

The V-SVZ and DG neurogenic niches exhibit many similarities that simultaneously allow for the maintenance of adult neural stem cells, whilst also promoting the differentiation of newborn neurons throughout life. They share a number of cellular components, including endothelial cells, astrocytes, microglia, mature neurons and neural stem cell progeny, that all contribute to the creation of an appropriate microenvironment to regulate neurogenesis throughout adulthood (reviewed by (Ming et al., 2011)) (Figures 1.2 and 1.3). For example, the vasculature is highly organised throughout the V-SVZ and DG and is closely associated with the NSCs from both niches to regulate their behaviour via blood borne factors and cell-cell interactions (see Section

1.3.2) (Delgado et al., 2014; Moss et al., 2016; Gebara et al., 2016; Licht et al., 2016). Astrocytes also secrete a variety of signalling molecules that regulate multiple stages of adult neurogenesis in both niches and microglia phagocytose cells that have undergone apoptosis to maintain the homeostasis of baseline adult neurogenesis (Sierra et al., 2010; Song et al., 2002). Additionally, the mature and immature progeny of NSCs also form an integrated part of both niches, providing diffusible and contact-mediated signals to regulate multiple stages of adult neurogenesis (Alfonso et al., 2012; Liu et al., 2005; Kawaguchi et al., 2013; Berg et al., 2013).

Whilst the two neurogenic niches share a number of common properties, there are distinct differences between the V-SVZ and the DG as well as differences in the adult neurogenesis that occurs between both niches. As stated above, the neurogenic niches are comprised of similar cellular components, however the V-SVZ is unique due to the presence of ependymal cells lining the ventricular wall (Figure 1.2). This ependymal cell lining is closely associated with the NSCs of the V-SVZ and actively regulates their activation and neuronal fate choice through the release of Noggin (Lim et al., 2000). In addition, factors within the cerebral spinal fluid such as sphingosine-1-phosphate and prostaglandins provide unique regulation of V-SVZ adult neurogenesis that is not present in the DG (Codega et al., 2014). The two niches are also distinct in terms of their architecture, as NSCs are located in a “pinwheel” organisation in the V-SVZ (Mirzadeh et al., 2008) and are localised to the SGZ in the DG. In addition, the adult neurogenesis of the hippocampus is locally restricted to the DG with neuroblasts and newborn granule neurons settling in the GCL, a short distance away from the NSCs in the SGZ (Sun et al., 2015a). This contrasts with the V-SVZ where neuroblasts enter the RMS and migrate away from the niche to settle in the olfactory bulb (Lois et al., 1994; Luskin. 1993; Doetsch et al., 1996; Lois et al., 1996). This shows that the DG NSCs are in close proximity to the granule neurons they produce unlike the V-SVZ NSCs which do not contact their progeny in the olfactory bulb (Obernier et al., 2019).

The NSCs themselves also share many key characteristics between these two neurogenic regions, such as their expression of stem cell specific markers (GFAP, Nestin and Sox2), their quiescent state, their connections to surrounding niche components and their restricted lineage potential. Single cell transcriptomic studies are useful tools to examine differences in the transcriptomes of different cell types (Haque et al., 2017). Thus far, a direct comparison of single cell RNA Sequencing datasets generated from NSCs isolated from the V-SVZ and DG simultaneously, has not been performed in the same study. Nevertheless, the independent single cell transcriptomic studies of the V-SVZ NSCs and DG NSCs, have allowed for the global

comparison between the gene expression profiles of NSCs isolated from these two neurogenic regions, despite employing different sorting strategies. Indeed, Dulken and colleagues directly compare their single cell RNA sequencing dataset of NSCs isolated from the V-SVZ with the dataset generated by Shin and colleagues of NSCs isolated from the DG (Dulken et al., 2017; Shin et al., 2015). Dulken and colleagues show that the overall gene expression profiles are similar between these two datasets, highlighting the transcriptomic similarities between the NSCs of both neurogenic niches (Dulken et al., 2017; Shin et al., 2015). Additionally, by employing pseudotime analysis to order cells according to their activation state, Dulken and colleagues show that the molecular phenotypes of quiescence and activation are partially conserved between the NSCs of the V-SVZ and DG (Dulken et al., 2017). Gene ontology analysis of published datasets show an enrichment of genes associated with lipid metabolism, glycolysis, cell signalling, and cell adhesion in quiescent V-SVZ and DG NSCs whereas cell cycle, DNA/RNA metabolism, transcription and protein translation are enriched in active NSCs from both niches (Llorens-Bobadilla et al., 2015; Mizrak et al., 2019; Shin et al., 2015; Artegiani et al., 2017). However, transcriptomic analyses have identified differences between the NSCs of these two neurogenic niches. For example, NSCs isolated from the V-SVZ have been shown to express distinct combinations of lineage-specific transcription factors in a regionally defined manner (Llorens-Bobadilla et al., 2015; Mizrak et al., 2019). This further supports evidence showing that the fate potential of V-SVZ NSCs is regionally specified and is further discussed below. In contrast, single cell data from NSCs isolated from the DG identify a single population of NSCs, which do not demonstrate regional lineage restriction (Shin et al., 2015; Hochgerner et al., 2018; Artegiani et al., 2017). Overall, these single cell transcriptomic datasets are a useful tool to compare the molecular signatures of the NSCs from the V-SVZ and DG niches.

The neural stem cells from both neurogenic niches exhibit a restricted lineage specification, however they each generate unique neuronal subtypes and glia. In the DG the NSCs generate excitatory dentate granule neurons and astrocytes (Berg et al., 2019; Pilz et al., 2018; Encinas et al., 2011; Bonaguidi et al., 2011; DeCarolis et al., 2013) whereas in the V-SVZ the NSCs generate inhibitory interneurons, periglomerular neurons and oligodendrocytes (Fuentealba et al., 2015; Merkle et al., 2007). As mentioned above, progeny subtypes are specified according to the NSC location along the dorsal-ventral axis in the V-SVZ indicating a form of positional heterogeneity within the V-SVZ NSCs (Merkle et al., 2007). This contrasts with the NSCs in the DG that generate granule neurons and astrocytes throughout the SGZ, however more research is needed to confirm this homogeneity (Bonaguidi et al., 2011; Encinas et al., 2011; Berg et al., 2019). Interestingly, both V-SVZ and DG NSCs are able to differentiate into all three lineages

(neurons, astrocytes and oligodendrocytes) *in vitro* (Palmer et al., 1997; Reynolds et al., 1992) indicating that the *in vivo* niche may limit adult NSC potential (Bond et al., 2015; Urbán et al., 2019).

The NSCs within the V-SVZ and DG also exhibit contrasting modes of division. The NSCs of the V-SVZ primarily divide symmetrically to produce two identical daughter cells (Obernier et al., 2018; Basak et al., 2018). The majority of V-SVZ NSCs undergo “consuming divisions” to generate two daughter IPCs, which depletes the size of the stem cell pool (Obernier et al., 2018). However, a smaller proportion (20-30%) of V-SVZ NSCs undergo “self-renewing divisions” to generate two daughter NSCs, which expands the pool of NSCs (Obernier et al., 2018). In contrast, the NSCs of the DG predominately divide asymmetrically to generate an NSC and either an IPC or astrocyte, which maintains the pool of NSCs whilst simultaneously meeting neurogenic demands (Bonaguidi et al., 2011; Pilz et al., 2018). A smaller proportion of DG NSCs are able to divide symmetrically in either self-renewing or consuming divisions (Bonaguidi et al., 2011; Pilz et al., 2018) (See Section 1.2.3). Asymmetric divisions couple the regulation of self-renewal with the generation of differentiated progeny, whereas symmetric divisions uncouple this regulation (Urbán et al., 2019). More work is needed to understand how these different modes of division are regulated within the V-SVZ and DG neurogenic niches and to determine how they impact the long-term dynamics of these two NSC populations (Urbán et al., 2019).

The NSCs within both niches are regulated by a variety of niche-derived signals including Notch, Sonic hedgehog (Shh), Bone Morphogenetic Proteins (BMPs) and Wnts. Notch signalling has been shown to promote quiescence of both V-SVZ and DG NSCs, as deletion of Notch downstream components in the NSCs of both niches leads to increased activation and depletion of the quiescent NSC pool (Imayoshi et al., 2010; Ehm et al., 2010). NSCs from both the V-SVZ and DG express three Notch receptors (Notch 1, 2 and 3) (Kawai et al., 2017; Breunig et al., 2007), however they exhibit differential roles in V-SVZ and DG NSCs. For example, deletion of Notch 1 in DG NSCs results in the loss of the NSC and IPC pool (Ables et al., 2010). Conversely, deletion of Notch 1 in V-SVZ NSCs promotes NSC proliferation without the loss of the quiescent NSC pool as observed in the DG (Basak et al., 2012). This highlights the context dependency of Notch signalling within the NSCs of the V-SVZ and DG niches. Similarly, BMP signalling also maintains NSC quiescence in both niches (Mira et al., 2010; Lim et al., 2000; Douet et al., 2012; Mercier et al., 2014) and also promotes the fate choice of V-SVZ progenitors in a dose-dependent manner. Basal levels of BMP signalling in the V-SVZ promotes a neuronal lineage specification (Colak et al., 2008), whereas higher BMP signalling levels inhibits neurogenesis

by promoting glial differentiation (Lim et al., 2000). Shh signalling in the V-SVZ has been shown to play a role in regulating NSC maintenance, activation and proliferation (Palma et al., 2005; Petrova et al., 2013; Daynac et al., 2016). Deletion of the primary cilium, which is required for Shh signalling, in DG NSCs impairs progenitor proliferation and promotes cell cycle exit (Breunig et al., 2008; Amador-Arjona et al., 2011), however a direct role in regulating quiescent DG NSC activation has yet to be established. Finally, the NSCs in both niches respond to canonical Wnt signalling which has been shown to promote NSC self-renewal and progenitor proliferation (Lie et al., 2005; Qu et al., 2013; Bowman et al., 2013) as well as neuronal lineage choice in the DG (Lie et al., 2005; Seib et al., 2013). In the V-SVZ non-canonical Wnt signalling has been shown to maintain the quiescent state of NSCs by promoting their anchorage to the niche via the small GTPase CDC42 (Chavali et al., 2018). This could suggest that the activation of quiescent NSCs requires a switch from non-canonical to canonical Wnt signalling, however this mechanism has yet to be elucidated (Urbán et al., 2019). Overall, whilst the niche-derived signals share some common regulatory mechanisms between the V-SVZ and DG, there are subtle context dependent differences in how these signalling pathways regulate adult neurogenesis within the two niches. This is evidenced by transplantation studies showing that the neuronal fate choice of transplanted NSCs is dependent on their niche location (Suhonen et al., 1996) and highlights the importance of understanding how adult neurogenesis is regulated independently in both of these neurogenic niches. The regulation of adult hippocampal neurogenesis will be further explored in Section 1.3.

1.1.7 Functions of Adult Neurogenesis

To understand the function of adult neurogenesis it is important to consider how this process evolved. In non-mammalian vertebrates, such as fish, reptiles, amphibians and birds, adult neurogenesis is widespread throughout various brain regions and may be related to post-embryonic brain growth in response to sensory system maturation (Kaslin et al., 2008). In contrast, mammalian adult neurogenesis is restricted to discrete neurogenic regions, which argues that the process of adult neurogenesis has declined during the course of evolution (Kaslin et al., 2008; Lindsey et al., 2006). It has been suggested that this decreased propensity for neurogenesis in the adult mammalian brain is due to a resistance to integrate new neurons into an already established neural network (Rakic. 2004; Rakic. 1985b). In opposition to this view, Gerd Kempermann proposed that the specific neurogenesis of the adult hippocampus is instead a late-evolved trait, conferring plasticity and adaptability in response to environmental challenges (Kempermann. 2012). Indeed, computational studies have shown that rigid networks

cannot acquire new information, whereas highly flexible networks are unable to retain information (Wiskott et al., 2006). As such, adult hippocampal neurogenesis provides an elegant solution to the stability vs plasticity problem (Kempermann. 2012).

The adult born neurons generated in the rodent SVZ and SGZ, integrate into existing neural networks and contribute to the complexity and continued plasticity of the adult brain (Deng et al., 2010; Jessberger et al., 2009; Sahay et al., 2011a; Lledo et al., 2006). Adult neurogenesis in the rodent SVZ gives rise to neuroblasts that migrate along the RMS to the olfactory bulb where they mature and integrate into olfactory circuits. SVZ adult neurogenesis has been implicated in maintaining olfactory bulb circuitry, regulating olfactory discrimination and mediating olfactory memory (reviewed by (Lledo et al., 2006)). These functions have been elucidated by ablating SVZ adult neurogenesis, however these studies have often reported contradictory results due to the unspecific nature of the experimental approaches used (reviewed by (Lledo et al., 2006)). Nevertheless, these studies provide useful information on the function of SVZ adult neurogenesis.

The adult hippocampus plays a crucial role in learning and memory, spatial navigation, pattern separation, and emotional behaviour (Deng et al., 2010). The functional integration of newborn neurons in the DG of the hippocampus, has been shown to be important in modulating many of these hippocampal dependent functions (Hastings et al., 1999; van Praag et al., 2002; Jessberger et al., 2003; Deng et al., 2010). One key function of the adult hippocampus is its role in pattern separation, which is the formation of distinct representations of similar inputs (Marr et al., 1971; Clelland et al., 2009). Computational modelling (Aimone et al., 2010) and behavioural studies (Clelland et al., 2009; Sahay et al., 2011a) have shown that adult hippocampal neurogenesis is important for optimal pattern separation functions as immature newborn neurons provide the plasticity required to integrate new information, without affecting the existing information stored by mature granule neurons (Deng et al., 2010; Danielson et al., 2016). Newborn neurons exhibit enhanced synaptic plasticity and excitability compared to mature granule neurons (Schmidt-Hieber et al., 2004; Ge et al., 2007; Mongiat et al., 2009; Gu et al., 2012) and are less influenced by the activity of inhibitory interneurons that depresses the activation of mature granule neurons (Marín-Burgin et al., 2012; Dieni et al., 2013; Sahay et al., 2011b; Groisman et al., 2020). These unique characteristics of immature newborn neurons favours their activation and recruitment during the formation of new memories and indicates their involvement in hippocampal learning and memory functions (Rodriguez-Iglesias et al., 2019; Sahay et al., 2011b). Indeed, abrogating adult hippocampal neurogenesis impairs

hippocampal dependent trace (Shors et al., 2001), spatial (Dupret et al., 2008) and long-term memory (Bruel-Jungerman et al., 2005), thus highlighting key roles for newborn neurons in hippocampal dependent learning and memory. However, there are reported inconsistencies across studies that ablate adult hippocampal neurogenesis to investigate the function of newborn neurons in hippocampal learning and memory (Deng et al., 2010; Shors et al., 2002). This is in part due to different ablation techniques and behavioural tasks employed across various studies and suggests that the involvement of adult neurogenesis in hippocampal learning and memory is context dependent (Deng et al., 2010; Shors et al., 2002).

1.1.8 Adult Neurogenesis in Ageing and Disease

Another clue as to the function of adult hippocampal neurogenesis lies within the pathological phenotypes of neuropsychiatric and neurodegenerative disorders that present with dysregulated adult hippocampal neurogenesis. In rodents, age-related cognitive decline has been linked to decreased levels of adult hippocampal neurogenesis (Knoth et al., 2010; Driscoll et al., 2006), however this direct link has yet to be made in humans (Lazarov et al., 2013). Reduced adult hippocampal neurogenesis is also a key feature of anxiety, stress and depressive disorders and may directly contribute to their progression (Jacobs et al., 2000; Miller et al., 2015). Indeed, many antidepressants have been shown to work by stimulating adult hippocampal neurogenesis and some require adult hippocampal neurogenesis to be effective (Sahay et al., 2007; Miller et al., 2015). Epileptic seizures have been shown to promote the production of newborn neurons in the hippocampus and prolonged/multiple seizures can cause alterations in the dendrite morphology of newborn neurons, which contributes to epileptic disease (Jessberger et al., 2015). Neurodegenerative disorders, such as Alzheimer's disease, Parkinson's disease and Huntington's disease also exhibit alterations in adult hippocampal neurogenesis despite the depletion of different neural populations targeted by the pathological proteins associated with each disease (Winner et al., 2015). Early symptoms of these diseases include depression, anxiety and cognitive impairment associated with deficits in adult hippocampal neurogenesis (Winner et al., 2015). Whether dysregulated adult neurogenesis represents a cause or consequence of neuropsychiatric and neurodegenerative disorders currently remains to be seen as, whilst depression is associated with decreased hippocampal volume (reviewed by (Kang et al., 2016)), ablation of adult hippocampal neurogenesis fails recapitulate a "depressive-like" state in animal models (Airan et al., 2007). In addition, as neurodegenerative diseases exhibit a progressive pathology, it remains to be determined when and how defects in adult neurogenesis switch from being causative to a direct consequence of neurodegeneration (Lazarov et al., 2010;

Gil-Mohapel et al., 2011; Regensburger et al., 2014). Overall, the dysregulated adult hippocampal neurogenesis in various disease states, ageing and depression, highlight important clinical and therapeutic implications in understanding how endogenous adult hippocampal neurogenesis is regulated.

1.2 Adult Hippocampal Stem Cell Activation States

Adult stem cells can be characterised based on their capacity for self-renewal and their ability to differentiate into specialised cell types to meet the demands of the local tissue. In the following section I will describe the stem cells of the adult hippocampus in terms of their origin, heterogeneity, activation states and behaviours. I will then outline some of the intrinsic mechanisms that regulate the activation of AHSCs from quiescence.

1.2.1 AHSC Origin and Heterogeneity

AHSCs share many characteristics with glial cells and indeed GFAP+ astrocytes were initially believed to be the source of new neurons in the adult DG (Seri et al., 2001). Subsequently these GFAP+ astrocytes were further defined as radial-glial-like cells that are derived from the radial glia of the embryonic dentate neuroepithelium during development and maintain their neurogenic potential in the adult (Doetsch et al., 1999; Seri et al., 2001; Eckenhoff et al., 1984; Alvarez-Buylla et al., 2001). Recent single cell transcriptomics and clonal lineage tracing techniques have shown a shift in embryonic radial glial identity towards an adult RGL identity during the second postnatal week, suggesting that AHSCs are a continuation of embryonic radial glial cells (Berg et al., 2019; Hochgerner et al., 2018). Alternatively, there is evidence suggesting that AHSCs might be descended from Shh-responsive cells in the ventral hippocampus during late gestation (Li et al., 2013). This could suggest that AHSCs originate from both embryonic and late-gestational sources, however the precise embryonic origin of AHSCs is currently unknown. Whilst no single marker has been identified to uniquely label the AHSC population, fate mapping studies in mice using the inducible Cre recombinase system, showed that AHSCs express astrocytic markers, such as Glast (Namba et al., 2005) and GFAP and progenitor markers such as Sox2 (Suh et al., 2007) and Nestin (Fukuda et al., 2003; Seri et al., 2004) (reviewed by (Dhaliwal et al., 2011)). These studies have also provided evidence for the functional heterogeneity of AHSCs (Urbán et al., 2019; DeCarolis et al., 2013). Using NestinCreERT2; Rosa26YFP and GlastCreERT2; Rosa26YFP mice, DeCarolis and colleagues

showed that Nestin+ and Glast+ AHSCs contribute differently to adult hippocampal neurogenesis. They found that Glast+ AHSCs were more proliferative and had a higher neurogenic output compared to Nestin+ AHSCs. (DeCarolis et al., 2013). This suggests that heterogeneity within the AHSC pool is required to maintain long-term neurogenesis. Single-cell transcriptomic analysis of AHSCs has thus far not provided any evidence of independent heterogeneous subtypes, but has shed light on the changes that occur during the transition from a quiescent to active state, suggesting that the molecular diversity of AHSCs is correlated with their activation state (Shin et al., 2015; Hochgerner et al., 2018; Artegiani et al., 2017). This highlights the possibility that AHSCs are differentially regulated to meet the changing demands of the hippocampal neurogenic niche.

1.2.2 Quiescent and Active AHSCs

Quiescence is defined as a reversible state of cell cycle exit, where cells exist in G0 of the cell cycle but retain the ability to re-enter the cell cycle when necessary. This is distinct from senescent and terminally differentiated cells, which apart from extreme circumstances, have irreversibly withdrawn from the cell cycle (Cheung et al., 2013). The quiescent state was first identified from the observation that cell populations proliferate at different rates, with some non-proliferative cells in somatic tissues only proliferating in response to external stimuli (Cheung et al., 2013; Baserga. 1968). Originally, this non-proliferative state was considered to be a prolonged G1 phase, however evidence of a distinct quiescent state was demonstrated in 1974, with the identification of a restriction point in G1 that determines whether a cell exits or progresses through the cell cycle (Pardee. 1974). Adult stem cells are maintained in a quiescent state to ensure the long-lasting integrity of the stem cell pool, and prevent them from accumulating environmental damage, thus ensuring that sufficient numbers of stem cells are available throughout life (Cheung et al., 2013). Whilst originally considered a passive state, recent advances in transcriptomic analyses show that quiescence is actively maintained and regulated by both extrinsic and intrinsic factors (Cheung et al., 2013).

The majority of AHSCs remain out of the cell cycle in quiescence to preserve their numbers throughout life. However, a small proportion of AHSCs are active and do express cell cycle markers such as Ki67 and MCM2 or incorporate the nucleotide analogues 5-ethynyl-2'-deoxyuridine (EdU) and BrdU (Andersen et al., 2014; Urbán et al., 2016). In the absence of a unique quiescence marker, quiescent AHSCs can be identified based on their AHSC characteristics (GFAP+ radial process with a Sox2+ nucleus residing in the SGZ of the DG) and

lack of proliferation markers (Figure 1.5). The transition from a quiescent to an active state is not only restricted to the upregulation of cell cycle genes. Activation of quiescent AHSCs is accompanied by many changes in cellular physiology, including changes in cellular metabolism (Figure 1.5) (Urbán et al., 2019). Quiescent AHSCs predominately use glycolysis and fatty acid oxidation to meet their energy demands, however upon activation cells switch to using oxidative phosphorylation (Figure 1.5) (Beckervordersandforth et al., 2017; Llorens-Bobadilla et al., 2015; Knobloch et al., 2013; Knobloch et al., 2017). Recent transcriptomic studies have also highlighted many differences between the transcriptomes of quiescent and active AHSCs and have identified genes that are enriched in quiescent AHSCs (Shin et al., 2015; Hochgerner et al., 2018; Artegiani et al., 2017). For example, the homeodomain-only protein HopX is highly expressed in quiescent AHSCs and is downregulated upon their activation making HopX a putative marker of quiescent AHSCs (Shin et al., 2015; Berg et al., 2019; Li et al., 2015). Active AHSCs are enriched for genes associated with transcription, translation, cell cycle and DNA repair, whereas quiescent AHSCs are enriched for genes involved in cell signalling, cell-cell communication and cell adherence (Figure 1.5) (Shin et al., 2015; Hochgerner et al., 2018; Artegiani et al., 2017). The enrichment in cell signalling and cell-cell communication genes suggests that quiescent AHSCs are constantly monitoring changes in the local niche microenvironment and are poised to respond to meet these demands (Shin et al., 2015; Hochgerner et al., 2018; Artegiani et al., 2017; Cheung et al., 2013). Not all the signals in the niche promote activation meaning that quiescent AHSCs receive both quiescent and activation signals alike and coordinate these to ensure the appropriate response (Section 1.3) (Urbán et al., 2019).

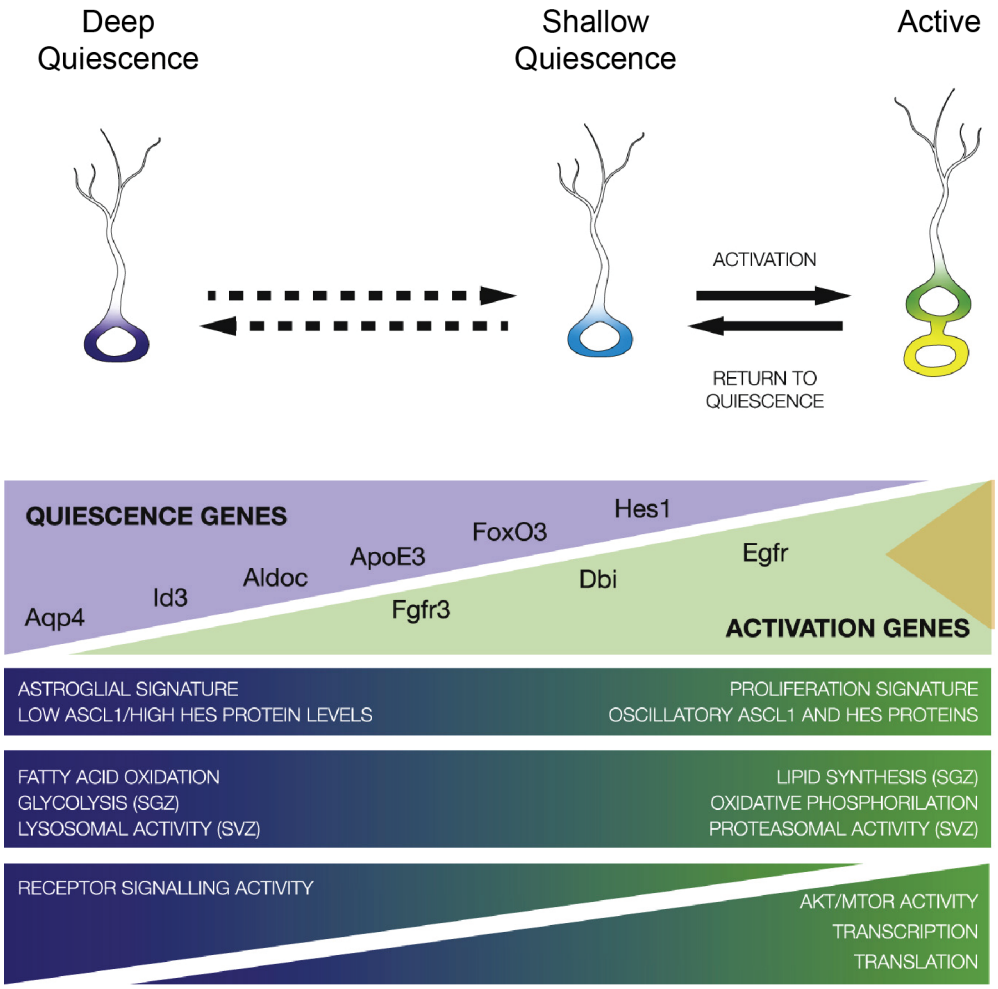


Figure 1.5: Characteristics of quiescent and active AHSCs.

Schematic of AHSC activation states and their defining characteristics. AHSCs undergo vast changes in gene expression and cellular physiology as they transition from different depths of quiescence to an active state. Image adapted from (Urbán et al., 2019) with permission from the rights holder, Elsevier.

1.2.3 AHSC Behaviours

Active AHSCs have the dual roles of renewing the AHSC population whilst also generating differentiated progenies (Urbán et al., 2019). To do this, they adopt different modes of division; symmetrical and asymmetrical divisions. Lineage tracing of AHSCs by clonal analysis and live imaging experiments have shown that most AHSCs divide asymmetrically to generate two daughter cells; another AHSC and an IPC or astrocyte (Bonaguidi et al., 2011; Pilz et al., 2018). This simultaneously allows for the renewal of the AHSC pool whilst generating a cell that can continue along the neurogenic lineage. Additionally, some AHSCs were found to divide symmetrically to either provide two daughter AHSCs (amplifying divisions) or two daughter

progenitor cells (consuming divisions) (Bonaguidi et al., 2011; Pilz et al., 2018). Long-term lineage tracing of Nestin+ AHSCs *in vivo* showed that a large proportion of clones retained an AHSC surrounded by neurons and astrocytes, highlighting the long-term ability of AHSCs to self-renew, whilst also contributing to multilineage differentiation (Bonaguidi et al., 2011). In contrast, *in vivo* live imaging showed that Ascl1+ AHSCs undergo limited rounds of symmetric and asymmetric divisions before being lost from the niche (Pilz et al., 2018). These differences could perhaps reflect the heterogeneity of the AHSC population and offer an insight into how AHSCs maintain life-long adult neurogenesis (Pilz et al., 2018; Urbán et al., 2016; Bonaguidi et al., 2011).

The rate of adult hippocampal neurogenesis declines with age and is coupled to a decrease in the number of AHSCs (Encinas et al., 2011). To explain this decline in adult neurogenesis with age, Encinas and colleagues propose a model whereby AHSCs undergo multiple rounds of asymmetric division before undergoing terminal astrocytic differentiation (Encinas et al., 2011). This “disposable stem cell” model suggests that the decline in the number of AHSCs with age is a division-coupled process linked to the production of new neurons and astrocytes (Encinas et al., 2011). This is further supported by *in vivo* live imaging experiments that showed that the self-renewal ability of AHSCs is lost upon successive divisions (Pilz et al., 2018). However, evidence from Bonaguidi and colleagues directly contradicts the “disposable stem cell” model as they show that AHSCs are maintained in the long-term by returning to a quiescent state following their symmetric or asymmetric division (Bonaguidi et al., 2011). These differences could be technical due to the use of different reporters and performing analyses at the cellular and population levels, or could be due to the heterogeneity of the AHSC population. However, these differences could also reflect a change in AHSC behaviour with time. The rate of adult neurogenesis peaks during the first postnatal weeks and is associated with a rapid rate of AHSC depletion (Kalamakis et al., 2019; Encinas et al., 2011; Harris et al., 2020) which corroborates the “disposable stem cell” model proposed by Encinas and colleagues (Encinas et al., 2011). The rate of adult neurogenesis declines with age but the depletion rate of the AHSC pool also decreases with age as they increasingly return to a quiescent state following their activation (Bonaguidi et al., 2011; Urbán et al., 2016; Ziebell et al., 2018; Harris et al., 2020). This suggests that AHSCs progressively acquire the ability to return to a quiescent state with age and could provide a mechanism whereby adult neurogenesis persists throughout life. AHSCs that return to quiescence enter a shallower state of quiescence termed “resting AHSCs” and have a higher propensity to activate (Pilz et al., 2018; Urbán et al., 2016). Inhibiting AHSCs ability to return to quiescence severely impairs AHSC proliferation and shows that resting AHSCs significantly

contribute to the pool of active AHSCs (Urbán et al., 2016; Urbán et al., 2019). Overall, these studies suggest that AHSCs display a diverse range of behaviours to maintain their longevity and to meet the demands of the changing DG niche microenvironment.

1.3 Regulation of Adult Hippocampal Stem Cell States and Adult Hippocampal Neurogenesis

Progression along the hippocampal neurogenic lineage is a tightly regulated process influenced by extrinsic, intrinsic and niche-derived factors. This tight regulation is essential to ensure the long-term maintenance of the AHSC pool, whilst also meeting the demands for the generation of newborn neurons. Each stage along the neurogenic lineage is subject to regulation including quiescent AHSC activation, progenitor proliferation and survival, neuroblast migration and the integration and survival of newborn neurons (Kempermann et al., 2015). Extrinsic or systemic factors such as physical exercise and enriched environments have been shown to stimulate adult hippocampal neurogenesis, by regulating the multiple signalling pathways present in the hippocampal niche microenvironment (Urbán et al., 2014). These signals arise from a variety of sources within the hippocampal niche microenvironment including direct cell contact and cell-cell adhesion; diffusible signals from both lineage cells and non-lineage cells including niche astrocytes and interneurons; neuronal inputs; and from the vasculature. In an added level of complexity, many of the same signals regulate different events throughout this neurogenic process. One of the challenges currently facing this field is to decipher how these regulatory signals impact the various cell types along the neurogenic lineage. In this section, I aim to briefly describe the various extrinsic, intrinsic and niche-derived factors that regulate adult hippocampal neurogenesis with a focus on what is known about the regulation of quiescent AHSC activation.

1.3.1 Extrinsic Factors Regulating AHSCs and Adult Hippocampal Neurogenesis

Adult hippocampal neurogenesis is regulated by many extrinsic factors that impact the levels of adult neurogenesis in both positive and negative manners (Aimone et al., 2014). The first example of this came from studies of mice housed in enriched environments. An enriched environment is one that provides sensory, social and motor stimulation (Aimone et al., 2014). To achieve environmental enrichment, multiple mice were housed together in an enlarged enclosure containing tunnels, running wheels and other toys to provide stimulation (Aimone et al., 2014). It was shown that mice housed within this enriched environment showed significantly

higher numbers of newborn granule neurons than littermates housed in standard conditions (Kempermann et al., 1997). This effect has been shown to act as a survival stimulus for newborn neurons rather than promoting progenitor proliferation or quiescent AHSC activation and has been shown to enhance cognition in learning and memory based behavioural tasks (Kronenberg et al., 2003). Voluntary running also enhances adult hippocampal neurogenesis but does so by promoting progenitor proliferation rather than enhancing newborn neuron survival as in enriched environments (van Praag et al., 1999; Kronenberg et al., 2003; Steiner et al., 2008). This highlights how different extrinsic factors can positively affect levels of adult neurogenesis by acting via different mechanisms. Both enriched environment and voluntary running have been shown to promote angiogenesis, which increases the levels of circulating hormones and growth factors delivered to the hippocampus (Aimone et al., 2014; Olson et al., 2006). Circulating growth factors such as Vascular Endothelial Growth Factor (VEGF) and Insulin Growth Factor (IGF) are induced through exercise and have been shown to positively influence adult hippocampal neurogenesis (Fabel et al., 2003; Trejo et al., 2001). The effects of enriched environment and voluntary running are synergistic as levels of adult hippocampal neurogenesis are further enhanced when these two extrinsic factors are combined (Fabel et al., 2009). Interestingly, exercise is able to enhance neurogenesis in the aged hippocampus of old mice more robustly than in younger mice, indicating that external stimulation could provide a therapeutic intervention for age-associated cognitive decline (Kempermann et al., 1998; Kempermann et al., 2002). Whilst these studies show a benefit of enriched environments and exercise on the levels of adult hippocampal neurogenesis, they do not directly address whether this is due to enhanced quiescent AHSC activation.

In line with the positive effects of an enriched environment, negative social interactions, such as social isolation and psychological stress, can impair adult hippocampal neurogenesis. Acute psychological stress, induced by co-habitation with an aggressor, has been shown to decrease cell proliferation in the hippocampus of tree shrews and marmosets (Gould et al., 1997; Gould et al., 1998; Lieberwirth et al., 2012). Adult neurogenesis is also impaired in rodents housed with an aggressor, however, this was due to decreased newborn neuron survival rather than decreased cell proliferation (Thomas et al., 2007). Chronic stress, caused by long-term social isolation or mild environmental stressors, also impairs adult hippocampal neurogenesis by reducing cell survival (Lu et al., 2003; Mineur et al., 2007). Stress causes the release of glucocorticoids into the bloodstream, which have been shown to suppress adult hippocampal neurogenesis by preventing the birth of newborn neurons (Gould et al., 1992; Cameron et al., 1994) and promoting the quiescence of a pool of glucocorticoid receptor-expressing neural

progenitors (Schouten et al., 2019), thus providing a possible mechanism for how stress could impair adult hippocampal neurogenesis. Stress is one of the key contributing factors in depression, which is also associated with decreased levels of adult hippocampal neurogenesis. Understanding the mechanism behind this stress-induced inhibition of adult neurogenesis, could provide insights into therapeutic targets for depressive diseases.

Many of these extrinsic environmental factors have been shown to affect adult hippocampal neurogenesis, in part by modulating elements of the hippocampal neurogenic niche (Aimone et al., 2014). Most of these effects have been shown to occur downstream of AHSCs, which could reflect the requirement to preserve AHSC pool. However, changes within the niche microenvironment, induced by external stimuli, could influence AHSC behaviour. For example, adult hippocampal neurogenesis declines with age and is associated with decreased number of AHSCs and increased AHSC quiescence (Encinas et al., 2011; Seib et al., 2013; Kempermann. 2011a). These age-associated effects are ameliorated by exposure to blood-derived factors from young mice, indicating that age-associated changes within the niche microenvironment could contribute to age-related cognitive decline (Castellano et al., 2015). By understanding how the niche microenvironment impacts on adult hippocampal neurogenesis, we can begin to identify therapies to rejuvenate adult hippocampal neurogenesis and overcome age-associated cognitive impairments.

1.3.2 Niche-Derived Signals Regulating AHSCs and Adult Hippocampal Neurogenesis

1.3.2.1 Cell Adhesion

The cells of the hippocampal neurogenic lineage occupy defined locations within the niche microenvironment, to ensure that the different cell types are exposed to the correct signals at the correct point during their development. Very little is known about the role of cell adhesion in adult hippocampal neurogenesis, however quiescent AHSCs show an enrichment for the expression of cell adhesion genes, indicating that cell adhesion and niche positioning play a role in maintaining quiescence (Shin et al., 2015; Martynoga et al., 2013; Codega et al., 2014). Increased cell adhesion has been shown to enhance tissue stiffness (reviewed by (Smith et al., 2018b)) and suggests a role for the mechanical properties of the niche in regulating AHSC behaviour. Whilst this has not been explored in the DG *in vivo*, Saha and colleagues cultured AHSCs on gels of varying stiffness to identify a critical range of mechanical properties that support AHSC self-renewal and bias cells towards a neuronal cell fate (Saha et al., 2008). Stiffer

gels instructed a glial fate choice, highlighting the importance of the mechanical properties of the tissue in regulating AHSC behaviour (Saha et al., 2008). Furthermore, Kjell and colleagues used atomic force microscopy to show that the SVZ neurogenic niche is stiffer than non-neurogenic brain regions and found that NSCs cultured on hydrogels, mimicking the stiffness of the niche (200 Pa), generated more neuroblasts than those cultured on softer gels (Kjell et al., 2020). Further work is needed to fully understand how NSCs sense mechanical changes in their surrounding niche microenvironment and how this regulates their behaviour.

The role of cell adhesion molecules in adult neurogenesis has been explored more in the V-SVZ neurogenic niche. Vascular cell adhesion molecule-1 (VCAM1) is expressed by V-SVZ NSCs and is required to maintain their correct niche location and prevent their premature activation from quiescence (Kokovay et al., 2012). In addition, SVZ NSCs express the laminin receptor $\alpha 6\beta 1$-integrin, which facilitates adherence to laminin expressing endothelial cells and maintains NSC quiescence (Shen et al., 2008). Another study showed that direct endothelial-NSC signalling via both ephrinB2 and Jagged maintained NSCs in a quiescent state (Ottone et al., 2014). This suggests that NSC quiescence is maintained by both cell adhesion and their location within the niche microenvironment. However, the close localisation of quiescent NSCs to the vasculature somewhat contradicts evidence showing that endothelial cells promote proliferation of NSCs in co-culture systems (Shen et al., 2004) suggesting that different regulatory mechanisms could be induced as a result of soluble factors or direct cell contacts.

1.3.2.2 Notch Signalling

AHSC behaviour is also regulated by direct interactions between AHSC transmembrane receptors and their corresponding cell surface signalling molecules on neighbouring cells. Of these, Notch signalling has been shown to play an important role in maintaining the pool of quiescent AHSCs (Imayoshi et al., 2011; Kageyama et al., 2008). The Notch signalling pathway is composed of four Notch receptors (Notch 1-4), which are single-pass transmembrane heterodimers, five Notch ligands (Jag1, Jag2, Dll1, Dll3 and Dll4) and the DNA-binding transcription factor RBPJk. Cell surface Notch ligands activate downstream Notch signalling in neighbouring cells by binding to their cell surface Notch receptors in a *trans* interaction. Upon ligand binding, a γ-secretase protease cleaves the Notch receptor which releases the Notch intracellular domain (NICD) from the cell membrane allowing it to translocate to the nucleus to regulate target gene transcription. The nuclear NICD binds RBPJk and recruits' coactivators to activate the expression of Notch target genes including members of the Hes transcription factor

family. Hes proteins are basic helix-loop-helix transcription factors that, in the nervous system, repress the gene expression of proneuronal transcription factors, such as Neurogenins and Ascl1, thus maintaining progenitors in an undifferentiated state (Imayoshi et al., 2011; Kageyama et al., 2008).

In the DG, Notch ligands are expressed by IPCs and are thought to provide feedback signals to maintain the quiescent state of AHSCs and prevent their activation (Lavado et al., 2014; Ables et al., 2010). Indeed, Notch signalling has been shown to be active in AHSCs as evidenced by their expression of Notch pathway components such as the Notch 1, Notch2, and Notch3 receptors, the Notch target genes Hes1 and Hes5 and by the presence of NICD (Lugert et al., 2010; Breunig et al., 2007; Ehm et al., 2010; Imayoshi et al., 2010). Ablation of IPCs leads to an increase in AHSC activation and exhaustion of the AHSC pool (Lavado et al., 2010; Hodge et al., 2008), which is similarly observed following the ablation of Notch signalling in AHSCs by deletion of the Notch1 receptor or RBPJk (Ables et al., 2010; Ehm et al., 2010; Lavado et al., 2014). This highlights an integral role for Notch signalling in maintaining AHSC quiescence by preventing their activation.

Notch signalling also plays a role in modulating dendritic morphologies as loss of Notch signalling, caused by ablation of Notch 1 receptor, resulted in less complex dendritic arborisations whereas overexpression increased dendritic complexity in newborn neurons (Breunig et al., 2007). This highlights that the role of Notch signalling is context dependent across the cells of the neurogenic lineage as it promotes AHSC quiescence but also enhances neuronal differentiation at later stages. This context dependency could arise from the differential expression of Notch receptors in AHSCs vs immature granule neurons (Shimizu et al., 2002)

1.3.2.3 Vasculature and Blood-Derived Factors

The hippocampal neurogenic niche is a highly vascularised structure and direct contact with endothelial cells has been shown to regulate NSC quiescence in the V-SVZ (Section 1.3.2.1). In the DG, proliferating progenitors are closely associated with endothelial cells (Palmer et al., 2000) and many blood-derived factors, such as IGF1 and VEGF have been shown to regulate different processes during adult hippocampal neurogenesis (Section 1.3.2.6). Indeed, changes within the DG vasculature could be key in mediating the effects external stimuli have on adult hippocampal neurogenesis. For example, DG blood volume increases following voluntary exercise, which positively correlates with increased neurogenic output (Pereira et al., 2007; Van

der Borght et al., 2009). This could be due to the increased availability of blood-derived signals delivered to the DG niche by increased angiogenesis (Clark et al., 2009; Van der Borght et al., 2009). Blood components have been shown to change with age, which could contribute to the age-related decline in adult neurogenesis (reviewed by (Smith et al., 2018a)). For example, CCL11 is a blood-derived chemokine that has been shown to be able to cross the blood brain barrier in multiple brain regions, however the exact mechanics driving this brain influx from the blood still remains unclear (Erickson et al., 2014). CCL11 blood plasma levels increase with age in both mice and humans and correlates with reduced hippocampal neurogenesis when levels are increased in young mice (Villeda et al., 2011). In heterochronic parabiosis experiments, where the blood supply of young and old mice is joined, factors from the blood of young mice promoted the proliferation of Sox2+ cells in the hippocampi of old mice; whereas factors from the blood of old mice impaired Sox2+ progenitor proliferation in young mice (Villeda et al., 2011; Castellano et al., 2015; Rebo et al., 2016). Whilst these studies show that adult neurogenesis is impaired or enhanced by factors that cross the blood brain barrier from old and young blood respectively, further work is required to identify these blood derived factors and investigate the mechanics of their influx into the brain across the blood brain barrier. Understanding more about these factors, and their mechanisms for crossing the blood brain barrier, could highlight potential therapeutic targets or strategies for ameliorating the effects of age-associated cognitive decline. It will also be interesting to see if these blood-derived factors produced their pro- or anti-neurogenic effects by regulating AHSCs quiescence and activation.

1.3.2.4 Neurotransmitters

Several neurotransmitters have been shown to influence adult hippocampal neurogenesis, which provides a mechanistic link between neuronal activity and the regulation of adult neurogenesis (reviewed by (Berg et al., 2013)). Neurotransmitters are small diffusible molecules that provide chemical communication between neurons. Glutamate is an excitatory neurotransmitter that binds to several different ionotropic receptor subtypes, N-methyl-D-aspartate (NMDA), α-Amino-3-hydroxy-5-methyl-4-isoxazolepropionic acid (AMPA), kainic acid receptors and metabotropic G-protein coupled glutamate receptors (mGluR) (Faigle et al., 2013). NMDA receptors are expressed by AHSCs and maturing granule neurons in the adult hippocampus and have been shown to mediate activity-induced neurogenesis by promoting the expression of the proneuronal transcription factor NeuroD1 (Nácher et al., 2007; Deisseroth et al., 2004). Low level stimulation of kainic acid receptors with the kainic acid agonist *in vivo*, promotes quiescent AHSC activation and depletion of the AHSC pool (Sierra et al., 2015).

However, higher kainic acid doses induce seizures *in vivo*, and promotes the integration of functional newborn neurons with aberrant morphologies in the rat hippocampus, which has long-lasting effects on hippocampal functions and the progression of epileptic disease (Jessberger et al., 2007). This highlights the importance in the correct balancing of activity levels within the hippocampus to ensure the correct progression of adult neurogenesis without developing epileptic disease.

γ-aminobutyric acid (GABA) is the main inhibitory neurotransmitter in the adult brain and plays a key role during the synaptic integration of newborn granule neurons (Ge et al., 2006). Newborn granule neurons are tonically activated by GABA before being innervated by GABA- and glutamate-mediated synaptic inputs (Ge et al., 2006). As well as playing a role at the later stages of adult hippocampal neurogenesis, GABA signalling also plays a role in regulating AHSC quiescence due to their expression of $GABA_B$ receptors (Song et al., 2012; Giachino et al., 2014). Tonic GABA release from parvalbumin-expressing interneurons acts directly on AHSCs to maintain their quiescent state in response to neuronal activity (Song et al., 2012). This is further supported by evidence from Giachino and colleagues showing that genetic deletion of $GABA_B$ receptors in AHSCs, promotes their proliferation and differentiation *in vivo* (Giachino et al., 2014). This highlights a direct role for GABA signalling in the regulation of AHSC activity. AHSCs themselves can directly regulate their own response to GABA signalling by the cell autonomous production of diazepam binding inhibitor (DBI), which inhibits GABA activity to maintain proliferation (Dumitru et al., 2017). The levels of GABA within the hippocampal niche can also be regulated by glutamatergic projections from hilar mossy cells, which stimulate GABA release from parvalbumin-expressing interneurons when moderately activated to maintain AHSC quiescence (Yeh et al., 2018). Interestingly, when highly stimulated, mossy cells can promote the activation of quiescent AHSCs by releasing glutamate directly onto AHSCs (Yeh et al., 2018).

1.3.2.5 BMP Signalling

Bone Morphogenetic Protein (BMP) signalling has been shown to play an integral role in regulating AHSC quiescence. More than 20 BMP ligands have been identified in vertebrates and these form a subgroup of the Transforming Growth Factor β (TGFβ) superfamily (Bragdon et al., 2011). They signal by binding to the BMP serine-threonine kinase receptor complex, which is divided into two subgroups; the BMP type I receptors BMPRIA, BMPRIB and Activin receptor type 1 A (ACVR1); and the BMP type II receptor BMPRII, which heterodimerise upon ligand

binding (Dijke et al., 1996; Heldin et al., 1997). Downstream signalling is divided into SMAD-dependent (canonical) and SMAD-independent (non-canonical) pathways. In canonical BMP signalling, activation of type I receptors results in the phosphorylation of the DNA binding proteins SMAD1/5/8, which in turn form a stable heterodimer with SMAD4 (Choe et al., 2015). This heterodimer then translocates to the nucleus and, together with other co-factors, activates the transcription of BMP target genes (Choe et al., 2015). Secreted BMP ligands often bind to the extracellular matrix meaning they act as short-range morphogens (Hall et al., 2004).

In the adult DG, BMPs are secreted by granule neurons and the AHSCs themselves (Yousef et al., 2015). In addition, several BMP inhibitors, including Noggin and Chordin are also present within the niche microenvironment (Scott et al., 2000; Fan et al., 2003; Bonaguidi et al., 2005; Bonaguidi et al., 2008). BMP signalling has been shown to act differentially at two stages along the hippocampal neurogenic lineage depending on the expression of the BMP receptor subtypes. Nestin+/GFAP+ AHSCs express the BMPRIA receptor and its loss leads to an overactivation of AHSCs, resulting in their depletion from the niche (Mira et al., 2010). This suggests that BMP signalling plays a role in promoting AHSC quiescence (Mira et al., 2010). This is further supported by data showing that the BMP antagonist Noggin promotes NSC proliferation (Bonaguidi et al., 2008). In NSC cultures, BMPs have been shown to induce a quiescent state when combined with Fibroblast Growth Factor 2 (FGF2), thus providing a useful tool for investigating the molecular mechanisms that regulate NSC behaviour (Mira et al., 2010; Martynoga et al., 2013; Sun et al., 2011; Blomfield et al., 2019). It has also been shown to promote the expression of astrocytic genes *in vitro*, suggesting BMP signalling could play a role in maintaining the astrocytic characteristics of AHSCs (Sun et al., 2011). BMP signalling also plays a role in regulating the differentiation and maturation of granule neurons (Bond et al., 2014). Granule neurons express BMPRIB and stimulating BMP signalling suppresses their differentiation and maturation (Bond et al., 2014; Mira et al., 2010). BMP signalling may also play a role in mediating how external stimuli regulate adult hippocampal neurogenesis. For example, levels of the BMP inhibitor Noggin are increased following voluntary running, which inhibits BMP signalling and enhances neurogenesis (Gobeske et al., 2009). In addition, levels of BMP signalling increase with age, which may contribute to the age-associated decline in adult hippocampal neurogenesis by preventing progenitor proliferation (Yousef et al., 2015). This could mean that BMP signalling may provide a promising therapeutic target for promoting adult hippocampal neurogenesis and preventing its age-associated decline.

1.3.2.6 Growth Factors and Neurotrophic Factors

Growth factors comprise a large group of extracellular proteins that regulate cell proliferation and maintenance (Faigle et al., 2013). Fibroblast Growth Factor-2 (FGF2), Insulin Growth Factor-1 (IGF1) and Vascular Endothelial Growth Factor (VEGF) have all been shown to play a role in regulating adult hippocampal neurogenesis (Faigle et al., 2013). These growth factors share common downstream signalling pathways, including the Phosphoinositide 3-kinase (PI3k)/Akt and the Ras/Raf/MEK/Erk pathways, which are activated by the binding of each growth factor to its' respective cell surface receptor. FGF receptor 1 (FGFR1) is expressed by GFAP+ AHSCs suggesting a role for FGF signalling in regulating AHSC behaviour (Choubey et al., 2017). Indeed, over-expression of FGF2 has been shown to promote DG neurogenesis (Rai et al., 2007) and loss of FGFR1 in Nestin+ progenitors impairs proliferation and newborn neuron production (Zhao et al., 2007). In addition, levels of FGF signalling decline in the DG with age and neurogenic output is improved by an infusion of FGF2 (Kang et al., 2015; Jin et al., 2003). In *in vitro* cultures, FGF2 acts as a mitogen to promote the self-renewal of progenitors derived from the DG (Gage et al., 1995). Overall, these data suggest a role for FGF2 signalling in promoting adult hippocampal neurogenesis, however more work is needed to delineate the stages along the neurogenic lineage that are directly regulated by FGF2 signalling.

IGF signalling has been shown to promote proliferation and neuronal differentiation in the DG and the upregulation of blood-derived IGF1 following exercise has been shown to mediate the positive effects of physical exercise on adult hippocampal neurogenesis (Bracko et al., 2012; Trejo et al., 2008; Llorens-Martín et al., 2010). Infusion of IGF1 in adult rats promotes progenitor proliferation and enhances neurogenic output in the DG (Åberg et al., 2003). It has also been shown to ameliorate age-related decline in adult hippocampal neurogenesis (Lichtenwalner et al., 2001). In addition, IGF2 has been shown to directly stimulate proliferation in cultured DG neural progenitors by activating the Akt signalling pathway (Bracko et al., 2012). This positive effect of IGF signalling on progenitor proliferation could be due to the Akt dependent inactivation of the FoxO3 transcription factor, which is expressed by AHSCs to maintain their quiescent state (Calnan et al., 2008; Paik et al., 2009; Renault et al., 2009). Whilst these studies show a positive effect of IGF signalling on adult hippocampal neurogenesis, more work is needed to identify how AHSCs are directly affected by this signalling pathway.

VEGF is a blood derived factor that is also secreted by endothelial cells and has been shown to have pro-proliferative effects in DG progenitor cultures, which is mediated by VEGF receptor 2

(Flk-1) activation (Jin et al., 2002; Schänzer et al., 2004). VEGF has two high-affinity receptor tyrosine kinases, VEGF receptor 1 (Flt-1) and VEGF receptor 2 (Flk-1) which are expressed by both endothelial cells and DG neural progenitors (Yang et al., 2003; Palmer et al., 2000; Maurer et al., 2003). VEGF is also expressed by hippocampal neural precursors suggesting the possibility of an autocrine signalling loop (Maurer et al., 2003). As VEGF is also angiogenic, its' expression by hippocampal precursors could suggest that hippocampal precursors play a role in remodelling the niche vasculature to accommodate local demands (Maurer et al., 2003). Indeed, the density of blood vessels increases in the DG after voluntary running which could be to meet the demands of activity-enhanced adult hippocampal neurogenesis (Clark et al., 2009; Van der Borght et al., 2009). Peripheral VEGF has also been shown to mediate the pro-neurogenic effects of exercise indicating that VEGF signalling directly regulates activity-induced adult neurogenesis as well as promoting angiogenesis (Fabel et al., 2003).

Neurotrophic factors are extracellular signalling proteins that play diverse roles in both the developing and adult central nervous system (CNS) (Lu et al., 2005). Four neurotrophins have been identified in the adult mammalian brain; nerve growth factor (NGF), brain-derived neurotrophic factor (BDNF), neurotrophin 3 (NT3) and neurotrophin4 (NT4). Neurotrophins act by binding the tyrosine kinase receptors known as Trk and their co-receptor p75 neurotrophin receptor ($p75^{NTR}$). There are three Trk receptors, TrkA, TrkB and TrkC, which each selectively bind a different neurotrophin (Faigle et al., 2013). Ligand binding promotes the dimerization and autophosphorylation of Trk receptors resulting in the transduction of various downstream signalling cascades (Miller et al., 2001; Lee et al., 2001). The TrkB receptor, which preferentially binds BNDF and NT4, and the $p75^{NTR}$ co-receptor are expressed by quiescent neural precursors and maturing granule neurons in the adult DG (Donovan et al., 2008; Li et al., 2008). Out of all the neurotrophins, BDNF has been the most studied in the context of adult hippocampal neurogenesis. Chronic infusion of BDNF directly into the adult DG promotes adult neurogenesis by acting as a survival and maturation factor for newborn granule neurons (Scharfman et al., 2005). The impairment of newborn neuron maturation following deletion of the TrkB receptor in Glast+ progenitors, further supports a role for BDNF signalling in enhancing the survival and maturation of newborn neurons (Bergami et al., 2008). BDNF was also shown to be important in promoting the proliferation of Nestin+ progenitors, as conditional deletion of the TrkB receptor reduced proliferation *in vitro* and proliferation and neurogenesis *in vivo* (Li et al., 2008). In addition, BDNF signalling has been shown to play a role in mediating the pro-neurogenic effects of environmental enrichment, as BDNF knock-out mice did not display enhanced neurogenesis after being housed within an enriched environment (Rossi et al., 2006).

1.3.2.7 Shh Signalling

Sonic hedgehog (Shh) is a soluble extracellular signalling protein that mediates signalling by binding to its cell surface receptor Patched and G-protein coupled co-receptor Smoothened, which are located on the primary cilium. Upon ligand binding, Patched-mediated inhibition of Smoothened is released and Smoothened activates the expression of Gli zinc-finger transcription factors, which have both activating (Gli1) and repressive forms (Gli2, Gli3) (Rohatgi et al., 2007; Philipp et al., 2009). Shh ligands in the DG have been shown to originate from distant entorhinal cortical neurons and local hilar mossy cells and both AHSCs and astrocytes have been shown to respond to Shh signalling (Gonzalez-Reyes et al., 2019; Traiffort et al., 1999; Ahn et al., 2005; Garcia et al., 2010). Pharmacological inhibition of Shh signalling, by cyclopamine treatment, reduces hippocampal progenitor proliferation *in vivo* and postnatal progenitors fail to develop following Smoothened deletion in Nestin+ and GFAP+ precursors (Lai et al., 2003; Han et al., 2008b). This suggests that Shh signalling plays a role in maintaining neural precursors and promoting their proliferation. This is further supported by data showing that progenitor proliferation is decreased upon loss of the primary cilium in neural progenitors but no effect was reported in the quiescent AHSC population (Breunig et al., 2008). Stimulating the levels of Shh signalling has been shown to promote progenitor proliferation *in vitro* (Lai et al., 2003), however the direct effect of Shh signalling on quiescent AHSC activation is still under debate.

1.3.2.8 Wnt Signalling

Wnt signalling has been shown to promote progenitor proliferation and neuronal differentiation. The full role of Wnt signalling during adult hippocampal neurogenesis will be explored in detail in Section 1.5.3.

1.3.3 Intrinsic Mechanisms Regulating AHSC Activation States

As stated above, quiescence is a highly regulated state and requires the controlled expression of many genes to balance quiescence maintenance vs activation. To maintain this balance many extrinsic and niche derived signals modulate AHSC behaviour via intrinsic factors that mediate

their effects. In this section, I will outline how some of the known intrinsic factors regulate AHSC activity and behaviour (Figure 1.6).

Ascl1 (Achaete-scute like 1; Mash1) is a basic helix-loop-helix (bHLH) proneuronal transcription factor that is expressed at the protein level in proliferating progenitors and active AHSCs (Pleasure et al., 2000; Kim et al., 2007; Blomfield et al., 2019; Andersen et al., 2014). The Ascl1 bHLH domain facilitates the binding to DNA at specific E-box hexanucleotide sequences as well as enabling the heterodimerisation to E-protein binding partners to promote stability and expression of target genes (Bertrand et al., 2002; Imayoshi et al., 2014). Ascl1 is essential for AHSC activation and neuronal differentiation *in vivo* as genetic ablation of Ascl1 prevents quiescent AHSC activation and blocks adult hippocampal neurogenesis, even in response to a neurogenic stimulus (Andersen et al., 2014). This dramatic phenotype in Ascl1-deficient mice suggests that Ascl1 is a key player in regulating the initiation of neuronal differentiation and promoting quiescent AHSC activation (Figure 1.6). Indeed, downstream targets of Ascl1 include cell cycle regulators such as *CyclinD1*, indicating that it promotes proliferation by directly activating the expression of cell cycle genes (Figure 1.6) (Andersen et al., 2014). Several niche derived signals converge on regulating the levels Ascl1 highlighting the integral nature of this transcription factor in co-ordinating multiple signals from extrinsic sources (Andersen et al., 2014; Imayoshi et al., 2010; Urbán et al., 2016; Blomfield et al., 2019). For example, Notch and BMP signalling regulate *Ascl1* via the expression of Hes and Inhibitor of differentiation (Id) proteins respectively (Figure 1.6). Notch signalling has been shown to maintain AHSC quiescence by downregulating *Ascl1* transcription via its target genes, Hes1 and Hes5 (Sueda et al., 2019). Stable, high levels of Hes1 and Hes5 have been shown to downregulate *Ascl1* transcription, however lower oscillating levels of Hes proteins promote out of phase oscillations of *Ascl1*, which induces AHSC proliferation (Sueda et al., 2019). This switch between oscillating and stably high Hes protein expression patterns is in part regulated by the direct interaction between Hes and Id proteins. This interaction blocks the auto-repressive activity of Hes proteins resulting in their stable expression and repression of their target genes such as *Ascl1* (Sueda et al., 2019; Bai et al., 2007; Boareto et al., 2017). However, Hes proteins do not fully repress *Ascl1* transcription as *Ascl1* mRNA was found to be expressed in the majority of quiescent AHSCs *in vivo* (Blomfield et al., 2019). Id4 is upregulated in quiescent AHSCs (Blomfield et al., 2019) and has been shown to inhibit the interactions between other Id proteins (Id1-3) and their binding partners (Patel et al., 2015; Sharma et al., 2015). Therefore, upregulation of Id4 in quiescent AHSCs could maintain *Ascl1* transcription by blocking the stabilisation of Hes proteins and their subsequent repression of target genes such as *Ascl1*

(Blomfield et al., 2019). Id4 also plays a role in regulating the elimination of Ascl1 protein in quiescent AHSCs (Blomfield et al., 2019). Whilst *Ascl1* mRNA is expressed in quiescent AHSCs, Ascl1 protein is absent from these cells (Blomfield et al., 2019). The high levels of Id4, induced by BMP signalling in quiescent AHSCs, sequesters the E-protein binding partners of Ascl1, which are required to maintain Ascl1 stability (Blomfield et al., 2019). This means that Ascl1 is destabilised and rapidly degraded in quiescent AHSCs thus preventing their premature activation (Blomfield et al., 2019). Ascl1 is also regulated at the protein level by the HECT domain E3 ubiquitin ligase Huwe1, which targets Ascl1 for proteasomal degradation in active AHSCs (Urbán et al., 2016). The loss of Ascl1 protein in active AHSCs promotes the downregulation of Ascl1 pro-proliferative target genes, thus allowing AHSCs to return to a resting state of quiescence (Urbán et al., 2016). Overall, the multiple levels of Ascl1 regulation highlight the importance of this transcription factor in regulating AHSC activation states.

TLX is an orphan nuclear receptor encoded by the *Nr2e1* gene and is required to maintain the pro-proliferative and undifferentiated state of AHSCs (Qu et al., 2010; Zhang et al., 2008; Shi et al., 2004). Indeed, TLX deletion impairs proliferation and TLX overexpression is sufficient to enhance neurogenesis and cognition (Shi et al., 2004; Murai et al., 2014). The pro-proliferative effects of TLX have been shown to work via activation of the canonical Wnt signalling pathway (Qu et al., 2010). TLX promotes the expression of Wnt7a, which works in an autocrine/paracrine manner to stimulate the proliferation of cultured NSCs by directly activating the expression of the canonical Wnt target gene and cell cycle regulator *CyclinD1* (Qu et al., 2010). Other TLX target genes include the cell cycle inhibitors *p21* and *PTEN*, which are repressed by the TLX dependent recruitment of histone deacetylases (HDACs), to promote proliferation (Sun et al., 2007). TLX has also been shown to promote neuronal lineage commitment over glial differentiation by directly activating *Ascl1* expression, while simultaneously repressing astrocytic genes such as *GFAP* (Elmi et al., 2010). Despite its integral role in promoting progenitor proliferation and neuronal lineage commitment, very little is known about how TLX is regulated. MicroRNA-9 suppresses *TLX* expression to negatively regulate cell proliferation in favour of neuronal differentiation (Zhao et al., 2009). In addition, TLX represses microRNA-9 expression, thus forming a negative feedback loop to balance cell proliferation vs neuronal differentiation. (Zhao et al., 2009). TLX expression levels are also regulated by extrinsic factors such as inflammation, which negatively regulates adult hippocampal neurogenesis and contributes to neuropathologies such as depression and Alzheimer's disease (Koo et al., 2008; Ekdahl et al., 2003; Loftis et al., 2010; Wyss-Coray et al., 2012). Interleukin-1β (IL-1β), the most abundant

pro-inflammatory cytokine in the brain, has been shown to impair progenitor proliferation by repressing the expression of TLX (Ryan et al., 2013).

PTEN is a negative regulator of PI3k-Akt signalling and a potent tumour suppressor gene that has been shown to be essential for maintaining AHSC quiescence (Figure 1.6) and preserving the AHSC pool, as loss of PTEN results in AHSC depletion via their increased activation and differentiation (Bonaguidi et al., 2011). PTEN prevents cell cycle progression by preventing G0-G1 cell cycle entry, therefore loss of PTEN promotes proliferation by allowing cells in G0 to progress to G1 (Groszer et al., 2006). Additionally, loss of PTEN has also been shown to elevate cellular levels of the activated form of β-catenin (Persad et al., 2016). This could provide another mechanism for PTEN maintaining quiescence by preventing the activation of the canonical Wnt signalling pathway (Persad et al., 2016). In quiescent AHSCs, PTEN inhibits Akt signalling, which in turn releases the Akt dependent repression of the forkhead transcription factor **FoxO3**. FoxO3 is required for the maintenance of quiescence and the long-term maintenance of the AHSC pool, as loss of FoxO3 results in AHSC depletion (Paik et al., 2009; Renault et al., 2009). Interestingly, Chromatin immunoprecipitation sequencing (ChIP-Seq) analysis shows that FoxO3 shares many of the same target genes as Ascl1 (Webb et al., 2013). This suggests that FoxO3 may directly compete with Ascl1 for DNA binding sites and promote AHSC quiescence by suppressing the expression of Ascl1 target genes (Figure 1.6). Additionally, FoxO3 has been shown to directly activate the expression of the Wnt inhibitors sFRP1/2 (Paik et al., 2009), indicating that FoxO3 could maintain stem cell quiescence by inhibiting the canonical Wnt pathway, which has been reported to promote proliferation (Lie et al., 2005). Other target genes of FoxO3 include genes associated with glycolysis, which is the preferred metabolic pathway of quiescent AHSCs (Paik et al., 2009; Renault et al., 2009; Beckervordersandforth et al., 2017; Knobloch et al., 2013; Llorens-Bobadilla et al., 2015; Knobloch et al., 2017). Overall this suggests that FoxO3 regulates many cellular responses to maintain quiescence and prevent the loss of the NSC pool.

Regulation of **cellular metabolism** has been shown to play a role in regulating the activation state of NSCs. As stated previously in Section 1.2.2, quiescent AHSCs favour glycolysis and fatty acid oxidation and switch to oxidative phosphorylation once activated (Beckervordersandforth et al., 2017; Llorens-Bobadilla et al., 2015; Knobloch et al., 2013; Knobloch et al., 2017). Interestingly, inhibiting fatty acid oxidation in quiescent NSCs, by manipulating the levels of malonyl-CoA (the metabolite that regulates fatty acid oxidation levels), induced quiescence exit and enhanced proliferation (Knobloch et al., 2017). This suggests that

the metabolic state of NSCs is not just a passive consequence of their activation state, but also plays an integral role in regulating NSC quiescence and activation.

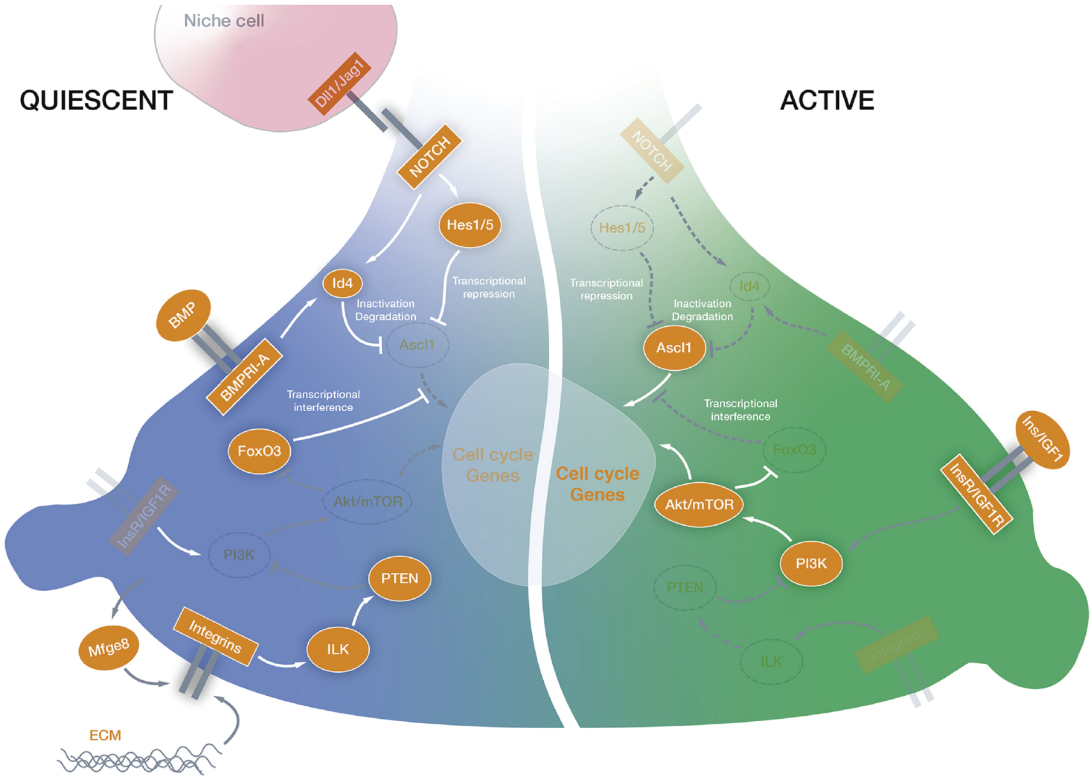


Figure 1.6: Intrinsic mechanisms regulating quiescent and active AHSCs.
Schematic highlighting some of the intrinsic mechanisms that regulate the activation states of AHSCs in response to extracellular stimuli. Image reproduced from (Urbán et al., 2019) with permission from the rights holder, Elsevier.

1.4 Wnt Signalling

The Wnt signalling pathway is a key regulator of both embryonic development and adult tissue homeostasis and mutations in this pathway can result in birth defects, cancer and other diseases (Logan et al., 2004; Clevers. 2006). The first member of the Wnt family *Wnt1* (or *Int1*) was identified in 1982 as an integration site for the mouse mammary tumour virus in virally induced breast cancers (Nusse et al., 1982). The *Wnt1* proto-oncogene encodes a secreted cysteine rich domain (CRD) protein, which was shown to be a homologue of the *Drosophila Wingless* (*Wg*) gene that controls segment polarity during larval development (Nüsslein-Volhard et al., 1980; Rijsewijk et al., 1987). Epistasis experiments investigating the relationships between segment polarity mutations in *Drosophila* facilitated the delineation of the core components of this signal transduction cascade (Noordermeer et al., 1994; Peifer et al., 1994b; Siegfried et al.,

1992). The injection of mouse *Wnt1* mRNA into early *Xenopus* embryos induced the duplication of the body axis and highlighted that Wnt signalling is shared between vertebrates and invertebrates, whilst also provided an assay to study the Wnt pathway in vertebrates (McMahon et al., 1989). The combined work in *Drosophila* and *Xenopus* identified a highly conserved signalling pathway that is activated by secreted Wnt proteins and has since been directly linked to human disease (Clevers. 2006; Clevers et al., 2012). Three separate pathways are currently known to be activated in response to Wnt receptor activation: the canonical/β-catenin dependent Wnt signalling pathway, and the non-canonical/β-catenin independent Wnt/PCP and Wnt/Ca^{2+} pathways. In the following sections I will briefly explain these three signal transduction cascades from the production of Wnt ligands through to their reception and transduction.

1.4.1 Production of Wnt Ligands

There are 19 Wnt ligands encoded within the human and mouse genomes, which introduces a level of complexity to the signalling cascade (Clevers et al., 2012). Wnt ligands are approximately 40kDa in size and contain many conserved cysteines (Tanaka et al., 2002). The first purification of the Wnt3a ligand highlighted that Wnt proteins are lipid modified by the attachment of a mono-unsaturated fatty acid (palmitoleic acid) to conserved serine and cysteine residues (Willert et al., 2003; Takada et al., 2006; Rios-Esteves et al., 2014; Rios-Esteves et al., 2013). This lipid modification is mediated by Porcupine (Porc), which is a multi-pass transmembrane O-acyltransferase located in the endoplasmic reticulum, active only in Wnt producing cells, and is essential for Wnt secretion (Figure 1.7) (Hofmann. 2000; Kadowaki et al., 1996; Rios-Esteves et al., 2013). The seven-transmembrane protein Wntless/Evi (Wls) is located to the Golgi network, endosomes and plasma membranes where it binds to the lipidated Wnt ligand to transfer it from the Golgi to the plasma membrane for secretion (Figure 1.7) (Bartscherer et al., 2006; Bänziger et al., 2006; Yu et al., 2014; Herr et al., 2012; Najdi et al., 2012). The lipid modification renders Wnt ligands insoluble which raises questions on how a Wnt morphogen gradient is established and how Wnt signals reach their target cells (Clevers et al., 2012; Nusse et al., 2017). Wnt ligands have been shown to be membrane tethered indicating that cell-cell contact is required to activate the Wnt signalling cascade (Alexandre et al., 2014). This would suggest that Wnt signalling occurs at close-range between neighbouring cells, which contradicts the assumption that Wnt ligands are long-range morphogens. However, there is evidence indicating that Wnt ligands are presented on the outside of secretory vesicles and exosomes making it available for receptor binding over longer distances (Figure 1.7) (Gross et

al., 2012; Korkut et al., 2009; McGough et al., 2016). Despite the recent advances in the field, there is still some way to go before the range of Wnt signalling is resolved.

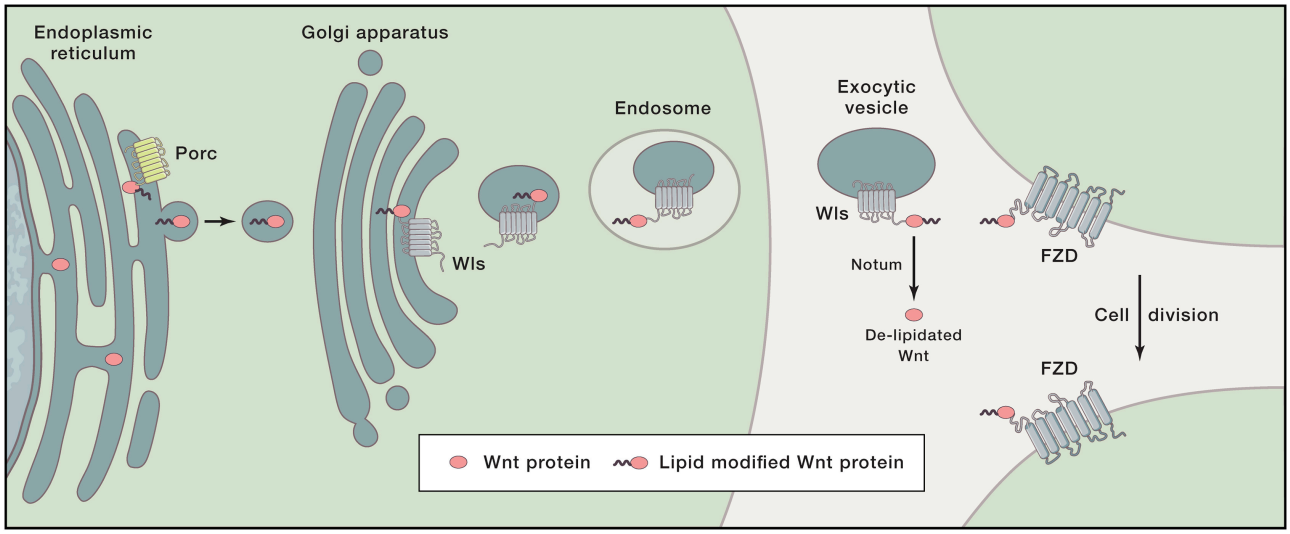


Figure 1.7: Schematic of Wnt secretion from the cell.

Wnt ligands are lipid modified by the O-acyltransferase Porcupine (Porc) in the endoplasmic reticulum. Transport of Wnt ligands is facilitated by Wntless (Wls) in endosomes and Wnts are secreted on exocytic vesicles or are tethered to the membrane. Notum is a Wnt inhibitor that de-acylates the Wnt ligand rendering it inactive. Wnt ligands bind to their Frizzled (Fzd) cell surface receptors, on recipient cells to activate the Wnt signalling cascade. Image adapted from (Nusse et al., 2017) with permission from the rights holder, Elsevier.

1.4.2 Wnt Cell Surface Receptors

On the cell surface of recipient cells, Wnt ligands bind to a heterodimeric receptor complex comprised of a Frizzled (Fzd) and LDL-Receptor-related Protein 5/6 (LRP5/6) (Figure 1.8) (Nusse et al., 2017). There are 10 mammalian Fzd proteins and these provide the primary platform for Wnt ligand binding (Dann et al., 2001; Janda et al., 2012). Fzd receptors are seven-transmembrane-domain receptors that contain a large N-terminal CRD (Bhanot et al., 1996). The CRD domain primarily forms the interaction with Wnt ligands due to the presence of a hydrophobic pocket that binds to the lipid modification on the Wnt ligand (Figure 1.7) (Janda et al., 2012). During Wnt ligand binding, Fzds co-operate with the single-pass transmembrane molecule LRP5/6 resulting in the heterodimerisation between the Fzd and LRP5/6 proteins (Figure 1.8) (Janda et al., 2017). This heterodimerisation leads to a conformational change in the receptors resulting in the phosphorylation of the cytoplasmic tail of LRP5/6 by multiple kinases, which initiates downstream Wnt signalling by recruiting the scaffold protein Axin (Figure

1.8) (Stamos et al., 2014). LRP5/6 phosphorylation is mediated in part by glycogen synthase kinase 3 β (GSK3β), which phosphorylates LRP5/6 on a serine located within a PPPSP motif (Stamos et al., 2014). This same motif is found in other GSK3β phosphorylation targets including β-catenin, Axin and APC (Zeng et al., 2005). LRP5/6 is also phosphorylated by the membrane tethered Casein Kinase 1γ (CK1γ), which phosphorylates LRP5/6 on serine/threonine residues located next to the PPPSP motifs (Davidson et al., 2005). Less information is known about the role of Fzds in Wnt reception. The Fzd cytoplasmic domain binds to Dishevelled (Dvl), which recruits Axin and forms a platform for the LRP5/6-Axin interaction to take place (Figure 1.8) (Tauriello et al., 2012). Axin and Dvl both contain DIX domains which polymerise in a head-to-tail fashion to facilitate the interaction between Axin and Dvl and encourage the formation of the Fzd-LRP5/6 heterodimer (Schwarz-Romond et al., 2007; Fiedler et al., 2011). The Wnt-Fzd interaction is promiscuous in that a single Wnt ligand can bind multiple Fzd receptors and vice versa, however there is some evidence suggesting that Wnt ligands have higher binding affinities for some Fzd receptors than others (Agostino et al., 2019; Agostino et al., 2017). In addition, it is not clear whether specific Wnt-Fzd bindings selectively activate the canonical or non-canonical Wnt signalling pathways. For example, Wnt8, Wnt3 and Wnt3a seem to preferentially activate canonical Wnt signalling, whereas Wnt5a favours the non-canonical pathways and Wnt11 and Wnt7a/b can activate both (Tao et al., 2005; Cadigan et al., 2006). Fzds similarly appear able to activate both canonical and non-canonical pathways (reviewed by (Cadigan et al., 2006)) indicating that the specific Wnt-Fzd combinations are not solely responsible for instructing the activation of a particular downstream Wnt signalling cascade (Komiya et al., 2008). It has been suggested that Wnt pathway specificity is determined by the availability of the Wnt co-receptors, as LRP5/6 is only implicated in transducing the canonical Wnt pathway (He et al., 2004).

1.4.3 Natural Wnt Agonists and Antagonists

The level of canonical Wnt signalling induced by Wnt ligand/receptor binding, is further regulated by the presence of natural Wnt agonists and antagonists. R-spondins (Rspo) are small secreted proteins containing two N-terminal furin domains and a thrombospondin domain (Kazanskaya et al., 2004). There are four Rspo proteins encoded in the vertebrate genome and were first found to enhance canonical Wnt signalling in *Xenopus* (Kazanskaya et al., 2004). Subsequently Rpso1 was shown to promote canonical Wnt dependent proliferation of intestinal crypt cells *in vivo* and *in vitro* (Kim et al., 2005; Sato et al., 2009). Rspo's bind to members of the seven-transmembrane leucine-rich repeat-containing G-protein coupled receptor (LGR) family and this

binding has been shown to enhance low level Wnt signalling (Carmon et al., 2011; de Lau et al., 2011; Glinka et al., 2011). The LGR family have been shown to mark adult stem cells of various adult tissues, such as the intestines and skin, and regulate these stem cell pools by maintaining Rspo receptor expression (Barker et al., 2007; de Lau et al., 2011; Yan et al., 2017; Füllgrabe et al., 2015; Snippert et al., 2010). The Rspo-LGR interaction has been shown to enhance Wnt signalling by reversing the Rnf43/Znrf3 E3 ligase mediated clearance of Wnt receptors in the plasma membrane (Hao et al., 2012). Rspo binds to LGR via one of its furin repeats which, facilitates the binding of Rspo to Rnf43/Znrf3 via its second furin repeat and promotes membrane clearance of the Rnf43/Znrf3 E3 ligases. This in turn results in the persistence of activated Wnt-Fzd-LRP5/6 receptor complexes at the plasma membrane thus enhancing Wnt signalling (de Lau et al., 2014).

Rnf43 and Znrf3 are single-pass transmembrane RING-type E3 ligases that are direct transcriptional targets of Wnt signalling (Koo et al., 2012; Hao et al., 2012). Rnf43 and Znrf3 mediate the multi-ubiquitination of lysines in Fzd cytoplasmic loops, thus inducing Fzd endocytosis and lysosomal degradation and downregulation of Wnt signalling levels (Koo et al., 2012; Hao et al., 2012). Therefore, Rnf43/Znrf3 act in a negative feedback loop to regulate the levels of Wnt signalling in cells (Koo et al., 2012; Hao et al., 2012).

Wnt signalling levels are also regulated by extracellular proteins that antagonise the Wnt-Fzd-LRP5/6 binding. For example, the Dickkopf (Dkk) family of secreted glycoproteins specifically inhibit the canonical Wnt pathway by binding the LRP5/6 co-receptors and preventing the formation of the Fzd-LRP5/6 heterodimer (Glinka et al., 1998; Ellwanger et al., 2008; Semënov et al., 2008). Similarly, WISE/SOST proteins also inhibit canonical Wnt signalling by binding to LRP5/6 and disrupting Fzd-LRP5/6 complexes (Semënov et al., 2005). Other Wnt antagonists include the secreted-frizzled related proteins (sFRPs) that sequester extracellular Wnt ligands away from their Fzd cell surface receptors thus preventing receptor activation of Wnt signalling (reviewed by (Bovolenta et al., 2008)). The sFRPs comprise the largest family of Wnt inhibitors with five family members identified in humans (Bovolenta et al., 2008). sFRPs contain a CRD similar to the one found in Fzd receptors and it is via this CRD that sFRPs bind to extracellular Wnt ligands and inhibit Wnt signalling (Bovolenta et al., 2008). Wnt-Inhibitory protein (WIF) also directly binds to extracellular Wnt ligands sequestering them away from their Fzd cell surface receptors, however the mechanism behind this binding is not yet understood (Hsieh et al., 1999; Cruciat et al., 2013). A more recently discovered Wnt inhibitor is Notum, which is a carboxylesterase enzyme that removes the palmitoleate lipid modification on Wnt ligands,

rendering it unable to bind to its Fzd cell surface receptor (Kakugawa et al., 2015; Zhang et al., 2015) (Figure 1.7). Altogether, the plethora of extracellular Wnt inhibitors provide different mechanisms for antagonising ligand receptor binding and allow the fine-tuning of Wnt signalling levels.

1.4.4 Canonical β-catenin Dependent Wnt Signalling Pathway

The canonical Wnt signalling pathway relies on the stabilisation and nuclear translocation of β-catenin to activate a Wnt dependent transcriptional profile. In the absence of Wnt-Fzd-LRP5/6 binding, cytoplasmic β-catenin is degraded by the β-catenin destruction complex, which consists of Axin, adenomatous polyposis coli (APC), Protein phosphatase 2A (PP2A), the E3 ubiquitin ligase β-TrCP, CK1γ and GSK3β (Figure 1.8) (Nusse et al., 2017). Within this complex, Axin acts as a scaffolding protein and interacts with all other members of the destruction complex and β-catenin (Figure 1.8) (Ikeda et al., 1998; Sakanaka et al., 1998). APC is a large protein that interacts with both Axin and β-catenin via interspersed Axin/β-catenin binding sites (Rubinfeld et al., 1993; Behrens et al., 1998). Whilst its exact function remains unresolved, APC is an integral member of the destruction complex and its deletion results in over-activation of canonical Wnt signalling and cancer (reviewed by (Kwong et al., 2009)). In the absence of a Wnt signal, CK1γ and GSK3β of the destruction complex, sequentially phosphorylate Axin bound β-catenin at its N-terminus. β-catenin is first phosphorylated by CK1γ at Ser45 followed by GSK3β mediated phosphorylation of Thr41, Ser37 and Ser33 (Liu et al., 2002; Yanagawa et al., 2002; Amit et al., 2002). These phosphorylated motifs provide a docking site for the E3 ubiquitin ligase β-TrCP that mediates β-catenin ubiquitination thus inducing its degradation via the proteasomal pathway (Figure 1.8) (Aberle et al., 1997; Kitagawa et al., 1999). Therefore, in the absence of Wnt-Fzd-LRP5/6 binding, β-catenin is degraded and canonical Wnt signalling is inactive (Figure 1.8).

Upon Wnt-Fzd-LRP5/6 binding, the destruction complex is recruited to the plasma membrane through the binding of Axin to the phosphorylated cytoplasmic tail of LRP5/6 (Figure 1.8). This recruitment inactivates the destruction complex resulting in the accumulation of non-phosphorylated β-catenin, which translocates to the nucleus to activate the transcription of Wnt target genes (Figure 1.8). The exact mechanism driving the inactivation of the destruction complex upon Wnt-Fzd-LRP5/6 binding has yet to be fully resolved, however various models have been proposed. Stamos and colleagues show that the phosphorylated LRP5/6 receptor

may act to directly inhibit GSK3β activity thus preventing β-catenin being phosphorylated for degradation (Stamos et al., 2014). An alternative model proposes that ubiquitination of the phosphorylated β-catenin protein is blocked by the destruction complexes' relocation to the plasma membrane (Li et al., 2012). In this model, the destruction complex becomes over-saturated with phosphorylated β-catenin, leading to the accumulation of newly synthesised β-catenin, which is able to translocate to the nucleus and activate Wnt target genes (Li et al., 2012).

The translocation of β-catenin into the nucleus is still poorly understood. β-catenin does not contain a nuclear-localisation signal but rather directly interacts with nuclear pore components to facilitate its nuclear translocation (Fagotto et al., 1998). It has been suggested that β-catenin could "piggy-back" into the nucleus as cargo of Axin or APC that also shuttle in and out of the nucleus (Cong et al., 2004; Rosin-Arbesfeld et al., 2000). Once in the nucleus, β-catenin forms a transcriptional activator complex with DNA bound T-cell factor/ Lymphoid enhancer-binding factor (TCF/LEF) transcription factors (Figure 1.8) (Behrens et al., 1996; Molenaar et al., 1996). TCF/LEF transcription factors bind to DNA at 5'-AGATCAAAGG-3' promoter motifs (van de Wetering et al., 1997) and these are widely used in Wnt reporter models to drive the expression of reporter genes and provide a read-out of Wnt signalling levels in cells (Maretto et al., 2003; Korinek et al., 1997). In the absence of Wnt-Fzd-LRP5/6 binding, TCF/LEFs interact with Gro proteins (Groucho in metazoan; Transducin-Like Enhancer of split (TLE) proteins in humans and Groucho-related-gene (Grg) proteins in mice) to repress gene transcription (Figure 1.8) (Cavallo et al., 1998; Roose et al., 1998). Upon activation of canonical Wnt signalling, nuclear β-catenin converts TCF/LEF to a transcriptional activator by displacing Gro proteins and binding to the N-terminus of TCF/LEF via its central Armadillo repeats (Figure 1.8) (Daniels et al., 2005; Behrens et al., 1996; Molenaar et al., 1996; van de Wetering et al., 1997). β-catenin also regulates TCF/LEF phosphorylation which further mediates its activation (Hikasa et al., 2010; Lee et al., 2009). The C-terminal domain of β-catenin mediates the recruitment of transcriptional co-activators such as the histone acetylase CBP, BCL9 and Brg1 of the SWI/SNF chromatin remodelling complex, thus inducing the remodelling of the local chromatin structure to aid the activation of Wnt target genes (reviewed by (Städeli et al., 2006)). Most Wnt target genes are context specific, however Axin2 is considered to be a global target of canonical Wnt signalling and is therefore commonly used as a read-out of canonical Wnt pathway activity (Figure 1.8) (Lustig et al., 2002). Axin2 is also a key component of the destruction complex, therefore its Wnt induced upregulation acts as a negative feedback loop to inhibit canonical Wnt signalling (Lustig et al., 2002).

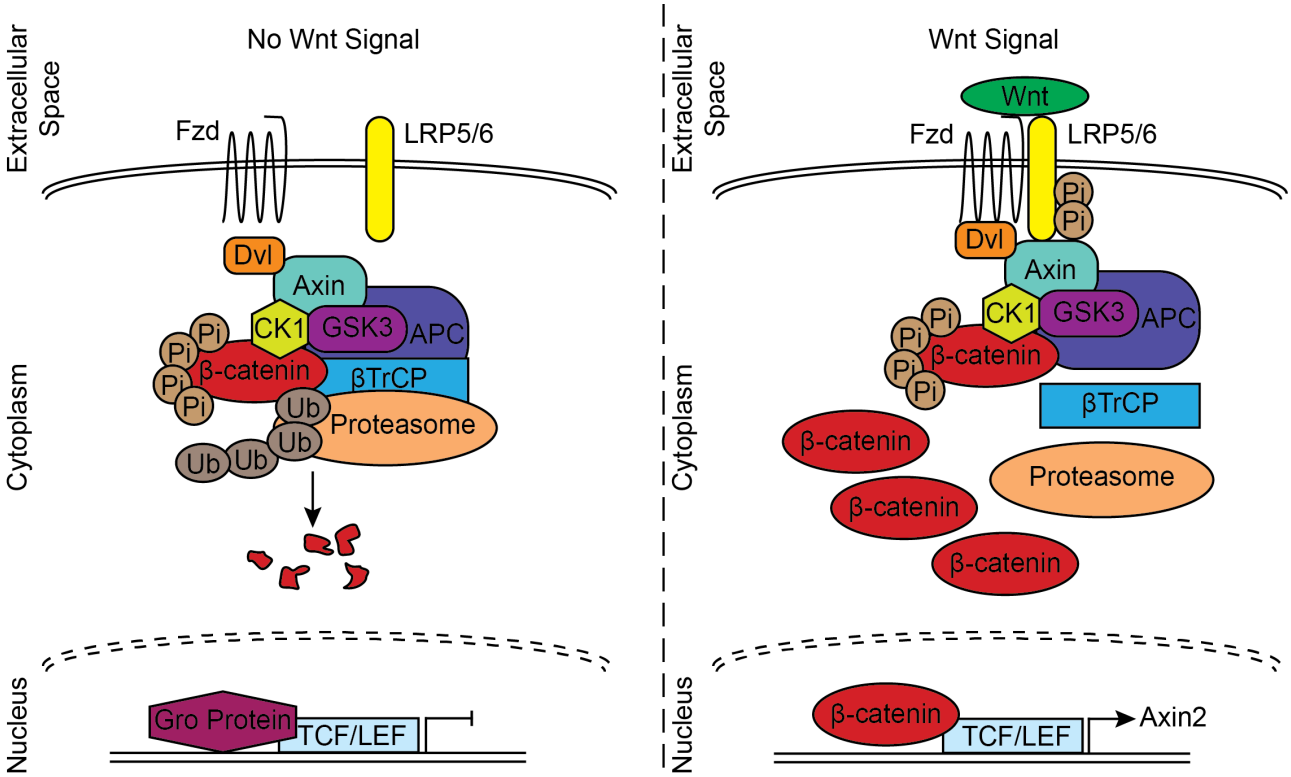


Figure 1.8: The canonical Wnt signalling pathway.

In the absence of a Wnt signal, the cytoplasmic destruction complex facilitates β-catenin degradation via GSK3β and CK1γ mediated phosphorylation and proteasome degradation. Therefore, β-catenin is unable to translocate to the nucleus and downstream canonical Wnt signalling is inactive. In the absence of a Wnt signal, TCF/LEF transcription factors are bound to DNA at target sites but their activity is repressed by Gro proteins. In the presence of a Wnt signal, binding of extracellular Wnts to their cell surface receptors, Fzds and LRP5/6, recruits the destruction complex to the cell membrane via Dvl, which disrupts its ability to degrade β-catenin. This promotes the accumulation of cytosolic β-catenin, which can then translocate to the nucleus and form a transcription activator complex with TCF/LEF by displacing Gro proteins. This β-catenin-TCF/LEF complex facilitates the activation of a Wnt dependent transcriptional program, including the expression of the canonical Wnt target gene Axin2. APC, adenomatous polyposis coli. CK1, casein kinase 1. Dvl, Dishevelled. Fzd, Frizzled. GSK3, glycogen synthase kinase 3. LRP5/6, low-density lipoprotein receptor-related protein 5/6. Pi, phosphate. TCF/LEF, T-cell factor/ Lymphoid enhancer-binding factor. Ub, ubiquitin. βTrCP, E3 ubiquitin ligase.

1.4.5 Structure and Functions of β-catenin

β-catenin plays a dual role in mediating both canonical Wnt signalling and cell-cell adhesion at cadherin-based adherens junctions. The β-catenin protein contains a central region consisting of 12 imperfect Armadillo (ARM) repeats that are flanked by N- and C-terminal domains (NTD and CTD respectively, Figure 1.9) (Valenta et al., 2012). The NTD and CTD are structurally flexible whereas the central ARM domain provides a rigid scaffold for many β-catenin binding partners, such as APC, TCF/LEF and cadherins (Figure 1.9) (Huber et al., 1997). The NTD contains the GSK3β and CK1γ phosphorylation sites and is therefore involved in regulating the stability of the β-catenin protein (Figure 1.9) (Yost et al., 1996). The CTD is responsible for recruiting transcriptional co-activators and therefore mediates gene transcription when bound with TCF/LEF transcription factors (Figure 1.9) (van de Wetering et al., 1997). The spatial segregation of β-catenin binding partners within the cell is important for determining the function of β-catenin and the conformational changes β-catenin undergoes are important in regulating this binding. For example, the NTD and CTD have been shown to fold back onto the central ARM domains to prevent binding to TCF/LEF and cadherins (Solanas et al., 2004). Interestingly, the CTD is essential for the signalling activity of β-catenin but is not required for its role in cell-cell adhesion indicating that different regions of the β-catenin protein are responsible for mediating its various function (Xing et al., 2008; Valenta et al., 2011).

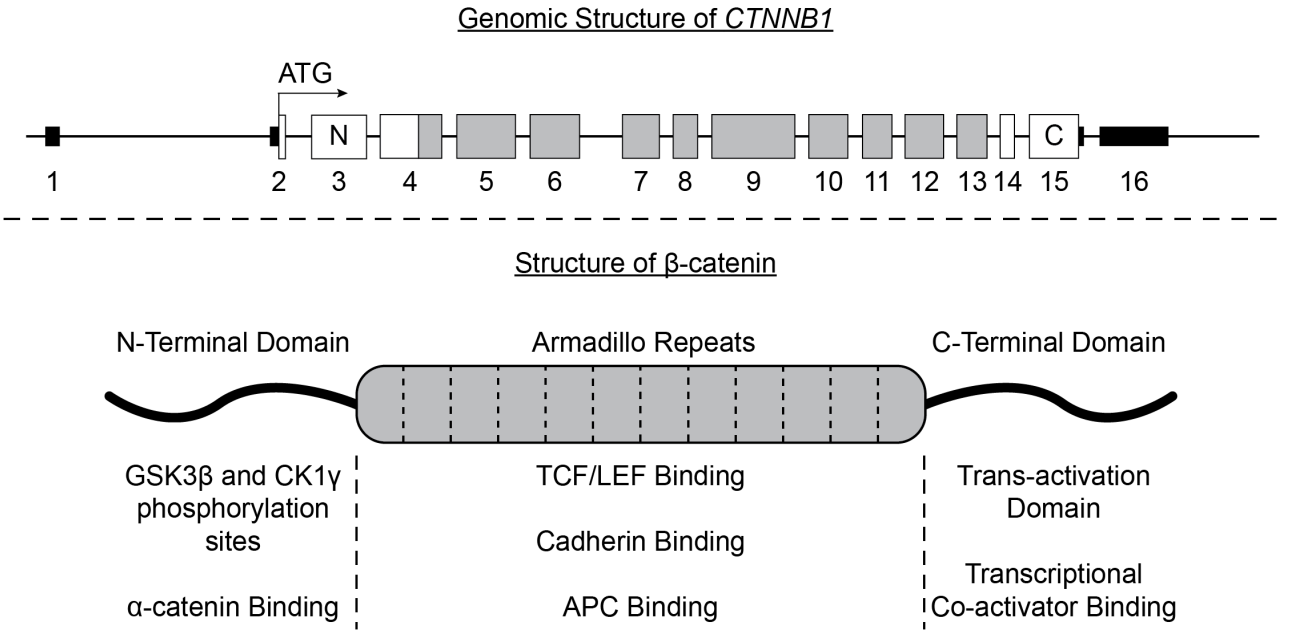


Figure 1.9: Genomic structure of *CTNNB1* and structure of β-catenin.

Cartoon of the genomic and protein structure of β-catenin. β-catenin is encoded by the *CTNNB1* gene, which contains 16 exons. The encoded β-catenin protein consists of three regions the N-terminal domain (N), Armadillo repeats and C-terminal domain (C). The N-terminal domain is encoded by exon 3 and encodes the GSK3β and CK1γ phosphorylation sites and the α-catenin binding site. The Armadillo repeats are encoded by exons 4-13 and form the central region of the protein responsible for binding TCF/LEF, cadherins and APC. The C-terminal domain is encoded by exon 15 and is responsible for recruiting transcriptional co-activators. Black boxes represent noncoding exons. Large boxes represent coding exons. Grey boxes indicate exons encoding the Armadillo repeats. N denotes the N-terminal domain. C denotes the C-terminal domain. Arrow indicates the ATG translational start codon. APC, adenomatous polyposis coli. CK1γ, casein kinase 1γ. GSK3β, glycogen synthase kinase 3. TCF/LEF, T-cell factor/ Lymphoid enhancer-binding factor.

Cadherin-based cell-cell junctions perform multiple roles including the initiation and stabilisation of cell-cell contacts, regulation of the actin cytoskeleton and regulation of intracellular signalling (reviewed by (Hartsock et al., 2008)). At these junctions, contact between neighbouring cells is mediated by cadherins, which are single-pass transmembrane glycoproteins named after the tissue they are predominately expressed in, such as Epithelial- and Neural-cadherin (E- and N-cadherin respectively) (Gooding et al., 2004). The cadherin extracellular domain forms a trans-cadherin interaction between neighbouring cells thus facilitating cell-cell adhesion and the formation of an adherens junction (Halbleib et al., 2006). The cytoplasmic region of cadherin interacts with the ARM domain of β-catenin, which is bound to α-catenin via its NTD (Huber et

al., 2001). α-catenin interacts directly with F-actin proteins, thus α/β-catenin provide a physical link between the transmembrane adhesion proteins and the actin cytoskeleton (Hur et al., 2013). This link to the cytoskeleton has been shown to be essential for maintaining cell adhesion functions as cells lacking either α- or β-catenin are unable to form cell-cell contacts (Knudsen et al., 1995). In addition, the binding between β-catenin and cadherins has been shown to be essential for the stability of both proteins as both are rapidly degraded by the proteasome when binding between these proteins is impaired (Hinck et al., 1994; Huber et al., 2001).

1.4.6 Non-canonical β-catenin independent Wnt signalling pathways: Wnt/PCP pathway and Wnt/Ca^{2+} pathway

The non-canonical Wnt signalling pathways are β-catenin-independent Wnt signalling cascades and include the planar cell polarity (PCP) pathway and the Ca^{2+} pathway (Figure 1.10). These pathways are favoured by Wnt4, Wnt5a and Wnt11 ligands, however other Wnt ligands are also able to activate non-canonical Wnt signalling (Grumolato et al., 2010). The Wnt/PCP pathway was first identified in *Drosophia* and regulates tissue polarity and cell migration (Adler. 2002; Veeman et al., 2003). This pathway involves the activation of small GTPases such as Rho and Rac to regulate cytoskeletal dynamics (Varela-Nallar et al., 2013). The Wnt/PCP pathway is thought to be mediated by Wnt-Fzd binding independently of LRP5/6, and uses the tyrosine kinases Ryk, PTK7 and ROR2 as alternative co-receptors (Figure 1.10) (He et al., 2004; Lu et al., 2004a; Lu et al., 2004b; Nishita et al., 2006). This signal is then transduced to Dvl, which uses separate domains to activate the GTPases Rho and Rac in parallel signalling pathways (Eaton et al., 1996; Fanto et al., 2000; Habas et al., 2003; Strutt et al., 1997; Tahinci et al., 2003). To activate Rho GTPase, Dvl forms a complex with the formin-homology protein Dishevelled associated activator of morphogenesis 1 (Daam1), which directly activates Rho GTPase (Figure 1.10) (Habas et al., 2001; Tanegashima et al., 2008). Activation of Rho GTPase leads to the activation of Rho-associated kinase (ROCK) and myosin resulting in cytoskeletal rearrangements (Figure 1.10) (Marlow et al., 2002; Weiser et al., 2007). The activation of Rac GTPase by Dvl is still poorly understood, but results in the activation of the JNK pathway and modulation of the cytoskeleton (Figure 1.10) (Habas et al., 2003).

The Wnt/Ca^{2+} pathway plays a role across a variety of developmental processes including the regulation of the dorsal-ventral axis, cardiac development and synapse formation (Kühl et al., 2000; Tian et al., 2010; McQuate et al., 2017). The Wnt/Ca^{2+} pathway was first identified following the observation that some Wnt ligands induced the release of Calcium ions (Ca^{2+}) from

the endoplasmic reticulum (ER) in a G-Protein dependent manner (Slusarski et al., 1997; Westfall et al., 2003). The Wnt-Fzd binding leads to the intracellular increase of inositol 1, 4, 5-triphosphate (IP3), which is produced from membrane-bound phospholipid phosphatidyl inositol 4, 5-bisphosphate by the action of membrane-bound phospholipase C (PLC) (De. 2011). IP3 interacts with calcium channels located in the ER and results in the release of Ca^{2+} into the cytoplasm (Figure 1.10) (De. 2011). The increase in intracellular Ca^{2+} levels activates several Ca^{2+} sensitive proteins including protein kinase C (PKC), calcium calmodulin-dependent kinase II (CamKII) and calcineurin (Figure 1.10) (Veeman et al., 2003; Kohn et al., 2005; Sheldahl et al., 2003; Kühl et al., 2000). These proteins then activate various downstream effectors including the transcription factors NFκB, CREB and NFAT that activate the expression of downstream target genes (Figure 1.10) (De. 2011; Hogan et al., 2003; Feske et al., 2003). CamKII also activates the TGFβ activated kinase (TAK) and Nemo-like kinase (NLK) which can antagonise canonical Wnt signalling, indicating that the different Wnt signalling branches are able to directly regulate each other (Ishitani et al., 1999).

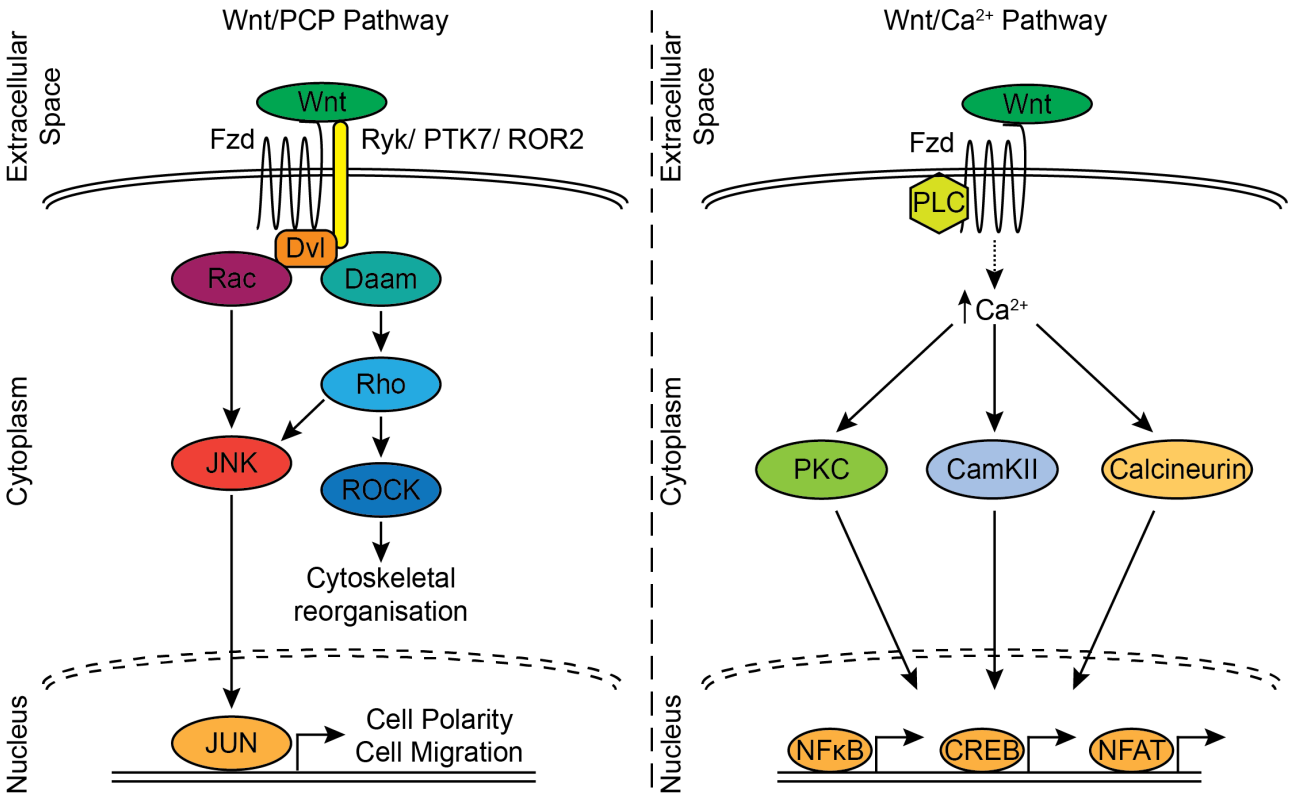


Figure 1.10: Schematic of the non-canonical β-catenin independent Wnt signalling pathways: the Wnt/PCP pathway and the Wnt/Ca^{2+} pathway.

The Wnt/PCP pathway activates the GTPases Rho and Rac, which in turn activate Rho associated kinase (ROCK) and JNK resulting in the reorganisation of the cytoskeleton. The Wnt/Ca^{2+} pathway triggers the increase in intracellular Ca^{2+} levels which in turn activates the calcium sensitive proteins calcium calmodulin-dependent kinase II (CamKII), protein kinase C (PKC), and calcineurin. These then activate various transcription factors that regulate the gene expression of various downstream target genes.

1.5 Role of Wnt Signalling During Neurogenesis

1.5.1 Role of Wnt Signalling in Neurogenesis During Development

Wnt signalling plays a crucial role throughout all stages of brain development including the anterior-posterior specification of the neural plate; the morphogenesis of the neural tube; the regulation of neural stem cell proliferation and neuronal differentiation; neuronal migration; axon growth and guidance; dendritic development and synapse formation (reviewed by (Mulligan et al., 2012)). During early vertebrate development, a Wnt signalling gradient, that is high in the posterior and low in the anterior, is integral for the correct anterior-posterior patterning of the neural plate (Kiecker et al., 2001). Ectopic stimulation of canonical Wnt signalling promotes the

expression of posterior neural markers while suppressing the expression of anterior markers (McGrew et al., 1995). Antagonism of Wnt signalling in the anterior neuroectoderm is achieved by the expression of the Wnt inhibitor Dkk1 and loss of anterior Wnt inhibition is associated with posteriorisation and loss of anterior fate (Glinka et al., 1998; Kazanskaya et al., 2000). After neural plate specification, the neuroectoderm invaginates to form the neural tube and the Wnt/PCP pathway plays a major role in regulating the closure of the neural tube (Mulligan et al., 2012). Many neural tube defects present with genetic disruptions in modulators of the Wnt/PCP pathway highlighting its integral role in regulating this process (Mulligan et al., 2012; Hamblet et al., 2002; Torban et al., 2008). Canonical Wnt signalling also plays a role in regulating neural tube closure, however whether it does so by interacting with the non-canonical Wnt signalling pathway is still unclear (Mulligan et al., 2012).

Canonical Wnt signalling has been shown to regulate both proliferation and neural specification of multipotent neural tube precursors (McMahon et al., 1990; Parr et al., 1993). Wnt1 and Wnt3a are expressed along the dorsal midline of the neural tube in a high-dorsal, low-ventral gradient and this correlates with the proliferative capacity of the progenitors along this gradient (Megason et al., 2002). High canonical Wnt signalling in the dorsal neural tube promotes proliferation by the direct upregulation of cell cycle genes such as *CyclinD1*, however in the ventral neural tube, where Wnt signalling is low, neuronal differentiation is favoured (Megason et al., 2002). Canonical Wnt signalling is also involved in specifying the dorsal fate of the developing telencephalon as loss of β-catenin in embryonic day 8 (E8) neural progenitors results in the upregulation of ventral restricted markers, such as *Ascl1* and loss of dorsal fate (Backman et al., 2005). In addition, ectopic expression of stabilised β-catenin in the ventral forebrain, results in the overexpression of dorsal-restricted markers, such as *Ngn2* and the repression of ventral markers, such as *Ascl1*, indicating that Wnt signalling also promotes a dorsal fate by repressing the expression of ventral markers (Zechner et al., 2007).

Wnt ligands and Fzd receptors are expressed in discrete and overlapping patterns in the developing forebrain, which correlates with areas of active canonical Wnt signalling, indicating that canonical Wnt signalling plays a role in early patterning events (Harrison-Uy et al., 2012; Maretto et al., 2003). The progenitor cells of the developing forebrain are initially a homogenous population, which become patterned as development progresses by key signalling centres from different regions along the neuroepithelium, such as the cortical hem. Components of the Wnt signalling pathway continue to be expressed following the completion of patterning events, suggesting that Wnt continues to play a role in later developmental processes (Harrison-Uy et

al., 2012). Cortical radial glia progenitors are located in a proliferative zone next to the lateral ventricles and undergo symmetric divisions to expand the progenitor pool during early development (Takahashi et al., 1996). As development progresses, radial glia switch to asymmetric divisions to generate one radial glial cell and either a neuron or IPC (Noctor et al., 2001; Noctor et al., 2004; Haubensak et al., 2004; Miyata et al., 2004). The IPCs then migrate away from the ventricular zone and symmetrically divide to generate two neurons (Noctor et al., 2004). Canonical Wnt signalling has been shown to promote the symmetrical divisions of radial glial cells thus expanding the progenitor pool at the expense of neuronal differentiation (Chenn et al., 2002; Wrobel et al., 2007; Machon et al., 2007; Woodhead et al., 2006). Wnt signalling also promotes the neuronal differentiation of IPCs, through the upregulation of pro-neuronal transcription factors such as Ngn1 and Ngn2 (Hirabayashi et al., 2004; Israsena et al., 2004; Kuwahara et al., 2010). This suggests that the response to Wnt signalling changes as progenitors mature indicating the context dependent role of Wnt signalling during cortical development. Interestingly, the dose of canonical Wnt signalling has been shown to determine cellular fate in the developing cortex where a gradient of canonical Wnt signalling regulates cell identity along the latero-medial axis in the developing dorsal telencephalon (Machon et al., 2007).

Wnt signalling also plays a role in the later stages of neuronal development during axon growth and guidance, dendrite development and synapse formation and function (reviewed by (Mulligan et al., 2012). Wnt ligands have been identified as guidance cues for axon growth cones that guide axon elongation towards their correct location (reviewed by (Guan et al., 2003)). Cerebellar granule neurons express Wnt7a, which mediates axon growth by inhibiting the GSK3β-mediated phosphorylation of microtubule associated proteins thus changing the organisation and stability of the cytoskeleton (Lucas et al., 1998; Lucas et al., 1997; Ciani et al., 2011). Dendrite development is also influenced by canonical Wnt signalling and is enhanced in hippocampal neuron cultures when dominant active β-catenin is over-expressed (Yu et al., 2003). Non-canonical Wnt signalling also enhances dendrite formation as inhibition/ knock-down of Wnt/PCP and Wnt/Ca^{2+} pathway components result in decreased dendritic branching (Rosso et al., 2005; Ciani et al., 2011). Additionally, Wnt7a plays a role in regulating synaptogenesis by promoting the clustering of Synapsin-1 at the presynaptic terminal and post-synaptic density protein-95 (PSD-95) at the postsynaptic terminal via the induction non-canonical Wnt signalling (Hall et al., 2000; Ciani et al., 2011). Wnt5a also mediates synapse function via the Wnt/Ca^{2+} pathway (Varela-Nallar et al., 2010; Cerpa et al., 2011; Varela-Nallar et al., 2012) and the

canonical Wnt signalling pathway has been shown to promote synaptic transmission (Chen et al., 2006).

Canonical Wnt signalling is also critical for the development of hippocampus. The cortical hem is a neuroepithelial structure located between the hippocampal anlage and the choroid plexus, characterised by high expression of Wnt and BMP ligands (Grove et al., 1998). These cortical hem signals influence the development of the hippocampus, starting at E14, and the hippocampus fails to develop in mouse models that lack the cortical hem (Grove et al., 1998; Tole et al., 2000; Theil et al., 1999). The importance of Wnt signalling during the development of the hippocampus is shown by the absence of the hippocampal structure in Wnt3a and LEF knock-out mice (Lee et al., 2000; Galceran et al., 2000). Wnt signalling also promotes the proliferation of hippocampal precursors, as in Wnt3a and LEF mutants, the number of BrdU+ cells are reduced in the medial wall of the developing telencephalon at E10.5 and E11.5 respectively (Galceran et al., 2000; Lee et al., 2000). Interestingly, proliferation is not affected at E12.5 and E13.5 suggesting that Wnt signalling regulates the initial expansion of the hippocampal progenitor pool but ongoing proliferation is supported independent of canonical Wnt signalling (Machon et al., 2003). In addition, the level of Wnt signalling is important in determining the cellular fate of the hippocampus, with high Wnt signalling specifying DG granule cells whereas a moderate level of canonical Wnt signalling specifies the CA layers (Machon et al., 2007). This indicates a dose-dependent effect for canonical Wnt signalling during hippocampal development (Machon et al., 2007). Overall, these studies show that Wnt signalling plays multiple roles across neurodevelopment which are also relevant to adult hippocampal neurogenesis and will be explored in the following sections.

1.5.2 Role of Non-Canonical Wnt Signalling During Adult Hippocampal Neurogenesis

The role of non-canonical Wnt signalling during adult hippocampal neurogenesis is relatively unknown but there is evidence suggesting the PCP and Wnt/Ca^{2+} pathway play a role in regulating the later stages of neuronal maturation, such as synapse formation and dendritic spine morphogenesis. As cells progress along the hippocampal neurogenic lineage they have been shown to transition from canonical to non-canonical Wnt signalling to promote the morphological maturation of newborn granule neurons (Schafer et al., 2015). Indeed, inhibition of the Wnt/PCP pathway, by deletion of pathway components, severely impairs dendritic growth, migration and dendritic orientation of adult born granule neurons (Schafer et al., 2015). The non-canonical Wnt5a ligand has been shown to activate non-canonical Wnt signalling cascades in

cultured hippocampal neurons where it plays an important role in modulating synapse structure and function (Farías et al., 2009; Cuitino et al., 2010; Varela-Nallar et al., 2010). Wnt5a induces the clustering of PSD-95 in a Wnt/JNK dependent manner (Farías et al., 2009). PSD-95 is a synaptic scaffolding protein enriched in the post-synaptic density, which is a network of proteins whose role is to organise the neurotransmitter receptors, such as glutamate receptors, at the synapse membrane (Li et al., 2003; Han et al., 2008a). Therefore, Wnt5a/JNK signalling plays a direct role in regulating glutamatergic synaptic transmission by directing the clustering and distribution of PSD-95 (Farías et al., 2009). Wnt5a also induces the recycling of functional $GABA_A$ receptors in hippocampal neurons via the Wnt/ Ca^{2+} pathway thus modulating inhibitory synapses as well as glutamatergic excitatory synapses. The synaptic integration of newborn granule neurons into the existing hippocampal neural circuitry requires the correct firing of inhibitory followed by excitatory synaptic inputs, suggesting that Wnt5a signalling could play a role in regulating the integration of newborn neurons by modulating synaptic activity (Varela-Nallar et al., 2012). Wnt5a and Wnt7a both promote dendritic spine morphogenesis via the Wnt/Ca^{2+} pathway and blockage of this signalling pathway leads to decreased spine density and decreased excitatory synaptic strength, indicating that non-canonical Wnt signalling could play an integral role during newborn neuron integration in the adult DG (Ciani et al., 2011; Varela-Nallar et al., 2010; Arredondo et al., 2019). In addition, Wnt5a treatment of hippocampal slices increased the activity and amplitude of synaptic events via the Wnt/ Ca^{2+} pathway (Varela-Nallar et al., 2010; Cerpa et al., 2011). Interestingly, Wnt5a levels are increased following training in the hidden platform Morris water maze task, which utilises hippocampal dependent long-term spatial memory (Tabatadze et al., 2012). This could suggest an indirect role for non-canonical Wnt signalling in promoting progenitor proliferation and neuronal differentiation by modulating hippocampal neurotransmission in response to an external stimulus (Varela-Nallar et al., 2010; Cerpa et al., 2011; Tabatadze et al., 2012; Varela-Nallar et al., 2013). During development Wnt/PCP pathway regulates polarisation and migration of newborn neurons, however this function during adult neurogenesis has yet to be established (reviewed by (Goodrich. 2008)).

1.5.3 Role of Canonical Wnt Signalling During Adult Hippocampal Neurogenesis

By using BATGAL Wnt reporter mice, that express β-galactosidase under the control of 7xTCF/LEF binding sites (Maretto et al., 2003), canonical Wnt signalling has been shown to be active within the SGZ and GCL of the adult hippocampus (Lie et al., 2005). Wnt ligands and Wnt inhibitors have been shown to be present within the adult hippocampal neurogenic niche, highlighting that Wnt is a regulated signalling pathway within the niche microenvironment (Lie et

al., 2005; Seib et al., 2013; Jang et al., 2013). Cultured adult hippocampal stem and progenitor cells (AHSPCs) express Wnt pathway components including *Dvl*, *β-catenin* and *LEF1* and also express *Fzds* and *LRP5/6* receptors (Lie et al., 2005; Wexler et al., 2009). Wnt receptors are differentially expressed across the cells of the neurogenic lineage, indicating stage specific roles for Wnt signalling in regulating different aspects of adult neurogenesis (Mardones et al., 2016). Adult hippocampal neural progenitors have also been shown to express Wnt ligands themselves, such as Wnt7a/b suggesting the presence of autocrine/paracrine Wnt signalling (Wexler et al., 2009; Qu et al., 2010; Qu et al., 2013). Wexler and colleagues used a Wnt reporter cell line, where GFP expression is driven by an enhanced TCF/LEF promoter, and found that co-culture with NSCs induced a 2-fold increase in fluorescence signal compared to fibroblast co-cultures, indicating that NSC derived Wnt ligands act locally on neighbouring cells (Wexler et al., 2009). However, other studies have failed to achieve a read-out of Wnt signalling using the classical TOP/FOPflash Wnt reporter assay (Lie et al., 2005; Wexler et al., 2009). The TOP/FOPflash assay uses luciferase expression under the control of TCF/LEF binding sites as a read-out of Wnt signalling levels (Molenaar et al., 1996). Luciferase has a relatively short half-life, which makes it difficult to detect low levels and cyclic changes in Wnt signalling activity, which Wexler and colleagues argue is the reason for not detecting baseline Wnt signalling in AHSPC cultures using the TOPflash Wnt reporter (Wexler et al., 2009). Nevertheless, deletion of Wnt7a and inhibition of Wnt signalling in cultured AHSPCs impairs proliferation, indicating that AHSPC derived Wnt ligands could act in an autocrine/paracrine manner to regulate AHSPC behaviour (Qu et al., 2010; Wexler et al., 2009; Qu et al., 2013).

Another source of Wnt ligands within the DG are the niche astrocytes (Lie et al., 2005). Lie and colleagues show that astrocyte derived Wnt3a promotes adult neurogenesis by enhancing proliferation and neuronal differentiation of neuronally committed precursors *in vitro* and *in vivo* (Lie et al., 2005). They found that stimulating canonical Wnt signalling, by overexpression of Wnt3a *in vitro* and Wnt3 *in vivo*, played a role in regulating neuronal fate choice and enhanced proliferation of neuronally committed precursors (Lie et al., 2005). The selective role of canonical Wnt signalling in neuronally committed precursors is further supported by evidence from Seib and colleagues (Seib et al., 2013). They found that loss of the Wnt inhibitor Dkk1 from progenitors enhanced the proliferation and maturation of neuronally committed progenitors *in vivo*, indicating a selective role for canonical Wnt signalling in enhancing adult neurogenesis (Seib et al., 2013). However, this is contradicted by data from Jang and colleagues who use clonal analysis to show that loss of sFPR3 from granule neurons, and the subsequent increase in niche Wnt signalling levels, activates quiescent AHSCs to generate IPCs, astrocytes and

AHSCs equally, thus indicating that canonical Wnt signalling does not exclusively favour neuronal lineage commitment (Jang et al., 2013). These differences could be due to the different experimental techniques used to stimulate canonical Wnt signalling, differences between *in vitro* and *in vivo* assays, as well as examining the effects at different stages along the neurogenic lineage. For example, Jang and colleagues use clonal analysis to look at the identities of cells in activated clones of Nestin+ AHSCs in the adult DG of sFRP3 knock-out mice (Jang et al., 2013). On the other hand, Seib and colleagues conditionally ablate Dkk1 in Nestin+ progenitors and use BrdU labelling to characterise and quantify the number of newly generated lineage cells (Seib et al., 2013). Finally, Lie and colleagues use a lentiviral vector to overexpress Wnt3 in the adult DG and examine the proportion of BrdU+ DCX+ neuroblasts (Lie et al., 2005). Additionally, Seib et al 2013 and Jang et al 2013 use Dkk1 and sFRP3 knock-out mice respectively for some analyses. Whilst they comment on no overall gross abnormality in the DG of adult mice, this doesn't exclude potential developmental contributions towards the reported phenotypes (Seib et al., 2013; Jang et al., 2013).

Canonical Wnt signalling has also been reported to play a role at the later stages of adult neurogenesis during neuronal maturation. Indeed, loss of sFRP3 accelerates the maturation of newborn neurons by enhancing dendritic branching and dendritic spine formation (Jang et al., 2013). Similarly, loss of Dkk1 also enhances dendritic complexity of DCX+ neuroblasts indicating a role for canonical Wnt signalling in promoting the maturation of newborn neurons (Seib et al., 2013). Transcriptional targets of canonical Wnt signalling include the pro-neuronal transcription factors *Neurogenin2* (*Ngn2*) and *NeuroD1*, showing that canonical Wnt signalling plays a direct role in regulating neuronal differentiation (Kuwabara et al., 2009; Gao et al., 2009). NeuroD1 is dual regulated by both Sox2 and canonical Wnt signalling, where its expression is repressed in Sox2+ progenitors but is activated by canonical Wnt signalling to promote neuronal differentiation (Kuwabara et al., 2009). Indeed, loss of β-catenin in Sox2+ progenitors impairs the number of newborn neurons without affecting the maintenance of the Sox2+ progenitor pool indicating a stage specific role for canonical Wnt signalling during adult hippocampal neurogenesis (Kuwabara et al., 2009). However, the authors do not robustly distinguish between AHSCs with radial morphology and Sox2+ IPCs in their *in vivo* conditional deletion of β-catenin models, which warrants further investigation to understand the role of canonical Wnt signalling during the early stages of adult neurogenesis. In addition, they conditionally delete β-catenin in β-catenin$^{fl/fl}$ mice through the stereotaxic injection of a Sox2-Cre-GFP retrovirus (Kuwabara et al., 2009), which infects mitotically active cells (Suh et al., 2007). Therefore, the quiescent AHSC

population is largely unaffected in this *in vivo* model meaning that the role of canonical Wnt signalling in regulating quiescent AHSC activation remains unresolved.

Adult neurogenesis declines with age as do the levels of canonical Wnt signalling in the DG in part due to the increased levels of the Wnt inhibitor Dkk1 and decreased levels of astrocyte derived Wnt3a ligands (Seib et al., 2013; Okamoto et al., 2011; Miranda et al., 2012). Loss of Dkk1 restored the levels of adult hippocampal neurogenesis in aged mice, suggesting that lower levels of canonical Wnt signalling could contribute to the age-related decline in adult hippocampal neurogenesis (Seib et al., 2013). Indeed, progenitor proliferation and neurogenic output are dramatically reduced by the inhibition of canonical Wnt signalling and impairs hippocampal dependent behaviours such as spatial memory retention and object recognition memory (Lie et al., 2005; Jessberger et al., 2009). This indicates that canonical Wnt mediated adult hippocampal neurogenesis contributes to overall hippocampal function and could provide a target for therapeutic intervention to combat age-related cognitive decline (Jessberger et al., 2009).

Levels of canonical Wnt signalling are also decreased in many neuropsychiatric disorders that also display impaired adult hippocampal neurogenesis, such as depression, Alzheimer's disease and schizophrenia (Fiorentini et al., 2010; Wexler et al., 2007; Mao et al., 2009; Hussaini et al., 2014). Disruptions in *Disrupted In Schizophrenia 1 (DISC1)* gene function are associated with bipolar disorder, autism spectrum disorders and schizophrenia (Mao et al., 2009). *DISC1* is expressed in hippocampal progenitors where it inhibits GSK3β, thus stabilises β-catenin and activates canonical Wnt signalling to promote progenitor proliferation (Mao et al., 2009). Loss of *DISC1* impairs progenitor proliferation and induces hyperactive and depressive behaviours, which are normalised by treatments with a GSK3β inhibitor to restore canonical Wnt signalling levels (Mao et al., 2009). Additionally, treatment with the GSK3β inhibitor lithium chloride, a treatment for manic depression, stimulates proliferation and neuronal fate commitment in a mouse model of Alzheimer's disease and hippocampal NSC cultures in a canonical Wnt dependent manner (Fiorentini et al., 2010; Wexler et al., 2007). These studies indicate an important link between canonical Wnt dependent adult hippocampal neurogenesis and neuropsychiatric disorders and highlight the clinical and therapeutic importance in understanding how canonical Wnt signalling regulates adult hippocampal neurogenesis.

Interestingly, exercise has been shown to increase the expression of Wnt3a in the adult hippocampus which has a positive effect on adult neurogenesis in the aged hippocampus

(Okamoto et al., 2011). Additionally, the Wnt inhibitor sFRP3, is produced by granule neurons in an activity-dependent manner (Jang et al., 2013). Both exercise and electroconvulsive stimulation (ECS) decrease the expression of granule neuron derived sFRP3 and promote progenitor proliferation via activation of the canonical Wnt signalling pathway (Jang et al., 2013). This positive effect of ECS on adult neurogenesis was abolished by the infusion of sFRP3 into the adult DG, indicating that the reduction in sFRP3 levels, and concomitant increase in levels of canonical Wnt signalling, are required for this activity dependent increase in neurogenesis (Jang et al., 2013). Overall, these studies implicate a role for canonical Wnt signalling in regulating the pro-neurogenic effects of external stimuli.

As previously stated, the direct Wnt-induced transcriptional activation of pro-neuronal transcription factors, such as *NeuroD1* and *Neurogenin2*, has been identified as a potential mechanism driving the pro-neurogenic effects of canonical Wnt signalling (Kuwabara et al., 2009). Additionally, *Prox1* is another direct transcriptional target of canonical Wnt signalling that is required for the differentiation and survival of newborn granule neurons (Karalay et al., 2011). The molecular mechanisms underlying the pro-proliferative effects of canonical Wnt signalling are currently not well defined. *CyclinD1* is a direct transcriptional target of the canonical Wnt signalling pathway and plays an integral role in regulating progression through the G1-S phase of the cell cycle alongside its cyclin dependent kinase binding partners CDK4 and CDK6 (Jun-ya Kato. 1993; Shtutman et al., 1999). Therefore, the pro-proliferative effects of canonical Wnt signalling during adult hippocampal neurogenesis could be due to the direct upregulation of *CyclinD1* expression.

Whilst the current literature indicates a role for canonical Wnt signalling in regulating various aspects of adult hippocampal neurogenesis, the identities of the cells along the neurogenic lineage that are directly responding to and affected by canonical Wnt signalling have yet to be robustly characterised. Indeed, studies highlighting a role for canonical Wnt signalling in regulating neural stem and progenitor cell behaviour are predominately performed *in vitro* (Lie et al., 2005; Wexler et al., 2009; Qu et al., 2010; Qu et al., 2013) and *in vivo* studies do not distinguish between AHSCs with radial morphology and IPCs (Kuwabara et al., 2009; Seib et al., 2013; Jang et al., 2013), which could be differentially regulated by canonical Wnt signalling given the context dependency of this pathway across various cell types. In addition, AHSCs exhibit unique characteristics according to their activation state, which could influence their response to niche-derived signalling pathways (Figure 1.5). However, the role of canonical Wnt signalling in quiescent and active AHSCs has not yet been explored. Furthermore, the activation

of quiescent AHSCs represents a key regulatory step during adult hippocampal neurogenesis, that balances the preservation of the AHSC pool with the neurogenic demands of the hippocampus. However, the role of canonical Wnt signalling in regulating quiescent AHSC activation is still unclear.

1.6 Project Aims

Since the establishment of neurogenesis in the adult mammalian hippocampus, much research has focussed on understanding how this process is regulated by extrinsic, niche-derived and intrinsic factors. The fact that adult hippocampal neurogenesis is impaired in a number of disease states and is associated with age-related cognitive decline, highlights important clinical and therapeutic implications in understanding how it is regulated. By deciphering these regulatory mechanisms, we can develop therapies to help alleviate the symptoms of neuropsychiatric disease and perhaps mitigate the changes associated with age-related cognitive decline.

The first key stage in the regulation of adult hippocampal neurogenesis is the decision of quiescent AHSCs to activate. The majority of the AHSC pool remains out of the cell cycle in quiescence to preserve their numbers throughout life. The decision to activate must balance the long-term preservation of the stem cell pool, whilst also meeting the neurogenic demands of the hippocampus. The unique microenvironment of the hippocampal neurogenic niche supplies AHSCs with a variety of signals, which they co-ordinate and integrate to regulate their behaviour. Much work has gone into understanding how these various niche-derived signals regulate adult hippocampal neurogenesis, however how these signals independently regulate specific stages of adult hippocampal neurogenesis still remains to be defined. The canonical Wnt signalling pathway is one example of a niche derived signal that has been shown to regulate adult hippocampal neurogenesis, however its precise role in AHSCs has yet to be elucidated.

Canonical Wnt signalling is actively regulated within the hippocampal neurogenic niche and has been shown to play a role at both early and late stages of adult hippocampal neurogenesis; in promoting neural precursor proliferation and instructing a neuronal fate. However, it is still unclear which cells along the neurogenic lineage are responding to canonical Wnt signalling and how they are affected by changing Wnt signalling levels. For example, canonical Wnt signalling has been shown to induce proliferation within the adult DG, however whether this is due to increased progenitor proliferation or increased activation of quiescent AHSCs remains unknown.

As such, the overall aim of this PhD work is to characterise the role of canonical Wnt signalling in the AHSC population, with a particular focus on the role of canonical Wnt signalling in the quiescence-activation transition of AHSCs. I aim to investigate the role of canonical Wnt signalling in AHSCs in the following ways:

1. Characterise both active and quiescent AHSCs under physiological conditions for their response to canonical Wnt signalling *in vivo* and *in vitro*.
2. Investigate the function of canonical Wnt signalling in AHSCs *in vivo* and *in vitro*, with a particular focus on the role of canonical Wnt signalling in regulating quiescent AHSC activation, by inhibiting their ability to respond to canonical Wnt signalling.
3. Determine how quiescent and active AHSCs respond to changing levels of canonical Wnt signalling, particularly in regards to quiescent AHSC activation, by stimulating canonical Wnt signalling in AHSCs *in vivo* and *in vitro*.

Chapter 2. Materials and Methods

2.1 Experimental Models

2.1.1 Mouse Models

All procedures involving animals and their husbandry were performed according to the guidelines of the Francis Crick Institute and in compliance with the following statutory regulations: Animals (Scientific Procedures) Act 1986 [ASPA], Animal Welfare Act 2006 and Welfare of Animals in Transport Order. This study was approved by The Crick Biological Research Facility Strategic Oversight Committee (BRF-SOC), Animal Welfare and Ethical Review Body (AWERB) and the UK Home Office (PPL PB04755CC). Mice were housed in standard cages under a 12hr light/dark cycle, with ad libitum access to food and water. All mouse husbandry requirements were met by Crick BRF staff members. Mice were genotyped by Transnetyx®.

All experimental mice were of a mixed genetic background. Founder mice were crossed with MF1 mice, and then backcrossed to littermates of the F1 generation. Glast-CreERT2 ($Slc1a3^{tm(cre/ERT2)Mgoe}$) (Mori et al., 2006) mice were crossed with Rosa26-floxed-stop-YFP (RYFP; $Gt(ROSA)26Sor^{tm1(EYFP)Cos}$) (Srinivas et al., 2001) mice to generate AHSC specific tamoxifen inducible mice with a YFP recombination reporter. These mice were then crossed with our experimental strains: β-$cat^{fl/fl\ ex3-6}$ *(*$Ctnnb1^{tm2Bir}$*)* (Huelsken et al., 2001), β-$cat^{fl/fl\ ex2-6}$ *(*$Ctnnb1^{tm2Kem}$*)* (Brault et al., 2001) and Cat-ca *(*$Ctnnb1^{tm1Mmt}$*)* (Harada et al., 1999). Glast-CreERT2; β-$cat^{fl/fl\ ex3-6}$; RYFP mice, Glast-CreERT2; β-$cat^{fl/fl\ ex2-6}$; RYFP mice and Glast-CreERT2; Cat-ca; RYFP mice were crossed with BATGAL Wnt reporter mice (Maretto et al., 2003) to introduce the BATGAL Wnt reporter allele. BATGAL Wnt reporter mice were also crossed with Axin2-mTurQ ($Axin2^{em1Fstl}$) (de Roo et al., 2017) mice and TCF/Lef:H2B:mCherry ($(no\ gene)^{Tg(TCF/Lef1-HISTH2B/mCherry)}$) (Metzis et al., 2018). Nestin-GFP reporter mice have been previously described (Mignone et al., 2004).

Experimental groups included a combination of mice from different litters within each strain and both males and females were used for all *in vivo* studies.

2.1.2 Generation and Maintenance of Primary Cell Cultures

Primary adult hippocampal stem and progenitor cell (AHSPC) cultures were derived from 7-8-week-old BATGAL and β-cat$^{fl/fl\ ex3-6}$; RYFP mice. Animals were processed separately or in pools of up to two mice. Mice were sacrificed and the dentate gyrus (DG) was dissected as previously described (Walker et al., 2014). DGs were dissociated using the Neural Tissue dissociation kit (P) (Milteny Biotec, 130-092-628) and AHSPCs were amplified in non-adherent conditions as neurospheres for at least two passages. Neurospheres were maintained in Complete Neurosphere media consisting of Supplemented Neurosphere media (DMEM:F12 + Glutamax (Gibco, 11320), 1mg/ml KCl (Sigma, P5405) and 2mg/ml BSA (Sigma, A9056)) + 1x Neurocult Supplement (Stem Cell Technologies, 05701) + 1x Penicillin/Streptomycin (ThermoFischer Scientific, 15140) + 10ng/ml Fibroblast Growth Factor 2 (FGF2, Protech, 450-33) + 20ng/ml Epidermal Growth Factor (EGF, Protech, 315-09) + 2μg/ml Heparin (Sigma, A9056). Neurospheres were incubated at 37°C, 5% CO_2.

Once >400,000 AHSCs were obtained from the neurosphere cultures (quantified using a haemocytometer during passaging), they were dissociated and transferred to adherent culture conditions in a T25 flask. Adherent flasks were incubated with AHSPC media for a minimum of 1hr at 37°C before passaging to allow for Laminin pre-coating. AHSPC media consists of basal media (DMEM/F-12 + Glutamax (Invitrogen, 31331-093)) + 1x N2 Supplement (R&D Systems, AR009) + 1x Penicillin/Streptomycin (ThermoFischer Scientific, 15140) + 2μg/ml Laminin (Sigma, L2020) + 5μg/ml Heparin (Sigma, A9056) + 10-20ng/ml FGF2 (Protech, 450-33) + 20ng/ml EGF (Protech, 315-09). AHSPCs were incubated in AHSPC media at 37°C, 5% CO_2 until 80% confluent at which point they were either passaged or frozen down. AHSPCs were detached from the flask using Accutase (Sigma, A6964) and Accutase was stopped by washing the AHSPCs in phosphate buffered saline (PBS). AHSPCs in PBS were then centrifuged for 4.5min at 0.2rcf. AHSPC pellets were resuspended in AHSPC media and transferred to a fresh laminin pre-coated flask for propagation or were processed for freezing. For freezing, pelleted AHSPCs were resuspended in AHSPC media containing 10% dimethyl sulfoxide (DMSO, Sigma, D2650) and chilled slowly to -80°C before being transferred to liquid nitrogen for long-term storage.

To transition AHSPCs from AHSPC media containing both 20ng/ml FGF2 and 20ng/ml EGF to 20ng/ml FGF2 only, AHSPCs were grown in 20ng/ml FGF2 + 20ng/ml EGF AHSPC media until 80% confluent, at which point the AHSPC media was aspirated and refreshed with AHSPC

media containing 20ng/ml FGF2 only. AHSPCs were then incubated at 37°C, 5% CO_2 in the presence of 20ng/ml FGF2 only for 2-3 days until 100% confluent. Cells were then passaged in the presence of 20ng/ml FGF2 only for at least 2 passages before being used for any experiments to allow the cells time to acclimatise to the FGF2 only conditions.

2.1.3 *in vitro* Model of Active and Quiescent AHSPCs

AHSPCs were maintained in an active state using the culture conditions described above. 20ng/ml FGF2 + 20ng/ml EGF AHSC media and 20ng/ml FGF2 only AHSPC media were used to maintain active culture conditions.

To induce quiescence, media from active culture conditions (either 20ng/ml FGF2 +20ng/ml EGF AHSPC media or 20ng/ml FGF2 only AHSPC media) was replaced with 20ng/ml FGF2 only AHSPC media containing 20ng/ml recombinant BMP4 (R&D Systems, 5020-BP) (Blomfield et al., 2019). AHSPCs were then incubated at 37°C, 5% CO_2 for 48-72hrs to induce quiescence (Blomfield et al., 2019). Quiescent AHSPC media was refreshed every 72hrs where necessary. In all experiments, active AHSPCs were plated onto laminin pre-coated P6 well plates (200,000 cells/well), P24 well plates containing laminin pre-coated coverslips (50,000 cells/well) or laminin pre-coated 10cm dishes (1million cells/dish) and incubated overnight to allow AHSPCs to settle and adhere. The next day active AHSPC media was refreshed for quiescent AHSPC media and AHSPCs were incubated for 48-72hrs at 37°C, 5% CO_2 to establish quiescence prior to commencing experimental conditions.

2.2 Method Details

2.2.1 Tamoxifen and EdU Administration *in vivo*

To induce nuclear translocation of the CreERT2 recombinase in Glast+ AHSCs *in vivo*, 2-month-old adult mice were administered 2mg (57-67mg/kg) 4-hydroxy-tamoxifen (Sigma, H6278) or tamoxifen (Sigma, T5648) by intraperitoneal (ip) injection, at the same time each day for 5 consecutive days. All tamoxifen injections were performed by Crick BRF staff members. Brain tissue was collected by transcardial perfusion 6, 10 and 30 days after the first tamoxifen injection or was collected and dissected as fresh tissue for fluorescence-activated cell sorting (FACS) 10 days after the first tamoxifen injection.

To mark active AHSCs following 4x tamoxifen injections to induce recombination, GlastCreERT2; Cat-ca; RYFP P65 adult mice were administered 50mg/kg EdU by intraperitoneal injections 3 times in one day (09:00, 13:00 and 17:00). All EdU injections were performed by Crick BRF staff members. Brain tissue was collected by transcardial perfusion 1 day later.

2.2.2 Tissue Preparation and Immunofluorescence

For immunofluorescence of brain tissue, mice were transcardially perfused, under terminal anaesthesia, for 2 mins with PBS followed by 4% paraformaldehyde (PFA) in PBS for 12mins. Brains were post-fixed overnight in 4% PFA at 4°C with rocking and were then transferred to PBS containing 0.02% Sodium Azide. Brains were sectioned coronally at a thickness of 40μm using a vibratome (Leica) and sections were stored serially in P12 plates in PBS containing 0.02% sodium azide at 4°C. Brains were sectioned with the assistance of L. Chen. For immunofluorescence of cultured AHSPCs on coverslips, AHSPCs were fixed with 4% PFA/PBS for 10min at room temperature and were then washed and stored at 4°C with PBS.

Antigen retrieval was performed in brain sections prior to immunofluorescence. For antigen retrieval, samples were transferred to sodium citrate buffer (10mM, pH6.0) and incubated at 95°C for 2min. Following antigen retrieval, samples were blocked with 10% normal donkey serum (NDS) in 1% Triton-PBS for 2 hours at room temperature with rocking. Fixed AHSPCs were blocked with 10% NDS in 0.1% Triton-PBS for 1hr at room temperature.

For all sections and fixed AHSPCs on coverslips, primary antibodies were diluted as described in Table 1 in 10% NDS in 0.1% Triton-PBS and incubated with samples at 4°C overnight. The following day, samples were washed 3x 10-15min with 0.1% Triton-PBS. Secondary antibodies were diluted 1:500 in 10% NDS in 0.1% Triton-PBS and incubated with samples for 2hrs at room temperature with rocking. Samples were then washed 1x 10-15min with 0.1% Triton-PBS followed by 2x 10-15min washes with PBS. 4',6-diamidino-2-phenylindole (DAPI) was diluted 1:5,000 in 50% PBS:H_2O and incubated with brain sections for 30mins or fixed AHSPCs for 10mins at room temperature. Samples were then transferred to 50% PBS:H_2O in preparation for mounting. All washes and incubations of brain sections were 15mins with rocking and washes and incubations of fixed AHSPCs were 10mins. Primary and secondary antibodies are listed in Table 1.

EdU detection was performed following secondary antibody incubation and 2x washes in PBS and prior to DAPI incubation using the Click-iT™ EdU Alexa Fluor® 647 detection kit (Invitrogen, C10340) following manufacturer's instructions.

Immunostained sections were arranged onto a slide in PBS and excess PBS was carefully aspirated. Aqua Polymount (Polysciences, 18606) was applied to the edge of the slide and a 1.0 glass coverslip was carefully lowered over the samples ensuring even distribution of the Aqua Polymount across all sections. Slides were kept in the dark at room temperature overnight to dry before storing at 4°C prior to imaging.

Fixed AHSPCs on coverslips were mounted onto glass slides using Aqua Polymount. Six coverslips were arranged per slide and were carefully lowered onto a small amount of Aqua Polymount applied directly to the slide. Mounted coverslips were left to dry overnight in the dark at room temperature to dry before storing at 4°C prior to imaging.

Target Molecule	Species	Procedure	Dilution	Supplier	Catalogue #
Actin	Rabbit	WB	1:1000	Sigma-Aldrich	A2066
Ascl1	Mouse	IF	1:100	In house	N/A
Axin2	Rabbit	IF	1:1000	Abcam	ab32197
β-catenin	Mouse	IF-*in vivo*	1:100	BD Biosciences	610154
		IF-*in vitro*	1:250		
		WB	1:2000		
β-catenin (ABC)	Mouse	IF	1:200	Merck	05-665
β-catenin	Rabbit	IF	1:500	Sigma	C2206
β-galactosidase	Chicken	IF	1:1000	Aves Lab Inc.	BGL-1010
CyclinD1	Rabbit	IF	1:25	ThermoScientific	RM-9104
DCX	Goat	IF	1:50	Santa-Cruz	Discontinued
GFAP	Rat	IF	1:800	Invitrogen	13-0300
GFP	Chicken	IF	1:2000	Abcam	ab13970
Ki67	Mouse	IF	1:100	BD Biosciences	550609
Map2	Mouse	IF	1:200	Sigma	M4403
mCherry	Rabbit	IF	1:500	GeneTex	GTX128508
Sox2	Rat	IF	1:400	EBioscience	14-9811-82

Tbr2	Rabbit	IF	1:200	Abcam	ab183991
TdTomato	Goat	IF	1:1000	Sicgen	ABB181-200
Tuj1	Rabbit	IF	1:400	Covance	PRB-435P
Tuj1	Mouse	IF	1:400	Covance	MMS-435P
Wnt7a	Rabbit	WB	1:500	Abcam	ab100792
Chicken IgG	Donkey	IF-488	1:500	Jackson	703-545-155
Mouse IgG	Donkey	IF-488	1:500	Jackson	715-546-151
Rat IgG	Donkey	IF-Cy3	1:500	Jackson	712-166-153
Rabbit IgG	Donkey	IF-Cy3	1:500	Jackson	711-166-152
Mouse IgG	Donkey	IF-Cy3	1:500	Jackson	715-166-151
Goat IgG	Donkey	IF-647	1:500	Jackson	705-605-147
Mouse IgG	Donkey	IF-647	1:500	Jackson	715-606-151
Rabbit IgG	Donkey	IF-647	1:500	Jackson	711-606-152
Rat IgG	Donkey	IF-647	1:500	Jackson	112-175-167
Mouse IgG	Rabbit	WB-HRP	1:1000	Dako	P0161
Rabbit IgG	Goat	WB-HRP	1:1000	Dako	P0448

Table 1: Antibodes.

Colours indicate the conjugated fluorophores of the secondary antibodies used for immunofluorescence.

2.2.3 RNA *in situ* Probe Preparation

Primers were designed to generate an RNA *in situ* probe that spans exons 3-6 of β-catenin (from nt301 to nt1223 of National Centre for Biotechnology Information (NCBI) reference number NM_007614.3). Primers were designed with the addition of the sequence for the T7 polymerase binding sites (5'-TAATACGACTCACTATAGGG-3') on the Reverse Antisense and Forward Sense primers: Forward Antisense primer: 5'-CTGACCTGATGGAGTTGGAC-3' (Tm = 43.4°C). Reverse Antisense Primer + T7: 5'-TAATACGACTCACTATAGG GCTTGCTCTCTTGATTGCCAT-3' (Tm 44.1°C). Forward Sense Primer + T7: 5'-TAATACGACTCACTATAGGGCTGACCTGATGGAGTTGGAC-3' (Tm = 48.8°C). Reverse Sense Primer: 5'-CTTGCTCTCTTGATTGCCAT-3' (Tm = 24.8°C). Primer specificity was checked using Basic Local Alignment Tool (BLAST) from NCBI. This showed 100% homology with mouse β-catenin.

Mouse β-catenin^{ex3-6} probe was generated by PCR using the Q5 Hot Start High-Fidelity 2X Master Mix (New England Biolabs, M0494S) following manufacturer's instructions. Complementary DNA (cDNA) from cultured wild type (WT) active AHSPCs was used as template for the PCR reaction. 1μl of the PCR reaction was run on a 1% polyacrylamide gel to confirm successful amplification. PCR product was purified using the QIAquick PCR clean-up kit (Qiagen, 28104) following manufacturer's instructions.

Digoxigenin-(DIG) labelled probes were generated using the DIG RNA Labelling Mix 10X, (Roche, 11277073910) following manufacturer's instructions for a 20μl reaction. 1μg of purified PCR product was used to generate the DIG-labelled probe using the T7 Taq Polymerase (Roche, 10881775001). Generated probes were treated with DNase (Roche, 04716728001) according to manufacturer's instructions and 1.86μl 0.5M Ethylenediaminetetraacetic acid (EDTA) was added to stop the DNase reaction. The DIG-labelled probe was purified by adding 6.25μl 4M lithium chloride and 200μl 100% ethanol at -20°C and incubated at -80°C for 15mins, followed by centrifugation at 16,000rpm at 4°C for 10mins. The supernatant was removed and 20μl DEPC water, 2.5μl 4M lithium chloride and 75μl 100% ethanol at -20°C was added before repeating the incubation at -80°C and centrifugation steps listed above. After the second centrifugation, the supernatant was removed and the pellet re-suspended in 20μl DEPC water. Purified DIG-labelled probes were run on a Bioanalyser (Aligent Technologies Inc.) to check purity. 180μl of hybridisation buffer was added to the purified DIG-labelled probe and this was stored at -20°C. 50ml of hybridisation buffer consisted of: 25ml deionised formamide, 12.5ml 20x SSC, 1.25ml tRNA (10mg/ml), 2.5ml 100X Denhardt's solution, 2.5ml 500mg/ml herring sperm and 6.25ml H_2O. The hybridisation buffer was stored at -20°C until use.

2.2.4 Tissue Preparation and *in situ* hybridisation

For *in situ* experiments, mice were transcardially perfused as described above. Brains were cryoprotected in 30% sucrose/PBS at 4°C before embedding in OCT compound (Fisher Scientific, 12678646), freezing at -80°C, and coronally sectioned at a thickness of 40μm using a cryostat (Leica). Sections were stored serially in a P12 plate in PBS at 4°C.

Sections were washed 3x 5mins in PBS before being incubated in acetylation solution for 10mins. Acetylation solution recipe for 200ml is as follows: 2.66ml Triethanolamine (TEA), 0.32ml 36% hydrochloric acid (HCl), 0.5ml acetic anhydride and H_2O up to 200ml. Sections were

then washed 3x 5mins in PBS followed by an incubation in hybridisation buffer for 2 hrs at room temperature. During this incubation the probe was diluted 1:100 in hybridisation buffer, denatured for 10mins at 95°C, vortexed and kept on ice until use. Sections were then incubated overnight at 70°C in a humidified chamber. The following day, sections were washed with 5X saline-sodium citrate buffer (SSC) for 10mins at room temperature followed by 2x30mins washes with 0.2X SSC at 70°C. Sections were then washed in 0.2X SSC for 5mins at room temperature followed by 2x 5mins washes in Buffer 1 at room temperature. Buffer 1 recipe for 1L is as follows: 100ml 1M Tris-HCl pH7.5, 30ml 5M sodium chloride (NaCl) and H_2O up to 1L. Sections were blocked with 10% normal goat serum (NGS) in Buffer 1 for 1hr at room temperature. Sections were then incubated over-night at 4°C with anti-digoxygenin AP-antibody diluted 1:1500 in 10% NGS in Buffer 1. The next day sections were washed 3x 5mins with Buffer 1 at room temperature followed by 2x 10mins washes with NTMT at room temperature. NTMT recipe for 50ml is as follows: 1ml 5M NaCl, 5ml 1M Tris-HCl pH9.5, 2.5ml 1M magnesium chloride ($MgCl_2$) 0.5ml 10% Tween-20 and H_2O up to 50ml. NBT/BCIP Stock Solution (Roche, 11681451001) was prepared 1:100 in NTMT and incubated with sections at 37°C protected from light with gentle shaking for 2hrs until signal developed. Sections was briefly washed in NTMT followed by 3x 5mins washes with PBS. Sections were fixed with 4%PFA at room temperature for 10min before beginning the immunofluorescence protocol listed above.

2.2.5 Microscopic Analysis and Quantifications

Immunofluorescence samples were imaged using a SP5 confocal microscope (Leica). For brain sections both left and right DG of every twelfth 40μm section along the rostro-caudal axis were imaged. Whole 40μm sections were imaged with a 1μm z-step. For AHSPCs on coverslips, 3 random regions of each coverslip were imaged with a 1μm z-step.

RNA *in situ* hybridisation samples were imaged using a Zeiss Apotome microscope. Whole 40μm sections were imaged with a 1μm z-step and bright field and fluorescence channels were overlaid to identify AHSCs as described below.

2.2.6 Dentate Gyrus Dissections and Fluorescence-activated Cell Sorting (FACS)

Mice were sacrificed and the dentate gyrus was dissected as previously described (Walker et al., 2014). Dentate gyri were dissociated using the Neural Tissue dissociation kit (P) (Milteny

Biotec, 130-092-628) according to manufacturer's instructions. Dissociated cells were resuspended in 750μl recovery media (recipe for 50ml of recovery media: 45ml DMEM/F12 media without phenol red (Sigma, DG434) and 5ml 5% PBS-BSA) and 7.5μl DAPI (100X) was added to check for cell viability. All cells were sorted on a MoFLo XDP cell sorter machine (Beckman Coulter) using a 100μm nozzle at a maximum sort speed of 5000 events per second and an efficiency of more than 80%. The MoFLo XDP cell sorter machine (Beckman Coulter) was operated by the Crick Flow Cytometry Science Technology Platform (STP). Events were first gated to remove debris, aggregates and dead cells. Cells were then gated for YFP expression using a YFP negative control mouse. For experiments involving Glast-CreERT2; β-cat$^{fl/fl\ ex3-6}$; RYFP and Glast-CreERT2; β-cat$^{fl/fl\ ex2-6}$; RYFP strains, mice were processed for FACS separately and YFP+ cells from individual samples were collected directly in 700μl RL lysis buffer from the RNeasy® Mini Kit (Qiagen, 74104) for RNA extraction. Dissections and FACS of YFP+ cells from Glast-CreERT2; β-cat$^{fl/fl\ ex3-6}$; RYFP and Glast-CreERT2; β-cat$^{fl/fl\ ex2-6}$; RYFP strains were performed in collaboration with L. Harris and the Crick Flow Cytometry STP. Nestin-GFP mice were processed for FACS in pools of up to 5 mice and GFP+ cells were collected in 700μl recovery media and processed for single cell RNA sequencing. Dissections of Nestin-GFP mice were performed by L. Harris, M. Masdeu and myself. FACS of Nestin-GFP mice was performed by L. Harris and M. Masdeu in collaboration with the Crick Flow Cytometry STP.

2.2.7 RNA Extraction, Complementary DNA synthesis and Quantitative PCR

FACS sorted YFP+ cells from Glast-CreERT2; β-cat$^{fl/fl\ ex3-6}$; RYFP and Glast-CreERT2; β-cat$^{fl/fl\ ex2-6}$; RYFP strains collected in RL lysis buffer from the RNeasy® Mini Kit (Qiagen, 74104) were processed for RNA extraction according to manufacturer's instructions. Complementary DNA (cDNA) synthesis was performed using the Maxima First Strand cDNA Synthesis Kit for quantitative PCR (qPCR) (ThermoScientific, K1641) according to manufacturer's instructions.

Cultured AHSPCs were plated in P6 wells (200,000 cell/well) and were lysed by the direct addition of 700μl TRIzol reagent (Ambion, 15596018) to the P6 wells. RNA was extracted using the Direct-zol™ RNA MiniPrep Kit (Zymo Research, R2052) according to manufacturer's instructions. cDNA was synthesised using the High Capacity cDNA Reverse Transcription Kit (Applied Biosystems, 4387406) according to manufacturer's instructions.

Gene expression level was measured using TaqMan Gene expression assays (Applied Biosystems) and qPCR was performed on a QuantStudio Real-Time PCR machine (ThermoFisher). TaqMan probes used for qPCR were listed in Table 2 Gene expression was calculated relative to the endogenous controls *GAPDH* and *ActinB*, and normalised to control to provide a delta delta cycle threshold (ddCt) value.

Gene	Assay ID	Catalogue Number
ActinB	Mm00607939_s1	4352933E
Ascl1	Mm03058063_m1	4331182
Axin2	Mm00443610_m1	4331182
CyclinD1	Mm00432359_m1	4331182
Eomes (Tbr2)	Mm01351988_m1	4331182
GAPDH	Mm99999915_g1	4352932E
GFAP	Mm01253033_m1	4331182
Hes5	Mm00439311_g1	4331182
HopX	Mm00558630_m1	4331182
Id4	Mm00499701_m1	4331182
Nestin	Mm00450205_m1	4331182
Ngn2	Mm00437603_g1	4331182
Olig1	Mm00497537_s1	4331182
Olig2	Mm01210556_m1	4331182
CDKN1C (p57)	Mm00438170_m1	4331182
Slc1a3 (Glast)	Mm00600697_m1	4331182
Sox2	Mm00488369_s1	4331182
Tubb3 (Tuj1)	Mm00727586_s1	4331182
β-catenin exons 13-14	Mm00483039_m1	4331182
β-catenin exons 4-5	Mm01350386_g1	4351372

Table 2: List of TaqMan probes from Applied Biosystems used for qPCR gene expression assays.

2.2.8 RNA Sequencing and Analysis with Seurat

Dissections of Nestin-GFP DGs for single cell RNA sequencing experiments were performed by L. Harris, M. Masdeu and myself. Single cell RNA sequencing experiments of Fluorescence

activated cell sorted (FAC sorted) Nestin-GFP+ cells were performed by L.Harris and M. Masdeu in collaboration with the Crick Sequencing STP. Analysis of single cell RNA sequencing data was performed by L. Harris, Z. Gaber and S. Vaga. Nestin-GFP+ cells were collected in 700μl recovery media following FAC sorting and were subsequently spun down at 500G for 5min at 4°C. After removing all but 50μl of supernatant, cells were resuspended and loaded into the 10x Chromium machine for single cell RNA sequencing. Libraries were prepared using with 10x Genomics Chemistry, Single Cell 3' version 2. Following sequencing, cellRanger count (Version 3.0.2) was used to map the FASTQ files to the mouse genome and was then read into Seurat (Version 3.1.1) (Stuart et al., 2019) for analysis. The Seurat object was transformed using the SCTransform function. The 3,000 most variable genes and anchors were identified and the data was integrated using the default parameters. This integrated dataset was visualised using UMAP (Becht et al., 2019) with the first 30 principle components. Clusters were identified based on the expression of known marker genes and expression levels of genes of interest was performed using the FeaturePlot function in Seurat.

Bulk RNA sequencing of AHSPCs in active and quiescent culture conditions was performed by I. Blomfield in collaboration with the Crick Sequencing STP and analysed by S. Vaga as previously described (Blomfield et al., 2019). Briefly, the KAPA mRNA HyperPrep Kit for Illumina (KAPA, Biosystems, Wilmington, MA, USA) was used to according to manufacturer's instructions to prepare the libraries for sequencing. Libraries were sequenced using Hiseq4000 (Illumina) and quality of reads was evaluated using FastQC (Version 0.11.2) (Andrews. 2010). Sequences that passed the quality assessment using Trimmomatic (Version 0.32) (Bolger et al., 2014), were aligned to the mm10 genome using tophat2 (Version 2.0.14) (Kim et al., 2013) with bowtie2 (Version 2.1.0) (Langmead et al., 2012) or for the quiescent AHSPC dataset, Cufflinks (Trapnell et al., 2010). Transcript abundance level (transcript count) was generated using HTSeq (Version 0.5.3p9) (Anders et al., 2015) and were further processed using R software environment for statistical computing and graphics (Version 3.4.0). Normalisation, removal of batch effects and other variants was performed using EDASeq R package (Risso et al., 2011) and RUVseq package (remove unwanted variation from RNA sequencing package) (Risso et al., 2014).

2.2.9 Constructs, Plasmid Transfection and Viral Transduction

The 7TGC Wnt reporter plasmid was a gift from Roel Nusse (Addgene, plasmid # 24304) (Fuerer et al., 2010) and was supplied as a bacterial stab. Bacteria were streaked for single colonies on

an ampicillin (100μg/ml) agar plate and grown overnight. Isolated single colonies were then picked to inoculate an overnight culture in 3ml of LB broth + 0.1mg/ml ampicillin. 500μl of this overnight culture was amplified in 100ml LB broth + 0.1mg/ml ampicillin overnight. 500μl of this overnight culture was mixed with 50% glycerol in dH2O in a cryotube and frozen at -80°C to produce a glycerol stock of the plasmid. The 100ml overnight culture was then centrifuged for 15mins at 6693rcf at 4°C and the supernatant discarded. Pellets were then processed for plasmid isolation (MaxiPrep) using the EndoFree® Plasmid Maxi Kit (Qiagen, 12362) according to manufacturer's instructions or stored at -20°C until the MaxiPrep protocol was performed. The 7TGC plasmid identity was confirmed by Sanger sequencing performed by the Crick Genomics Equipment Park STP using the following primers: 5'-GGCCCGAAGGAATAGAAG-3' (Tm: 52.5°C) and 5'-AACGGGCCACTCCTC-3' (Tm: 57.8°C).

Active AHSPCs were cultured in laminin pre-coated T75 flasks in 20ng/ml FGF2 + 20ng/ml EGF AHSPC media prior to nucleofection with the 7TGC Wnt reporter plasmid. Active AHSPCs were detached using Accutase, as described previously, and counted. $5x10^6$ cells were used per 10μg of 7TGC plasmid for each nucleofection. Nucleofection was performed using the Amaxa mouse neural stem cell nucleofector kit (Lonza, VPG-1004) with an Amaxa Nucleofector II machine on programme A-033 according to manufacturer's instructions. Following nucleofection, $5x10^6$ cells were resuspended in 4ml 20ng/ml FGF2+ 20ng/ml EGF active AHSPC media and distributed between 8x laminin pre-treated coverslips in P24 wells (approximately $6.25x10^5$ cells, however many cells die after the nucleofection) and active AHSPC media (20ng/ml FGF2 + 20ng/ml EGF) was refreshed the next day. 48hrs after nucleofection, cells on coverslips in P24 wells were fixed with 4% PFA/PBS for 10mins at room temperature before being stored at 4°C in PBS until they were processed for immunofluorescence protocols. To induce quiescence in 7TGC nucleofected active AHSPCs, media was changed to quiescent culture conditions (20ng/ml FGF2 + 20ng/ml BMP4 AHSPC media) 24hrs after nucleofection and maintained for 72hrs before fixation as described above.

Cre adenovirus (Ad-CMV-iCre, Vector Biolabs, 1045) was used to induce the deletion of β-catenin in AHSPCs derived from β-cat$^{fl/fl\ ex3-6}$; RYFP mouse strain. β-cat$^{fl/fl\ ex3-6}$ AHSPCs in active AHSPC media (20ng/ml FGF2 + 20ng/ml EGF and 20ng/ml FGF2) were plated onto laminin pre-coated coverslips in P24 wells (50,000 cells/well), P6 wells (200,000 cells/well) or 10cm Petri dishes (1million cells). The following day, the active AHSPC media was refreshed with active AHSPC media only (non-transduced Control), active AHSPC media with 100 multiplicity

of infection (moi) empty adenovirus (Ad-CMV-Null, Vector Biolabs, 1300) or active AHSPCs media with 100moi Cre Adenovirus and incubated overnight. The following morning, active AHSPC media (20ng/ml FGF2 + 20ng/ml EGF and 20ng/ml FGF2) was refreshed and the AHSPCs collected for immunofluorescence, qPCR and Western blot analysis 24-, 48- and 72hrs post-virus transduction. To induce deletion of β-catenin in quiescent β-cat$^{fl/fl\ ex3-6}$ AHSPCs, the media was refreshed for quiescent AHSPC media (20ng/ml FGF2 + 20ng/ml BMP4), 24hrs after plating the active AHSPCs as described above. 72hrs later, the quiescent AHSPC media was refreshed with quiescent AHSPC media only (non-transduced Control), quiescent AHSPC media with 100moi empty adenovirus or quiescent AHSPCs media with 100moi Cre Adenovirus and incubated overnight. The quiescent AHSPC media was refreshed the following morning.

2.2.10 Cell Treatments

To inhibit and activate canonical Wnt signalling in active and quiescent AHSPC cultures, small molecule Wnt antagonists and agonists were added to active or quiescent AHSPC media and incubated with AHSPCs at 37°C, 5% CO_2 for various times before analysis. All treatments were performed in duplicate wells to generate technical repeats of each experimental condition for each biological replicate. Biological replicates constitute individual experiments initiated on separate days from consecutive AHSC passages. Experiments were repeated with three biological replicates (n=3) unless stated otherwise.

To inhibit canonical Wnt signalling in active AHSPC cultures, the following small molecule Wnt inhibitors were incubated with active AHSPCs for 24hrs or 48hrs: C59 (gifted by the J. Smith lab), Dkk1 (R&D Systems, 5897-DK), IWR (gifted by the J. Smith lab), LF3 (Sigma, SML1752), LGK974 (Cayman Chemical, 14072), sFRP1 (R&D Systems, 5396-SF) and sFPR3 (R&D Systems, 592-FR). For these experiments, active AHSPCs were plated on laminin pre-coated coverslips in P24 wells (50,000 cells/well) or laminin pre-coated P6 wells (200,000 cells/well) and incubated overnight at 37°C, 5% CO_2. The following day, active AHSPC media was refreshed for active AHSPC media supplemented with either the vehicle Control for each Wnt antagonist (either DMSO or 0.1% BSA/PBS) or active AHSPC media supplemented with one of the Wnt antagonists listed above. AHSPCs were collected for immunofluorescence and qPCR analysis 24hrs or 48hrs later. In all cases, the concentration of the Wnt antagonists used were titrated to optimise experimental conditions and treatment media was refreshed every 24hrs where necessary.

For experiments treating 7TGC transfected active AHSPCs with the Wnt antagonist LGK974, active AHSPCs were nucleofected as described above and plated onto laminin pre-coated coverslips in P24 wells ($6.25x10^5$ cells/well). The following day, the active AHSPC media was refreshed for active AHSPC media supplemented with either DMSO vehicle Control or 1μM, 2.5μM and 5μM LGK974 and samples were collected for immunofluorescence 24hrs later.

For the proof of principle experiment of Wnt inhibition, active AHSPCs were plated onto laminin pre-coated P6 wells (200,000 cells/well) and incubated at 37°C, 5%CO_2. Active AHSPC media was refreshed 24hrs later for active AHSPC media supplemented with either DMSO vehicle Control, the Wnt agonist 5μM CHIR99021 (BioVision, 1677-5), the downstream Wnt antagonist 30μM LF3, or both 5μM CHIR99021+ 30μM LF3. Samples were collected for RNA extraction and qPCR analysis 48hrs later. Treatment media was refreshed every 24hrs where necessary.

To stimulate canonical Wnt signalling using the GSK3β inhibitor CHIR99021 in active AHSPCs, active AHSPCs (10ng/ml FGF2) were plated onto laminin pre-coated coverslips in P24 wells (50,000 cells/well) or onto laminin pre-coated P6 wells (200,000 cells/well). Active AHSPC media (10ng/ml FGF2) was refreshed the following day and supplemented with either DMSO vehicle Control or 1μM CHIR99021, or 5μM CHIR99021 or 10μM CHIR99021. Active AHSPCs were collected 72hrs later for immunofluorescence and qPCR analysis. Treatment media was refreshed after 36hrs.

To stimulate canonical Wnt signalling using the GSK3β inhibitor CHIR99021 in quiescent AHSPCs, active AHSPCs (20ng/ml FGF2+ 20ng/ml EGF) were plated onto laminin pre-coated coverslips in P24 wells (50,000 cells/well) or onto laminin pre-coated P6 wells (200,000 cells/well). The following day, active AHSPC media (20ng/ml FGF2 + 20ng/ml EGF) was replaced with quiescent AHSPC media (20ng/ml FGF2 + 20ng/ml BMP4) and cells were incubated at 37°C 5% CO_2 for 48hrs. Afterwards, the quiescent AHSPC media was refreshed and supplemented with either DMSO vehicle Control or the indicated concentrations of CHIR99021. Samples were collected 6hrs, 12hrs, 24hrs, 48hrs and 72hrs later as indicated for immunofluorescence or qPCR analysis.

To compare the phenotype of stimulating canonical Wnt signalling in quiescent AHSPCs using the GSK3β inhibitor CHIR99021 vs recombinant Wnt3a (R&D Systems, 1324-WN), active AHSPCs (20ng/ml FGF2) were plated onto laminin pre-coated coverslips in P24 wells (50,000

cells/well) or P6 wells (200,000 cells/well) and incubated overnight at 37°C 5%CO_2. The following day, active AHSPC media was replaced with quiescent AHSPC media (20ng/ml FGF2 + 20ng/ml BMP4) and AHSPCs were incubated at 37°C 5%CO_2 for 72hrs. Following this, the quiescent AHSPC media was refreshed and supplemented with either vehicle Control (DMSO or 0.1%BSA/PBS) or 5μM CHIR99021 or 250ng/ml rWnt3a or 500ng/ml rWnt3a. Samples were collected 48hrs later for immunofluorescence and qPCR analysis. Treatment media was refreshed every 24hrs where necessary.

To stimulate canonical Wnt signalling in active β-cat$^{fl/fl\ ex3-6}$ AHSPCs after β-catenin deletion, active β-cat$^{fl/fl\ ex3-6}$ AHSPCs were treated with active AHSPC media (20ng/ml FGF2) supplemented with 5μM CHIR99021 48hrs after Cre and Null virus transduction as described above. 24hrs later, samples were collected in 700μl TRIzol for RNA extraction, cDNA synthesis and qPCR analysis.

To determine the reactivation rate of quiescent β-cat$^{fl/fl\ ex3-6}$ AHSPCs upon returning to active culture conditions after β-catenin deletion, Cre and Null adenoviruses were applied to quiescent β-cat$^{fl/fl\ ex3-6}$ AHSPCs to facilitate the deletion of β-catenin as described above. 48hrs after virus transduction, quiescent AHSPC media (20ng/ml FGF2 + 20ng/ml BMP4) was replaced with active AHSPC media (20ng/ml FGF2) following 2x PBS washes to remove any residual BMP4 in the wells. At this point some wells were refreshed with quiescent AHSPC media to maintain AHSPCs in a quiescent state throughout the experiment. Samples in quiescent culture conditions were collected at this time point as time point 0hrs and further samples in both active and quiescent culture conditions were collected 3 days and 6 days later for immunofluorescence and qPCR analysis. Media was refreshed every 72hrs for all conditions.

To label cells in S-phase of the cell cycle, 0.5μl of 10mM EdU (Invitrogen, C10340) was added to the AHSPC media of cells on coverslips in P24 wells for a final concentration of 10μM EdU in each well. The plates were agitated slightly to ensure even mixing of the EdU in the media and AHSPCs were incubated with the EdU for 45min-1hr at 37°C 5% CO_2 prior to fixation with 4% PFA/PBS for 10mins at room temperature. To label the mitochondria of AHSPCs in culture, AHSCs on coverslips in P24 wells were incubated with 30nM MitoTracker™ Deep Red (LifeTechnologies, M22426) for 1hr at 37°C 5% CO_2 prior to fixation with 4% PFA/PBS for 10mins at room temperature. Coverslips were stored in PBS in a P24 plate at 4°C before processing for immunofluorescence and EdU detection as described above.

To determine the effect of chronic loss of β-catenin in β-cat$^{fl/fl\ ex3-6}$ AHSPCs, active β-cat$^{fl/fl\ ex3-6}$ AHSPCs were plated in a T25 flask and transduced with either Cre or Null adenovirus as described above. These cells were maintained in the long-term in active culture conditions (20ng/ml FGF2). At 6-, 12- and 18 days after virus transduction, AHSPCs were plated on laminin pre-coated coverslips in P24 wells (50,000 cells/well) and in laminin pre-coated P6 wells (200,000 cells/well) and assayed for their maintenance as active AHSPCs, ability to enter a quiescent state and the ability to differentiate into astrocytes and neurons. After plating, transduced active β-cat$^{fl/fl\ ex3-6}$ AHSPCs were collected for immunofluorescence and qPCR analysis at the indicated times. To determine how chronic β-catenin deletion affects quiescent entry, plated transduced β-cat$^{fl/fl\ ex3-6}$ AHSPCs were switched to quiescent culture conditions (20ng/ml FGF2 + 20ng/ml BMP4) and were collected for immunofluorescence and qPCR analysis 72hrs later. To determine how chronic β-catenin deletion affects neuronal and astrocytic differentiation, the active AHSPC media (20ng/ml FGF2) on transduced β-cat$^{fl/fl\ ex3-6}$ AHSPCs was changed to basal media + 2% B27 to promote neuronal differentiation and to basal media + 2% FBS to promote astrocytic differentiation. AHSPCs were cultured in these media conditions at 37°C 5% CO_2 and samples were collected 5 days later for analysis.

2.2.11 Protein Purification and Western Blots

For Western blot analysis of β-catenin protein in active β-cat$^{fl/fl\ ex3-6}$ AHSPCs following Cre and Null adenovirus transduction, active β-cat$^{fl/fl\ ex3-6}$ AHSPCs were plated in laminin pre-coated 10cm dishes (1million AHSPCs per dish) and virus transduction in active β-cat$^{fl/fl\ ex3-6}$ AHSPCs was performed as described above. Samples were collected at the various time points after virus transduction as indicated. Non-transduced quiescent β-cat$^{fl/fl\ ex3-6}$ AHSPCs and dissected P14 hippocampus samples were used for Wnt7a Western blots. Upon sample collection, dishes were kept on ice whilst the AHSPC media was aspirated and AHSPCs were washed with ice-cold PBS. 250μl of lysis buffer (ThermoFischer Scientific, 87788) supplemented with phosphatase inhibitor (ThermoFischer Scientific, 78420), EDTA (ThermoFischer Scientific, 87788) and protease inhibitor (ThermoFischer Scientific, 87786) was added to the dishes and cells were scraped from the dish and collected in a 500μl Eppendorf. Samples were lysed under rotation at 4°C for 20mins and then centrifuged at 13,000 rpm at 4°C for 20mins. 400μl of supernatant was transferred to a clean Eppendorf and an equal volume of Laemmli sample buffer (Sigma, S3401-10VL) was added before boiling at 95°C for 5mins.

Samples were run on a polyacrylamide gel at 120V and then transferred onto a nitrocellulose membrane. Membranes were then blocked with 5% BSA in TBS-Tween for 90mins at room temperature with rocking. After blocking, membranes were incubated with primary antibody, diluted as described in Table 1 in 5% BSA in TBS-Tween + 0.02% sodium azide, overnight at 4°C under rotation. The following day membranes were washed 5x 10mins with TBS-Tween prior to incubation with secondary antibody, diluted as described in Table 1 in 5% milk in TBS-Tween, for 2hrs at room temperature with rocking. Membranes were washed 5x 10mins with TBS-Tween followed by 2x 10mins washes with TBS under rocking. Detection was performed using ECL Western Blotting reagents (Sigma, GERPN2106) according to manufacturer's instructions and blots were developed using Kodak films.

For Actin Western blots following the development of Wnt7a Western blots, membranes were washed 3x 10mins with TBS and the incubated with stripping buffer (ThermoScientific, 46430) for 30mins at room temperature with rocking. Membranes were washed 3x 10mins with TBS before repeating the steps listed above starting from the blocking step and using a primary antibody against Actin.

2.3 Quantifications and Statistical Analysis

2.3.1 Quantification of Immunofluorescence

All samples were blinded by a third party prior to quantification. AHSCs in DG images were identified as having a DAPI+ (Sox2+) cell body located within the subgranular zone (SGZ) co-localised with a GFAP+ radial projection through the granule cell layer (GCL) spanning a minimum of 2 cell nuclei away from the AHSC nucleus. Displaced AHSCs were identified as above but with the DAPI+ Sox2+ cell body being located more than 2 nuclei's distance away from the SGZ.

For quantifying the proportion of cells expressing specific markers in DG images, a minimum of 200 cells were counted per animal for a minimum of 3 animals per genotype. For quantifying the total number of cells/SGZ length mm, a minimum of 3 sections per series per mouse was quantified for a minimum of 3 mice per genotype. The freehand line tool in Fiji (Schindelin et al., 2012) was used to measure the length of the SGZ in μm. Fiji was used to measure the nuclear signal intensity of immunolabelled cells by selecting for the DAPI+ area of the identified cell in a

single z-plane and measuring the intensity in the selected channel (0-255 Arbitrary Units (A.U.).). A DAPI negative area in the hilus was chosen to measure the background levels of the signal and this value (0-255 A.U.) was subtracted from the value obtained from the immunolabelled cell.

For quantification of cultured AHSPC immunolabelled samples, the DAPI channel was used to generate a mask of all nuclei using the Fiji software. This mask was used to measure the average pixel intensity for each channel within the area of each nuclei. The proportion of cultured AHSPCs expressing specific markers was quantified by setting a signal threshold and expressing the number of positive cells as a percentage of the total number of cells. For each experiment, at least 100 cells were quantified across 3 biological replicates unless stated otherwise.

2.3.2 Statistical Analysis

Statistical analyses were conducted using an unpaired Student's t-test; One-way ANOVA with Tukey's or Dunnett's multiple comparison tests; Two-way Anova with Sidak's or Tukey's multiple comparisons tests and Three-way Anova with Tukey's multiple comparisons as appropriate using the Prism software. All error bars represent the mean ± SEM. Significance is stated as follows: ns, $p>0.05$. *, $p<0.05$. **, $p<0.01$. ***, $p<0.001$. ****, $p<0.0001$. The statistical details for each experiment are recorded in the figure legends.

Chapter 3. Results 1: Adult Hippocampal Stem Cells Respond to Canonical Wnt Signalling Independent of their Activation State

To understand the role of canonical Wnt signalling in regulating adult hippocampal stem cell (AHSC) biology and behaviour, I first worked to establish how these cells respond to canonical Wnt signalling *in vivo* and *in vitro*. As such, the aim of this chapter is to characterise the response of AHSCs to canonical Wnt signalling both *in vivo* and in the *in vitro* model system of active and quiescent adult hippocampal stem and progenitor cells (AHSPCs). In this chapter, I will present RNA sequencing data showing that AHSCs *in vivo* and AHSPCs *in vitro* express components of the canonical Wnt signalling pathway, which agrees with published works (Lie et al., 2005; Wexler et al., 2009). This shows that AHSCs *in vivo* and AHSPCs *in vitro* possess the necessary machinery to respond to canonical Wnt signalling. I will also present data from Wnt reporter models showing that AHSCs *in vivo* and AHSPCs *in vitro* respond heterogeneously to endogenous levels of canonical Wnt signalling in a manner that is independent of their activation state.

3.1 Adult Hippocampal Stem Cells Express Components of the Canonical Wnt Signalling Pathway *in vivo* and *in vitro*

3.1.1 Adult Hippocampal Stem Cells *in vivo* Express the Machinery to Respond to Canonical Wnt Signalling

To determine whether AHSCs *in vivo* express components of the canonical Wnt signalling pathway, I utilised the *in vivo* single cell RNA sequencing dataset generated by members of the Guillemot lab. To generate this dataset M. Masdeu, L. Harris and myself dissected the dentate gyrus (DG) of 2 month old Nestin-GFP adult mice (Mignone et al., 2004) as described (Walker et al., 2014). M. Masdeu and L. Harris then dissociated the dissected tissue to achieve a single cell suspension which was Fluorescence-Activated Cell (FAC) Sorted, in collaboration with the Crick Flow Cytometry Science Technology Platform (STP), for the Nestin-GFP+ population. Nestin is an intermediate filament protein that is transiently expressed in AHSCs and intermediate progenitor cells (IPCs) and disappears during differentiation (Dahlstrand et al., 1995). Therefore, FAC Sorting for Nestin-GFP+ cells selects for AHSCs and IPCs, although some astrocytes, oligodendrocyte precursor cells and oligodendrocytes were also obtained in

these preparations perhaps due to leaky expression of the randomly integrated Nestin-GFP reporter (Mignone et al., 2004). These cells were then processed for single cell RNA sequencing by M. Masdeu and L. Harris in collaboration with the Crick Sequencing STP. Analysis of these datasets was performed by S. Vaga, Z. Gaber and L. Harris. Datasets were merged using Seurat (Stuart et al., 2019) and visualised using Uniform Manifold Approximation and Projection (UMAP) for dimension reduction (Becht et al., 2019). The cluster identities were determined according to the expression of cell specific markers. Astrocytes and oligodendrocyte precursor cells/oligodendrocytes were removed from the dataset based on the expression of astrocyte and oligodendrocyte markers, such as *Aldoc* and *Mog*, and the data was re-clustered to visualise the AHSCs and IPCs only. The “AHSC” cluster was identified by the high expression of the AHSC markers *HopX* and *Apoe* and the low expression of the astrocyte marker *Aqp4* (Figure 3.1A). This cluster predominately contains AHSCs in a quiescent state due to their low expression of cell cycle genes such as *Mcm2*. In this dataset, active AHSCs could not be distinguished from proliferating IPCs due to their low numbers, therefore active AHSCs cluster alongside the IPCs according to their stage in the cell cycle. “G1 IPCs” were identified by the high expression levels of *Tbr2* as well as genes associated with G1 of the cell cycle such as *MCM2-7* (Figure 3.1A). The “G2/M/S Proliferating Cells” cluster was identified by the expression of genes associated with G2/M/S of the cell cycle such as Ki67 and includes active AHSCs and IPCs (Figure 3.1A). The “Differentiating IPCs” cluster was identified based on the expression of neuronal differentiation genes such as *NeuroD1* and *DCX* (Figure 3.1A). Visualisation of the cellular clusters in low-dimensional space using UMAP revealed that the AHSCs cluster away from the proliferating and differentiating IPCs, highlighting intrinsic differences between the quiescent AHSC and proliferating IPC populations.

Single cell RNA sequencing datasets are limited by the low sensitivity of sequencing methods detecting lowly expressed transcripts in some cells, highlighting that a lack of detection does not necessarily mean a lack of expression (Haque et al., 2017). Nevertheless, single cell RNA sequencing datasets are useful tools to compare the transcriptomes of different cell types and assess transcriptional heterogeneity within cell populations (Haque et al., 2017). I therefore used this single cell RNA sequencing dataset to examine the expression of Wnt associated genes within the AHSC and IPC clusters (Figure 3.1A). I found that subsets of cells within each cluster express components of the canonical Wnt signalling pathway. The Wnt receptors *Fzd1*, *Fzd2* and *Lrp6* (Figure 3.1B, 3.1C and 3.1D) are expressed in a proportion of both AHSCs and IPCs in a salt and pepper manner highlighting the heterogeneity of gene expression within these clusters. *Fzd3* (Figure 3.1E) appears to be more abundant in IPCs compared to AHSCs

suggesting a difference in the demand for Wnt signalling between AHSCs and IPCs. *Lrp5*, *Fzd6* and *Fzd9* (Figure 3.1F, 3.1G and 3.1H) are expressed in both the AHSC and IPC clusters, however, fewer cells express these Wnt receptors. *Fzds 4*, *7* and *8* are expressed by very few cells within the AHSC and IPC clusters (data not shown).

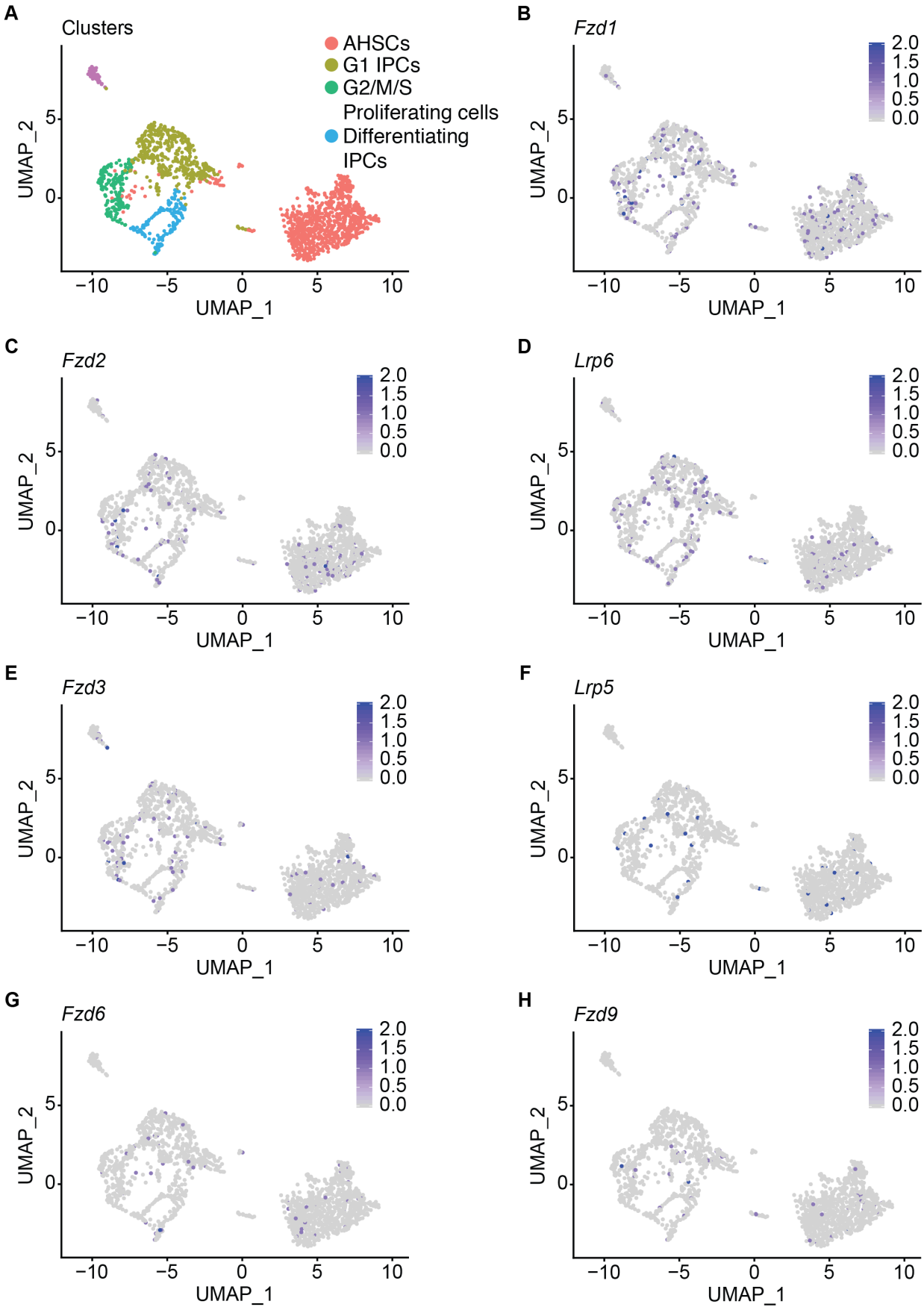


Figure 3.1: *in vivo* single cell RNA sequencing data showing the expression of Wnt receptors in Nestin-GFP+ AHSCs and IPCs.

Dissection of Nestin-GFP mice was performed by M. Masdeu, L. Harris and myself. Samples were processed for FAC Sorting by M. Masdeu and L. Harris and GFP+ cells were sorted in collaboration with the Crick Flow Cytometry STP. Single cell RNA sequencing of Nestin-GFP+ cells was performed by M. Masdeu and L. Harris in collaboration with the Crick Sequencing STP. Analysis of this data was performed by S. Vaga, Z. Gaber and L. Harris and is used here with permission.

(A) UMAP plot showing the clusters of cells FAC Sorted from 2-month-old Nestin-GFP mice. Cluster identities were determined based on the expression patterns of cell specific markers.

(B, C, D, E, F, G, H) UMAP plots showing the gene expression patterns of the Wnt receptors *Fzd1* **(B)**, *Fzd2* **(C)**, *Lrp6* **(D)**, *Fzd3* **(E)**, *Lrp5* **(F)**, *Fzd6* **(G)** and *Fzd9* **(H)** within the AHSC and IPC clusters described in **(A)**.

Both AHSCs and IPCs express downstream Wnt pathway components such as *APC* and *GSK3β* of the β-catenin destruction complex (Figure 3.2B and 3.2C). AHSCs, and to a higher extent IPCs, also express the transcription factor *β-catenin*, which is essential for the activation of a canonical Wnt dependent transcriptional programme (Figure 3.2D). They also express the co-transcription factors *Lef1* and *TCF7l2* (Figure 3.2E and 3.2F) of the transcription activator complex indicating that they are expressing the machinery that will allow them to respond to canonical Wnt signalling. Axin2 is a component of the β-catenin destruction complex and is a direct target gene of canonical Wnt signalling (Yan et al., 2001b; Jho et al., 2002). As such, *Axin2* expression is commonly used as a read-out of canonical Wnt signalling levels in cells (Yan et al., 2001b; Jho et al., 2002). Few cells express *Axin2* in both the AHSC and IPC clusters (Figure 3.2G), which could indicate that the endogenous level of canonical Wnt signalling is low in AHSCs and IPCs. However, the low detection of *Axin2* expression levels could reflect the limitations of single cell RNA sequencing, as genes that are lowly expressed can remain undetected using this technique (Haque et al., 2017).

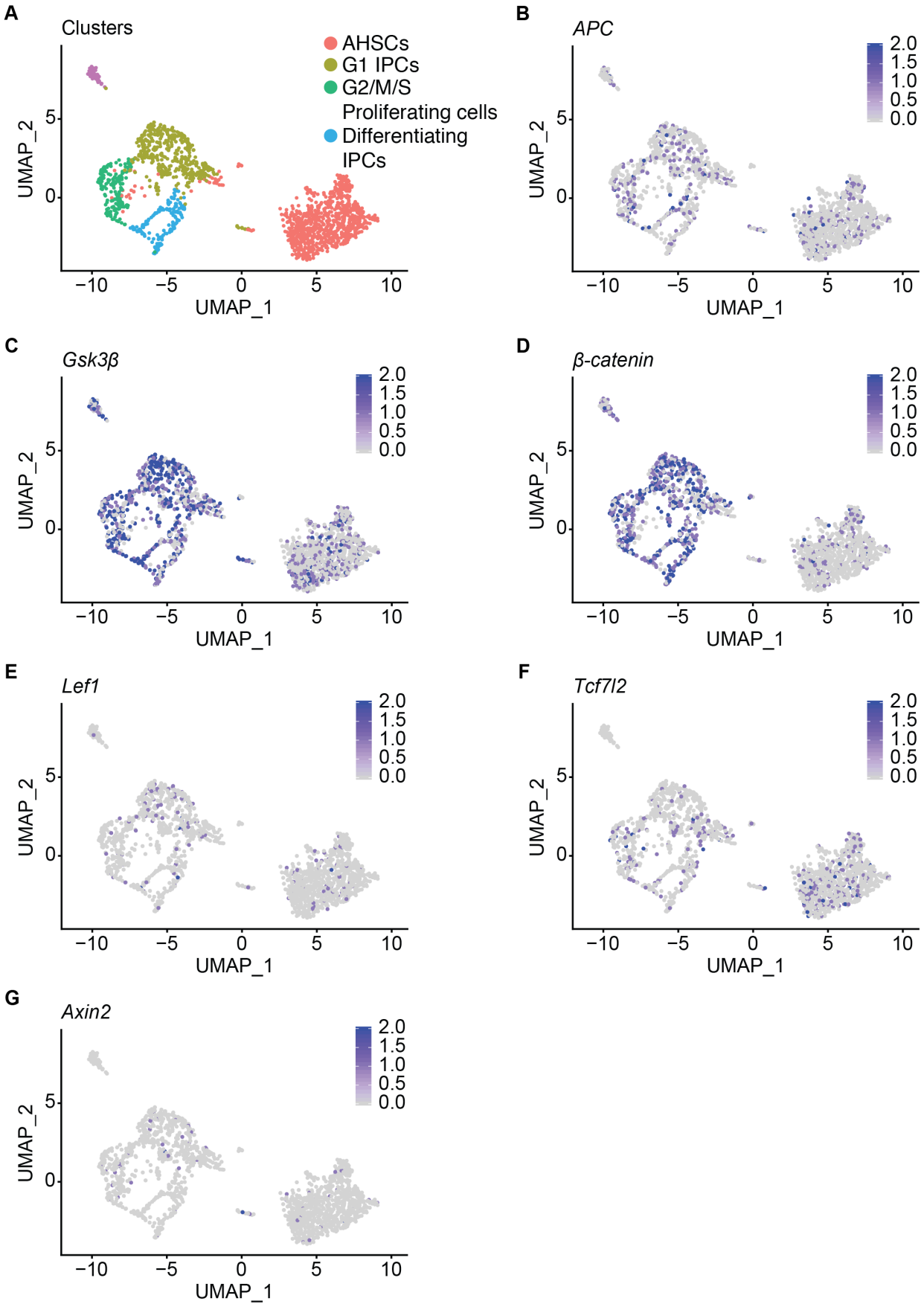


Figure 3.2: *in vivo* single cell RNA sequencing data showing the expression of Wnt pathway components in Nestin-GFP+ AHSCs and IPCs.

(A) UMAP plot showing the clusters of cells FAC Sorted from Nestin-GFP 2-month-old mice. Cluster identities were determined based on the expression patterns of cell specific markers. **(B, C, D, E, F, G)** UMAP plots showing the gene expression patterns of the Wnt pathway components *APC* **(B)**, *Gsk3β* **(C)**, *β-catenin* **(D)**, *Lef1* **(E)**, *Tcf7l2* **(F)** and *Axin2* **(G)** within the AHSC and IPC clusters described in **(A)**.

A subset of AHSCs and IPCs also express Wnt ligands such as *Wnt5a*, *Wnt7a*, *Wnt7b* and *Wnt8b* (Figure 3.3B, 3.3C, 3.3D and 3.3E), suggesting that these cells could be producing their own Wnt ligands within the DG niche. In addition, AHSCs and IPCs express the Wnt inhibitors *Dkk3* and *sFRP1* (Figure 3.3F and 3.3G), indicating that these cells play a role in regulating Wnt signalling levels within the DG neurogenic niche.

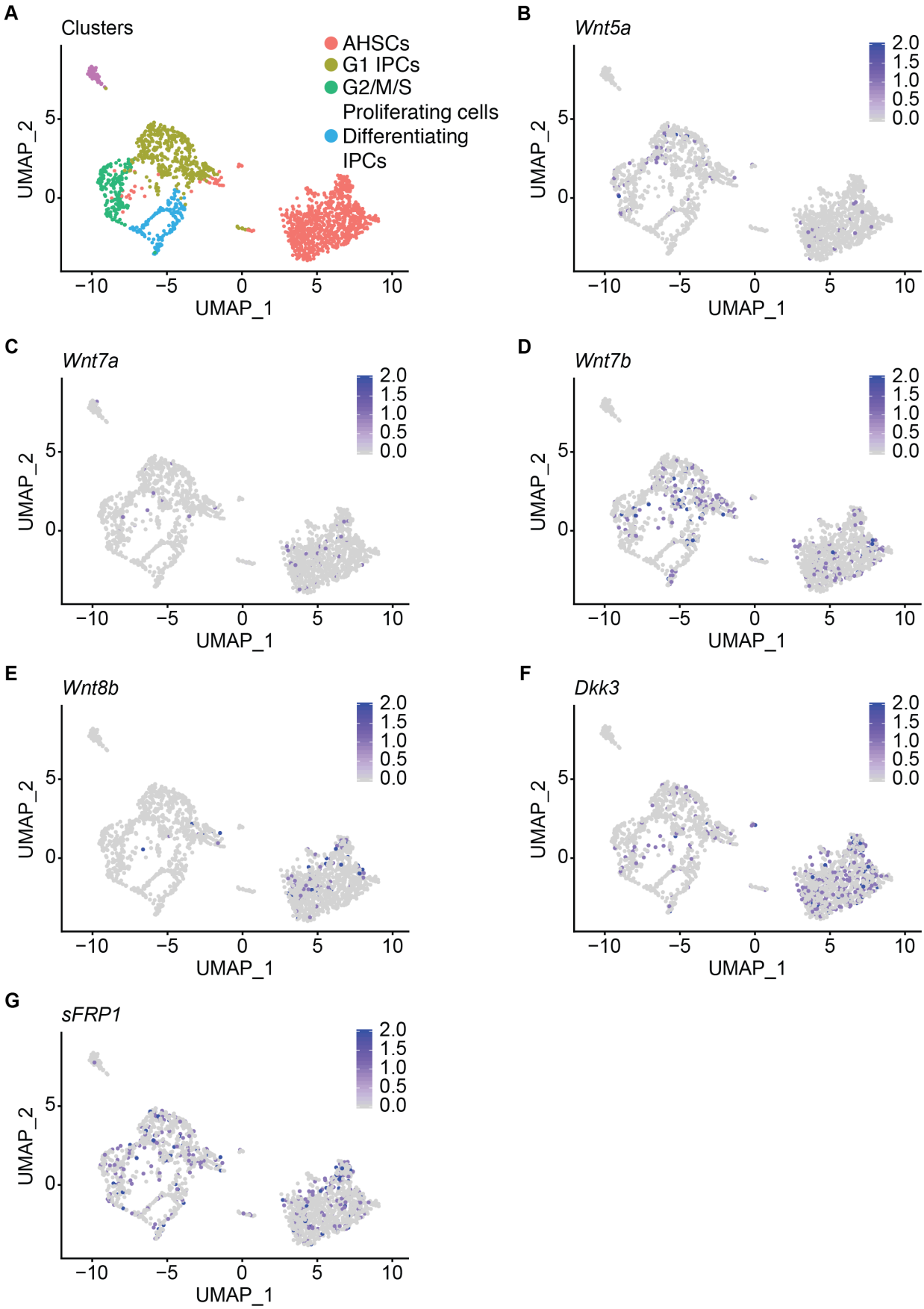


Figure 3.3: *in vivo* single cell RNA sequencing data showing the expression of Wnt ligands and Wnt inhibitors in Nestin-GFP+ AHSCs and IPCs.

(A) UMAP plot showing the clusters of cells FAC Sorted from Nestin-GFP 2-month-old mice. Cluster identities were determined based on the expression patterns of cell specific markers. **(B, C, D, E, F, G)** UMAP plots showing the gene expression patterns of the Wnt ligands and inhibitors *Wnt5a* **(B)**, *Wnt7a* **(C)**, *Wnt7b* **(D)**, *Wnt8* **(E)**, *Dkk3* **(F)** and *sFRP1* **(G)** within the AHSC and IPC clusters described in **(A)**.

I also used immunofluorescence techniques to determine the protein expression of β-catenin in AHSCs *in vivo*, which is the key transcription factor essential for the transduction of canonical Wnt signalling (Molenaar et al., 1996). AHSCs can be identified based on their expression of cell markers such as glial fibrillary associated protein (GFAP), their subgranular zone (SGZ) cell body location and their characteristic radial morphology. Therefore, in these sections AHSCs were identified as having a DAPI+ cell body located in the SGZ of the DG with a GFAP+ radial projection through the granule cell layer (GCL) (Figure 3.4, arrowheads). Co-immunolabelling of AHSCs with two different antibodies against the C-terminal domain of β-catenin showed that AHSCs are positive for β-catenin protein (Figure 3.4). Overall, this data shows that AHSCs *in vivo* express canonical Wnt pathway components at both the mRNA and protein level, indicating that they have the necessary machinery to respond to canonical Wnt signalling.

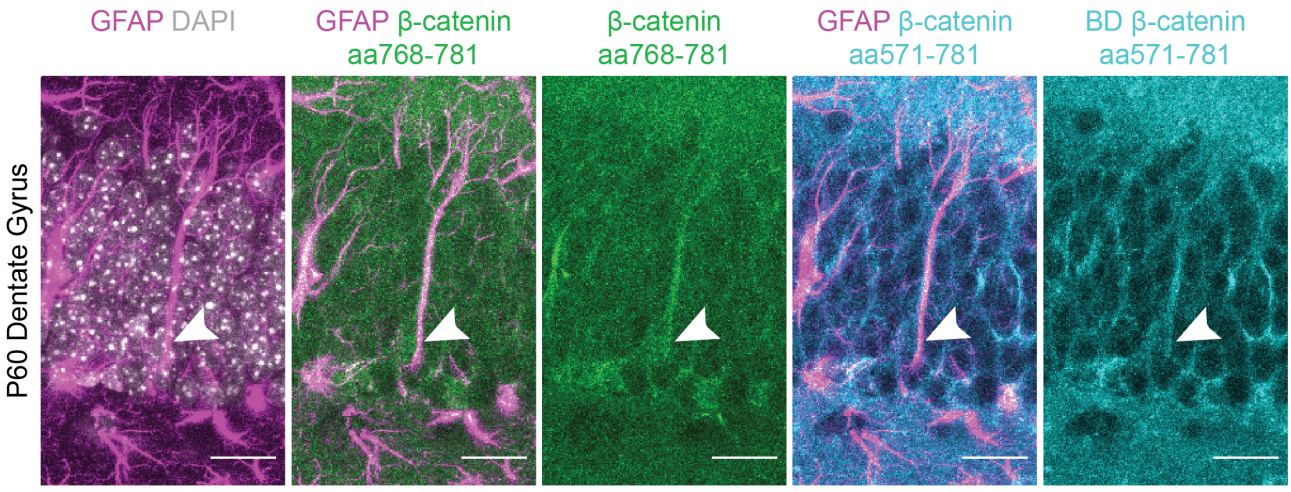


Figure 3.4: AHSCs express β-catenin at the protein level.

Representative images of a GFAP+ β-catenin+ AHSC in the dentate gyrus (DG) of a 2-month-old mouse. AHSCs were identified as cells with an SGZ located DAPI+ cell body with a GFAP+ radial projection through the GCL. Co-immunolabelling with two different antibodies raised against the C-terminal domain of β-catenin highlighted β-catenin+ AHSCs (arrowhead). Scale bars represent 20μm.

3.1.2 Active and Quiescent AHSPC Cultures Recapitulate the Gene Expression Patterns of Wnt Pathway Components Observed *in vivo*.

As previously described, I. Blomfield of the Guillemot lab established an *in vitro* model of AHSPCs in both an active and quiescent state (Blomfield et al., 2019). In this model, active AHSPCs are maintained in an active/proliferative state by culturing them in the presence of high concentrations of mitogens (10-20ng/ml FGF2 + 20ng/ml EGF or 10-20ng/ml FGF2 only) (Blomfield et al., 2019). A reversible state of quiescence can be induced in active AHSPC cultures through the addition of BMP4 (10-20ng/ml FGF2+ 20ng/ml BMP4) (Blomfield et al., 2019). This model not only allows me to investigate the role of canonical Wnt signalling in active and quiescent AHSPCs, but also allows me to investigate the role of canonical Wnt signalling in the switch between these two AHSPC states. Additionally, it is a useful tool to investigate the molecular mechanisms induced by canonical Wnt signalling in AHSPCs. Before investigating these molecular mechanisms, I first needed to establish whether the AHSPC cultures express components of the canonical Wnt signalling pathway as they do *in vivo* (Figures 3.1, 3.2 and 3.3). To do this, I used bulk RNA sequencing datasets generated by I. Blomfield of both active (10ng/ml FGF2) and quiescent (10ng/ml FGF2 + 20ng/ml BMP4) AHSPC cultures. Using these datasets, I compared the gene expression levels of Wnt pathway components between active and quiescent AHSPC cultures and compared this to the *in vivo* data.

AHSPCs *in vitro* express a variety of Frizzled (Fzd) Wnt receptors such as *Fzd1*, *Fzd2*, *Fzd3*, *Lrp5* and *Lrp6* (Figure 3.5A) recapitulating the *in vivo* observations. These Wnt receptors appear to be differentially expressed between the active and quiescent cultures, for example *Fzd2*, *Fzd9*, *Fzd8* and *Lrp5* are more highly expressed in active AHSPCs, whereas *Fzd1*, *Fzd3* and *Fzd5* are more highly expressed in quiescent AHSPCs. This could reflect varying demands for Wnt signalling between active and quiescent AHSPCs. Other Wnt pathway components, such as *β-catenin*, *Gsk3β* and *Dvl3* (Figure 3.5B) are more highly expressed in active AHSPCs compared to quiescent AHSPCs, which could again reflect a greater demand for canonical Wnt signalling in active AHSPCs. However, the Wnt target gene *Axin2* (Figure 3.5B) is expressed at a similar level in both active and quiescent AHSPC cultures. This could indicate that *Axin2* is regulated by other transcription factors in AHSPCs *in vitro*. Alternatively, it could suggest that active and quiescent AHSPCs respond similarly to canonical Wnt signalling despite potential differing demands for the upstream pathway components and cell surface receptors.

I also found that active and quiescent AHSPCs express a number of Wnt ligands (Figure 3.5C) that have been shown to preferentially activate both the canonical and non-canonical Wnt signalling pathways. The non-canonical Wnts, *Wnt5a* and *Wnt5b* are differentially expressed between active and quiescent AHSPCs with *Wnt5a* being more highly expressed in both states compared to *Wnt5b* (Figure 3.5C). The canonical Wnts, *Wnt7a* and *Wnt7b*, are expressed in both active and quiescent AHSPCs but are more highly expressed in active AHSPCs (Figure 3.5C). Wnt ligand expression is translated into protein in these AHSPC cultures, as shown by Western blot of Wnt7a in quiescent AHSPC lysate (Figure 3.5D). The production of Wnt ligands alongside the expression of *Fzd* Wnt receptors in active and quiescent AHSPCs suggests the possibility of autocrine or paracrine Wnt signalling within these AHSPC cultures and highlights their ability to regulate their own behaviour.

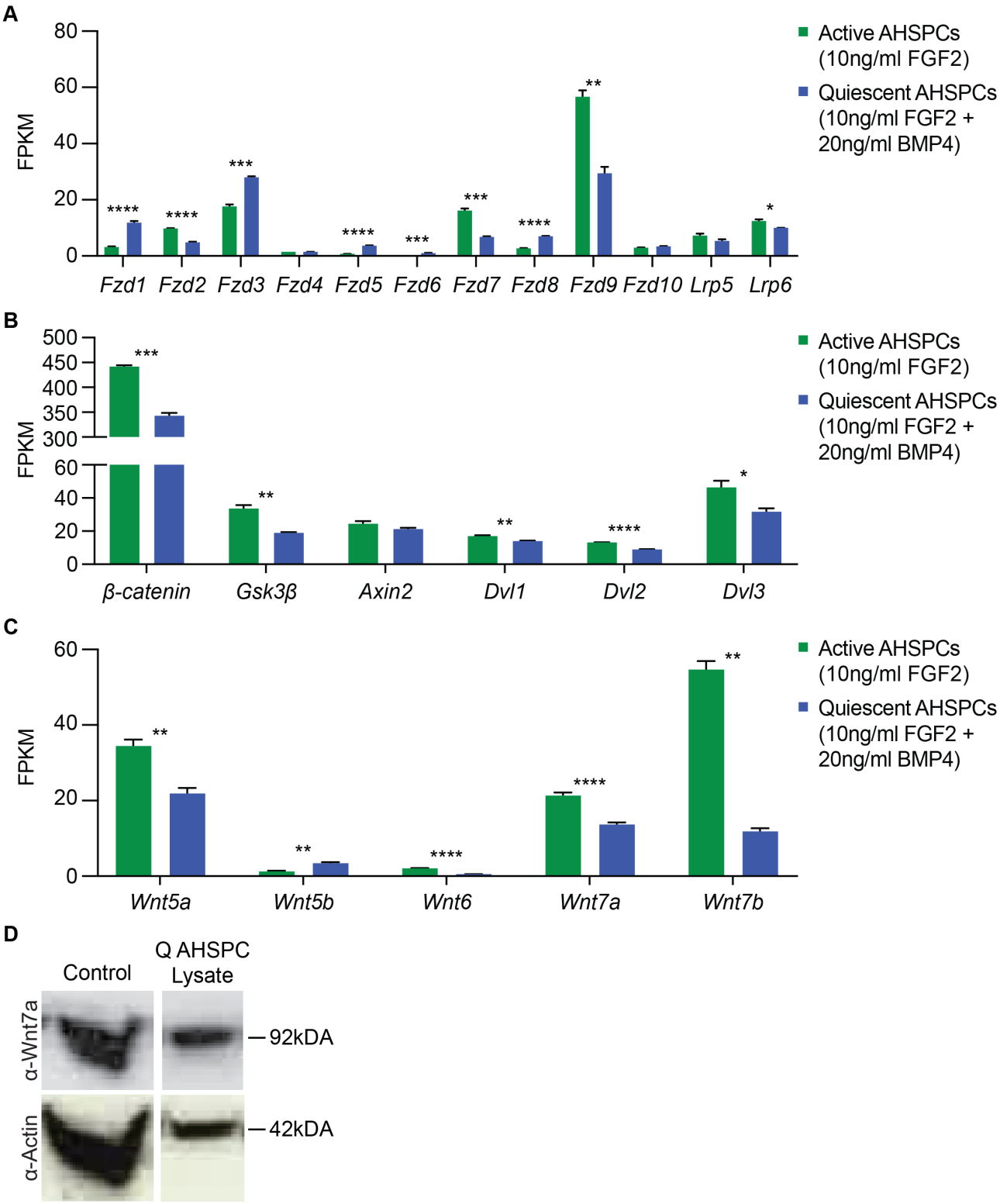


Figure 3.5: Bulk RNA sequencing and Western blot analysis of Wnt pathway components in active (10ng/ml FGF2) and quiescent (10ng/ml FGF2 + 20ng/ml BMP4) AHSPC cultures. RNA sequencing data from active and quiescent AHSPC cultures was produced by I. Blomfield and analysed by S. Vaga. These data are used here with permission. An unpaired Student's t-

test was used for statistical analysis, (*, p<0.05. **, p<0.01. ***, p<0.001. ****, p<0.0001). Error bars represent mean with SEM. n=3 biological replicates.

(A, B, C) RNA sequencing analysis comparing the gene expression levels of Wnt receptors **(A)**, Wnt pathway components **(B)** and Wnt ligands **(C)** between active (FGF2 10ng/ml) and quiescent (10ng/ml FGF2 + 20ng/ml BMP4) AHSPC cultures. **(A)** Differential expression of Wnt receptors between active and quiescent cultures could reflect different demands for canonical Wnt signalling between AHSPC states. **(B)** Similar expression levels of *Axin2* suggests similar levels of Wnt signalling in active and quiescent AHSPC cultures. **(C)** Expression of Wnt ligands in both active and quiescent AHSPC cultures highlights the possibility of autocrine/paracrine Wnt signalling. FPKM = Fragments per Kilobase of transcript per Million mapped reads.

(D) Wnt7a Western Blot in quiescent AHSPC lysates shows that quiescent AHSPCs produce Wnt protein. Lysate from dissected P14 hippocampus samples was used as a positive control.

3.2 AHSCs *in vivo* Respond to Canonical Wnt Signalling Independently of their Activation State

By using the *in vivo* single cell RNA sequencing dataset of Nestin-GFP+ FAC Sorted cells, I found that AHSCs express components of the canonical Wnt signalling pathway, indicating that they possess the machinery to respond to canonical Wnt signalling. I next wanted to investigate whether AHSCs respond to canonical Wnt signalling *in vivo* under normal conditions. The expression of the Wnt target gene *Axin2*, observed in some AHSCs from the single cell RNA sequencing dataset, indicated that some AHSCs *in vivo* respond to canonical Wnt signalling (Figure 3.2G). To investigate this further, I took advantage of available Wnt reporter mouse models that exploit the transcriptional activation mechanism of canonical Wnt signalling to provide a read-out of canonical Wnt signalling levels in cells. One model used was the BATGAL Wnt reporter mouse model (Maretto et al., 2003). These transgenic mice were engineered to express the *LacZ* gene under the control of 7 x β-catenin/TCF/LEF responsive elements (Maretto et al., 2003). This means that cells responding to canonical Wnt signalling in these mice will express nuclear β-galactosidase. The β-galactosidase reporter can be visualised through its reaction with X-gal (5-bromo-4-chloro-3-indolyl-β-D-galactopyranoside), which is a soluble colourless glycoside consisting of galactose linked to a substituted indolyl. β-galactosidase hydrolyses X-gal thus releasing the indolyl group from galactose (Trifonov et al., 2016). Dimerisation of two indolyl moieties and their subsequent oxidation results in the production of an insoluble blue/indigo precipitate that represents the expression of the β-

galactosidase reporter (Cotson et al., 1958; Trifonov et al., 2016). For all experiments throughout this thesis, β-galactosidase expression was visualised with immunofluorescence techniques using an antibody against β-galactosidase. This approach was used to allow for co-immunolabelling with cell specific markers to characterise the cells of the neurogenic lineage for their response to canonical Wnt signalling *in vivo*.

I used 2-month-old BATGAL mice to characterise the cells within the DG for their response to canonical Wnt signalling. Immunostaining for β-galactosidase in the DG of 2-month-old BATGAL mice, showed that a large number of cells within the DG were BATGAL+ (β-galactosidase+) and therefore responding to canonical Wnt signalling (Figure 3.6A). As the levels of Wnt ligands and Wnt inhibitors change with age (Seib et al., 2013; Okamoto et al., 2011; Miranda et al., 2012), I also looked at 7-month-old BATGAL mice, to see how the response to canonical Wnt signalling in the DG changes with age (Figure 3.6B). I found that there are fewer BATGAL+ cells in the DG of 7-month-old BATGAL mice (Figure 3.6B), which could reflect the age-dependent changes in the niche microenvironment (Seib et al., 2013; Okamoto et al., 2011; Miranda et al., 2012).

By combining immunostaining of the canonical Wnt reporter β-galactosidase with immunostaining of neurogenic lineage markers, I characterised the cells across the neurogenic lineage for their Wnt responsiveness. As before, AHSCs were identified by the localisation of their cell body in the SGZ and the presence of a GFAP+ radial process projecting through the GCL (Figure 3.6A and 3.6B). Quantifying the proportion of BATGAL+ AHSCs in 2-month-old and 7-month-old BATGAL mice showed that around 30% of the AHSCs were BATGAL+ in 2-month-old BATGAL mice compared with 20% BATGAL+ AHSCs in 7-month-old mice, however this was not statistically significant (Figure 3.6C). This indicates that AHSCs' response to canonical Wnt signalling slightly decreases with age, which could be due to the reported age-associated changes in the levels of canonical Wnt signalling within the hippocampal niche microenvironment (Seib et al., 2013; Okamoto et al., 2011). To determine the level of response to canonical Wnt signalling in AHSCs, I measured the signal intensity of the β-galactosidase staining in BATGAL+ AHSCs of 2-month-old and 7-month-old mice (Figure 3.6D). The range of values in the β-galactosidase signal intensity suggests that AHSCs respond heterogeneously to canonical Wnt signalling (Figure 3.6D). This heterogeneous response could be due to fluctuations in the levels of Wnt ligands or Wnt inhibitors throughout the niche microenvironment. Variations in the measured β-galactosidase signal intensities could also reflect different timings of activation between AHSCs. Therefore, it is possible that all AHSCs respond uniformly to

canonical Wnt signalling but exhibit a temporal heterogeneity in their response. Comparing the β-galactosidase signal intensity of BATGAL+ AHSCs in 2-month-old vs 7-month-old mice, shows that on average AHSCs respond similarly to canonical Wnt signalling with age (Figure 3.6D).

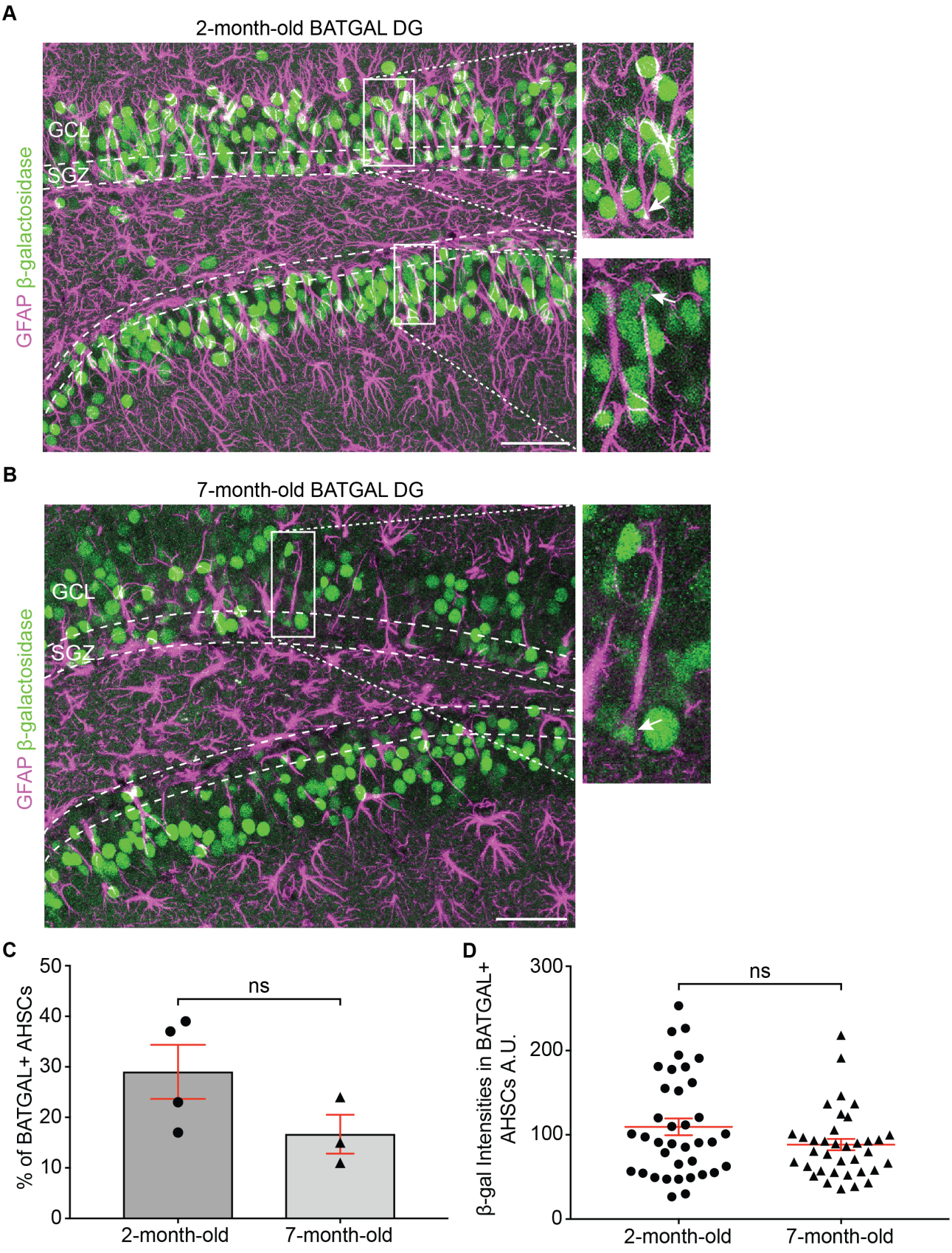


Figure 3.6: Wnt responding AHSCs in the Dentate Gyrus of 2-month-old and 7-month-old BATGAL Wnt reporter mice.

(A, B) β-galactosidase immunolabelling in the dentate gyrus of 2-month-old **(A)** and 7-month-old **(B)** BATGAL Wnt reporter mice, showing that cells in the SGZ and GCL respond to canonical Wnt signalling. Enlarged boxes indicate BATGAL+ AHSCs (identified as GFAP+ cells with radial morphology). Scale bars represent 50μm.
(C) Quantification of the proportion of BATGAL+ AHSCs in 2-month-old **(A)** and 7-month-old **(B)** mice. An unpaired Student's t-test was used for statistical analysis, (ns, $p>0.05$). Error bars represent mean with SEM. n=4 for 2-month-old and n=3 for 7-month-old.
(D) Quantification of the intensities of β-galactosidase immunolabelling in BATGAL+ AHSCs in young 2-month-old vs old 7-month-old mice. The spread of these values indicates a heterogeneous response to canonical Wnt signalling in AHSCs in young and old mice. A.U. = Arbitrary Units. An unpaired Student's t-test was used for statistical analysis (ns, $p>0.05$). Error bars represent mean with SEM. n=4 for 2-month-old and n=3 for 7-month-old.

As well as the AHSCs, I also characterised the cells along the neurogenic lineage for their response to canonical Wnt signalling in 2-month-old BATGAL mice. Co-immunolabelling of β-galactosidase alongside markers for IPCs (Sox2+ GFAP-) and neuroblasts (DCX+) highlighted that some IPCs and neuroblasts were BATGAL+ and therefore responding to canonical Wnt signalling (Figure 3.7A and 3.7B). However, quantifying the proportion of BATGAL+ IPCs and neuroblasts showed that very few responded to canonical Wnt signalling compared with AHSCs and neurons (Figure 3.7C). The proportion of Wnt responding astrocytes (GFAP+) is also slightly reduced compared to AHSCs and significantly reduced compared to neurons (Figure 3.7C). This highlights how the different cell types across the neurogenic lineage respond differently to canonical Wnt signalling despite residing within similar niche locations, emphasising the context dependency of their response. I also measured the β-galactosidase signal intensity in BATGAL+ cells across the neurogenic lineage as an indication of their level of response to canonical Wnt signalling (Figure 3.7D). AHSCs and neurons respond quite variably to canonical Wnt signalling whereas the few neuroblasts that were BATGAL+ exhibited lower β-galactosidase signal intensity (Figure 3.7D). On average, BATGAL+ IPCs respond similarly to canonical Wnt signalling compared to AHSCs and neurons, however they do not exhibit the same variability in β-galactosidase signal intensity (Figure 3.7D). This pattern of Wnt responsiveness across the cells of the neurogenic lineage suggests that canonical Wnt signalling has a role at both early and late stages of adult neurogenesis.

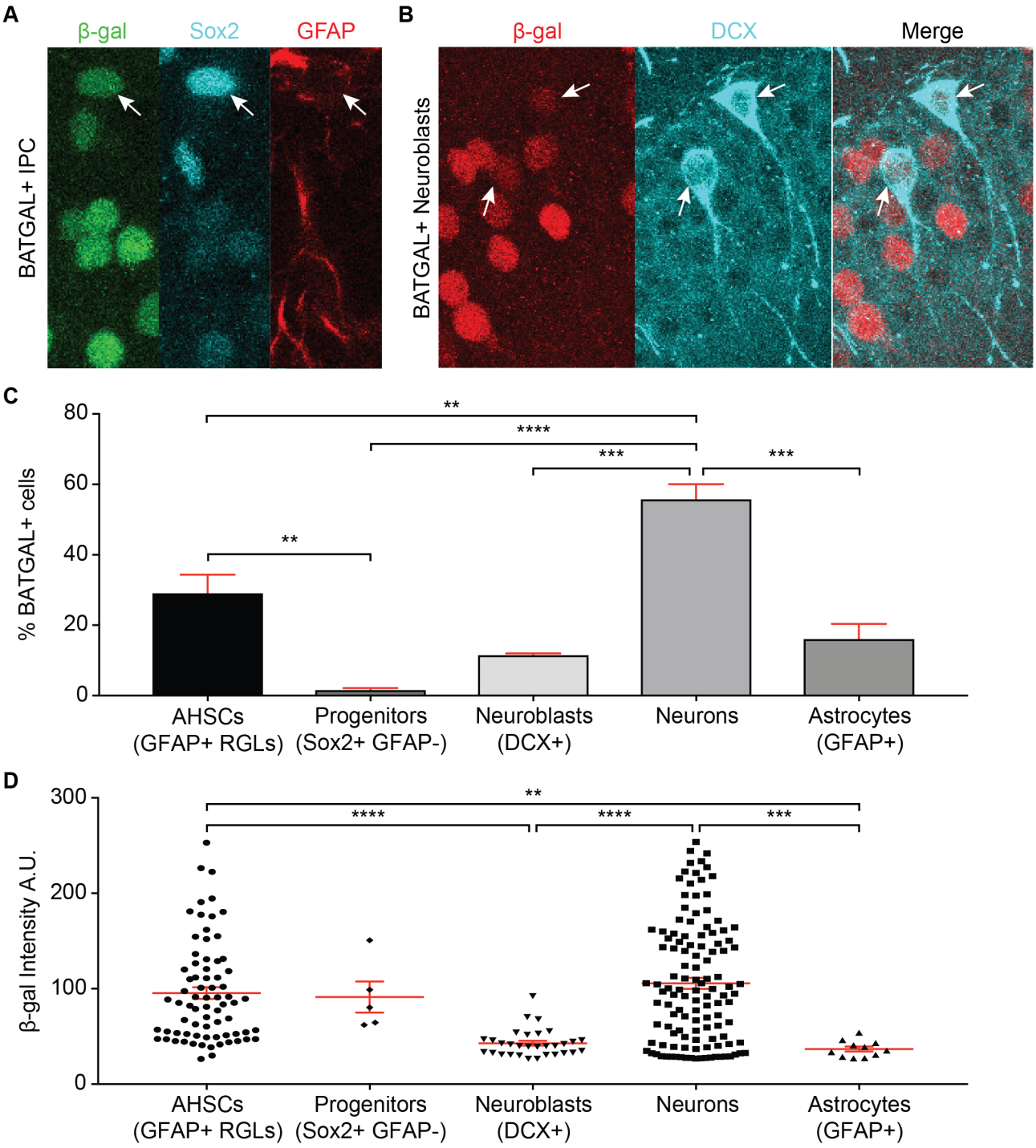


Figure 3.7: Wnt Responding IPCs and neuroblasts in the dentate gyrus of 2-month-old BATGAL Wnt reporter mice.

(A, B) β-galactosidase (β-gal) immunolabelling in Sox2+ GFAP- Intermediate Progenitor cells (IPCs) **(A)** and DCX+ neuroblasts **(B)** in 2-month-old BATGAL mice.

(C) Quantification of the proportion of BATGAL+ cells across the neurogenic lineage in 2-month-old BATGAL mice. A higher proportion of BATGAL+ AHSCs and neurons compared to neuroblasts, progenitors and astrocytes, indicates a role for canonical Wnt signalling at early and late stages of adult hippocampal neurogenesis. An ordinary one-way ANOVA with Tukey's

multiple comparison test was used for statistical analysis, (**, p<0.01. ***, p<0.001. ****, p<0.0001). Error bars represent mean with SEM. n=3.

(D) Intensities of β-galactosidase immunolabelling in BATGAL+ cells across the neurogenic lineage. AHSCs and neurons respond to Wnt signalling with a similar dynamic, whereas neuroblasts and astrocytes respond less to canonical Wnt signalling. BATGAL+ progenitors respond to Wnt similarly to AHSCs on average but less variably. A.U. = Arbitrary Units. An ordinary one-way ANOVA with Tukey's multiple comparison test was used for statistical analysis, (**, p<0.01. ***, p<0.001. ****, p<0.0001). Error bars represent mean with SEM. n=3.

The data I have shown so far shows that 30% of AHSCs in 2-month-old BATGAL Wnt reporter mice respond to canonical Wnt signalling. I next wanted to investigate whether the response to canonical Wnt signalling enriches for AHSC proliferation. To identify active/proliferating AHSCs within the AHSCs responding to Wnt, I co-immunolabelled for the pan cell cycle marker Ki67, alongside the AHSC marker GFAP and the Wnt reporter β-galactosidase (Figure 3.8A and 3.8B). I found both Ki67+ BATGAL- AHSCs (Figure 3.8A) and Ki67+ BATGAL+ AHSCs (Figure 3.8B), indicating that AHSC proliferation does not correlate with their response to Wnt signalling. I quantified the proportion of Ki67+ AHSCs within BATGAL+ and BATGAL- AHSCs and found no significant difference (Figure 3.8C). This suggests that AHSCs' response to canonical Wnt signalling does not enrich for proliferation and is independent of their activation state.

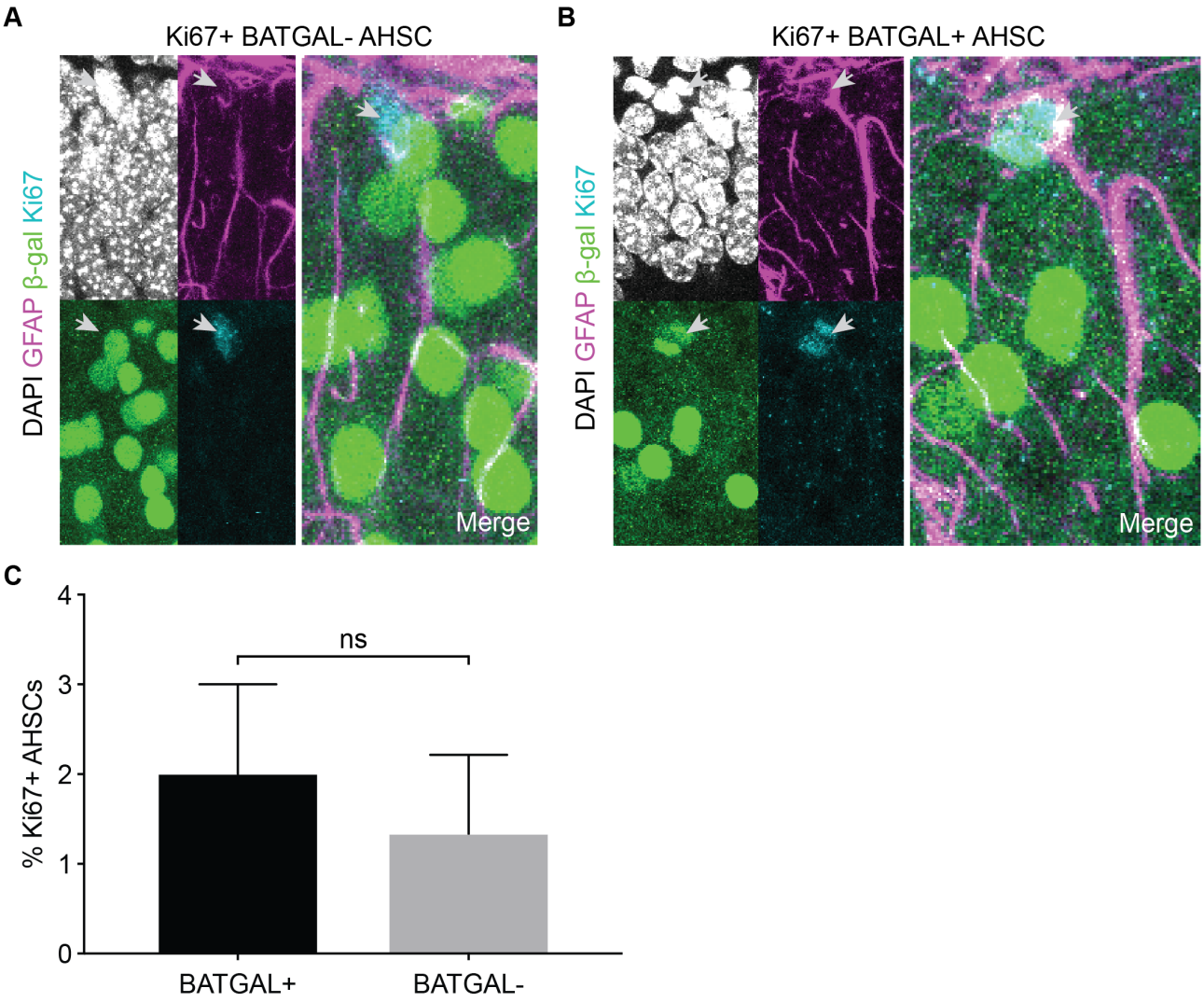


Figure 3.8: Response to canonical Wnt signalling does not enrich for AHSC proliferation in 2-month-old BATGAL Wnt reporter mice.

(A, B) β-galactosidase immunolabelling in active (Ki67+) AHSCs in 2-month-old BATGAL Wnt reporter mice. AHSCs' response to canonical Wnt signalling is independent of their activation state as shown by the presence of Ki67+ BATGAL- AHSCs **(A)** and Ki67+ BATGAL+ AHSCs **(B)**.

(C) Quantification of the data shown in **(A, B)**. The proportion of proliferating (Ki67+) AHSCs is similar between BATGAL+ and BATGAL- AHSCs indicating that AHSC activation/proliferation is not enriched in Wnt responding AHSCs. An unpaired Student's t-test was used for statistical analysis, (ns, $p>0.05$). Error bars represent mean with SEM. n=3 biological replicates.

Comparisons between different Wnt reporter mouse models have sometimes produced varying results (Al Alam et al., 2011; Garbe et al., 2012). Therefore, to validate the results obtained with the BATGAL Wnt reporter mice, I used two other Wnt reporter mouse models to characterise

the AHSCs for their response to canonical Wnt signalling. I used a second Wnt reporter mouse line that utilises multimerised TCF/LEF binding sites to drive the expression of histone tagged mCherry (TCF/LEF:H2B:mCherry) (Metzis et al., 2018). Immunolabelling of the Wnt reporter mCherry in 2-month-old TCF/LEF:H2B:mCherry mice showed a similar reporter pattern observed with the BATGAL Wnt reporter mice (Figure 3.9A). Co-immunolabelling for AHSC markers (GFAP+ cells with RGL morphology) alongside the mCherry Wnt reporter highlighted the presence of mCherry+ AHSCs indicating that AHSCs respond to canonical Wnt signalling *in vivo* as observed with the BATGAL Wnt reporter mice (Figure 3.9A panels).

In addition to using the BATGAL and TCF/LEF:H2B:mCherry Wnt reporter mice, that both use multimerised TCF/LEF binding sites to drive reporter gene expression, I also used an Axin2 knock-in Wnt reporter mouse line to further validate AHSCs' response to canonical Wnt signalling. Axin2 is a direct transcriptional target of canonical Wnt signalling and is used as a read-out of Wnt responding cells (Yan et al., 2001b; Jho et al., 2002). I used 2-month-old Axin2-membrane Turquoise (Axin2-mTurQ) knock-in mice (de Roo et al., 2017) to identify the Axin2+ Wnt responding cells within the DG. Immunolabelling of mTurQ using a GFP antibody generated results with a high level of background, despite optimisations with and without antigen retrieval, different detergents for permeabilization and different post-fixation times in 4%PFA (Figure 3.9B). Co-immunolabelling for AHSC markers (GFAP+ /Sox2+ cells with RGL morphology) alongside GFP to label the Axin2-mTurQ+ cells did show some Axin2-mTurQ+ AHSCs (Figure 3.9B panels). This indicates that some AHSCs *in vivo* respond to canonical Wnt signalling and reaffirms the results achieved with the BATGAL Wnt reporter mice. Overall, these data suggest that AHSCs *in vivo* respond heterogeneously to canonical Wnt signalling and that their response is independent of their activation state.

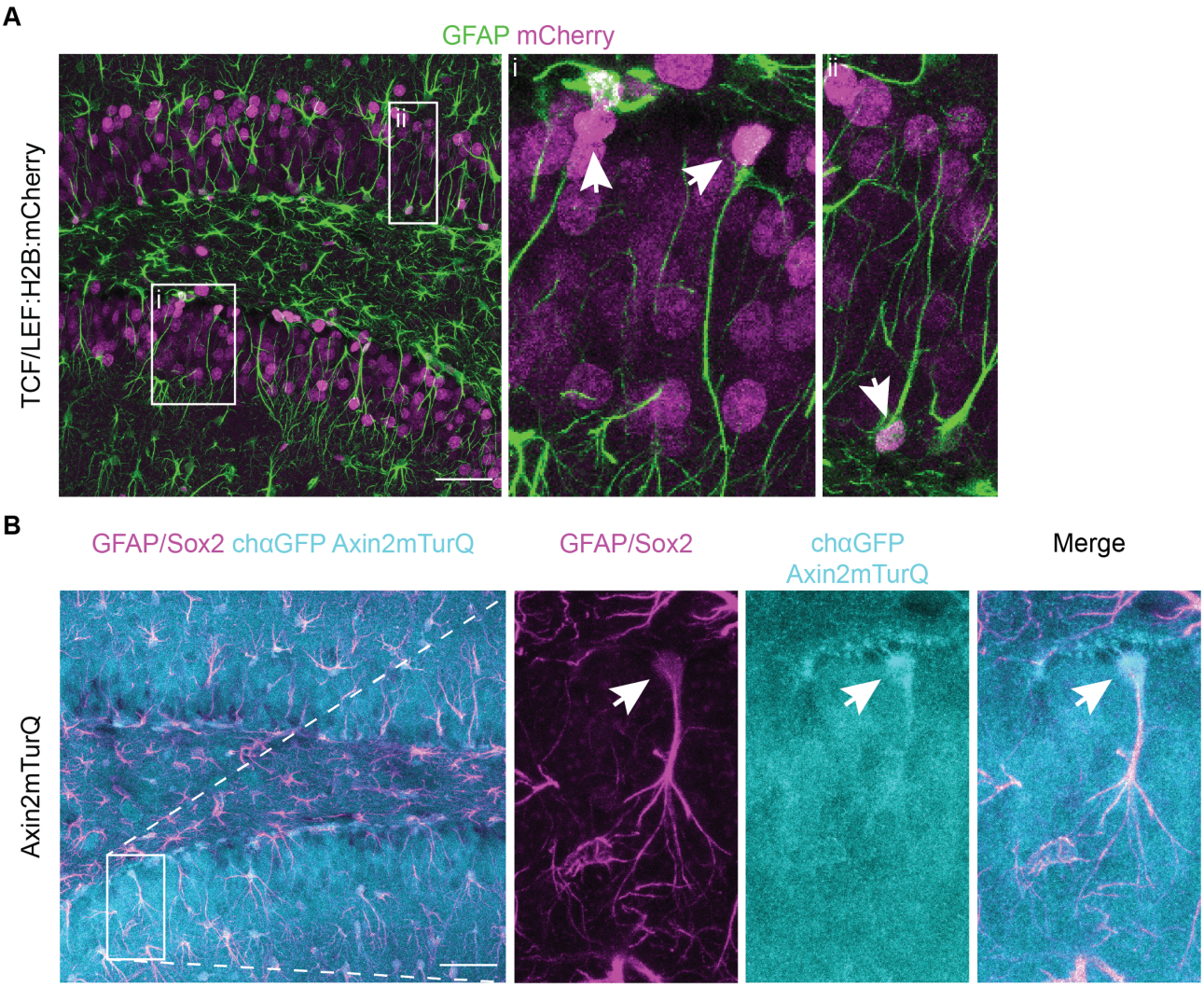


Figure 3.9: Characterisation of Wnt responding AHSCs using TCF/LEF:H2B:mCherry and Axin2-mTurQ Wnt reporter mice.

(A) Immunolabelling of AHSCs (GFAP+ cells with radial morphology) and mCherry in the dentate gyrus of 2-month-old TCF/LEF:H2B:mCherry Wnt reporter mice. Boxes highlight mCherry+ (Wnt responding) AHSCs and are enlarged in the adjacent panels. Scale bar represents 50μm.

(B) Immunolabelling of AHSCs (GFAP+/Sox2+ cells with radial morphology) and GFP (Axin2-mTurQ) in the dentate gyrus of 2-month-old Axin2-mTurQ Wnt reporter mice. Box indicates an Axin2-mTurQ+ AHSC, which is shown enlarged in the subsequent panels. Scale bar represents 50μm.

3.3 Active and Quiescent AHSPC Cultures Respond to Canonical Wnt Signalling in a Heterogeneous Manner

So far, using the bulk RNA sequencing dataset generated by I. Blomfield, I have established that the AHSPCs in active and quiescent culture conditions express Wnt pathway components, and therefore possess the machinery to respond to canonical Wnt signalling (Figure 3.5). I next wanted to determine whether active and quiescent AHSPCs *in vitro* respond to canonical Wnt signalling to validate using this model in future experiments to manipulate canonical Wnt signalling levels. To do this, I used the 7TGC Wnt reporter plasmid gifted by R. Nusse (Fuerer et al., 2010). This plasmid contains a 7xTCF-eGFP Wnt reporter cassette, upstream of a SV40-mCherry selection cassette (Figure 3.10A). This means that all nucleofected/transfected cells will express mCherry, but only those responding to canonical Wnt signalling will co-express eGFP, thus allowing the distinction between un-nucleofected and Wnt un-responsive cells (Figure 3.10A). Initial nucleofection tests using 10μg 7TGC plasmid DNA in Wild Type (WT) AHSPCs showed that both active and quiescent AHSPCs took up the plasmid DNA and expressed the mCherry selection marker, which was observed by immunolabelling for mCherry (Figure 10B). Quantification of the proportion of mCherry+ nucleofected cells was similarly low, at approximately 25%, in both active and quiescent culture conditions (Figure 3.10C). However, the presence of the mCherry selection cassette means that only mCherry+ cells were counted for further analysis on their Wnt responsiveness. To confirm that the 7TGC Wnt reporter plasmid provides a reliable read out of Wnt signalling levels in these AHSPC cultures, I treated 7TGC nucleofected active AHSPCs with the canonical Wnt agonist 5μM CHIR99021 for 24hrs. CHIR99021 is a competitive ATP inhibitor of GSK3β of the β-catenin destruction complex (Ring et al., 2003). GSK3β of the β-catenin destruction complex phosphorylates β-catenin at 3 residues, S33, S37 and T41, thus marking it for degradation in the absence of a Wnt signal (Daugherty et al., 2007; Sakanaka. 2002; Yost et al., 1996; Peifer et al., 1994a; Liu et al., 2002). Therefore, inhibiting the activity of GSK3β, prevents the degradation of β-catenin and activates downstream canonical Wnt signalling (Ring et al., 2003). Immunofluorescence of mCherry and eGFP in these samples allowed me to identify the AHSPCs that had taken up the plasmid and were responding to canonical Wnt signalling (Figure 3.10D). Normalising the eGFP grey values to mCherry grey values, allowed me to determine the level of the Wnt response in AHSPCs and AHSPCs treated with the Wnt agonist, independent of the amount of plasmid they have taken up. The eGFP/mCherry average ratio is 1.3x higher in 5μM CHIR99021 treated active AHSPCs compared with vehicle Control (Figure 3.10E). This indicates that the 7TGC Wnt reporter

plasmid serves as a readout of Wnt signalling levels in these AHSPC cultures. I therefore used this Wnt reporter plasmid to compare the Wnt responsiveness between the AHSPCs in active and quiescent culture conditions. Co-immunolabelling of mCherry and eGFP shows the presence of mCherry+/eGFP+ cells in both active and quiescent culture conditions (Figure 3.10F), indicating that they are responding to canonical Wnt signalling. As eGFP+ cells were found in both culture conditions, this suggests that AHSPCs' response to canonical Wnt signalling is independent of their activation state, which recapitulates the results observed *in vivo* using the BATGAL Wnt reporter mice (Figure 3.8C). In addition, these results were obtained without the addition of Wnt agonists, highlighting the presence of autocrine/paracrine Wnt signalling in active and quiescent AHSPC cultures. The range of eGFP/mCherry ratio values indicates a level of heterogeneity in their response to canonical Wnt signalling (Figure 3.10G), which also supports the variation of intensities observed in BATGAL+ AHSCs *in vivo* (Figure 3.6D). Although the spread of eGFP/mCherry ratios is similar between active and quiescent AHSPCs, the average eGFP/mCherry ratio value is higher in active AHSPCs indicating that they are more responsive to canonical Wnt signalling than AHSPCs in a quiescent state (Figure 3.10G).

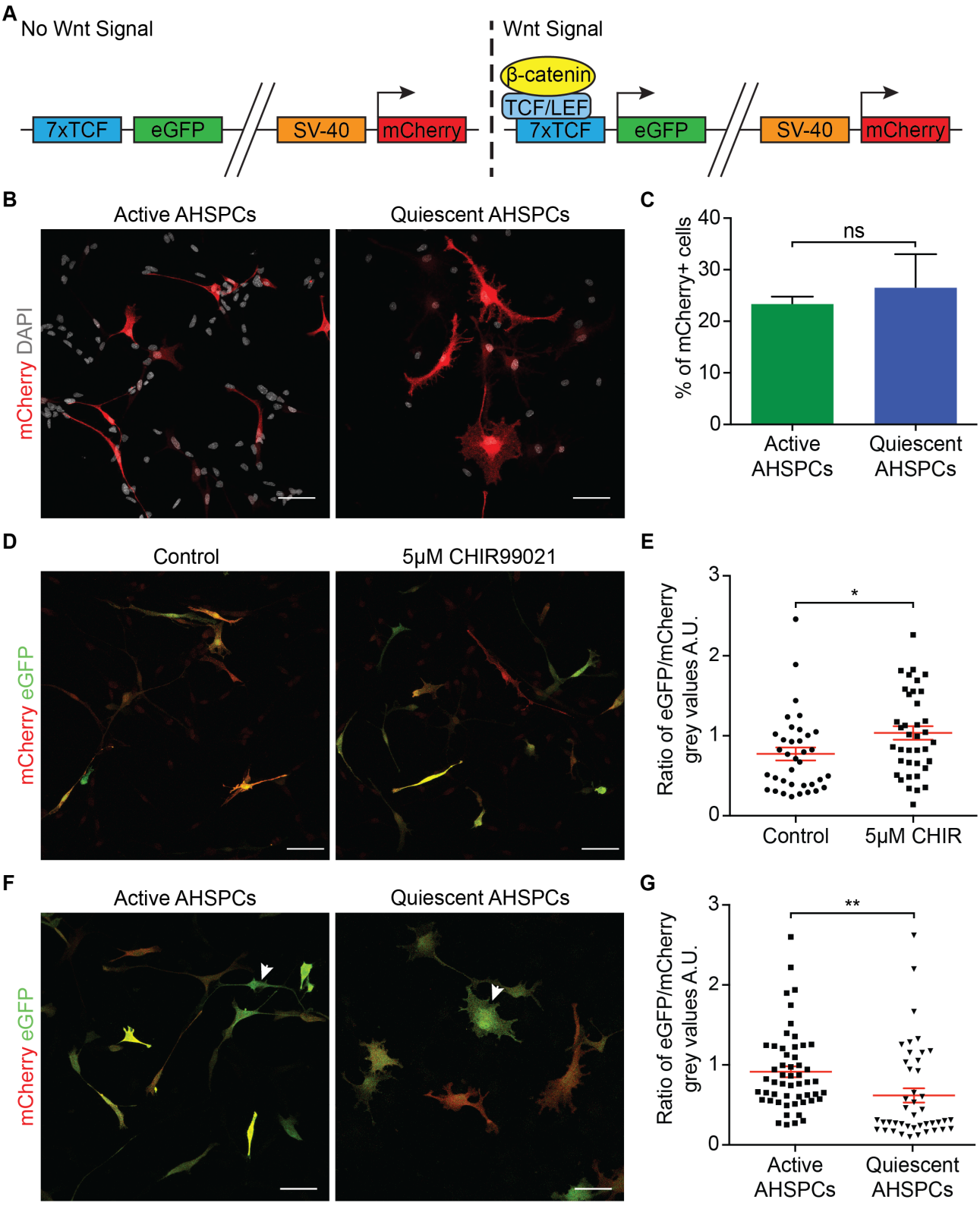


Figure 3.10: Analysis of active and quiescent AHSPCs nucleofected with the 7TGC Wnt reporter plasmid.

(A) Schematic of the 7TGC Wnt reporter plasmid. All nucleofected cells will express mCherry and Wnt responding cells will co-express eGFP. 7TGC plasmid was a gift from Roel Nusse (Fuerer et al., 2010).

(B) mCherry immunostaining in active (20ng/ml FGF2 + 20ng/ml EGF) and quiescent (20ng/ml FGF2 + 20ng/ml BMP4) AHSPCs transfected with 10μg of 7TGC plasmid. Images are representative of n=3 and n=2 biological repeats for active and quiescent AHSPCs respectively. Scale bars represent 50μm.

(C) Quantification of data represented in **(B)**. Quantification of the proportion of mCherry+ cells in active and quiescent AHSPCs transfected with 10μg of 7TGC plasmid. n=3 and n=2 biological repeats for active and quiescent AHSPCs respectively. An unpaired Student's t-test was used for statistical analysis, (ns, $p>0.05$). Error bars represent mean with SEM.

(D) mCherry and eGFP immunostaining in 7TGC nucleofected active AHSPCs treated with the Wnt agonist 5μM CHIR99201 for 24hrs vs Control. Images are representative of n=1 biological replicate. Scale bars represent 50μm.

(E) Treatment of 7TGC nucleofected active AHSPCs with the Wnt agonist CHIR99021 for 24hrs increases the average ratio of eGFP/mCherry grey values confirming that the 7TGC Wnt reporter plasmid provides a readout of the levels of canonical Wnt signalling in nucleofected cells. A.U. = Arbitrary units. An unpaired Student's t-test was used for statistical analysis, (*, $p<0.05$). Error bars represent mean with SEM. Data shown is of technical repeats from n=1 biological replicate.

(F) mCherry and eGFP immunostaining in active and quiescent AHSPCs nucleofected with 10μg of 7TGC plasmid. eGFP+ cells in both active and quiescent AHSPC cultures indicates the presence of endogenous canonical Wnt signalling in both culture conditions. Images are representative of n=3 and n=2 biological replicates for active and quiescent AHSPCs respectively. Scale bars represent 50μm.

(G) Ratio of eGFP/mCherry grey values indicates the Wnt responsiveness of AHSPCs, independent of the amount of plasmid in each cell. The range of values suggests that active and quiescent AHSPCs *in vitro* respond heterogeneously to endogenous canonical Wnt signalling. A.U. = Arbitrary units. n=3 and n=2 biological replicates for active and quiescent AHSPCs respectively. An unpaired Student's t-test was used for statistical analysis, (**, $p<0.01$). Error bars represent mean with SEM.

To corroborate the results obtained with the 7TGC Wnt reporter plasmid in wild type (WT) AHSPCs, I used an AHSPC line that was derived from the BATGAL Wnt reporter mice by N. Urban as described in Section 2.1.2. Immunolabelling of β-galactosidase in active BATGAL AHSPCs, showed β-galactosidase staining in the nuclei of approximately 37% of active AHSPCs (Figure 3.11A and 3.11B). These preliminary results suggest that some active BATGAL

AHSPCs respond to canonical Wnt signalling, which recapitulates the observations with the 7TGC Wnt reporter plasmid in WT active AHSPCs (Figure 3.10F). Measuring the intensity of the β-galactosidase immunolabelling across the nucleus in a single z-plane, highlights the specificity of the β-galactosidase reporter immunolabelling to the cell nucleus (Figure 3.11C).

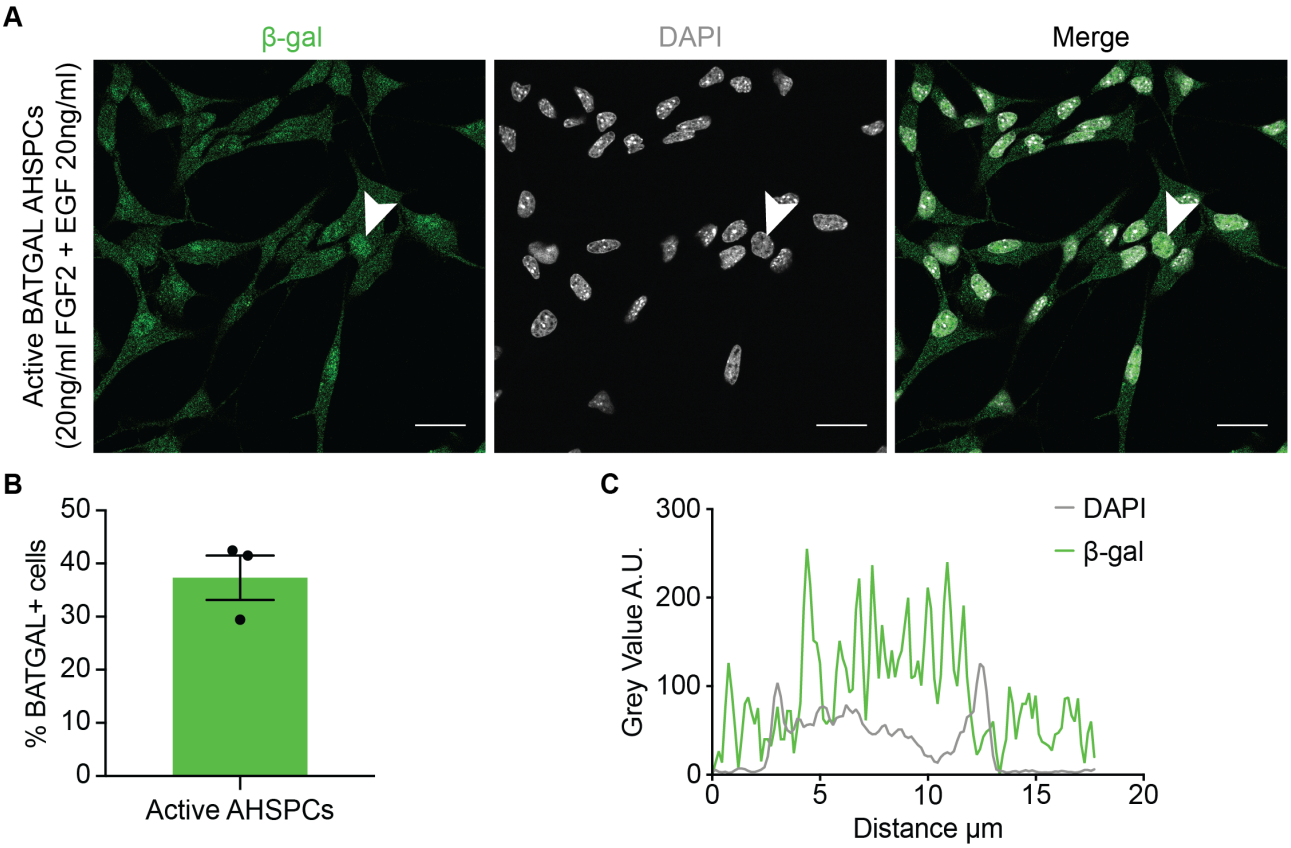


Figure 3.11: Active AHSPC cultures derived from BATGAL mice respond to endogenous canonical Wnt signalling.

(A) Nuclear β-galactosidase immunostaining in AHSPC cultures derived from BATGAL mice shows that active (20ng/ml FGF2 + 20ng/ml EGF) AHSPCs respond to endogenous canonical Wnt signalling. Arrows indicate a β-galactosidase+ active BATGAL AHSPC. Images represent a single z-plane of a confocal stack containing the nucleus. Images are representative of n=1 biological replicate. Scale bars represent 20µm.

(B) Quantification of the proportion of BATGAL+ active AHSPCs represented in **(A)**. Error bars represent mean with SEM. Data shown is of technical repeats from n=1 biological replicate.

(C) Intensity of β-galactosidase immunostaining measured across the DAPI+ nucleus indicated by the arrow in **(A)**. The intensity of the β-galactosidase immunostaining increases across the nucleus indicating a BATGAL+ cell.

Chapter 4. Results 2: Adult Hippocampal Stem Cells are Unaffected by Deletion of β-catenin

In the previous chapter, I established that adult hippocampal stem cells (AHSCs) respond heterogeneously to canonical Wnt signalling under normal conditions *in vivo* and *in vitro*, independently from their activation state. I next sought to investigate the role of this endogenous canonical Wnt signalling in AHSCs. It has previously been reported that loss of canonical Wnt/β-catenin dependent signalling has very little effect on adult hippocampal neural progenitor behaviour (Kuwabara et al., 2009), however, the effect in active and quiescent AHSCs has not been explored in detail. Conversely, other studies have shown that inhibition of endogenous canonical Wnt signalling induces a loss of multipotency and impairs proliferation in adult hippocampal stem and progenitor cell (AHSPC) cultures (Wexler et al., 2009; Qu et al., 2010; Qu et al., 2013). Therefore, to decipher the role of endogenous canonical Wnt signalling in AHSCs, I designed experiments to inhibit canonical Wnt signalling in AHSCs using both *in vivo* and *in vitro* experimental techniques.

In this chapter, I will present data showing that various small molecule Wnt inhibitors fail to inhibit baseline canonical Wnt signalling in active AHSPC cultures. Similarly, deleting β-catenin in active AHSPCs fails to abolish their response to endogenous canonical Wnt signalling but does prevent AHSPCs from responding to a canonical Wnt agonist. I will also present data showing that AHSPC homeostasis and differentiation potential is unaffected by the loss of β-catenin *in vitro*. Next, I will present the characterisation of a mouse model designed to inhibit canonical Wnt signalling in AHSCs *in vivo*, by inducing the deletion of β-catenin, and I will provide evidence for the unsuccessful recombination and deletion of β-catenin in this *in vivo* model. Finally, I will present data from a second successful *in vivo* model of AHSC specific β-catenin deletion, showing that whilst AHSCs are unaffected by loss of β-catenin, the process of adult neurogenesis is impaired.

4.1 Small Molecule Wnt Inhibitors Do Not Inhibit Baseline Canonical Wnt Signalling in Active AHSPC Cultures

To understand the role of endogenous canonical Wnt signalling observed in AHSPC cultures (Section 3.3), I aimed to investigate the functional and molecular alterations that occur following

treatment of AHSPCs with various small molecule Wnt inhibitors (Figure 4.1). There is a large repertoire of available small molecule Wnt inhibitors that block canonical Wnt signalling at different points along the pathway (Figure 4.1A). The Wnt inhibitors sFPR1 and sFPR3 sequester Wnt ligands extracellularly and Dkk1 prevents the binding between Wnt ligands and their LRP5/6 cell surface co-receptors (Figure 4.1A) (Finch et al., 1997; Glinka et al., 1998; Mao et al., 2001; Bafico et al., 2001; Semënov et al., 2001). The porcupine inhibitors LGK974 and C59 inhibit the activity of the o-acyl-transferase Porcupine, preventing the lipid modification and secretion of Wnt ligands (Figure 4.1A) (Liu et al., 2013; Proffitt et al., 2013). The tankyrase inhibitor IWR, stabilises Axin protein and inhibits canonical Wnt signalling by stabilising the β-catenin destruction complex (Figure 4.1A) (Chen et al., 2009; Huang et al., 2009). Finally, LF3 prevents the formation of the transcription activator complex in the nucleus by antagonising the binding of β-catenin with TCF/LEF partners (Figure 4.1A) (Fang et al., 2016). Using these different small molecule Wnt inhibitors in parallel experiments ensures that any observed phenotypes are due to inhibiting canonical Wnt signalling and not off target effects.

To optimise experimental conditions, I titrated each individual Wnt inhibitor in active AHSPCs for 24hrs. I determined the concentrations of the Wnt inhibitors used based on their previous use in the literature at non-toxic levels. *Axin2* is a direct transcriptional target of canonical Wnt signalling and its expression is used as read out of Wnt signalling levels in cells (Yan et al., 2001b; Jho et al., 2002). Thus, inhibiting canonical Wnt signalling should result in a decrease in *Axin2* expression levels, which I investigated using qPCR analysis. Active AHSPCs treated with 0.1μg/ml and 0.5μg/ml sFRP1 for 24hrs showed a modest decrease in *Axin2* expression levels indicating a mild inhibition of canonical Wnt signalling (Figure 4.1B). However, *Axin2* gene expression levels were unchanged in active AHSPCs treated with sFPR3 (Figure 4.1C), Dkk1 (Figure 4.1D) or LGK974 (Figure 4.1E) for 24hrs at all indicated concentrations. This indicates that canonical Wnt signalling was not inhibited under these experimental conditions. To further confirm that canonical Wnt signalling was not impaired by treatment with these Wnt antagonists, I treated active AHSPCs, nucleofected with the 7TGC Wnt reporter plasmid, with different concentrations of LGK974 for 24hrs (Figure 4.1F). As described in the previous chapter, this 7TGC Wnt reporter plasmid contains a constitutively active mCherry selection cassette downstream of an eGFP Wnt reporter cassette, meaning all nucleofected cells express mCherry and only those responding to canonical Wnt signalling co-express eGFP (Figure 3.10A). By immunostaining for mCherry and eGFP, I found mCherry+ eGFP+ cells in both control active AHSPCs and active AHSPCs treated with all three concentrations of LGK974 (1μM, 2.5μM and 5μM LGK974). This suggests that LGK974 treatment has failed to inhibit canonical Wnt

signalling in active AHSPCs (Figure 4.1F). Indeed, active AHSPCs treated with increasing concentrations of the Wnt inhibitor LGK974 (1μM, 2.5μM and 5μM LGK974), do not show a significant decrease in the average eGFP/mCherry ratio (Figure 4.1G). This further supports a failure to inhibit canonical Wnt signalling in active AHSPCs under these experimental conditions.

I also treated active AHSPCs with Wnt inhibitors for 48hrs as further optimisation of these experimental conditions. I found that 48hrs treatment of active AHSPCs with the small molecule Wnt inhibitors LGK974, IWR, LF3 and C59, at the indicated concentrations, also failed to decrease *Axin2* expression levels compared to Control (Figure 4.1H). This contrasts with the increase in *Axin2* expression levels achieved with 48hrs treatment with the Wnt agonist CHIR99021 (5μM) (Figure 4.1H). This shows that active AHSPCs are able to respond to a canonical Wnt stimulus, but baseline levels of canonical Wnt signalling are difficult to inhibit under these experimental conditions. As a proof of principle experiment, to determine whether Wnt inhibition is possible using small molecule Wnt inhibitors in AHSPC cultures, I treated active AHSPCs with the Wnt agonist CHIR99021, that stimulates Wnt at the level of the β-catenin destruction complex, in combination with the Wnt antagonist LF3, that inhibits Wnt signalling downstream of the β-catenin destruction complex at the level of the transcriptional activation complex (Figure 4.1A). Other Wnt inhibitors were not suitable for this proof of principle experiment as they inhibit the signalling cascade upstream of the β-catenin destruction complex and would therefore not be able to counteract CHIR99021 stimulated canonical Wnt signalling (Figure 4.1A). I found that 48hrs of 5μM CHIR99021 treatment alone upregulates *Axin2* gene expression, whereas 48hrs of 30μM LF3 treatment alone fails to decrease *Axin2* gene expression compared to Control (Figure 4.1I). Active AHSPCs treated with both 5μM CHIR99021 and 30μM LF3 for 48hrs also show a significant increase in *Axin2* gene expression levels (Figure 4.1I). This indicates that 30μM LF3 is unable to inhibit 5μM CHIR99021 stimulated canonical Wnt signalling in active AHSPCs under these experimental conditions.

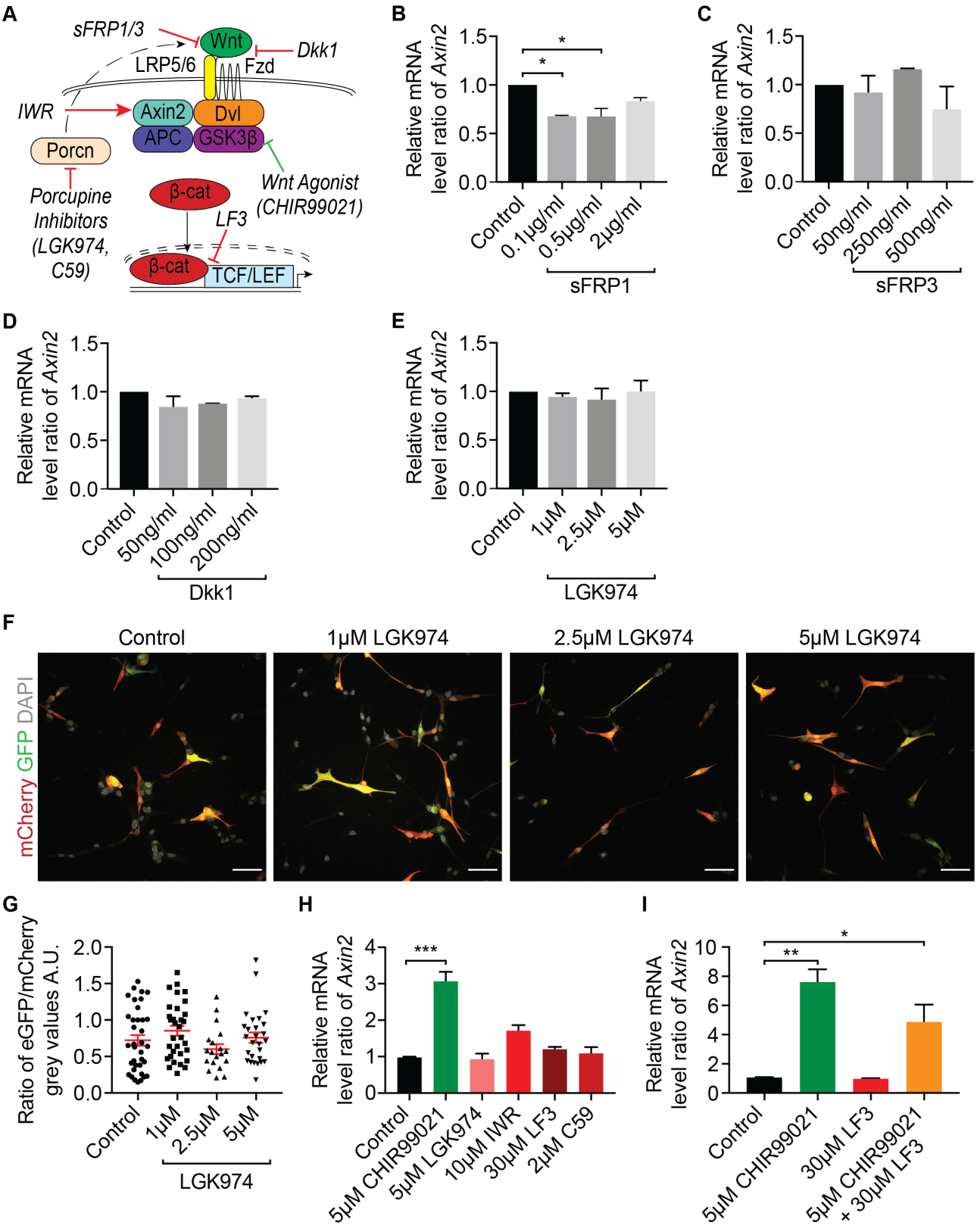


Figure 4.1: Expression of the Wnt target gene *Axin2* and activity of the Wnt reporter plasmid 7TGC is unaffected in active AHSPCs treated with small molecule Wnt inhibitors. **(A)** Schematic of the canonical Wnt signalling pathway highlighting the target points of the small molecule Wnt modulators used in subsequent experiments. sFRP1 and sFRP3 sequester Wnt

ligands extracellularly and Dkk1 inhibits the binding between Wnt ligands and their LRP5/6 cell surface co-receptors. LGK974 and C59 are inhibitors of the o-acyl-transferase Porcupine and inhibit the secretion of Wnt ligands. IWR is a tankyrase inhibitor that stabilises Axin within the β-catenin destruction complex. LF3 antagonises the binding of β-catenin with TCF/LEF transcription factor partners. The Wnt agonist CHIR99021, stimulates canonical Wnt signalling by inhibiting the activity of GSK3β of the β-catenin destruction complex.

(B, C, D, E) qPCR results of *Axin2* gene expression levels in active AHSPCs treated with the Wnt inhibitors sFRP1 **(B)**, sFRP3 **(C)**, Dkk1 **(D)** and LGK974 **(E)** for 24hrs. mRNA levels were normalised to *GAPDH* and *ActinB* mRNA and expressed relative to Control. An ordinary one-way ANOVA with Dunnett's multiple comparisons test was used for statistical analysis, (*, $p<0.05$). Error bars represent mean with SEM. Data shown are technical repeats of one biological replicate. n=1 biological replicate.

(F) mCherry and eGFP immunolabelling in active AHSPCs nucleofected with the 7TGC Wnt reporter plasmid and treated with 1μM, 2.5μM and 5μM LGK974 for 24hrs. Scale bars represent 50μm.

(G) Quantification of the data shown in **(F)**. Normalisation of eGFP grey values to mCherry grey values indicates the Wnt responsiveness of AHSPCs independent of the amount of plasmid in each cell. Active AHSPCs treated with LGK974 do not show a significant decrease in the average eGFP/mCherry ratio. A.U. = Arbitrary units. An ordinary one-way ANOVA with Dunnett's multiple comparisons test was used for statistical analysis, (ns, $p>0.05$). Error bars represent mean with SEM. Data shown is technical repeats of one biological replicate. n=1 biological replicate.

(H) qPCR results of *Axin2* gene expression levels in active AHSPCs treated with the Wnt agonist CHIR99021 and the Wnt inhibitors LGK974, IWR, LF3 and C59 for 48hrs at the indicated concentrations. *Axin2* expression is significantly upregulated in active AHSPCs treated with 5μM CHIR99021 for 48hrs indicating stimulated canonical Wnt signalling. *Axin2* expression levels do not decrease in active AHSPCs treated with the Wnt inhibitors 5μM LGK974, 10μM IWR, 30μM LF3 and 2μM C59 for 48hrs indicating that canonical Wnt signalling is not inhibited using these small molecule inhibitors under these experimental conditions. mRNA levels were normalised to *GAPDH* and *ActinB* mRNA and expressed relative to Control. An ordinary one-way ANOVA with Dunnett's multiple comparisons test was used for statistical analysis, (***, $p<0.001$). Error bars represent mean with SEM. Data shown is technical repeats of one biological replicate. n=1 biological replicate.

(I) *Axin2* gene expression changes in a proof of principle experiment of Wnt inhibition. Active AHSPCs were treated with the Wnt agonist 5μM CHIR99021, the Wnt inhibitor 30μM LF3 and both 5μM CHIR99021 and 30μM LF3 for 48hrs. 5μM CHIR99021 alone upregulates *Axin2* expression, however, 30μM LF3 alone does not change *Axin2* expression compared to control. Combined treatments of 5μM CHIR99021 and 30μM LF3 causes an increase in *Axin2* expression levels suggesting that LF3 is unable to inhibit CHIR99021 stimulated canonical Wnt signalling under these experimental conditions. mRNA levels were normalised to *GAPDH* and *ActinB* mRNA and expressed relative to Control. An ordinary one-way ANOVA with Dunnett's multiple comparisons test was used for statistical analysis, (*, $p<0.05$. **, $p<0.01$). Error bars represent mean with SEM. Data shown is technical repeats of one biological replicate. n=1 biological replicate.

4.2 *in vitro* AHSPC Cultures are Unaffected by Loss of β-catenin

4.2.1 β-catenin is Robustly Deleted in Active β-cat$^{fl/fl\ ex3-6}$ AHSPCs, Which Prevents Their Response to a Canonical Wnt Stimulus, But Fails to Inhibit Baseline Canonical Wnt Signalling

As well as using small molecule Wnt inhibitors, I took advantage of an AHSPC line, derived by N. Urban from a mouse model designed to inhibit canonical Wnt signalling in AHSPCs *in vivo* by deleting β-catenin. β-catenin is the key transcriptional mediator of canonical Wnt signalling, therefore deleting β-catenin in AHSPCs should prevent them from responding to canonical Wnt signalling (Papkoff et al., 1996; Peifer et al., 1994b). Mice from the GlastCreERT2; β-cat$^{fl/fl\ ex3-6}$; RYFP line that were wild type for the GlastCreERT2 allele and homozygous for both the β-cat$^{fl/fl\ ex3-6}$ and RYFP alleles were used for the derivation of this β-cat$^{fl/fl\ ex3-6}$ AHSPC line. The β-cat$^{fl/fl\ ex3-6}$ mice contain LoxP sites flanking exons 3-6, which encode the N-terminal domain and armadillo repeats 1-4 of β-catenin (Huelsken et al., 2001) (Figure 4.2A). Recombination of these LoxP sites causes a deletion/frame-shift mutation fusing exon 2 with exon 7, which generates a truncated mRNA but does not produce protein (Huelsken et al., 2001) (Figure 4.2A). The RYFP (Rosa26-floxed-stop-YFP) allele is included as a reporter of recombination (Srinivas et al., 2001). *EYFP* was inserted into the Rosa26 locus preceded by a LoxP-flanked-Stop sequence (Srinivas et al., 2001). Recombination of the LoxP-flanked-Stop sequence results in the expression of *EYFP*, thus marking recombined cells as YFP+ (Srinivas et al., 2001). By including the RYFP allele, we are able to identify recombined AHSCs and target our immunofluorescence

analysis to this population. Recombination of the β-cat$^{fl/fl\ ex3-6}$ and RYFP alleles *in vitro* was achieved through the overnight exposure of AHSPCs to a Cre adenovirus (Figure 4.2A).

To validate the deletion of β-catenin in this AHSPC line, I treated active β-cat$^{fl/fl\ ex3-6}$ AHSPCs with either Control or Cre adenovirus overnight and collected samples 24hrs, 48hrs and 72hrs after virus transduction. As stated above, recombined cells will be YFP+ due to the inclusion of the RYFP recombination reporter allele. Therefore, to identify recombined YFP+ AHSPCs, I performed immunostaining using a GFP antibody in Control and β-cat$^{del\ ex3-6}$ AHSPCs (Figure 4.2B). I did not find any YFP+ AHSPCs in Control active AHSPCs, showing that they have not undergone recombination (Figure 4.2B and 4.2C). The majority of active β-cat$^{del\ ex3-6}$ AHSPCs were YFP+ indicating a high level of recombination under these experimental conditions (Figure 4.2B and 4.2C). Immunostaining for an antibody raised against the C-terminal domain of β-catenin showed that active Control AHSPCs were largely positive for cytoplasmic and membrane β-catenin at all time points (Figure 4.2B). In contrast, YFP+ active β-cat$^{del\ ex3-6}$ AHSPCs were largely β-catenin negative, indicating that Cre mediated recombination successfully deletes β-catenin under these experimental conditions (Figure 4.2B). β-catenin immunolabelling can be seen in YFP- cells in active β-cat$^{del\ ex3-6}$ AHSPCs at all time points after Cre adenovirus transduction, indicating that they have not recombined (Figure 4.2B). This provides an internal control showing that the loss of β-catenin is specific to AHSPCs that have undergone successful recombination.

I next performed qPCR analysis for two different regions of β-catenin to confirm that the floxed region (*β-catenin*$^{ex3-6}$) has been deleted. The gene expression levels of a region outside the LoxP sites (TaqMan probe spanning *β-catenin*$^{ex13-14}$) is unchanged between Control and β-cat$^{del\ ex3-6}$ active AHSPCs at all time points following virus transduction, indicating that this region is unaffected by Cre mediated recombination (Figure 4.2D). However, the gene expression levels of a region within the floxed region of β-catenin (TaqMan probe spanning *β-catenin*$^{ex4-5}$) is abolished in active β-cat$^{del\ ex3-6}$ AHSPCs compared to Control (Figure 4.2E). This indicates that Cre adenovirus treatment induces the recombination of the floxed region of β-catenin even at 24hrs after virus transduction (Figure 4.2E). Western blot analysis, using an antibody against the C-terminal domain of β-catenin, shows that at 24hrs after virus transduction, β-catenin protein levels are greatly reduced in β-cat$^{del\ ex3-6}$ active AHSPCs compared to Control and is completely abolished 48hrs after virus transduction (Figure 4.2F). This shows that these experimental conditions are optimal to achieve robust deletion of β-catenin in active β-cat$^{fl/fl\ ex3-6}$

AHSPCs. As the canonical Wnt signalling pathway relies on β-catenin to mediate a Wnt dependent transcriptional programme, deleting β-catenin should result in the decreased expression of the Wnt target gene *Axin2* (Yan et al., 2001b; Jho et al., 2002). However, *Axin2* expression levels are unchanged in active β-cat$^{fl/fl\ ex3-6}$ AHSPCs compared to Control at all time points following virus transduction (Figure 4.2G). This suggests that active β-cat$^{del\ ex3-6}$ AHSPCs might still be able to respond to endogenous canonical Wnt signalling, even in the absence of β-catenin. It also highlights the possibility that *Axin2* could be regulated independently of canonical/β-catenin Wnt signalling in these cells and therefore might not be a good read-out for inhibiting canonical Wnt signalling levels.

I next sought to determine whether active β-cat$^{del\ ex3-6}$ AHSPCs are able to respond to a canonical Wnt signalling stimulus. As such, 48hrs after virus transduction, I treated Control and β-cat$^{del\ ex3-6}$ active AHSPCs with the Wnt agonist CHIR99021 (5μM) for 24hrs and analysed *Axin2* expression levels (Figure 4.2H). In Control AHSPCs, 5μM CHIR99021 treatment induced a significant upregulation of *Axin2* (Figure 4.2H), confirming the activation of canonical Wnt signalling. However, in active β-cat$^{del\ ex3-6}$ AHSPCs, 5μM CHIR99021 treatment failed to upregulate *Axin2* expression as observed in Control AHSPCs (Figure 4.2H). This indicates that, whilst β-catenin deletion fails to abrogate baseline canonical Wnt signalling, intact β-catenin is essential for active AHSPCs to respond to an external stimulus of canonical Wnt signalling.

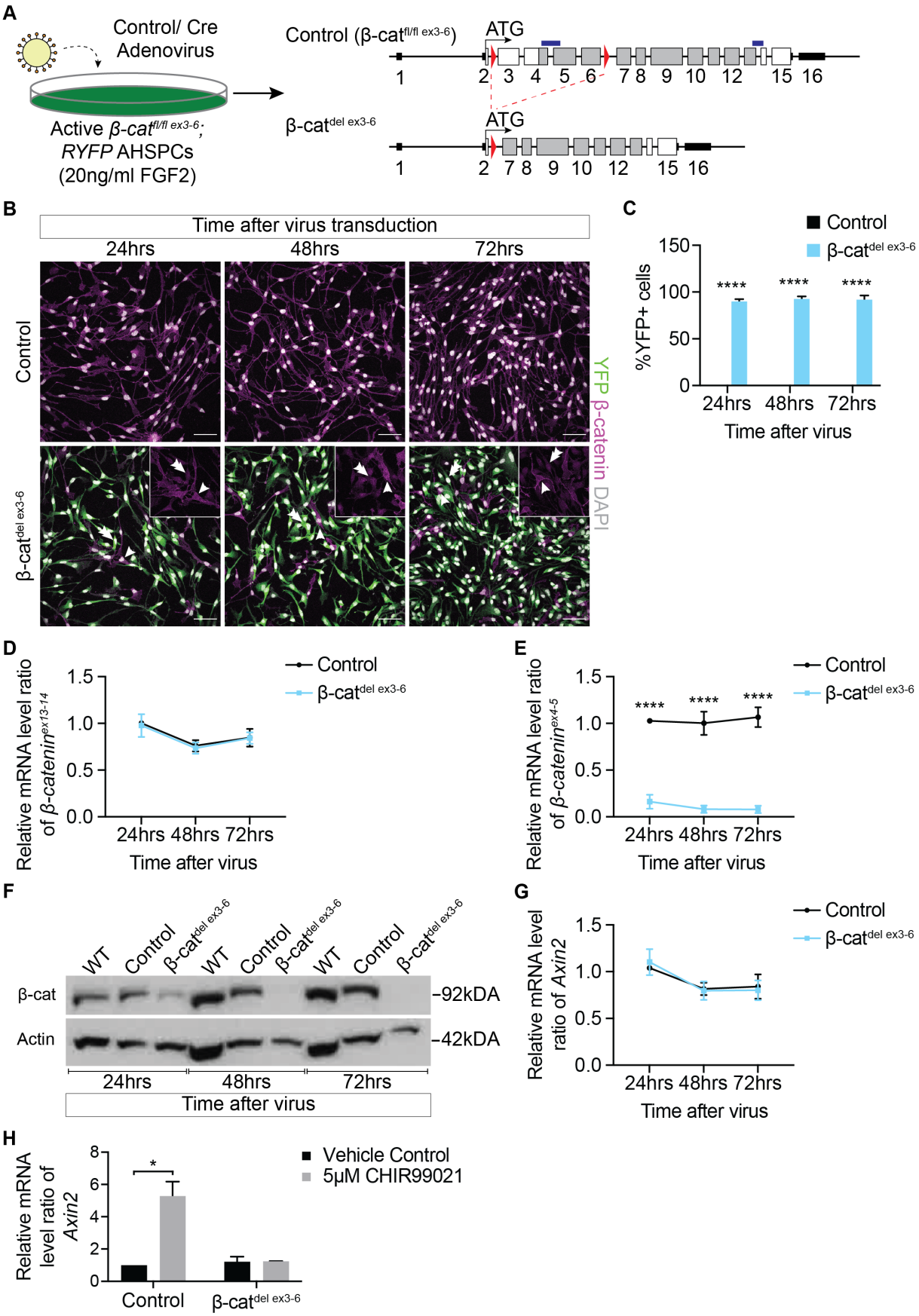


Figure 4.2: Robust deletion of β-catenin in active AHSPCs fails to inhibit baseline canonical Wnt signalling but prevents their response to an external Wnt stimulus.

(A) Schematic of experimental design including a scheme of the genomic structure of β-catenin before and after Cre induced recombination of the β-cat$^{fl/fl\ ex3-6}$ allele. Active β-cat$^{fl/fl\ ex3-6}$ AHSPCs were exposed to Control and Cre adenovirus overnight to facilitate the recombination of the β-cat$^{fl/fl\ ex3-6}$ allele. Media was refreshed the following morning and samples collected 24hrs, 48hrs and 72hrs after virus transduction for immunolabelling, qPCR and western blots. In the β-cat$^{fl/fl\ ex3-6}$ allele, LoxP sites (red triangles) flank exons 3-6 which encode the N-terminal domain and armadillo repeats 1-4 (grey boxes). Upon Cre-mediated recombination, a deletion/frame-shift mutation is introduced fusing exon 2 with exon 7, which does not encode a functional protein (Huelsken et al., 2001). Black boxes indicate non-coding exons. Large boxes indicate coding exons. Grey boxes indicate armadillo repeats. Red arrows indicate LoxP sites. Blue boxes indicate the TaqMan probes used for qPCR analysis.

(B) Immunolabelling of YFP (GFP antibody used), β-catenin and DAPI in active (20ng/ml FGF2) Control and β-cat$^{del\ ex3-6}$ AHSPCs 24hrs, 48hrs and 72hrs after Control and Cre virus transduction. Cells exposed to Control virus remain YFP- and retain β-catenin protein (top panels). YFP+ staining indicates AHSPCs that have undergone Cre adenovirus-mediated recombination and have lost β-catenin protein (bottom panels double arrow heads). Some β-cat$^{del\ ex3-6}$ AHSPCs have not recombined (YFP-) and retain β-catenin protein (bottom panels single arrow heads). Scale bars represent 50μm. Data shown are representative images from n=3 biological repeats.

(C) Quantification of the proportion of YFP+ cells shown in **(B)** indicating a high level of recombination in β-cat$^{del\ ex3-6}$ AHSPCs. Two-way Anova with Sidak's multiple comparisons test was used for statistical analysis, (****, $p<0.0001$). Error bars represent mean with SEM. n=3 biological replicates.

(D) qPCR gene expression analysis of *β-catenin$^{ex13-14}$*. *β-catenin$^{ex13-14}$* lies outside the floxed region of β-catenin and is similarly expressed between Control and β-cat$^{del\ ex3-6}$ AHSPCs. n=3 biological replicates.

(E) qPCR gene expression analysis of *β-catenin^{ex4-5}*. *β-catenin^{ex4-5}* lies within the floxed region of β-catenin and is downregulated in β-cat$^{del\ ex3-6}$ AHSPCs vs Control active AHSPCs. Two-way Anova with Sidak's multiple comparisons test was used for statistical analysis, (****, $p<0.0001$). Error bars represent mean with SEM. n=3 biological replicates.

(F) Western Blot analysis of β-catenin protein levels in Wild Type, Control and β-cat$^{del\ ex3-6}$ active AHSPCs 24hrs, 48hrs and 72hrs after virus transduction. β-catenin protein levels are abolished 48hrs after virus transduction.

(G) qPCR gene expression levels of *Axin2* are unaffected by β-catenin deletion. This indicates that baseline levels of canonical Wnt signalling in active AHSPCs are not impaired by deletion of β-catenin. Two-way Anova with Sidak's multiple comparisons test was used for statistical analysis, (ns, $p>0.05$). Error bars represent mean with SEM. n=3 biological replicates.
(H) qPCR gene expression levels of *Axin2* in Control and β-cat$^{del\ ex3-6}$ active AHSPCs following treatment with the Wnt agonist CHIR99021 (5μM). CHIR99021 treatments were started 48hrs after virus transduction and maintained for 24hrs. *Axin2* levels increase in Control active AHSPCs treated with 5μM CHIR99021 indicating stimulation of canonical Wnt signalling. However, *Axin2* expression levels are unchanged in β-cat$^{del\ ex3-6}$ AHSPCs treated with 5μM CHIR99021 compared to vehicle Control, indicating that in the absence of β-catenin protein, β-cat$^{del\ ex3-6}$ AHSPCs are unable to respond to a Wnt stimulus. An unpaired Student's t-test was used for statistical analysis, (*, $p<0.05$). Error bars represent mean with SEM. Data shown is technical repeats of one biological replicate. n=1 biological replicate.

4.2.2 Active AHSPCs Do Not Require Intact β-catenin Signalling to Maintain Their Stemness or Their Activation State

I next wanted to see whether intact β-catenin signalling was required for active AHSPCs to maintain their active state or to retain their stem-like properties. To investigate any changes in their active state following β-catenin deletion, I examined proliferation in Control and β-cat$^{del\ ex3-6}$ AHSPCs 24hrs, 48hrs and 72hrs after virus transduction. EdU (5-ethynyl-2'-deoxyuridine) is a thymidine analogue that is incorporated into DNA during active DNA synthesis in S-phase of the cell cycle (Salic et al., 2008). EdU is detected using the Click-iT™ EdU Alexa Fluor® 647 detection kit (Invitrogen, C10340), which uses a Click copper catalysed reaction between the alkyne in EdU and the azide in the Alexa Fluor® 647 to fluorescently label incorporated EdU (Salic et al., 2008). This fluorescence can then be visualised to identify cells in S-phase of the cell cycle. I pulsed Control and β-cat$^{del\ ex3-6}$ AHSPCs with EdU for 1hr before sample collection to label cells in S-phase of the cell cycle. Immunolabelling of EdU, using the Click-iT™ EdU Alexa Fluor® 647 detection kit (as described in Section 2.2.2) showed the presence of proliferating cells in both Control and β-cat$^{del\ ex3-6}$ AHSPCs (Figure 4.3A). Quantification of the proportion of EdU+ cells is similar between both Control and β-cat$^{del\ ex3-6}$ AHSPCs across all time points (Figure 4.3B), indicating that proliferation is unaffected by β-catenin deletion. Furthermore, the expression levels of the G1 cell cycle gene *CyclinD1* are also unaffected

between active Control and β-cat$^{del\ ex3-6}$ AHSPCs (Figure 4.3C). Overall, this suggests that the loss of β-catenin signalling does not affect AHSPCs' ability to maintain an active proliferative state under these culture conditions.

To understand whether AHSPCs' stemness is affected by loss of β-catenin signalling, I used qPCR analysis to compare the expression levels of AHSPC associated genes, between Control and β-cat$^{del\ ex3-6}$ AHSPCs. The similarity in the expression levels of *Nestin*, *Ascl1, Glast* and *Sox2* (Figure 4.3D, 4.3E, 4.3F and 4.3G) highlight that AHSPCs' stem-like state is unaffected by loss of β-catenin signalling under these experimental conditions.

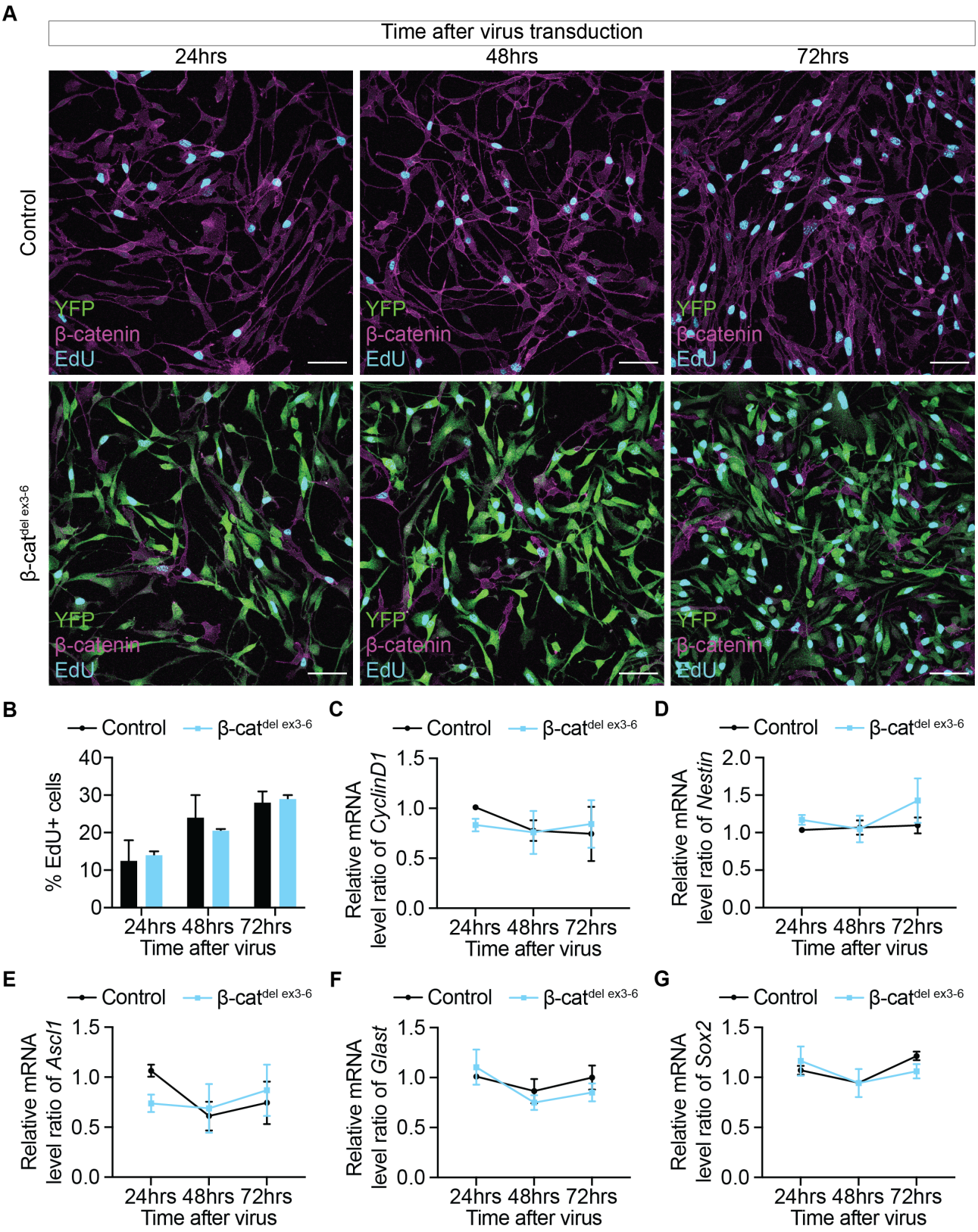


Figure 4.3: Loss of β-catenin signalling does not affect AHSPCs' ability to maintain an active state or retain their stem-like properties.

(A) YFP (GFP antibody), β-catenin and EdU immunolabelling in active (20ng/ml FGF2) Control and β-cat$^{del\ ex3-6}$ AHSPCs 24hrs, 48hrs and 72hrs following virus transduction. Scale bars represent 50μm. Representative images of n=3 biological replicates.
(B) Quantification of the proportion of EdU+ AHSPCs shown in **(A)**. The proportion of EdU+ cells is similar between Control and β-cat$^{del\ ex3-6}$ active AHSPCs indicating that proliferation is unaffected by loss of β-catenin signalling. The proportion of EdU+ cells increases with time in active culture conditions. Proportion of EdU+ cells in active β-cat$^{del\ ex3-6}$ AHSPCs was calculated as a proportion of the YFP+ (recombined) AHSPCs. Two-way Anova with Sidak's multiple comparisons test was used for statistical analysis, (ns, $p>0.05$). Error bars represent mean with SEM. n=3 biological replicates.
(C, D, E, F, G) qPCR gene expression analysis of *CyclinD1* **(C)**, *Nestin* **(D)**, *Ascl1* **(E)**, *Glast* **(F)** and *Sox2* **(G)**. *CyclinD1* **(C)** is a cell cycle marker, expressed during G1 of the cell cycle, and the similarity in its expression levels between Control and β-cat$^{del\ ex3-6}$ active AHSPCs, indicates that proliferation is unaffected by the loss of β-catenin signalling. The similarities in the expression levels of the of stem cell markers *Nestin* **(D)**, *Ascl1* **(E)**, *Glast* **(F)** and *Sox2* **(G)** highlight that active AHSPC stemness is unaffected by loss of β-catenin signalling. Two-way Anova with Sidak's multiple comparisons test was used for statistical analysis, (ns, $p>0.05$). Error bars represent mean with SEM. n=3 biological replicates.

4.2.3 Under Normal Culture Conditions, β-catenin Deletion Does Not Affect Quiescent AHSPC Activation

I have shown above that intact β-catenin signalling is not essential for AHSPCs to maintain an active/proliferative state when cultured in active culture conditions. Quiescent AHSPC activation is distinctly regulated from the maintenance of a proliferative state once activated, as quiescent AHSPCs must first re-enter the cell cycle from G0. Therefore, I next wanted to investigate whether intact β-catenin signalling was required for quiescent AHSPCs to re-activate upon returning to active culture conditions. To achieve this, I exposed quiescent β-cat$^{fl/fl\ ex3-6}$ AHSPCs to Control and Cre adenovirus overnight to induce recombination and deletion of β-catenin (Figure 4.4A). 48hrs after virus transduction, I either maintained Control and β-cat$^{del\ ex3-6}$ AHSPCs in quiescent culture conditions (20ng/ml FGF2 + 20ng/ml BMP4) or changed the media for active culture conditions (20ng/ml FGF2) (Figure 4.4A). I then collected samples for qPCR and immunofluorescence analysis (following a 1hr pulse with EdU) 3 and 6 Days after this media change (Figure 4.4A). I used immunolabelling for GFP, to mark the YFP+ recombined AHSPCs,

and combined this with immunolabelling for the proliferation markers EdU and Ki67 to provide a read-out of AHSPC re-activation rates (Figure 4.4B). Quantification of the proportion of YFP+ AHSPCs in β-cat$^{del\ ex3-6}$ AHSPCs ranged from 40%-70% across the course of the experiment indicating successful recombination (Figure 4.4C). The proportion of EdU+ (Figure 4.4D) and Ki67+ (Figure 4.4E) AHSPCs increases at a similar rate in both Control and β-cat$^{del\ ex3-6}$ AHSPCs returned to active culture conditions. This suggests that loss of β-catenin signalling does not impair quiescent AHSPC activation upon returning to active culture conditions. In addition, the proportion of EdU+ (Figure 4.4D) and Ki67+ (Figure 4.4E) AHSPCs remained low in Control and β-cat$^{del\ ex3-6}$ AHSPCs maintained in quiescent culture conditions. This indicates that intact β-catenin signalling is not essential for the maintenance of AHSPC quiescence *in vitro*.

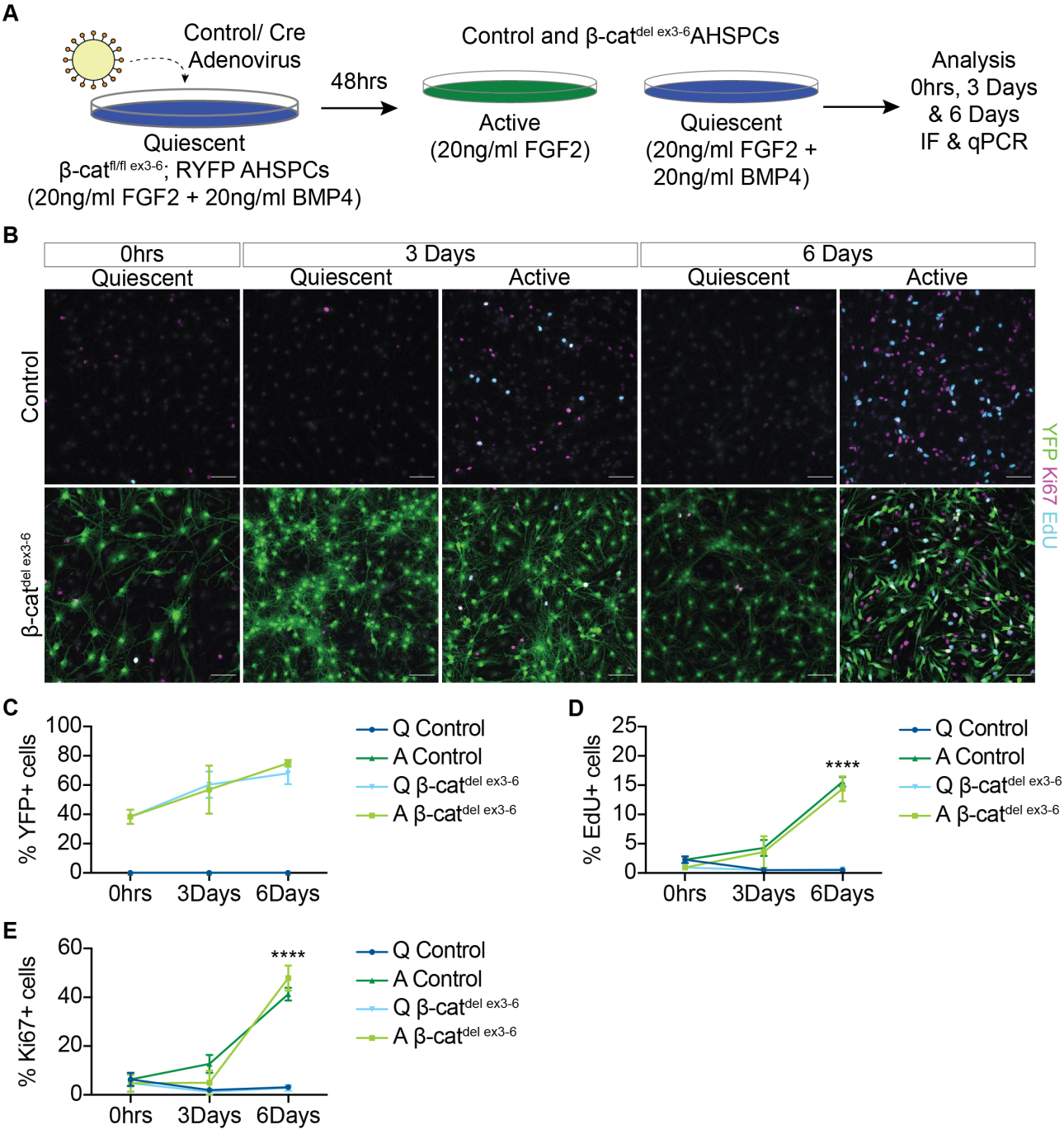


Figure 4.4: Quiescent β-cat$^{del\ ex4-5}$ AHSPCs re-activate and proliferate similarly to quiescent Control AHSPCs when returned to active culture conditions.

(A) Schematic of experimental design. 48hrs after Cre adenovirus transduction, quiescent (20ng/ml FGF2 + 20ng/ml BMP4) Control and β-cat$^{del\ ex3-6}$ AHSPCs were either maintained in quiescent culture conditions or changed to active (20ng/ml FGF2) culture conditions. Media was refreshed every 48hrs and samples collected 3 and 6 Days after changing to active culture conditions.

(B) Immunolabelling of YFP (GFP antibody), Ki67 and EdU in Control and β-cat$^{del\ ex3-6}$ AHSPCs maintained in quiescent culture conditions and those changed to active culture conditions at all

time points. YFP immunolabelling marks recombined cells. Ki67 and EdU immunolabelling was used as markers of proliferation as a measurement of quiescent AHSPCs re-activation upon change to active culture conditions. Scale bars represent 50μm. Data shown are representative images from n=3 biological repeats.

(C, D, E) Quantification of the proportion of YFP+ **(C)**, EdU+ **(D)** and Ki67+ **(E)** cells shown in **(B)**. The proportion of YFP+ cells **(C)** in β-cat$^{del\ ex3-6}$ AHSPCs indicates successful Cre mediated recombination. The proportion of EdU+ **(D)** and Ki67+ **(E)** cells indicates a similar re-activation rate between quiescent Control and β-cat$^{del\ ex3-6}$ AHSPCs changed to active conditions. The proportion of proliferating AHSPCs is unchanged in Control and β-cat$^{del\ ex3-6}$ AHSPCs maintained in quiescent culture conditions. In β-cat$^{del\ ex3-6}$ AHSPCs, the proportion of proliferating AHSPCs was determined as a proportion of the YFP+ (recombined) AHSPCs. Statistical significance was achieved for the proportion of EdU+ **(D)** and Ki67+ **(E)** cells between Active and Quiescent culture conditions over time. A = active culture conditions (20ng/ml FGF2). Q = quiescent culture conditions (20ng/ml FGF2 + 20ng/ml BMP4). A three-way Anova with Tukey's multiple comparisons test was used for statistical analysis, (****, $p<0.0001$). Error bars represent mean with SEM. n=3 biological replicate.

The above data shows that quiescent AHSPCs are able to re-activate normally in the absence of intact β-catenin signalling, which suggests that β-catenin signalling is not essential for the re-activation of quiescent AHSPCs. However, the re-activation of quiescent β-cat$^{del\ ex3-6}$ AHSPCs could be due to a compensatory mechanism that by-passes the need for intact β-catenin signalling to promote quiescent AHSPC activation. Therefore, I wanted to investigate any potential mechanistic differences between the re-activation of quiescent Control AHSPCs and quiescent β-cat$^{del\ ex3-6}$ AHSPCs. To do this, I analysed the expression levels of genes associated with an active or quiescent state in Control and β-cat$^{del\ ex3-6}$ AHSPCs that were either maintained in quiescent culture conditions or returned to active culture conditions to re-activate. To confirm successful β-catenin deletion, I checked the expression levels of *β-catenin exons 4-5* and observed a 50% decrease in the expression level of *β-catenin^{ex4-5}* in β-cat$^{del\ ex3-6}$ AHSPCs vs Control (Figure 4.5A). This 50% reduction in the expression of *β-catenin^{ex4-5}*, is consistent with the proportion of YFP+ (recombined) AHSPCs recorded in β-cat$^{del\ ex3-6}$ AHSPCs (Figure 4.4C). This confirms that β-catenin has been deleted in β-cat$^{del\ ex3-6}$ AHSPCs, however the expression of the Wnt target gene *Axin2* is unchanged (Figure 4.5B), which again suggests that baseline canonical Wnt signalling is not impaired. *CyclinD1* is expressed during G1 of the cell cycle and is used as a marker of AHSPC activation and proliferation. The gene expression levels of

CyclinD1 are similarly upregulated in both Control and β-cat$^{del\ ex3-6}$ AHSPCs that have been returned to active culture conditions (Figure 4.5C), supporting the previous observation that β-catenin is not necessary for the re-activation of quiescent AHSPCs under these experimental conditions. In addition, *CyclinD1* remains lowly expressed in both Control and β-cat$^{del\ ex3-6}$ AHSPCs maintained in quiescent conditions (Figure 4.5C), indicating that β-catenin is not required to maintain AHSPC quiescence. This is also supported by the gene expression levels observed with the quiescent AHSPCs marker *HopX*. *HopX* expression remains consistent in Control and β-cat$^{del\ ex3-6}$ AHSPCs maintained in quiescent culture conditions, but decreases in Control and β-cat$^{del\ ex3-6}$ AHSPCs returned to active culture conditions (Figure 4.5D). This again indicates that AHSPCs' maintenance of quiescence is not affected by the loss of β-catenin signalling. Overall, these data show that Control and β-cat$^{del\ ex3-6}$ AHSPCs re-activate similarly under these experimental conditions, indicating that intact β-catenin signalling is not essential for quiescent AHSPC re-activation.

Finally, I checked the expression levels of genes associated with stemness to determine whether loss of β-catenin signalling affects the maintenance of a stem-like state during this quiescence to activation switch. The expression levels of the AHSPCs markers *Ascl1* (Figure 4.5E) and *Sox2* (Figure 4.5F) remain consistent across both Control and β-cat$^{fl/fl\ ex3-6}$ AHSPCs in all conditions and time points. This indicates that the absence of β-catenin signalling does not affect AHSPCs' ability to maintain a stem-like state when activating from a quiescent state.

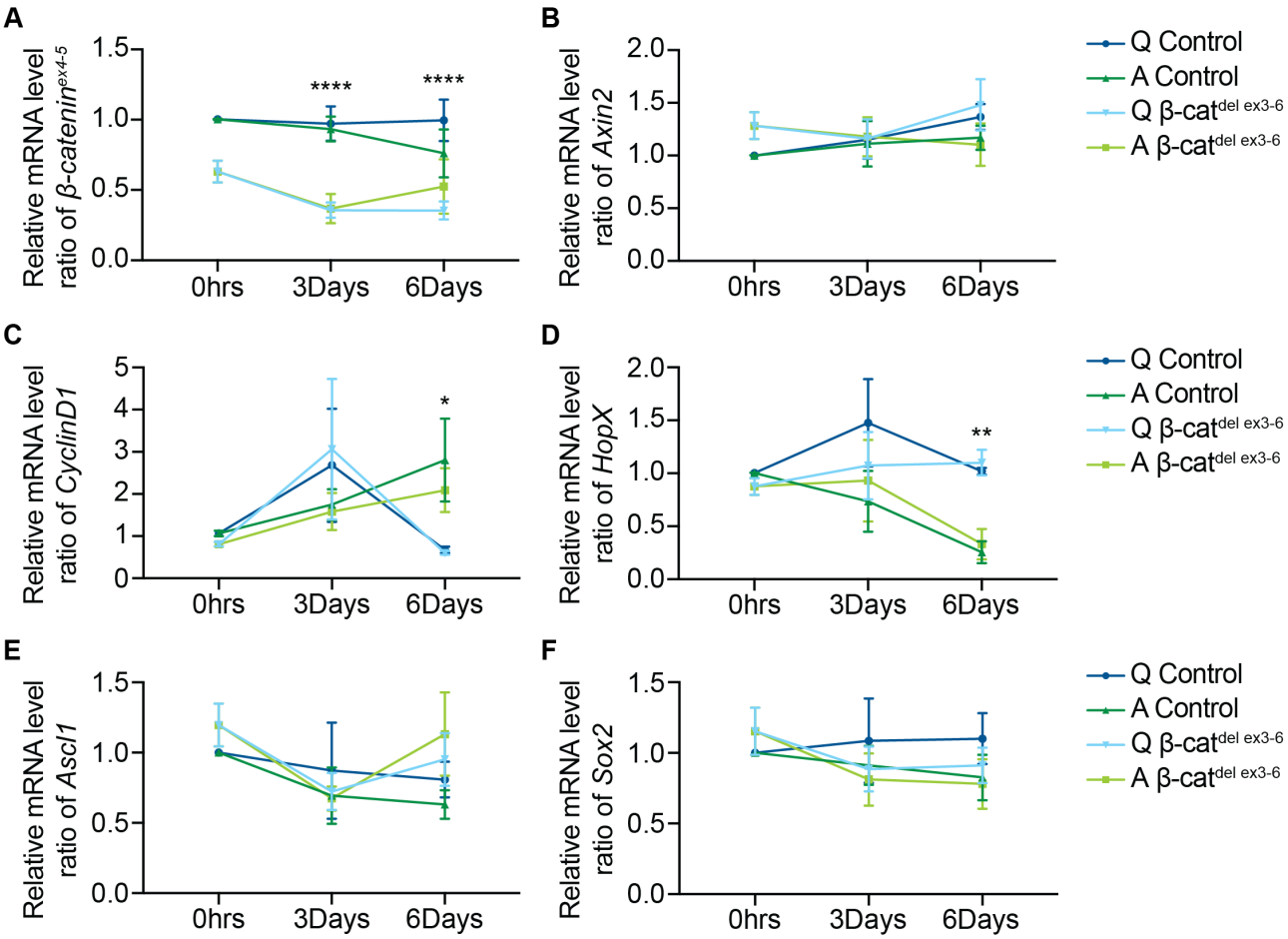


Figure 4.5: Loss of β-catenin signalling does not alter the mechanism of quiescent AHSPC activation nor does it affect quiescent AHSPC maintenance.

(A, B, C, D, E, F) qPCR gene expression analysis of *β-catenin*$^{ex4-5}$ **(A)**, *Axin2* **(B)**, *CyclinD1* **(C)**, *HopX* **(D)**, *Ascl1* **(E)** and *Sox2* **(F)**. The floxed region of *β-catenin* **(A)** is robustly deleted in β-cat$^{del\ ex3-6}$ AHSPCs. *Axin2* **(B)** gene expression levels are unchanged between Control and β-cat$^{del\ ex3-6}$ AHSPCs, indicating that β-catenin deletion does not affect baseline levels of canonical Wnt signalling. *CyclinD1* **(C)** expression levels are increased in active culture conditions vs quiescent culture conditions irrespective of the presence or absence of β-catenin. The quiescent marker *HopX* **(D)** is increased in quiescent culture conditions vs active culture conditions irrespective of the presence or absence of β-catenin. *Ascl1* **(E)** and *Sox2* **(F)** expression levels are unchanged, indicating that β-catenin deletion does not affect AHSPC stemness. Gene expression changes are shown normalised to *ActinB* and *GAPDH* expression levels and shown relative to 0hrs in quiescent culture conditions. A = active culture conditions (20ng/ml FGF2). Q = quiescent culture conditions (20ng/ml FGF2 + 20ng/ml BMP4). A three-way Anova with Tukey's multiple comparisons test was used for statistical analysis, (*, $p<0.05$. **, $p<0.01$. ****, $p<0.0001$). Error bars represent mean with SEM. n=3 biological replicates.

4.2.4 Chronic Loss of β-catenin Does Not Affect AHSPCs' Stemness, Their Ability to Enter a Quiescent State or Their Ability to Differentiate into Astrocytes and Neurons

It has been reported that levels of the Wnt inhibitor Dkk1 increase in the mouse DG with age, which impairs progenitor self-renewal and/or survival (Seib et al., 2013). Indeed, I found that the proportion of Wnt responding AHSCs is decreased in 7-month old BATGAL Wnt reporter mice compared with 2-month-old BATGAL mice (Figure 3.6D). This implies that age-related changes in AHSCs' response to canonical Wnt signalling could affect AHSC behaviour and impair adult neurogenesis. I addressed this *in vitro* by investigating how AHSPCs respond to a chronic loss of β-catenin signalling. I exposed active β-cat$^{fl/fl\ ex3-6}$ AHSPCs to Control and Cre adenovirus overnight, and refreshed the active AHSPC media the following day. I maintained Control and β-cat$^{del\ ex3-6}$ AHSPCs in active culture conditions through serial passaging and collected samples for qPCR and immunofluorescence analysis at 6-, 12- and 18-days following virus transduction (Figure 4.6A). I wanted to investigate whether the maintenance of AHSPCs' active state and stem-like characteristics are affected by a chronic loss of β-catenin signalling. Co-immunolabelling for YFP (GFP antibody) and β-catenin shows that β-catenin levels are decreased in YFP+ (recombined) β-cat$^{del\ ex3-6}$ AHSPCs (Figure 4.6B). The proportion of EdU+ AHSPCs is similar in Control and β-cat$^{del\ ex3-6}$ active AHSPCs at all time points, indicating that their proliferation rate is unaffected by loss of β-catenin signalling (Figure 4.6C). By qPCR analysis, I confirmed that the expression level of *β-catenin^{ex4-5}* is decreased in active β-cat$^{del\ ex3-6}$ AHSPCs compared to Control (Figure 4.6D) indicating successful deletion of β-catenin. As before, I also found that *Axin2* expression levels were unchanged despite the successful deletion of *β-catenin* (Figure 4.6E). In addition, the expression levels of the AHSPC markers *Sox2*, *Nestin* and *Glast* (Figure 4.6F, 4.6G and 4.6H respectively) are unchanged between Control and β-cat$^{del\ ex3-6}$ active AHSPCs across all time points. This indicates that active AHSPC stemness is unaffected by chronic loss of β-catenin signalling.

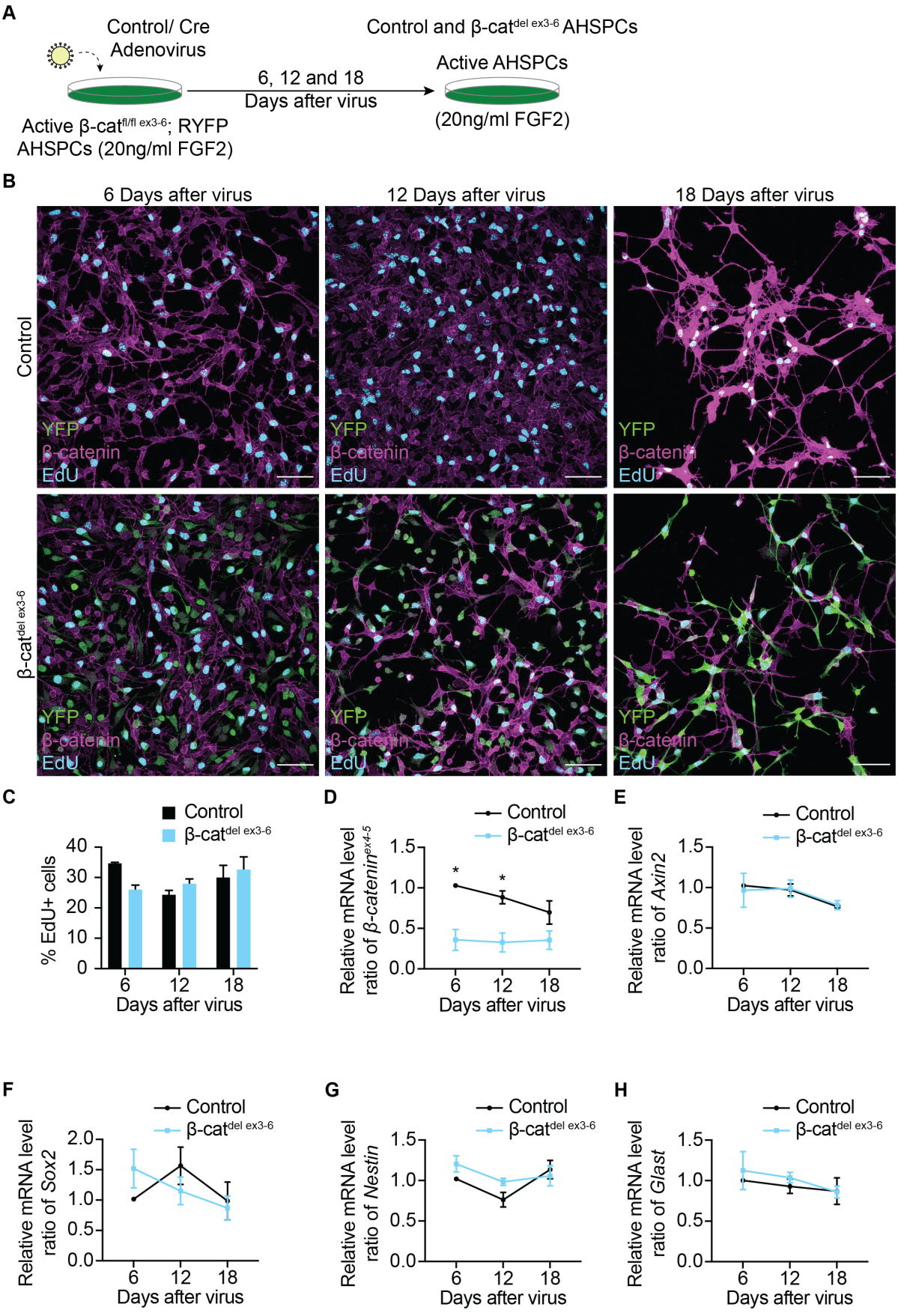


Figure 4.6: Maintenance of AHSPCs' active state and stem-like characteristics are unaffected by chronic loss of β-catenin.

(A) Schematic of experimental design. Active (20ng/ml FGF2) β-cat$^{fl/fl\ ex3-6}$ AHSPCs were exposed to Control and Cre adenovirus overnight to induce recombination. Control and β-cat$^{del\ ex3-6}$ AHSPCs were maintained in active culture conditions through serial passages and samples were collected 6-, 12- and 18-Days following virus transduction for qPCR and immunofluorescence analysis.
(B) Immunolabelling of YFP (GFP antibody), β-catenin and EdU in Control and β-cat$^{del\ ex3-6}$ active AHSPCs at 6-, 12- and 18-Days after virus transduction. YFP immunolabelling marks recombined cells. β-catenin immunolabelling shows that levels of β-catenin are decreased in YFP+ AHSPCs. The proliferation marker EdU was used as an indicator of AHSC activity. Scale bars represent 50μm. Data shown are representative images from n=1 biological replicate.
(C) Quantification of the proportion of EdU+ AHSPCs shown in **(B)**. For β-cat$^{del\ ex3-6}$ active AHSPCs, the proportion of EdU+ AHSPCs was calculated from the YFP+ population. Two-way Anova with Sidak's multiple comparisons test was used for statistical analysis, (ns, $p>0.05$). Error bars represent mean with SEM. Data shown is technical repeats of one biological replicate. n=1 biological replicate.
(D, E, F, G, H) qPCR analysis of the gene expression levels of *β-catenin^{ex4-5}* **(D)**, *Axin2* **(E)**, *Sox2* **(F)**, *Nestin* **(G)** and *Glast* **(H)** in Control and β-cat$^{del\ ex3-6}$ active AHSPCs collected 6-, 12- and 18-Days after virus transduction. Gene expression changes are shown normalised to *ActinB* and *GAPDH* expression levels and shown relative to active Control AHSPCs at 6-days after virus transduction. Two-way Anova with Sidak's multiple comparisons test was used for statistical analysis, (ns, $p>0.05$. *, $p<0.05$). Error bars represent mean with SEM. Data shown is technical repeats of one biological replicate. n=1 biological replicate.

A key feature for the long-term maintenance of AHSPCs is their ability to enter and maintain a quiescent state. I therefore wanted to investigate whether chronic loss of β-catenin signalling affects AHSPCs' ability to enter quiescence. To test this, at 6-, 12- and 18-Days after virus transduction, I plated Control and β-cat$^{del\ ex3-6}$ AHSPCs in quiescent culture conditions (20ng/ml FGF2 + 20ng/ml BMP4) for 72hrs before collecting for qPCR and immunofluorescence analysis (Figure 4.7A). Co-immunolabelling of β-catenin and YFP shows that β-catenin is deleted in YFP+ AHSPCs (Figure 4.7B). EdU immunolabelling shows that very few Control and β-cat$^{del\ ex3-6}$ AHSPCs are proliferating after 72hrs in quiescent culture conditions, indicating that they have entered a quiescent state (Figure 4.7B). In addition, quantification of the proportion of EdU+ Control and β-cat$^{del\ ex3-6}$ AHSPCs after 72hrs in quiescent culture conditions, is similar across all time points (Figure 4.7C). This indicates the chronic loss of β-catenin signalling does not affect

AHSPCs ability to enter a quiescent state under these *in vitro* conditions. The decreased expression of *β-catenin*$^{ex4-5}$ confirms that β-catenin has successfully recombined (Figure 4.7D) and maintained *Axin2* expression levels continue to show that this deletion of β-catenin does not impair baseline canonical Wnt signalling levels (Figure 4.7E). Finally, I checked the gene expression levels of known markers of quiescence. *HopX*, *Id4* and *p57* (Figure 4.7F, 4.7G and 4.7H respectively) are similarly expressed in Control and β-cat$^{del\ ex3-6}$ AHSPCs at all time points following virus transduction and 72hrs in quiescent culture conditions. Overall this indicates that quiescence entry is unaffected by chronic loss of β-catenin signalling under these *in vitro* experimental conditions.

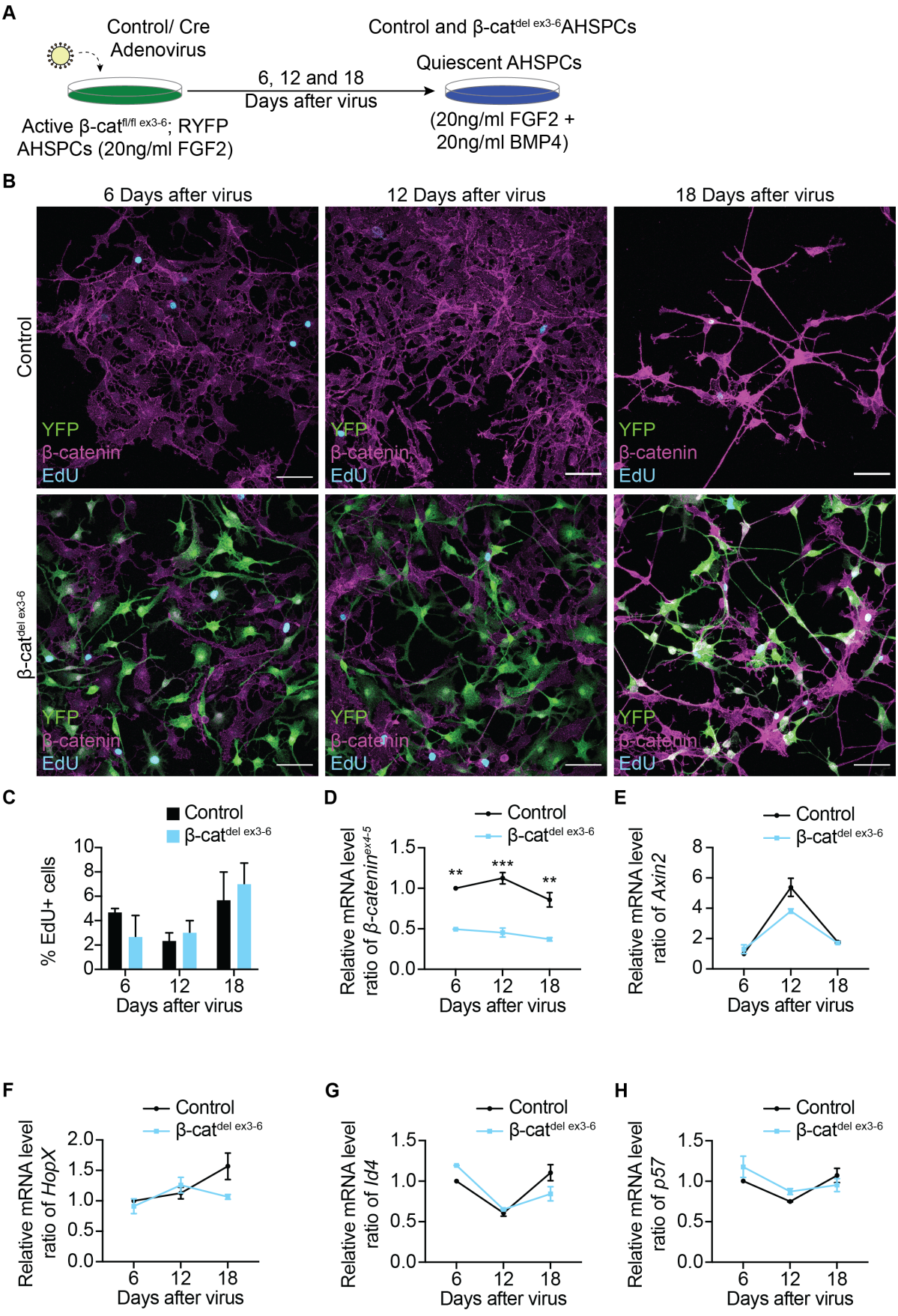


Figure 4.7: Chronic loss of β-catenin signalling does not affect AHSPCs ability to enter quiescence.

(A) Schematic of experimental design. Active (20ng/ml FGF2) β-cat$^{fl/fl\ ex3-6}$ AHSPCs were exposed to Control and Cre adenovirus overnight to induce recombination and active culture media was refreshed the following morning and maintained. At 6-, 12- and 18- Days after virus transduction, Control and β-cat$^{del\ ex3-6}$ AHSPCs were changed to quiescent (20ng/ml FGF2 + 20ng/ml BMP4) culture conditions for 72hrs to induce quiescence before collection for immunofluorescence and qPCR analysis.
(B) Immunolabelling of YFP (GFP antibody), β-catenin and EdU in Control and β-cat$^{del\ ex3-6}$ AHSPCs at 6-, 12- and 18- Days after virus transduction, following 72hrs in quiescent culture conditions. YFP immunolabelling marks recombined cells and β-catenin immunolabelling shows that levels of β-catenin are decreased in YFP+ AHSPCs. The proliferation marker EdU was used as an indicator of AHSPC activity. Scale bars represent 50μm. Data shown are representative images from n=1 biological replicate.
(C) Quantification of the proportion of EdU+ AHSPCs shown in **(B)**. For β-cat$^{del\ ex3-6}$ quiescent AHSPCs, the proportion of EdU+ AHSPCs was calculated from the YFP+ population. Two-way Anova with Sidak's multiple comparisons test was used for statistical analysis, (ns, $p>0.05$). Error bars represent mean with SEM. Data shown is technical repeats of one biological replicate. n=1 biological replicate.
(D, E, F, G, H) qPCR analysis of the gene expression levels of *β-catenin^{ex4-5}* **(D)**, *Axin2* **(E)**, *HopX* **(F)**, *Id4* **(G)** and *p57* **(H)** in Control and β-cat$^{del\ ex3-6}$ AHSPCs collected 6-, 12-, 18- Days after virus transduction, following 72hrs in quiescent culture conditions. Gene expression changes of *HopX* **(F)**, *Id4* **(G)** and *p57* **(H)** are significant across time (not shown) but not between Control and β-cat$^{del\ ex3-6}$ AHSPCs. Gene expression changes are shown normalised to *ActinB* and *GAPDH* expression levels and shown relative to quiescent Control AHSPCs at 6-days after virus transduction. Two-way Anova with Sidak's multiple comparisons test was used for statistical analysis, (ns, $p>0.05$. **, $p<0.01$. ***, $p<0.001$). Error bars represent mean with SEM. Data shown is technical repeats of one biological replicate. n=1 biological replicate.

β-catenin signalling, via the canonical Wnt signalling pathway, has been shown to promote AHSPC differentiation towards the neuronal and astrocyte lineages with a preference towards neuronal differentiation (Lie et al., 2005; Jang et al., 2013; Seib et al., 2013). Therefore, I wanted to investigate whether chronic loss of β-catenin signalling affected AHSPCs' ability to differentiate into neurons and astrocytes *in vitro*. To do this, I plated Control and β-cat$^{del\ ex3-6}$ active AHSPCs 6-, 12- and 18-days after virus transduction and cultured them for 5 days in conditions to promote neuronal (FGF2 withdrawal and B27 addition) and astrocyte (FGF2

withdrawal and FBS addition) differentiation (Figure 4.8A). To identify differentiated neurons in B27 treated Control and β-cat$^{del\ ex3-6}$ AHSPCs, I immunolabelled cells for the neuronal marker Map2 (Figure 4.8B). I did not observe any morphological differences between the Map2+ neurons generated from Control or β-cat$^{del\ ex3-6}$ AHSPCs (Figure 4.8B). In addition, the proportion of Map2+ cells is similar in both Control and β-cat$^{del\ ex3-6}$ AHSPCs at all time points after virus transduction (Figure 4.8C). This indicates that neuronal differentiation is not impaired by chronic loss of β-catenin signalling under these *in vitro* experimental conditions. To identify differentiated astrocytes in FBS treated Control and β-cat$^{del\ ex3-6}$ AHSPCs, I immunolabelled cells for the astrocyte marker GFAP (Zhang et al., 2019) (Figure 4.8D). The GFAP+ astrocytes generated from Control and β-cat$^{del\ ex3-6}$ AHSPCs were morphological similar at all time points after virus transduction (Figure 4.8D). The proportion of GFAP+ cells is similar between Control and β-cat$^{del\ ex3-6}$ AHSPCs at both 6- and 12- days after virus transduction indicating that loss of β-catenin signalling does not affect astrocyte differentiation at these time points (Figure 4.8E). At 18 Days after virus transduction the proportion of GFAP+ cells is greater in β-cat$^{del\ ex3-6}$ AHSPCs compared with Control (Figure 4.8E). These preliminary results could suggest that differentiation towards the astrocyte lineage is enhanced by a chronic loss of β-catenin signalling.

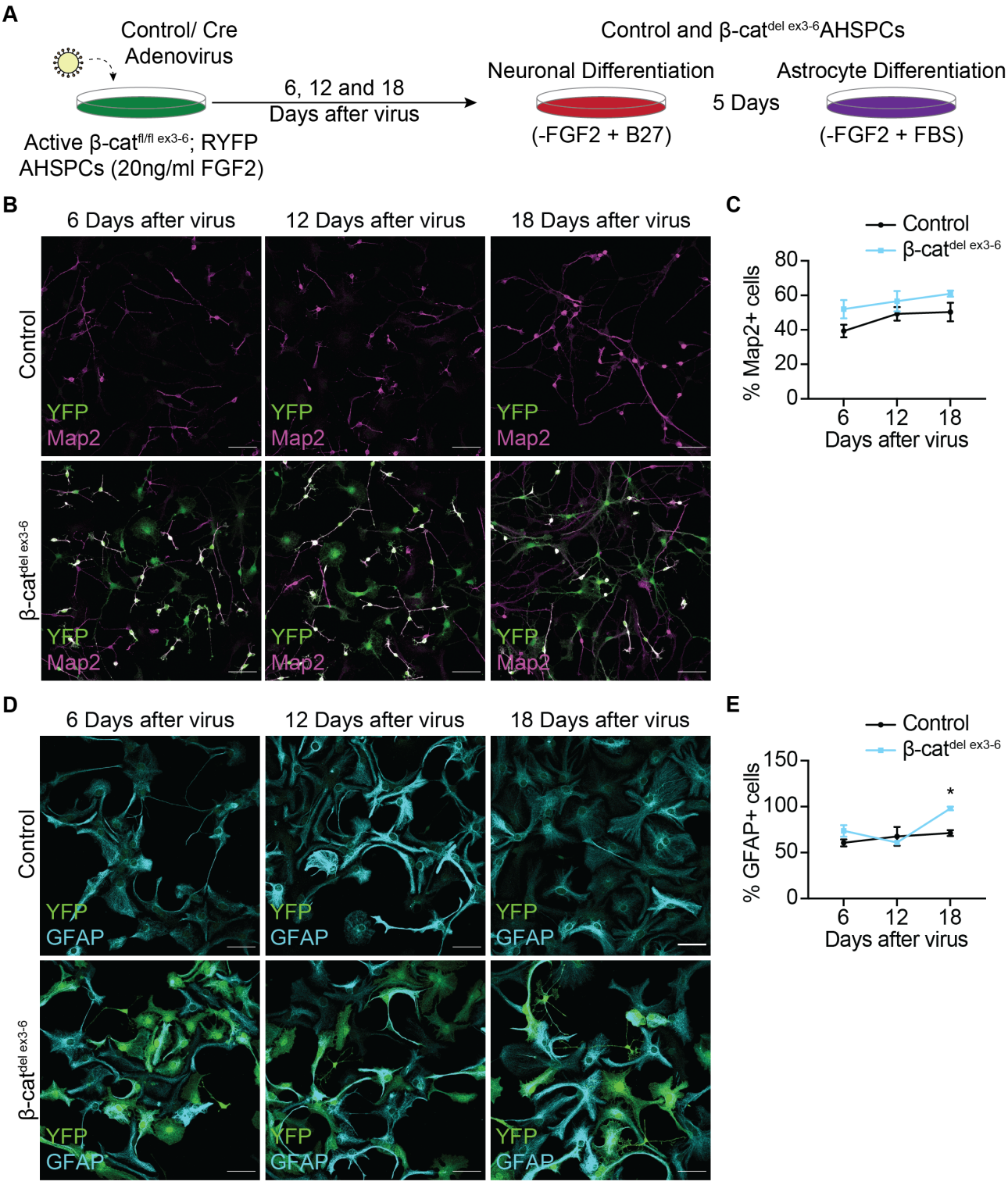


Figure 4.8: Chronic loss of β-catenin signalling does not impair AHSPCs ability to differentiate into neurons and astrocytes *in vitro*.

(A) Schematic of experimental design. Active (20ng/ml FGF2) β-cat$^{fl/fl\ ex3-6}$ AHSPCs were treated with Control and Cre adenovirus overnight and active culture media was refreshed the following morning and maintained. At 6-, 12- and 18- Days after virus transduction, Control and β-cat$^{del\ ex3-6}$ AHSPCs were cultured in conditions to promote neuronal or astrocytic differentiation. The

growth factor FGF2 was withdrawn and either B27 for neuronal differentiation or FBS for astrocyte differentiation was added. Control and β-cat$^{del\ ex3-6}$ AHSPCs were cultured in these differentiation conditions for 5 days before collection.

(B) YFP (GFP antibody) and Map2 co-immunostaining in Control and β-cat$^{del\ ex3-6}$ cultured in B27 for 5 days at 6-, 12- and 18- Days after virus transduction. YFP labels recombined cells in β-cat$^{del\ ex3-6}$ samples. Map2 is a neuronal marker and is used here to label differentiated neurons. Scale bars represent 50μm. Data shown are representative images from n=1 biological replicate.

(C) Quantification of the proportion of Map2+ neurons shown in **(B)**. For β-cat$^{del\ ex3-6}$ samples, the proportion of Map2+ neurons were calculated from the YFP+ population. Two-way Anova with Sidak's multiple comparisons test was used for statistical analysis. Error bars represent mean with SEM. Data shown is technical repeats of one biological replicate. n=1 biological replicate.

(D) YFP and GFAP co-immunostaining in Control and β-cat$^{del\ ex3-6}$ AHSPCs cultured in FBS for 5 days at 6, 12 and 18 Days after virus transduction. YFP labels recombined cells in β-cat$^{del\ ex3-6}$ samples. GFAP is an astrocyte marker and is used here to label differentiated astrocytes. Scale bars represent 50μm. Data shown are representative images from n=1 biological replicate.

(E) Quantification of the proportion of GFAP+ astrocytes shown in **(D).** For β-cat$^{del\ ex3-6}$ samples, the proportion of GFAP+ astrocytes were calculated from the YFP+ population. Two-way Anova with Sidak's multiple comparisons test was used for statistical analysis, (*, $p<0.05$). Error bars represent mean with SEM. Data shown is technical repeats of one biological replicate. n=1 biological replicate.

4.3 *in vivo* Model Fails to Reliably Delete β-catenin and Inhibit Canonical Wnt Signalling in AHSCs

In Chapter 3, using the BATGAL Wnt reporter mouse model, I showed that AHSCs *in vivo* respond to canonical Wnt signalling. To understand the role of canonical Wnt signalling in these Wnt responding AHSCs *in vivo*, I generated transgenic inducible knock-out mice to inhibit AHSCs' response to canonical Wnt signalling within the *in vivo* context. I generated GlastCreERT2; β-cat$^{fl/fl\ ex3-6}$; RYFP mice as described in Section 2.1.1 to conditionally delete β-catenin in Glast-expressing AHSCs by tamoxifen-inducible Cre-mediated recombination. Mice

from this line were used to generate the *in vitro* AHSPC line presented above (Figure 4.2A). As stated previously, β-catenin is the key downstream mediator of canonical Wnt signalling, therefore deleting β-catenin should prevent the transduction of canonical Wnt signalling in recombined cells (Papkoff et al., 1996; Peifer et al., 1994b). Glast encodes a glutamate aspartate transporter protein that is expressed in AHSCs, IPCs and astrocytes (Mori et al., 2006). Cre is fused to a mutated ligand binding domain of the oestrogen receptor and is retained in the cytoplasm of Glast+ cells in the absence of tamoxifen (Mori et al., 2006; Feil et al., 1997). Upon tamoxifen administration, Cre translocates to the nucleus of Glast+ cells and recombines the LoxP sites within the β-cat$^{fl/fl\ ex3-6}$ allele thus generating a truncated form of β-catenin mRNA, which is unable to produce protein (Mori et al., 2006; Feil et al., 1997; Huelsken et al., 2001) (β-cat$^{del\ ex3-6}$ Figure 4.2A). The inclusion of the RYFP reporter allows the identification of recombined cells based on their YFP expression.

4.3.1 Unsuccessful β-catenin Deletion in AHSCs *in vivo*, Means That Canonical Wnt Signalling Remains Intact in the AHSCs of β-cat$^{del\ ex3-6}$ Mice

I first set out to validate this mouse model for the deletion of β-catenin and inhibition of canonical Wnt signalling in the recombined AHSCs of β-cat$^{del\ ex3-6}$ mice. To do this, I crossed GlastCreERT2; β-cat$^{fl/fl\ ex3-6}$; RYFP mice to the BATGAL Wnt reporter mice that express *LacZ* under the control of 7 x β-catenin/TCF/LEF responsive elements (Maretto et al., 2003). This means that Wnt responding cells express nuclear β-galactosidase, which I can visualise using immunofluorescence techniques. Therefore, β-galactosidase immunostaining should be decreased in recombined (YFP+) β-cat$^{del\ ex3-6}$ AHSCs that are unable to respond to canonical Wnt signalling as a consequence of β-catenin deletion.

2-month-old GlastCreERT2; β-cat$^{fl/wt\ ex3-6}$; RYFP; BATGAL (Control) and GlastCreERT2; β-cat$^{fl/fl\ ex3-6}$; RYFP; BATGAL (β-cat$^{del\ ex3-6}$) mice were injected once daily with tamoxifen for 5 consecutive days and sacrificed 30 days after the first injection by transcardial perfusion (Figure 4.9A). Immunostaining for recombined AHSCs (YFP+ GFAP+ with radial morphology) and β-galactosidase of the BATGAL Wnt reporter, highlighted the presence of BATGAL+ YFP+ AHSCs in both Control and β-cat$^{del\ ex3-6}$ mice 30 days after tamoxifen (Figure 4.9B). This suggests that AHSCs are still able to respond to canonical Wnt signalling in β-cat$^{del\ ex3-6}$ mice. Indeed, the

proportion of BATGAL+ YFP+ AHSCs is similar between Control and β-cat$^{del\ ex3-6}$ mice (Figure 4.9C), indicating that AHSCs in β-cat$^{del\ ex3-6}$ mice are still responding to canonical Wnt signalling.

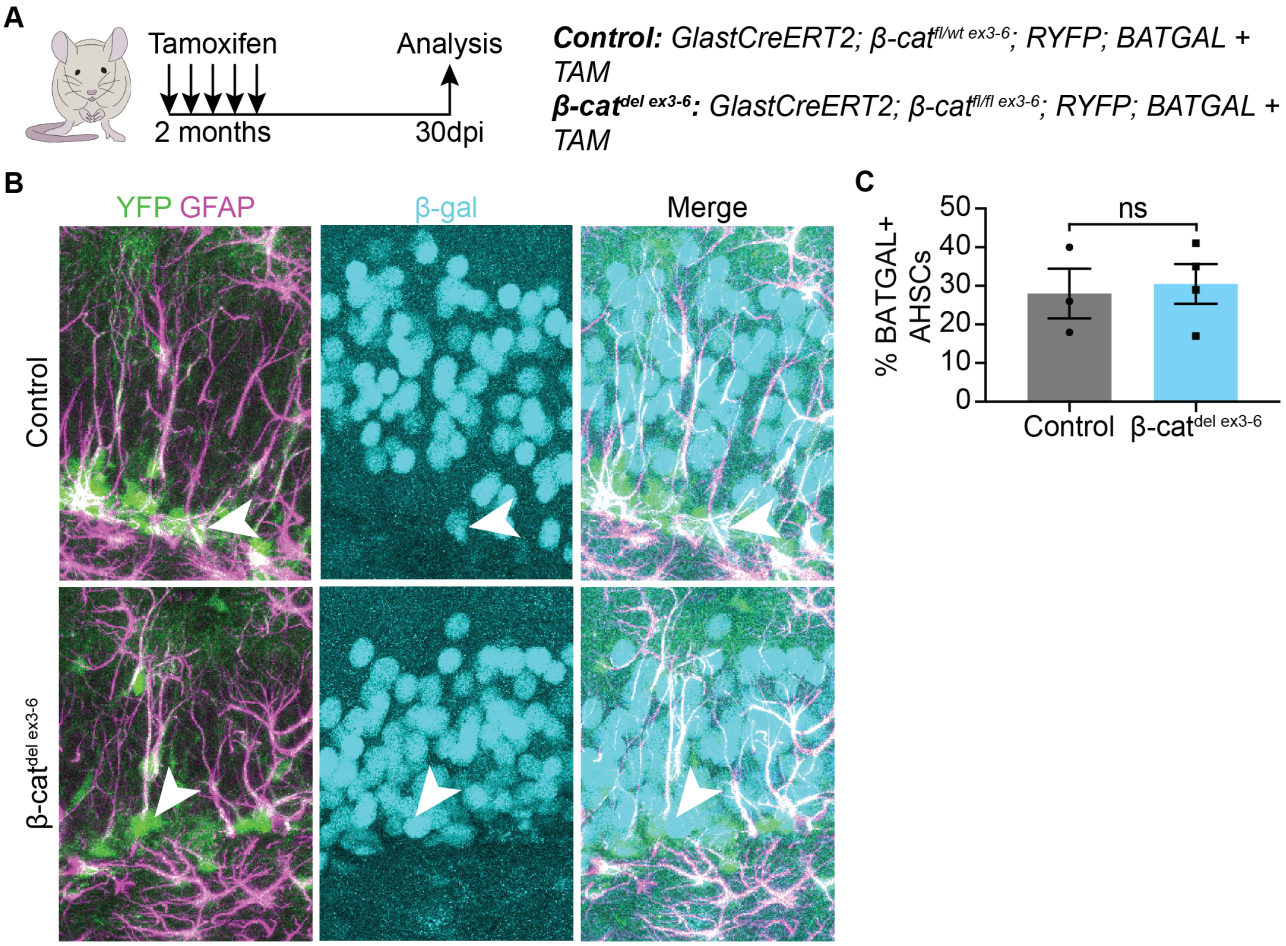


Figure 4.9: Canonical Wnt signalling is not inhibited in YFP+ AHSCs of β-cat$^{del\ ex3-6}$ mice 30 days after tamoxifen.

(A) Schematic of experimental design. 2-month-old GlastCreERT2; β-cat$^{fl/wt\ ex3-6}$; RYFP; BATGAL (Control) and GlastCreERT2; β-cat$^{fl/fl\ ex3-6}$; RYFP; BATGAL (β-cat$^{del\ ex3-6}$) mice were injected once daily with tamoxifen for 5 consecutive days and sacrificed 30 days after the first injection by transcardial perfusion.

(B) β-galactosidase, YFP (GFP antibody) and GFAP immunolabelling in the DG of Control and β-cat$^{del\ ex3-6}$ mice 30 days after the first tamoxifen injection. Wnt responding AHSCs that have recombined (YFP+ BATGAL+ GFAP+ cells with radial morphology) can been seen in both Control and β-cat$^{del\ ex3-6}$ mice. This indicates that AHSCs in β-cat$^{del\ ex3-6}$ mice are still able to respond to canonical Wnt signalling. Arrowheads indicate recombined Wnt responding AHSCs (YFP+ BATGAL+ GFAP+ cells with radial morphology).

(C) Quantification of the proportion of BATGAL+ (Wnt responding) YFP+ AHSCs in Control and β-cat$^{del\ ex3-6}$ mice 30 days after the first tamoxifen injection. The proportion of BATGAL+ YFP+ AHSCs is similar between Control and β-cat$^{del\ ex3-6}$ mice, indicating that AHSCs are still able to respond to canonical Wnt signalling in β-cat$^{del\ ex3-6}$ mice. An unpaired Student's t-test was performed for statistical analysis (ns, $p>0.05$). n=3 and n=4 biological replicates for Control and β-cat$^{del\ ex3-6}$ mice respectively.

The presence of BATGAL+ YFP+ AHSCs in β-cat$^{del\ ex3-6}$ mice, prompted me to investigate whether β-catenin was successfully deleted in β-cat$^{del\ ex3-6}$ mice upon tamoxifen administration. To see whether β-catenin protein levels are reduced in the DG of β-cat$^{del\ ex3-6}$ mice, I immunolabelled Control and β-cat$^{del\ ex3-6}$ brain sections using an antibody against the C-terminal domain of β-catenin (Figure 4.10A). Overall, β-catenin protein levels do not appear to be decreased in the DG of β-cat$^{del\ ex3-6}$ mice 30 days after the first tamoxifen injection (Figure 4.10A). Also, the proportion of β-catenin+ YFP+ AHSCs is similar between Control and β-cat$^{del\ ex3-6}$ mice (Figure 4.10B), which indicates that β-catenin protein is still present in YFP+ AHSCs of β-cat$^{del\ ex3-6}$ mice.

I next used *in situ* hybridisation to confirm whether the floxed region of β-catenin had been deleted in YFP+ AHSCs of β-cat$^{del\ ex3-6}$ mice. I designed primers to generate an RNA *in situ* probe that spans exons 3-6 of β-catenin (*β-cat^{ex3-6}*) and used cDNA from *in vitro* WT active AHSPCs as template for the PCR reaction. The PCR product was sent for Sanger sequencing to confirm specificity of the amplification and the *in situ* probe was generated as described in Section 2.2.3. *in situ* hybridisation using the designed antisense probe showed that *β-cat^{ex3-6}* is still expressed in the DG of Control and β-cat$^{del\ ex3-6}$ mice 30 days after tamoxifen injection (Figure 4.10C). The specificity of the probe was confirmed upon comparison with the sense Control probe, which did not report any signal (Figure 4.10C). To determine whether the mRNA levels of the floxed region of β-catenin was decreased in recombined AHSCs, I combined the *β-cat^{ex3-6} in situ* probe with immunofluorescence to identify recombined AHSCs (Figure 4.10C outlined cells). However, the inability to generate single z-plane images of the *β-cat^{ex3-6} in situ*, made it difficult to assign the *in situ* signal to individual AHSCs.

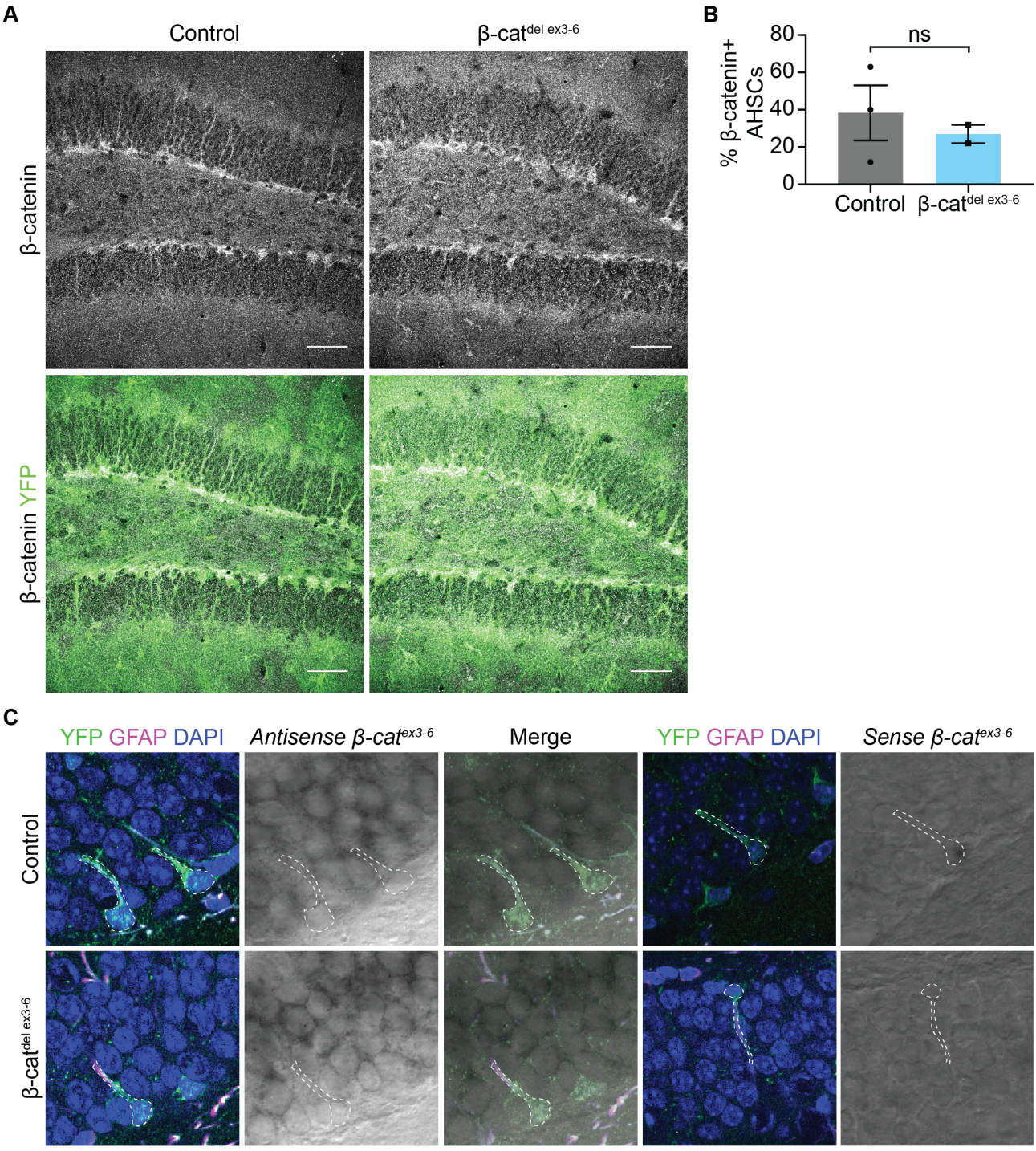


Figure 4.10: β-catenin immunolabelling and *in situ* analysis in the DG of Control and β-cat$^{del\ ex3-6}$ mice 30 days after the first tamoxifen injection.

(A) β-catenin and YFP (GFP antibody) immunolabelling in the DG of Control and β-cat$^{del\ ex3-6}$ mice 30 days after the first tamoxifen injection. β-catenin immunolabelling is widespread in the SGZ of both Control and β-cat$^{del\ ex3-6}$ mice, indicating that β-catenin protein is still present in the SGZ of β-cat$^{del\ ex3-6}$ mice. Scale bars represent 50μm.

(B) Quantification of the proportion of YFP+ β-catenin+ AHSCs in Control and β-cat$^{del\ ex3-6}$ mice 30 days after the first tamoxifen injection. Students' t-test was performed for statistical analysis (ns, p>0.05). Error bars represent mean with SEM. n=3 and n=2 biological repeats for Control and β-cat$^{del\ ex3-6}$ respectively.

(C) *in situ* hybridisation of antisense and sense *β-cat^{ex3-6}* with YFP, GFAP and DAPI immunolabelling in Control and β-cat$^{del\ ex3-6}$ mice 30 days after the first tamoxifen injection. Outlined cells indicate AHSCs in Control and β-cat$^{del\ ex3-6}$ mice. n=2 biological replicates.

Due to the difficulty in assigning the *β-cat^{ex3-6} in situ* signal to individual YFP+ AHSCs, I next used qPCR analysis to determine whether the floxed region of β-catenin was recombined. To do this, I FAC Sorted the YFP+ cells from Control and β-cat$^{del\ ex3-6}$ mice and performed qPCR analysis to investigate the expression levels of the floxed region of β-catenin (Figure 4.11A). I injected 2-month-old GlastCreERT2; β-cat$^{fl/wt\ ex3-6}$; RYFP (Control) and GlastCreERT2; β-cat$^{fl/fl\ ex3-6}$; RYFP (β-cat$^{del\ ex3-6}$) with tamoxifen, once daily for 5 consecutive days to induce recombination (Figure 4.11A). Ten days after the first tamoxifen injection, I dissected the DG of individual Control and β-cat$^{del\ ex3-6}$ mice and processed these samples for FAC Sorting of YFP+ cells (Figure 4.11A). The dissection and FAC Sorting were performed in collaboration with L. Harris and the Crick Flow Cytometry Science Technology Platform (STP). The number of YFP+ cells collected from each individual sample ranged from 400-7,000 cells. I then extracted the RNA from the collected YFP+ cells, and synthesised cDNA for the qPCR analysis. The amount of RNA used for cDNA synthesis was normalised according to the lowest number of YFP+ cells collected for each replicate. I next performed qPCR analysis using TaqMan probes for both an unfloxed region of *β-catenin* (*β-cat$^{ex13-14}$*) and the floxed region of *β-catenin* (*β-cat^{ex4-5}*) (Figure 4.11B). The gene expression level of the unfloxed region *β-cat$^{ex13-14}$* is unchanged in YFP+ cells from Control and β-cat$^{del\ ex3-6}$ mice, indicating that these cells express *β-catenin* (Figure 4.11C). Two out of the three β-cat$^{del\ ex3-6}$ mice dissected showed no difference in the gene expression level of *β-cat^{ex4-5}* compared to Control (Figure 4.11D) This indicates that they have failed to successfully recombine the floxed region of β-catenin upon tamoxifen administration (Figure 4.11D). However, one β-cat$^{del\ ex3-6}$ mouse did show a decrease in the expression level of *β-cat^{ex4-5}*, meaning that recombination has occurred in the YFP+ cells collected from this mouse (Figure 4.11D). I also checked the gene expression level of the Wnt target gene *Axin2* and found no difference between Control and β-cat$^{del\ ex3-6}$ mice (Figure 4.11E). This suggests that canonical Wnt signalling is not inhibited in YFP+ cells of β-cat$^{del\ ex3-6}$ mice due to the failure to reliably

delete β-catenin. Overall, these data show that recombination of the floxed region of *β-catenin* only occurs in one third of β-cat$^{del\ ex3-6}$ mice making this an inefficient model for deleting β-catenin and inhibiting canonical Wnt signalling in AHSCs *in vivo*.

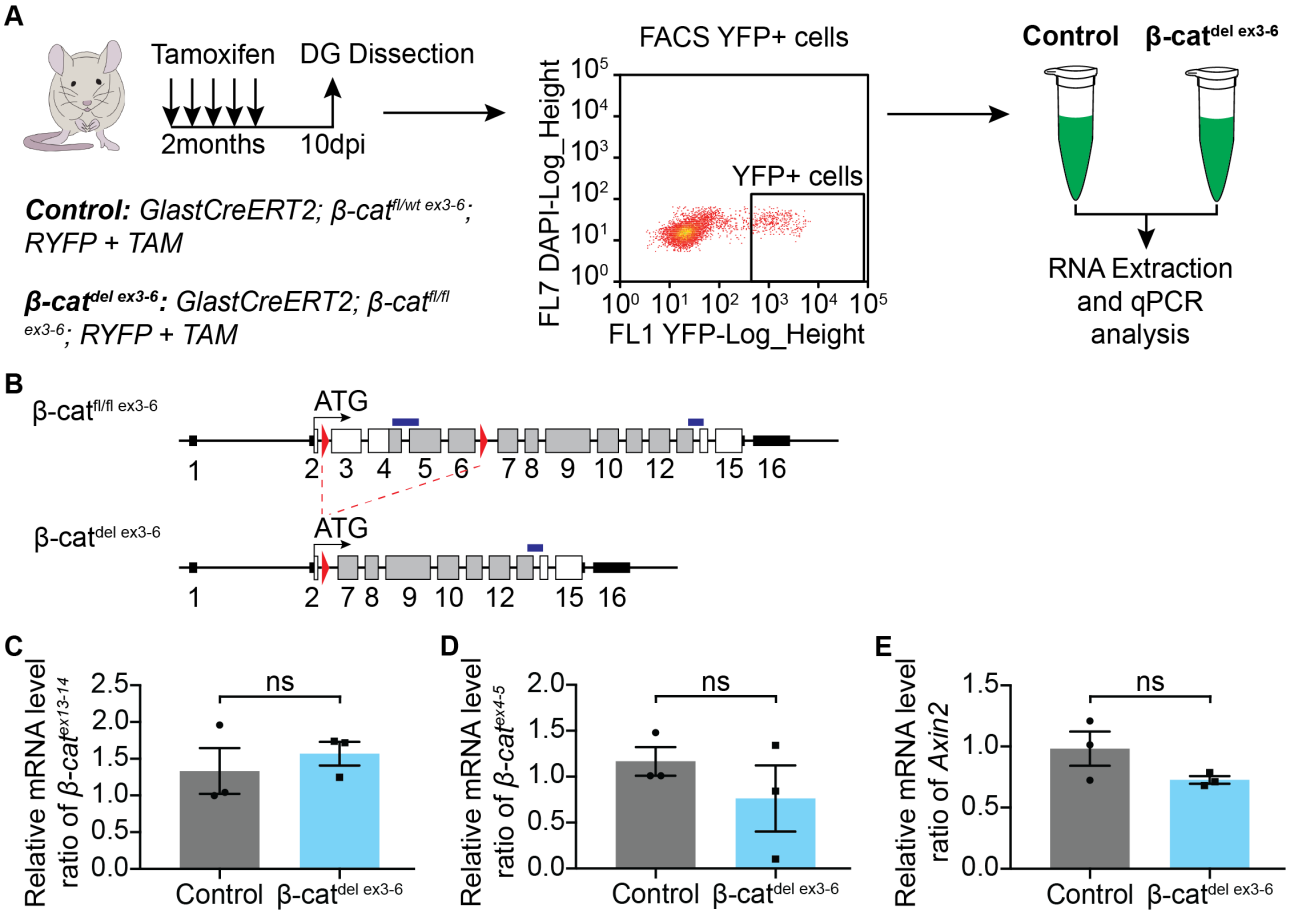


Figure 4.11: Recombination of the floxed region of *β-catenin* is inefficient in FAC Sorted YFP+ cells from β-cat$^{del\ ex3-6}$ mice.

(A) Schematic of experimental design. 2-month-old GlastCreERT2; β-cat$^{fl/wt\ ex3-6}$; RYFP (Control) and GlastCreERT2; β-cat$^{fl/fl\ ex3-6}$; RYFP (β-cat$^{del\ ex3-6}$) were injected with tamoxifen once daily for 5 consecutive days. 10 days after the first tamoxifen injection, the DG of individual mice was dissected and YFP+ cells were FAC Sorted and collected for RNA extraction and qPCR analysis.

(B) Schematic of *β-cat$^{fl/fl\ ex3-6}$* allele before and after tamoxifen induced Cre mediated recombination. LoxP sites (red triangles) flank exons 3-6 which encode the N-terminal domain and armadillo repeats 1-4 (grey boxes). Upon tamoxifen induced Cre-mediated recombination, a deletion/frame-shift mutation is introduced fusing exon 2 with exon 7, which generates truncated mRNA but does not encode a functional protein (Huelsken et al, 2001). Black boxes indicate non-coding exons. Large boxes indicate coding exons. Grey boxes indicate armadillo

repeats. Red arrows indicate LoxP sites. Blue boxes indicate the TaqMan probes used for qPCR analysis.

(C) qPCR analysis of the gene expression levels of an unfloxed region of *β-catenin (β-cat$^{ex13-14}$)*. The TaqMan probe used spans exons 13-14 which is outside the floxed region and its' expression levels are unaffected by tamoxifen induced Cre-mediated recombination in YFP+ cells from both Control and β-cat$^{del\ ex3-6}$ mice.

(D) qPCR analysis of the gene expression levels of the floxed region of *β-catenin (β-cat^{ex4-5})*. The TaqMan probe used spans exons 4-5 which is within the floxed region. Two out of the three β-cat$^{del\ ex3-6}$ repeats show a similar expression level to Control indicating that the YFP+ cells in these samples have not recombined *β-cat$^{fl/fl\ ex3-6}$*. One sample has undergone successful recombination of the floxed region of β-catenin.

(E) qPCR analysis of the gene expression levels of the Wnt target gene *Axin2*. *Axin2* levels are unchanged between YFP+ cells from Control and β-cat$^{del\ ex3-6}$ mice indicating that canonical Wnt signalling is not inhibited due to the failure to reliably delete β-catenin.

For all qPCR analysis a Student's t-test was used for statistical analysis (ns, $p>0.05$). Error bars represent mean with SEM. n=3 biological replicates for Control and β-cat$^{del\ ex3-6}$ mice.

4.3.2 Adult Neurogenesis is Unaffected in β-cat$^{del\ ex3-6}$ Mice Due to Failed Recombination

As this model failed to successfully recombine and delete β-catenin in Glast+ cells, I anticipated that adult neurogenesis would be unaffected in this mouse model. To confirm this, 2-month-old GlastCreERT2; β-cat$^{fl/wt\ ex3-6}$; RYFP (Control) and GlastCreERT2; β-cat$^{fl/fl\ ex3-6}$; RYFP (β-cat$^{del\ ex3-6}$) mice were administered tamoxifen, by intraperitoneal (ip) injection, once daily for 5 consecutive days and were transcardially perfused 30 days after the first tamoxifen injection (30dpi) for analysis (Figure 4.12A). Collecting samples 30 days after the initial tamoxifen injection allowed me to investigate the resulting phenotype in the AHSC population and the whole process of adult neurogenesis. I performed immunofluorescence staining for AHSC markers (YFP+ GFAP+ cells with radial morphologies) to investigate whether the AHSC population was affected. Quantification of the total number of YFP+ AHSCs normalised to the SGZ length showed no difference between Control and β-cat$^{del\ ex3-6}$ mice 30 days after tamoxifen induced recombination at 2 months, as expected (Figure 4.12C). I also stained for the proliferation marker Ki67 (Figure 4.12B) and found no difference in the percentage of Ki67+ AHSCs between Control and β-cat$^{del\ ex3-6}$ mice (Figure 4.12D). In addition, the total number of Ki67+ cells normalised to the SGZ length, which includes active AHSCs, IPCs and proliferating

neuroblasts, was similar in both Control and β-cat$^{del\ ex3-6}$ mice 30 days after tamoxifen administration (Figure 4.12E). This confirms that AHSCs and their progeny are unaffected in this mouse model as β-catenin has not been deleted.

Doublecortin (DCX) is a microtubule-associated protein (MAP) that is expressed in late progenitors and neuroblasts (NBs) of the hippocampal neurogenic lineage and is commonly used to detect levels of adult neurogenesis (Brown et al., 2003). Therefore, I used DCX immunolabelling in brain sections from Control and β-cat$^{del\ ex3-6}$ mice, 30 days after tamoxifen, to compare the levels of adult hippocampal neurogenesis in this model (Figure 4.12F). The morphologies of DCX+ neuroblasts are similar between Control and β-cat$^{del\ ex3-6}$ mice (Figure 4.12F), indicating that neuroblast maturation is unaffected. In addition, the total number of DCX+ neuroblasts is not significantly changed between Control and β-cat$^{del\ ex3-6}$ mice 30 days after the first tamoxifen injection (Figure 4.12G). This indicates that adult neurogenesis is unaffected in β-cat$^{del\ ex3-6}$ mice due to the failure to successfully recombine and delete β-catenin.

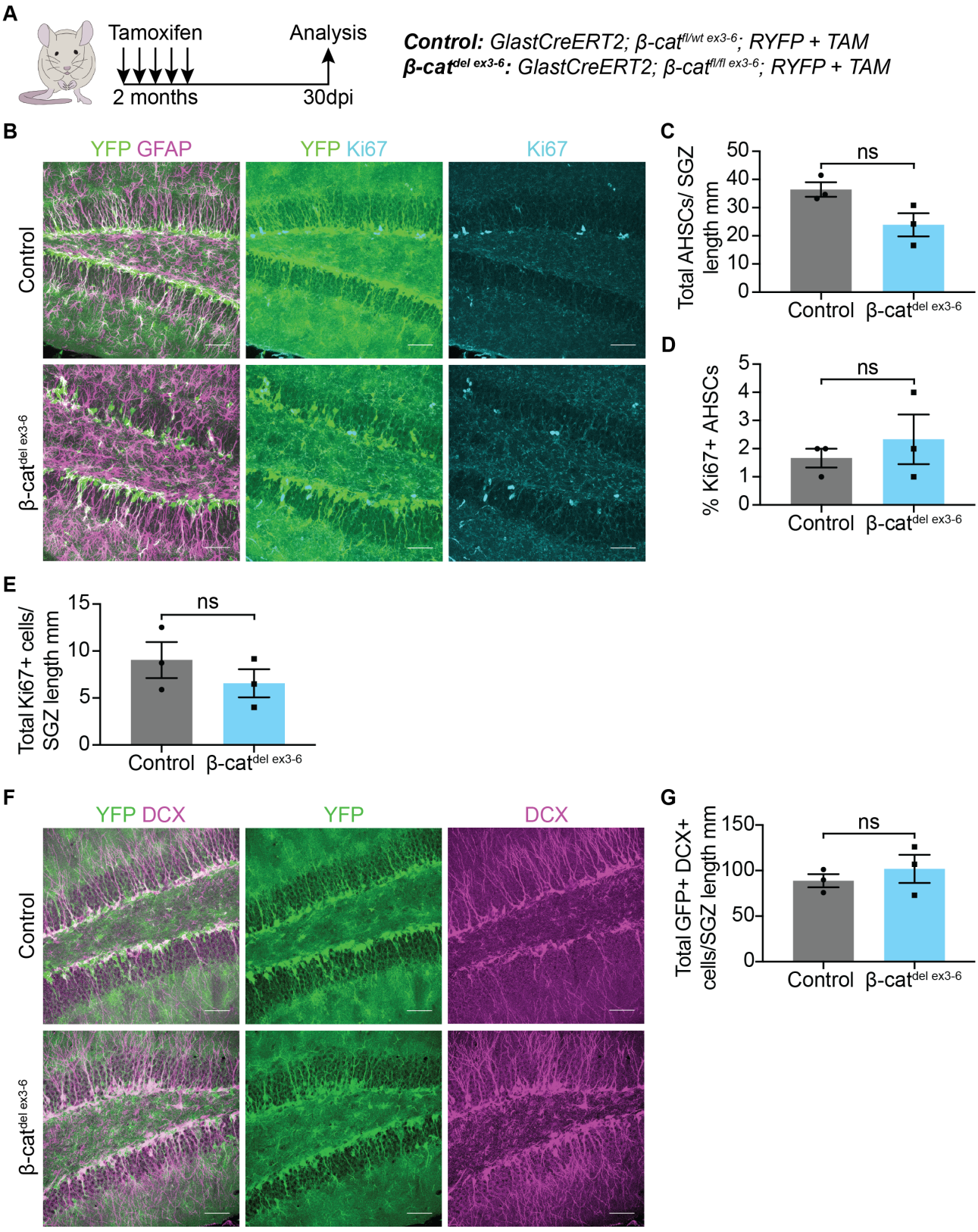


Figure 4.12: Adult neurogenesis is unaffected in β-cat$^{del\ ex3-6}$ mice 30 days after tamoxifen.

(A) Schematic of experimental design. 2-month-old mice were injected with tamoxifen for 5 consecutive days and sacrificed 30 days after the first tamoxifen injection for analysis.

Tamoxifen was administered to both GlastCreERT2; β-cat$^{fl/wt\ ex3-6}$;RYFP (Control) mice and GlastCreERT2; β-cat$^{fl/fl\ ex3-6}$;RYFP (β-cat$^{del\ ex3-6}$) mice.

(B) Immunolabelling of AHSCs (GFAP+ YFP+ cells with radial morphologies) and the proliferation marker Ki67 in the DG of Control and β-cat$^{del\ ex3-6}$ animals 30 days after tamoxifen administration. No gross overall phenotype can be observed between Control and β-cat$^{del\ ex3-6}$ animals. GFP antibody was used to label YFP+ cells. Scale bars represent 50μm.

(C) Quantification of the total number of YFP+ AHSCs normalised to the length of the SGZ in Control and β-cat$^{del\ ex3-6}$ animals 30 days after tamoxifen administration. No significant difference is observed between Control and β-cat$^{del\ ex3-6}$ animals. An unpaired Student's t-test was used for statistical analysis, (ns, $p>0.05$). Error bars represent mean with SEM. Data shown is of n=3 biological replicates for each genotype.

(D) Quantification of the proportion of Ki67+ YFP+ AHSCs in Control and β-cat$^{del\ ex3-6}$ animals 30 days after tamoxifen administration. No significant difference is observed between Control and β-cat$^{del\ ex3-6}$ animals. An unpaired Student's t-test was used for statistical analysis, (ns, $p>0.05$). Error bars represent mean with SEM. Data shown is of n=3 biological replicates for each genotype.

(E) Quantification of the total number of YFP+ Ki67+ cells normalised to the length of the SGZ in Control and β-cat$^{del\ ex3-6}$ animals 30 days after tamoxifen administration. Ki67+ YFP+ cells include active AHSCs, IPCs and neuroblasts. No significant difference is observed between Control and β-cat$^{del\ ex3-6}$ animals. An unpaired Student's t-test was used for statistical analysis, (ns, $p>0.05$). Error bars represent mean with SEM. Data shown is of n=3 biological replicates for each genotype.

(F) Immunolabelling of YFP and DCX (neuroblasts) in the DG of Control and β-cat$^{del\ ex3-6}$ animals 30 days after tamoxifen administration. No gross overall phenotype can be observed in the morphologies or numbers of DCX+ neuroblasts between Control and β-cat$^{del\ ex3-6}$ animals. Scale bars represent 50μm.

(D) Quantification of the total number of YFP+ DCX+ neuroblasts normalised to the length of the SGZ in Control and β-cat$^{del\ ex3-6}$ animals 30 days after tamoxifen administration. No significant difference is observed between Control and β-cat$^{del\ ex3-6}$ animals. An unpaired Student's t-test was used for statistical analysis, (ns, $p>0.05$). Error bars represent mean with SEM. Data shown is of n=3 biological replicates for each genotype.

4.4 Deletion of β-catenin in AHSCs from a Second β-catenin$^{fl/fl}$ Mouse Model Does Not Affect AHSCs But Does Impair Adult Neurogenesis

4.4.1 β-catenin is Successfully Deleted in YFP+ Cells from The DG of β-cat$^{del\ ex2-6}$ Mice

As β-catenin was not reliably deleted in the AHSCs of the previous mouse model, (GlastCreERT2; β-cat$^{fl/fl\ ex3-6}$; RYFP mice), I generated a second β-catenin floxed mouse line to investigate the role of canonical Wnt signalling in AHSCs *in vivo*. This second β-catenin floxed line contains LoxP sites flanking exons 2-6 of β-catenin (β-cat$^{fl/fl\ ex2-6}$), which encode the N-terminal domain, ATG translational start codon and Armadillo repeats 1-4 of β-catenin (Brault et al., 2001). Tamoxifen induced Cre-mediated recombination of these LoxP sites flanking exons 2-6 of β-catenin generates the β-cat$^{del\ ex2-6}$ allele, which is unable to generate a functional protein (Brault et al., 2001) (Figure 4.13A). I crossed β-cat$^{fl/fl\ ex2-6}$ mice with GlastCreERT2; RYFP mice to generate GlastCreERT2; β-cat$^{fl/fl\ ex2-6}$; RYFP mice. As described previously, tamoxifen administration will promote Cre translocation to the nucleus of Glast+ cells, where it facilitates the recombination of the LoxP sites within the β-cat$^{fl/fl\ ex2-6}$ allele. By including the RYFP reporter of recombination allele, I am able to identify the cells that have successfully recombined as being YFP+.

To confirm β-cat$^{fl/fl\ ex2-6}$ recombination in this mouse model, I FAC Sorted the YFP+ cells from the DG of 2-month-old GlastCreERT2; β-cat$^{wt/wt\ ex2-6}$; RYFP (Control) and GlastCreERT2; β-cat$^{fl/fl\ ex2-6}$; RYFP (β-cat$^{del\ ex2-6}$) mice 10 days after tamoxifen administration and performed qPCR analysis for both floxed and unfloxed regions of β-catenin (Figure 4.13B). The dissection and FAC Sorting were performed in collaboration with L. Harris and the Crick Flow Cytometry STP and were identically processed for qPCR analysis as described for the previous mouse model (Figure 4.11). qPCR analysis for an unfloxed region of *β-catenin* (*β-cat$^{ex\ 13-14}$*) shows a similar expression level between Control and β-cat$^{del\ ex2-6}$ mice, indicating that these cells express β-catenin (Figure 4.13C). The expression level of the floxed region of *β-catenin* (*β-cat$^{ex\ 4-5}$*) is significantly decreased in β-cat$^{del\ ex2-6}$ mice compared to Control (Figure 4.13D). This confirms successful recombination of the *β-cat$^{fl/fl\ ex2-6}$* allele upon tamoxifen administration in GlastCreERT2; β-cat$^{fl/fl\ ex2-6}$; RYFP mice. All three biological replicates behaved in a similar manner (Figure 4.13D), showing that this recombination event is more efficient in this mouse model compared with the previous one. I also checked the gene expression levels of the Wnt target gene *Axin2*, to determine whether the successful recombination of the *β-cat$^{fl/fl\ ex2-6}$* allele

inhibits canonical Wnt signalling in YFP+ cells (Figure 4.13E). However, I did not observe a significant decrease in *Axin2* expression levels between Control and β-cat$^{del\ ex2-6}$ mice (Figure 4.13E) suggesting that canonical Wnt signalling levels are not impaired by loss of β-catenin. This recapitulates my *in vitro* observations in Section 4.2.1, that loss of β-catenin does not inhibit AHSCs' baseline response to canonical Wnt signalling. It again also raises the possibility that *Axin2* expression is not strictly dependent on canonical Wnt signalling levels in these cells and therefore may not provide a reliable read-out for inhibited canonical Wnt signalling.

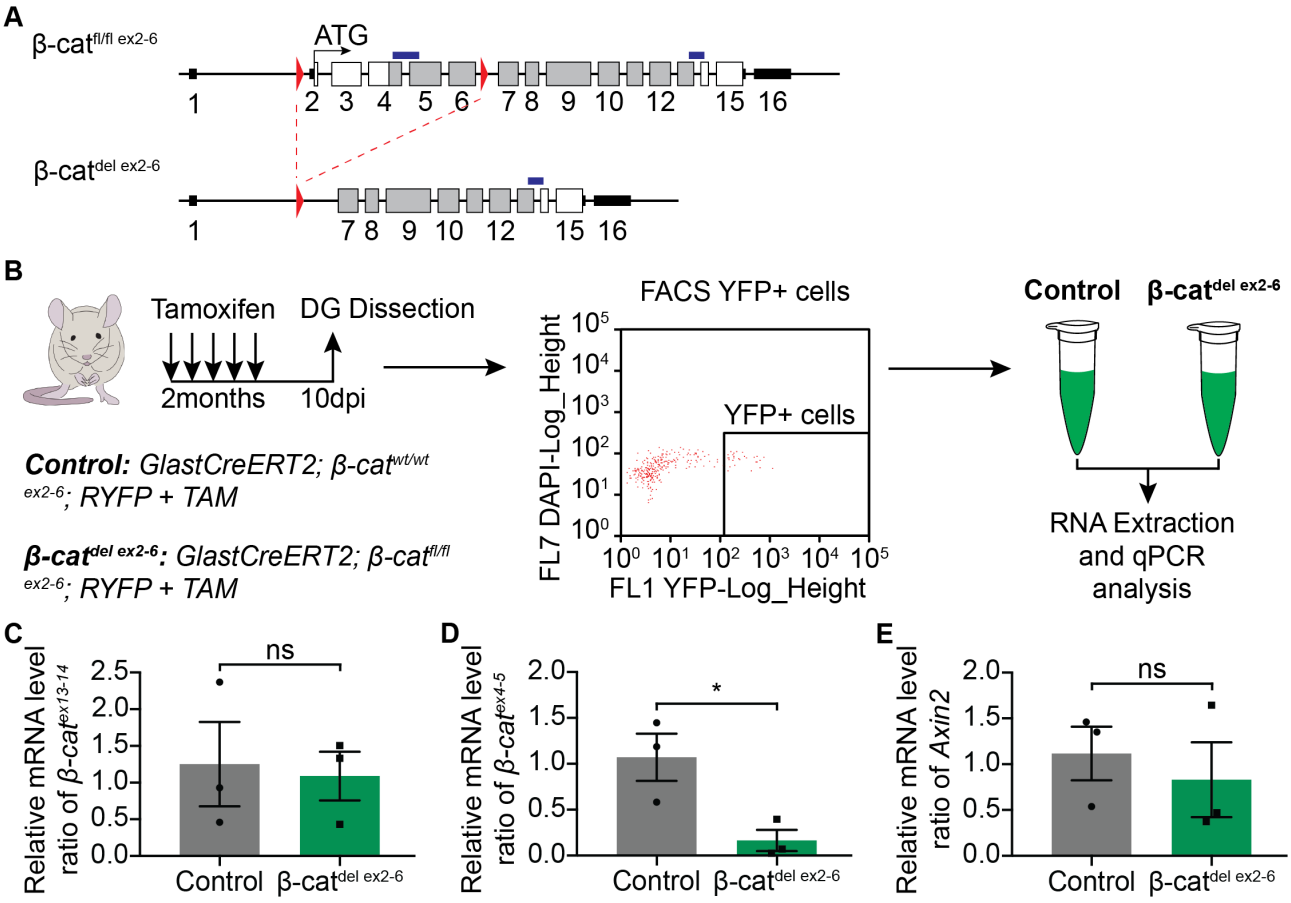


Figure 4.13: *β-cat*$^{fl/flex\ 2-6}$ allele is successfully recombined in FAC Sorted YFP+ cells from β-cat$^{del\ ex2-6}$ mice.

(A) Schematic of *β-cat*$^{fl/fl\ ex2-6}$ allele before and after tamoxifen induced Cre mediated recombination. LoxP sites (red triangles) flank exons 2-6 which encode the ATG translational start codon, the N-terminal domain and armadillo repeats 1-4 (grey boxes). Tamoxifen induced Cre-mediated recombination, generates the *β-cat*$^{del\ ex2-6}$ allele, which is unable to generate functional protein (Brault et al., 2001). Black boxes indicate non-coding exons. Large boxes indicate coding exons. Grey boxes indicate armadillo repeats. Red arrows indicate LoxP sites. Blue boxes indicate the TaqMan probes used for qPCR analysis.

(B) Schematic of experimental design. 2-month-old GlastCreERT2; β-cat$^{wt/wt\ ex2-6}$; RYFP (Control) and GlastCreERT2; β-cat$^{fl/fl\ ex2-6}$; RYFP (β-cat$^{del\ ex2-6}$) were injected with tamoxifen once daily for 5 consecutive days. 10 days after the first tamoxifen injection, the DG of individual mice was dissected and YFP+ cells were FAC Sorted and collected for RNA extraction and qPCR analysis.

(C) qPCR analysis of the gene expression levels of an unfloxed region of *β-catenin* (*β-cat*$^{ex13-14}$). Expression levels of *β-cat*$^{ex13-14}$ is unaffected by tamoxifen induced Cre-mediated recombination in YFP+ cells from both Control and β-cat$^{del\ ex2-6}$ mice.

(D) qPCR analysis of the gene expression levels of the floxed region of *β-catenin* (*β-cat*$^{ex4-5}$). The expression levels of *β-cat*$^{ex4-5}$ is significantly decreased in β-cat$^{del\ ex2-6}$ mice compared to control, confirming successful recombination in all biological repeats.

(E) qPCR analysis of the gene expression levels of the Wnt target gene *Axin2*. *Axin2* levels are unchanged between YFP+ cells from Control and β-cat$^{del\ ex2-6}$ mice indicating that canonical Wnt signalling is not inhibited despite the successful recombination of the *β-cat*$^{fl/fl\ ex2-6}$ allele.

For all qPCR analysis a Students' t-test was used for statistical analysis (ns, $p>0.05$. *, $p<0.05$). Error bars represent mean with SEM. n=3 biological replicates for Control and β-cat$^{del\ ex3-6}$ mice.

The above results show that the *β-cat*$^{fl/fl\ ex2-6}$ allele is successfully recombined in YFP+ cells 10 days after tamoxifen induced Cre mediated recombination in GlastCreERT2; β-cat$^{fl/fl\ ex2-6}$; RYFP mice (Figure 4.13). I next wanted to confirm that this recombination event resulted in the loss of β-catenin protein levels. For this, I injected 2-month-old GlastCreERT2; β-cat$^{wt/wt\ ex2-6}$; RYFP mice (Control) and GlastCreERT2; β-cat$^{fl/fl\ ex2-6}$; RYFP mice (β-cat$^{del\ ex2-6}$) once daily with tamoxifen for 5 consecutive days. 30 days after the first tamoxifen injection, Control and β-cat$^{del\ ex2-6}$ mice were sacrificed by transcardial perfusion and brain tissue was collected and processed for immunofluorescence techniques (Figure 4.14A). Analysing 30 days after the first tamoxifen injection allows me to investigate the effect deleting β-catenin in the AHSCs has on the whole process of adult neurogenesis. To confirm that *β-cat*$^{fl/fl\ ex2-6}$ recombination results in loss of β-catenin protein levels, I immunolabelled Control and β-cat$^{del\ ex2-6}$ brain sections with an antibody raised against the C-terminal domain of β-catenin (Figure 4.14B). By comparing the confocal images of this β-catenin immunofluorescence, I observed that the intensity of the β-catenin immunolabelling appears to be decreased in the DG of β-cat$^{del\ ex2-6}$ mice compared to Control (Figure 4.14B). This suggests that *β-cat*$^{fl/fl\ ex2-6}$ recombination does result in decreased β-catenin protein levels in the DG of β-cat$^{del\ ex2-6}$ mice, making this a more reliable model of deleting β-

catenin in AHSCs *in vivo*. Quantification of the proportion of β-catenin+ AHSCs is ongoing to further confirm this.

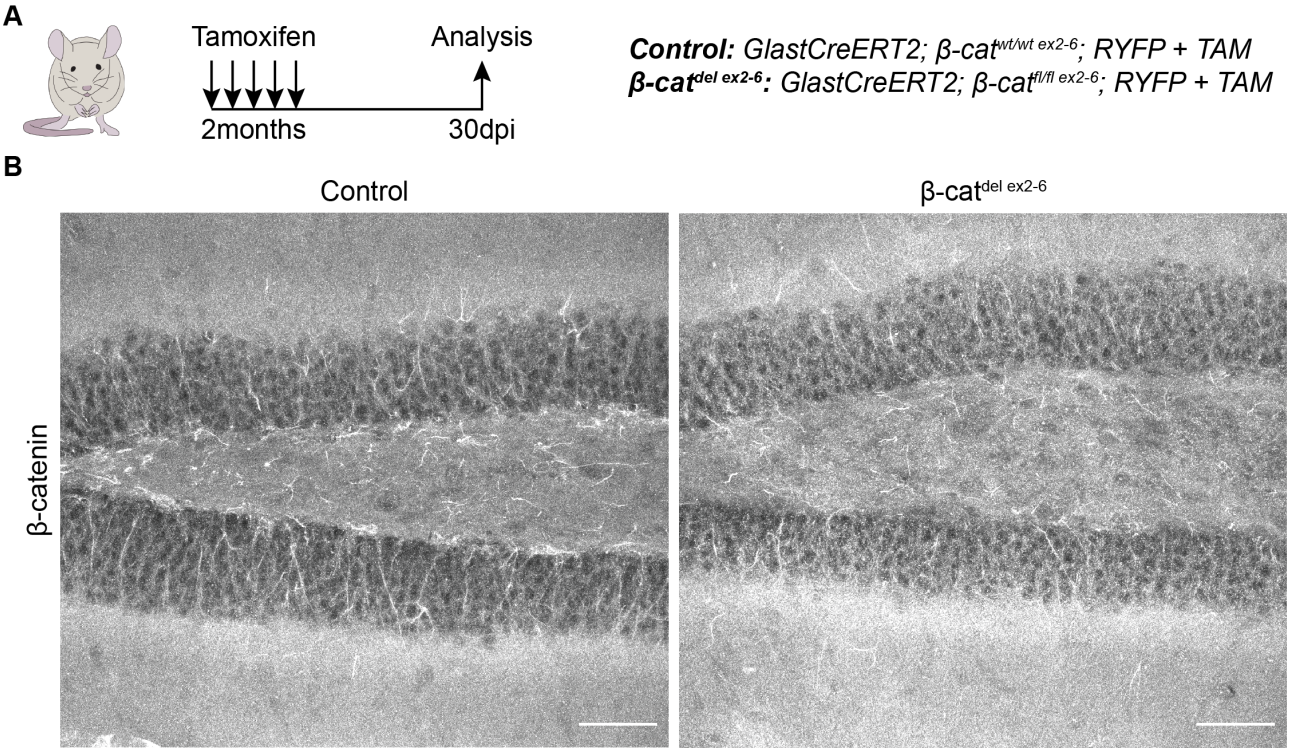


Figure 4.14: β-catenin protein levels are decreased in the DG of β-cat$^{del\ ex2-6}$ mice 30 days after tamoxifen induced Cre-mediated recombination of the *β-cat$^{fl/fl\ ex2-6}$* allele in Glast+ cells.

(A) Schematic of experimental design. 2-month-old GlastCreERT2; β-cat$^{wt/wt\ ex2-6}$; RYFP mice (Control) and GlastCreERT2; β-cat$^{fl/fl\ ex2-6}$; RYFP mice (β-cat$^{del\ ex2-6}$) were injected with tamoxifen once daily for 5 consecutive days. 30 days following the first tamoxifen injection, mice were sacrificed by transcardial perfusion and brains were processed for immunofluorescence techniques.

(B) Representative images of β-catenin immunostaining in the DG of Control and β-cat$^{del\ ex2-6}$ mice 30 days after tamoxifen administration. The β-catenin antibody used was raised against the C-terminal domain of β-catenin. Global levels of β-catenin immunostaining appear to be reduced in the DG of β-cat$^{del\ ex2-6}$ mice compared to Control suggesting loss of β-catenin protein. Scale bars represent 50μm.

4.4.2 AHSCs are Largely Unaffected by Deletion of β-catenin in β-cat$^{del\ ex2-6}$ Mice 30 Days After Tamoxifen Induced Cre-Mediated Recombination of the *β-cat$^{fl/fl\ ex2-6}$* Allele.

The results above confirm the successful recombination and deletion of β-catenin in the DG of β-cat$^{del\ ex2-6}$ mice. I next wanted to investigate how AHSCs are affected by this this loss of β-catenin signalling. To do this I used the same protocol described above whereby 2-month-old GlastCreERT2; β-cat$^{wt/wt\ ex2-6}$; RYFP mice (Control) and GlastCreERT2; β-cat$^{fl/fl\ ex2-6}$; RYFP mice (β-cat$^{del\ ex2-6}$) were injected once daily with tamoxifen for 5 consecutive days and analysed 30 days later (Figure 4.14A). Immunostaining for AHSC markers (GFAP+ Sox2+ cells with radial morphologies) showed that the overall morphologies and organisation of the AHSCs is similar in the DG of Control and β-cat$^{del\ ex2-6}$ mice (Figure 4.15A), indicating that AHSCs are not obviously affected by loss of β-catenin signalling. Indeed, the total number of AHSCs, normalised to the SGZ length, is similar between Control and β-cat$^{del\ ex2-6}$ mice 30 days after tamoxifen administration (Figure 4.15B). I used Ki67 immunostaining to identify proliferating cells and initially observed more Ki67+ cells in the DG of β-cat$^{del\ ex2-6}$ mice compared to Control (Figure 4.15A), suggesting that loss of β-catenin signalling in AHSCs could promote proliferation. However, the percentage of Ki67+ AHSCs is largely unchanged between Control and β-cat$^{del\ ex2-6}$ mice (Figure 4.15C). This indicates that the increased number of proliferating cells observed in the DG of β-cat$^{del\ ex2-6}$ mice (Figure 4.15A) is not due to increased AHSC proliferation, however more quantifications are needed to confirm this. IPCs in the DG can be characterised based on their proliferative nature, the absence of a GFAP+ radial process and their expression of cell specific markers such as Sox2. As such, I quantified the total number of Ki67+ Sox2+ IPCs, normalised to the length of the SGZ, to understand whether the increased proliferation in β-cat$^{del\ ex2-6}$ mice is due to increased numbers of proliferating IPCs (Figure 4.15D). I found an increase in the number of proliferating Sox2+ IPCs in β-cat$^{del\ ex2-6}$ mice vs Control (Figure 4.15D) suggesting that inhibiting canonical Wnt/ β-catenin signalling in AHSCs promotes the proliferation and/or generation of IPCs. More replicates are needed to improve the robustness of these quantifications; however, these preliminary data so far suggest that AHSCs are largely unaffected by loss of β-catenin signalling. The observed increase in the number of proliferating IPCs in β-cat$^{del\ ex2-6}$ mice suggests that there are consequences of deleting β-catenin in AHSCs further along the neurogenic lineage.

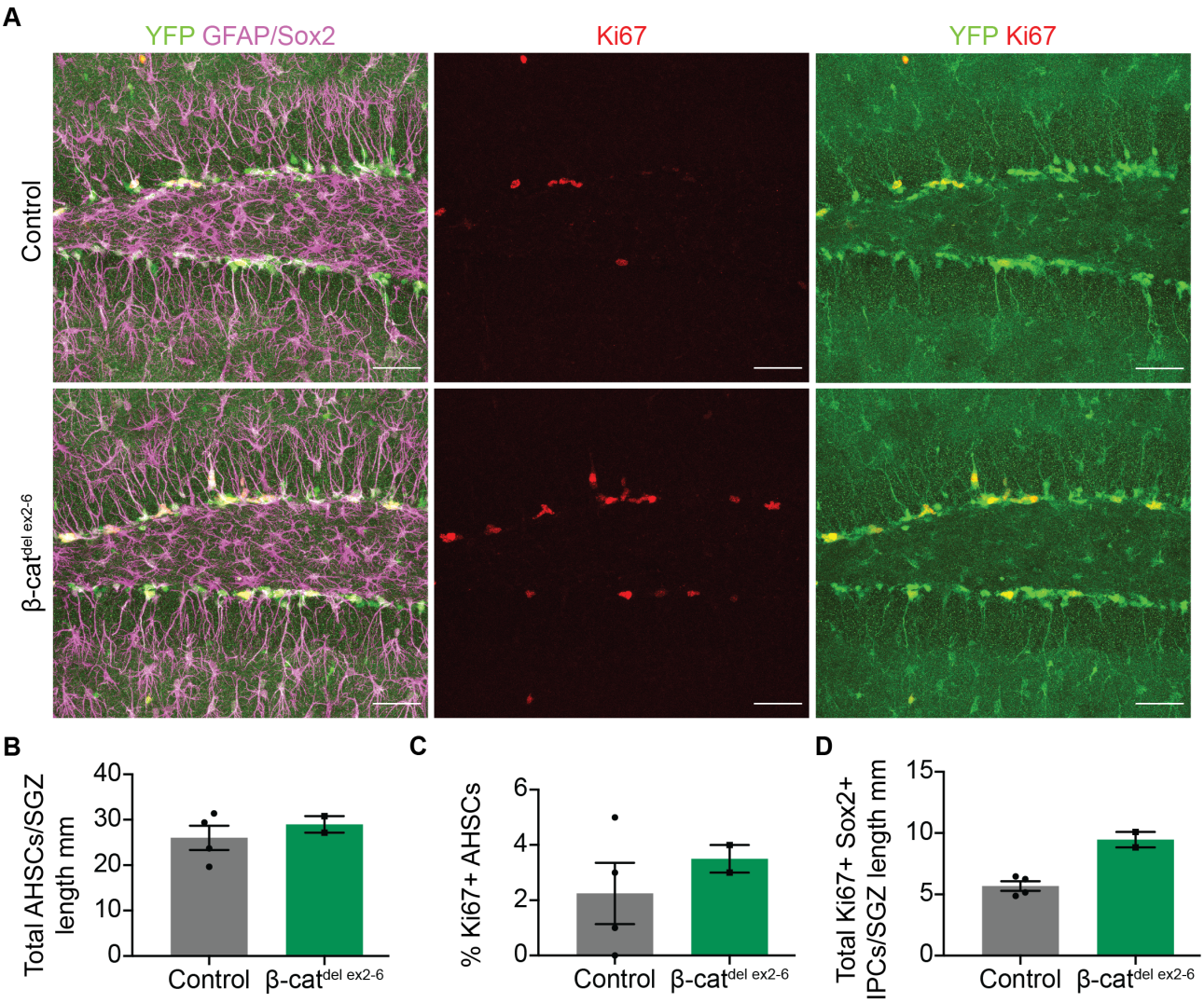


Figure 4.15: Immunostaining for AHSCs, IPCs and proliferation in the DG of Control and β-cat$^{del\ ex2-6}$ mice 30 days after tamoxifen administration.

(A) Immunostaining of GFAP, Sox2, YFP (GFP antibody) and Ki67 in the DG of Control and β-cat$^{del\ ex2-6}$ mice 30 days after the first tamoxifen injection. AHSCs are identified as having a DAPI+ Sox2+ cell body located in the SGZ, associated with a GFAP radial projection through the GCL. YFP immunostaining marks the recombined cells. Ki67 immunostaining is used to mark proliferating cells. Scale bars represent 50μm.

(B) Quantification of the total number of AHSCs normalised to the length of the SGZ (mm) in Control and β-cat$^{del\ ex2-6}$ mice.

(C) Quantification of the proportion of Ki67+ AHSCs in Control and β-cat$^{del\ ex2-6}$ mice.

(D) Quantification of the total number of Ki67+ Sox2+ IPCs normalised to the length of the SGZ (mm) in Control and β-cat$^{del\ ex2-6}$ mice.

Error bars represent mean with SEM. Statistics were not performed for these data due to insufficient biological replicates for β-cat$^{del\ ex2-6}$ samples. n=4 and n=2 biological replicates for Control and β-cat$^{del\ ex2-6}$ mice respectively.

4.4.3 Normal Progression Along the Neurogenic Lineage is Impaired by the Loss of β-catenin in AHSCs

To further investigate how adult neurogenesis is affected by the loss of β-catenin in AHSCs, I used immunofluorescence techniques to identify and characterise the different cell types along the neurogenic lineage in the DG of Control and β-cat$^{del\ ex2-6}$ mice 30 days after the first tamoxifen injection (Figure 4.14A). I used DCX immunostaining to label the neuroblast population and preliminary observations suggest that the number of DCX+ cells is markedly reduced in β-cat$^{del\ ex2-6}$ mice compared to Control (Figure 4.16A). In addition, the morphologies of the DCX+ neuroblasts in the DG β-cat$^{del\ ex2-6}$ mice appear to be less complex than in Control mice (Figure 4.16A). Overall, this could indicate that loss of β-catenin signalling in AHSCs, impairs the correct generation and/or survival of neuroblasts. However, as this is preliminary data, further analysis and quantifications are needed to confirm these observations.

I showed above that the number of proliferating Sox2+ early IPCs was increased in β-cat$^{del\ ex2-6}$ mice (Figure 4.15D). However, the defect observed above in the DCX+ neuroblast population would suggest that loss of β-catenin in AHSCs impairs the generation of neuroblasts. IPCs progress through various stages before differentiating into DCX+ neuroblasts (Urbán et al., 2014; Ming et al., 2011) (Figure 1.4). Therefore, I next wanted to investigate how the progenitor stages preceding DCX+ neuroblasts are affected by the loss of β-catenin in AHSCs. Tbr2 (T-box brain gene 2 or Eomes) is a T-box transcription factor that is expressed in Type IIb progenitors of the hippocampal neurogenic lineage and is therefore used as a marker for these later progenitor stages of adult hippocampal neurogenesis (Hodge et al., 2008; Hodge et al., 2012) (Figure 1.4). Preliminary observations of the Tbr2 immunostaining showed fewer Tbr2+ cells in the DG of β-cat$^{del\ ex2-6}$ mice vs Control 30 days after tamoxifen administration (Figure 4.16B). This suggests that loss of β-catenin in AHSCs promotes the proliferation of Sox2+ Tbr2- early IPCs but impairs their differentiation into later stage Tbr2+ IPCs. Overall, these data suggest the loss of β-catenin signalling in AHSCs impairs the progression along the neurogenic lineage and adult neurogenesis. However, as stated above, these are preliminary observations and require confirmation with further analysis and quantifications.

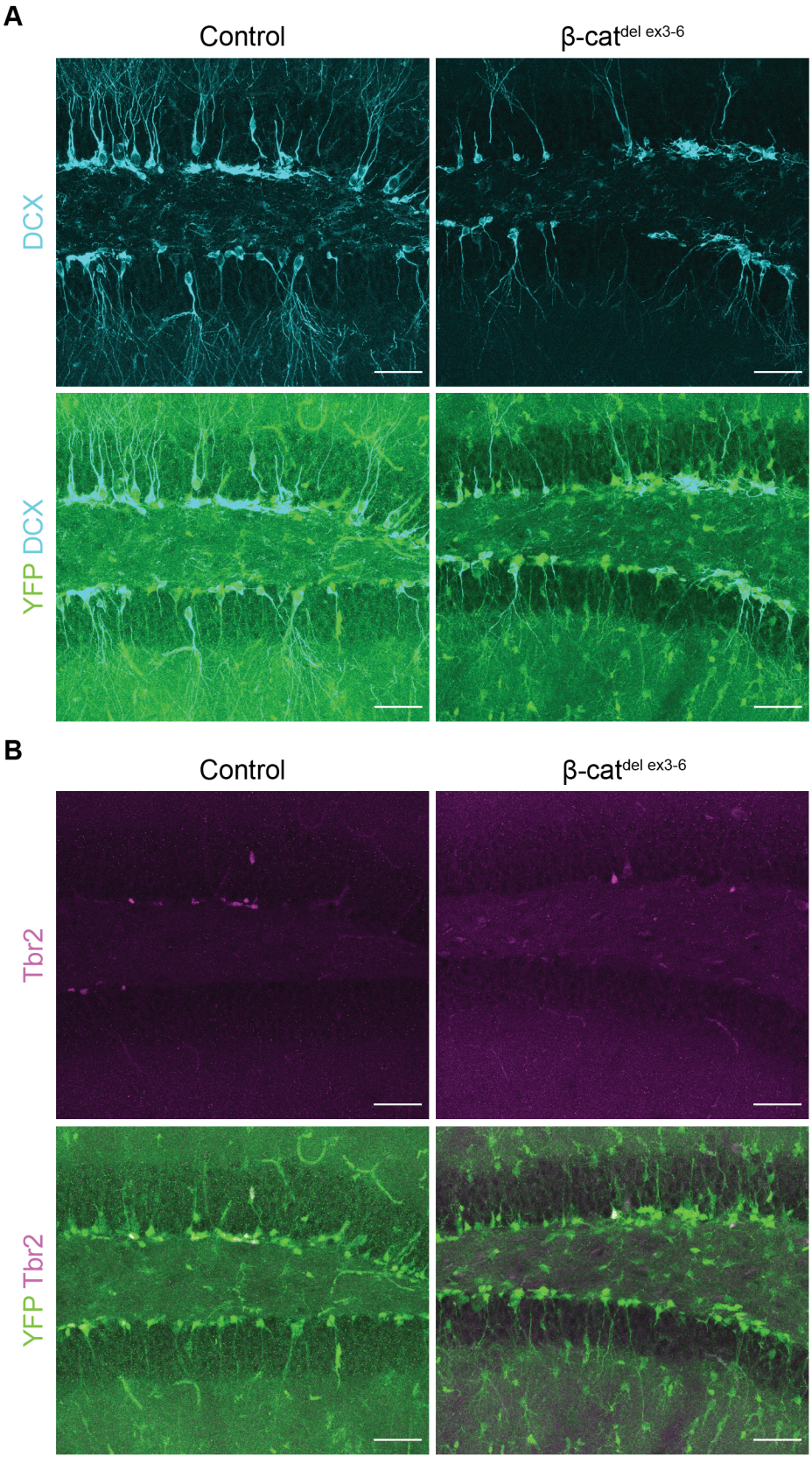


Figure 4.16: Progression along the neurogenic lineage is impaired in the DG of adult β-cat$^{del\ ex2-6}$ mice 30 days after the first tamoxifen injection.

(A) DCX and YFP (GFP antibody) immunostaining in the DG of Control and β-cat$^{del\ ex2-6}$ mice 30 days after the first tamoxifen injection at 2 months of age. YFP is used to label the recombined cells. DCX is used to label the neuroblast population. Scale bars represent 50μm.

(B) Tbr2 and YFP immunostaining in the DG of Control and β-cat$^{del\ ex2-6}$ mice 30 days after the first tamoxifen injection at 2 months of age. YFP is used to label the recombined cells. Tbr2 is used to label Type IIb later progenitors of the hippocampal neurogenic lineage. Scale bars represent 50μm.

Representative images of n=2 biological replicates for Control and β-cat$^{del\ ex2-6}$ mice.

Chapter 5. Results 3: Levels of Canonical Wnt Stimulation are Important for Determining a Proliferation or Neuronal Differentiation Response in Quiescent AHSCs

In the previous chapters, I have shown that AHSCs, *in vitro* and *in vivo*, respond heterogeneously to canonical Wnt signalling, however they are largely unaffected by inhibition of canonical Wnt signalling. In contrast, it has been reported that stimulating canonical Wnt signalling in AHSCs promotes both AHSC self-renewal and instructs neuronal differentiation (Lie et al., 2005; Seib et al., 2013; Jang et al., 2013; Wexler et al., 2009; Qu et al., 2010). I next wanted to understand how stimulating canonical Wnt signalling in AHSCs can produce these two different phenotypes. In this Chapter, I will present data showing that canonical Wnt stimulation in active AHSPCs drives neuronal differentiation, whereas the same level of Wnt stimulation in quiescent AHSPCs promotes their proliferation and activation from quiescence. A higher level of Wnt stimulation is required to promote neuronal differentiation of quiescent AHSPCs. This indicates that the levels of canonical Wnt stimulation in quiescent AHSPCs are important in determining a proliferation or neuronal differentiation response. Finally, I will present results from an *in vivo* model of canonical Wnt stimulation, where β-catenin protein is stabilised in AHSCs, to over-activate canonical Wnt signalling levels in Glast+ AHSCs. Here I found that stabilising β-catenin in AHSCs promotes their displacement from their correct niche location within the SGZ. This displacement appears to promote AHSC activation from quiescence possibly because they lose exposure to SGZ-located quiescent signals.

5.1 Stimulating Canonical Wnt Signalling in Active AHSPCs Initiates Neuronal Differentiation

To understand how AHSPCs respond to elevated canonical Wnt signalling levels, I treated active AHSPC cultures with a Wnt agonist to stimulate their canonical Wnt response. To stimulate canonical Wnt signalling *in vitro* I titrated the Wnt agonist CHIR99021 in active AHSPCs cultures for 72hrs and collected samples for immunofluorescence and qPCR analysis to assess any Wnt induced changes in proliferation and gene expression (Figure 5.1A). I used 1μM, 5μM and 10μM of CHIR99021 for a total of 72hrs in active AHSPC cultures. The 10μM CHIR99021 treatment in active AHSPCs caused massive cell death by 48hrs, indicating that this level of Wnt agonist and Wnt stimulation is toxic to active AHSPCs.

To confirm the activation of canonical Wnt signalling following CHIR99021 treatment, I checked the gene expression level of the Wnt target gene *Axin2* (Figure 5.1B). The expression levels of *Axin2* is upregulated in a dose-dependent manner in active AHSPCs treated with CHIR99021, which confirms the stimulation of canonical Wnt signalling (Figure 5.1B). Canonical Wnt signalling has been shown to play a role in promoting neuronal differentiation in the adult hippocampal neurogenic lineage (Lie et al., 2005; Seib et al., 2013; Jang et al., 2013). To understand whether neuronal differentiation is upregulated in CHIR99021 treated active AHSPCs, I used qPCR to check the gene expression levels of genes associated with stemness and neuronal differentiation. Ascl1 is a basic helix-loop-helix transcription factor that has been shown to been essential for the activation and proliferation of AHSCs *in vivo* (Andersen et al., 2014). Nestin is a class VI intermediate filament protein that is highly expressed in neural progenitors of both the developing and adult central nervous system (CNS) (Lendahl et al., 1990; Morshead et al., 1994; Palmer et al., 2000). Both *Ascl1* and *Nestin* are highly expressed in neural progenitors but are downregulated upon neuronal differentiation (Pleasure et al., 2000; Frederiksen et al., 1988; Dahlstrand et al., 1995). I found that CHIR99021 treatment in active AHSPCs decreased the gene expression levels of *Ascl1* and *Nestin*, however the downregulation of *Nestin* gene expression levels was not statistically significant and therefore only indicates a trend (Figure 5.1C and 5.1D). This suggests that stimulating canonical Wnt signalling in active AHSPCs promotes a loss of stem cell associated genes. To determine whether this canonical Wnt induced loss of stem cell associated genes is accompanied by an increase in neuronal differentiation, I checked the gene expression levels of neuronal differentiation markers. Neurogenin 2 (Ngn2) is neural-specific basic helix-loop-helix (bHLH) transcription factor that is expressed in neural progenitor cells and instructs a neuronal fate (Hodge et al., 2012; Galichet et al., 2008; Wilkinson et al., 2013). Tuj1 is a neuron-specific class III β-tubulin and is expressed early on during neuronal differentiation (Ambrogini et al., 2004). I found that the pro-neuronal markers *Tuj1* and *Ngn2* were upregulated in a dose-dependent manner in active AHSPCs treated with CHIR99021 (Figure 5.1E and 5.1F). However, as these results were not statistically significant this only indicates a trend of upregulation. This could indicate that stimulating canonical Wnt signalling in active AHSPCs initiates neuronal differentiation.

To confirm this neuronal differentiation phenotype, I immunolabelled Control, 1μM CHIR99021 and 5μM CHIR99021 treated active AHSPCs for Tuj1 (Figure 5.1G). No Tuj1+ cells were found in Control active AHSPC samples (Figure 5.1G and 5.1H). In contrast, I observed some Tuj1+

cells in active AHSPCs treated with 1μM CHIR99021 and significantly more Tuj1+ cells in 5μM CHIR99021 (Figure 5.1G). This confirms that stimulating canonical Wnt signalling in active AHSPCs promotes a neuronal fate. The proportion of Tuj1+ cells is higher in 5μM CHIR99021 treated active AHSPCs compared to 1μM CHIR99021 treated active AHSPCs, indicating that a higher level of canonical Wnt stimulation promotes neuronal differentiation of active AHSPCs more readily (Figure 5.1H).

The proliferative capacity of AHSPCs is a hallmark of multipotent progenitors (Ming et al., 2011). As progenitors differentiate towards a more committed cell fate, their proliferative capacity decreases as they become post-mitotic (Ming et al., 2011). To investigate proliferation changes in active AHSPCs treated with CHIR99021, I immunolabelled proliferating cells with the cell cycle markers EdU and Ki67 (Figure 5.1I). I found that the proportion of EdU+ and Ki67+ AHSPCs, was significantly decreased in active AHSPCs treated with 5μM CHIR99021 compared to Control (Figure 5.1J and 5.1K). 5μM CHIR99021 treatment also induced a significant increase in the proportion of Tuj1+ cells (Figure 5.1H). This indicates that stimulating canonical Wnt signalling in active AHSPCs, reduces their proliferative capacity as they initiate neuronal differentiation. Overall, these data suggest that stimulating canonical Wnt signalling in active AHSPC cultures instructs a neuronal fate and promotes neuronal differentiation.

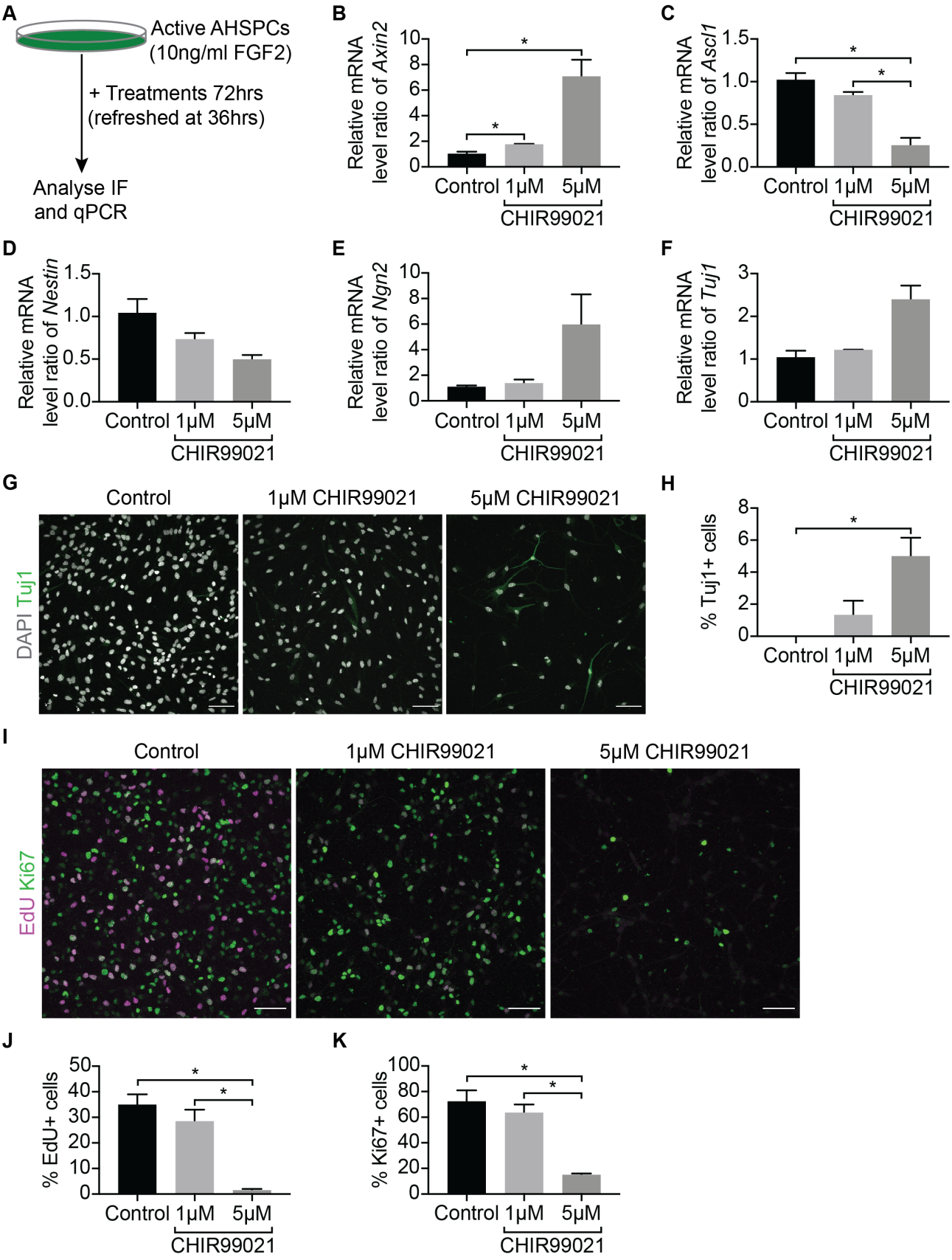


Figure 5.1: Treatment of active AHSPCs with the Wnt agonist CHIR99021 promotes neuronal differentiation.

(A) Schematic of experimental design. Active AHSPCs (10ng/ml FGF2) were treated with DMSO vehicle Control, 1μM CHIR99021, 5μM CHIR99021 and 10μM CHIR99021 for 72hrs. Treatments were refreshed at 36hrs. 10μM CHIR99021 treatment caused cell death in active AHSPCs.

(B, C, D, E, F) qPCR analysis of the expression levels of *Axin2* **(B)**, *Ascl1* **(C)**, *Nestin* **(D)**, *Ngn2* **(E)** and *Tuj1* **(F)**. The increasing expression levels of the Wnt target gene *Axin2* **(B)** shows that canonical Wnt signalling is stimulated in active AHSPCs upon CHIR99021 treatment. The decreasing expression levels of the stem cell markers *Ascl1* **(C)** and *Nestin* **(D)** indicate a loss of stemness with high levels of Wnt stimulation in active AHSPCs. The expression levels of the pro-neuronal markers *Ngn2* (*Neurogenin 2*) **(E)** and *Tuj1* **(F)** increase with 5μM CHIR99021, indicating that high levels of Wnt stimulation initiates neuronal differentiation in active AHSPCs. An unpaired Student's t-test was used for statistical analysis, (*, $p<0.05$). Error bars represent mean with SEM. n=2 biological repeats.

(G) Tuj1 and DAPI immunolabelling in active AHSPCs treated with 1μM CHIR99021 and 5μM CHIR99021 vs Control. Scale bars represent 50μm.

(H) Quantification of the data shown in **(G)**. The proportion of Tuj1+ cells is increased in active AHSPCs treated with CHIR99021, indicating that stimulating canonical Wnt signalling in active AHSPCs initiates neuronal differentiation. An unpaired Student's t-test was used for statistical analysis, (*, $p<0.05$). Error bars represent mean with SEM. n=2 biological repeats.

(I) Immunolabelling of proliferation markers, EdU and Ki67, in active AHSPCs treated with 1μM CHIR99021 and 5μM CHIR99021 verses Control. To label cells in S-phase of the cell cycle, AHSPCs were pulsed with 10μM EdU for 45min prior to fixation on the last day of treatment and EdU was detected using the Click-iT™ EdU Alexa Fluor® 647 detection kit. Scale bars represent 50μm.

(J, K) Quantification of the data shown in **(I)**. The proportion of EdU+ **(J)** and Ki67+ **(K)** immunolabelled cells decreases in active AHSPCs treated with CHIR99021, indicating that stimulating canonical Wnt signalling causes cells to become post-mitotic as they undergo neuronal differentiation. An unpaired Student's t-test was used for statistical analysis, (*, $p<0.05$). Error bars represent mean with SEM. n=2 biological repeats.

5.2 Stimulating Canonical Wnt Signalling in Quiescent AHSPCs Promotes Differential Effects Depending on the Levels of Wnt Stimulation

Quiescent AHSPCs differ from active AHSPCs in their proliferative capacity, metabolism and transcriptional program (Beckervordersandforth et al., 2017; Knobloch et al., 2017; Shin et al., 2015; Cheung et al., 2013). These differences allow quiescent AHSPCs to be maintained in a reversible state of dormancy, which is essential for the long-term maintenance of the AHSPC pool. It has also been suggested that quiescence allows stem cells to respond to more readily to external signals due to their high expression of cell surface receptors (Cheung et al., 2013). Due to these differences between active and quiescent AHSPCs, I next wanted to investigate how quiescent AHSPCs respond to stimulating canonical Wnt signalling.

5.2.1 Over-stimulating Canonical Wnt Signalling in Quiescent AHSCs Induces Neuronal Differentiation Whereas Lower Levels of Wnt Stimulation Promotes Proliferation

To stimulate canonical Wnt signalling in quiescent AHSCs, I again used the Wnt agonist CHIR99021. I used the same concentrations of CHIR99021 as I used to stimulate canonical Wnt signalling in active AHSPCs (1μM, 5μM and 10μM CHIR99021) and collected samples after 48hrs (Figure 5.2A). 10μM CHIR99021 treatment was toxic to active AHSPCs, however I did not observe any cell death in quiescent AHSPCs treated with 10μM CHIR99021. This indicates that active AHSPCs are more sensitive to levels of canonical Wnt stimulation compared to quiescent AHSPCs and highlights the difference in how active and quiescent AHSPCs perceive and respond to the same level of an external stimulus.

To confirm the activation of canonical Wnt signalling, I checked the gene expression levels of *Axin2* (Figure 5.2B). *Axin2* levels are significantly upregulated in a dose-dependent manner in quiescent AHSPCs treated with 1μM, 5μM and 10μM CHIR99021 (Figure 5.2B), indicating robust stimulation of the canonical Wnt signalling pathway. Similar to stimulating canonical Wnt signalling in active AHSPCs, over-activation of canonical Wnt signalling in quiescent AHSPCs also initiated neuronal differentiation. This is seen by the downregulation AHSPC markers such as *Ascl1* (Figure 5.2C) and *Sox2* (Figure 5.2D), alongside the upregulation of the pro-neuronal markers *Ngn2* (Figure 5.2E) and *Tuj1* (Figure 5.2F) in quiescent AHSPCs treated with 10μM CHIR99021. Indeed, immunolabelling for Tuj1 showed a significant increase in the proportion of

Tuj1+ cells in quiescent AHSPCs treated with 10μM CHIR99021 vs Control (Figure 5.2G and 5.2H). 5μM CHIR99021 treatment of quiescent AHSPCs also initiated neuronal differentiation, but to a lesser extent than 10μM CHIR99021. This suggests that higher levels of stimulating canonical Wnt signalling in quiescent AHSPCs are more effective at inducing neuronal differentiation.

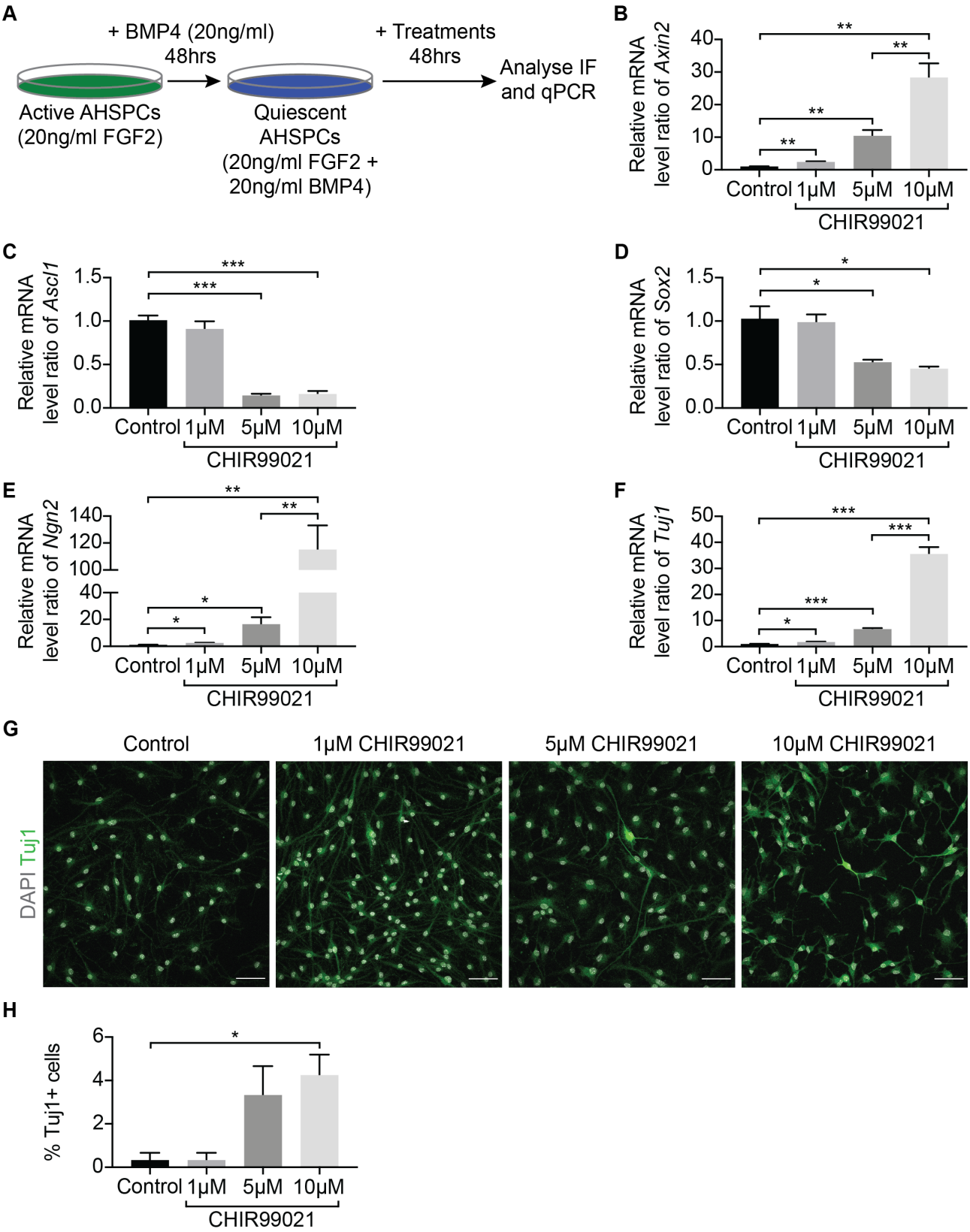


Figure 5.2: Over-stimulating canonical Wnt signalling using CHIR99021 in quiescent AHSPCs initiates neuronal differentiation.

(A) Schematic of experimental design. Active AHSPCs (20ng/ml FGF2) were plated and were transferred into quiescent culture conditions (20ng/ml FGF2 + 20ng/ml BMP4) 24hrs later.

CHIR99021 treatments were started 48hrs after quiescence induction and quiescent culture conditions were maintained throughout. Treatments include: DMSO vehicle control, 1μM CHIR99021, 5μM CHIR99021 and 10μM CHIR99021 for 48hrs.

(B) qPCR analysis of the expression levels of the Wnt target gene *Axin2* shows that canonical Wnt signalling is stimulated in quiescent AHSPCs treated with CHIR99021 in a dose-dependent manner.

(C, D) qPCR analysis of the expression levels of the AHSPC markers *Ascl1* **(C)** and *Sox2* **(D)**. Both *Ascl1* **(C)** and *Sox2* **(D)** expression levels decrease with 5μM and 10μM CHIR99021 indicating a loss of stemness with high levels of Wnt stimulation.

(E, F) qPCR analysis of the expression levels of pro-neuronal markers *Neurogenin2* (*Ngn2*) **(E)** and *Tuj1* **(F)**. *Ngn2* **(E)** and *Tuj1* **(F)** expression levels increase with 10μM CHIR99021 treatment indicating that high levels of Wnt stimulation initiates neuronal differentiation in quiescent AHSPCs.

(G) Immunolabelling of the neuronal differentiation marker Tuj1 in quiescent AHSPCs treated with 1μM CHIR99021, 5μM CHIR99021 and 10μM CHIR99021 verses Control. Scale bars represent 50μm.

(H) Quantification of the data shown in **(G)**. The proportion of Tuj1+ cells increases in quiescent AHSPCs treated with 5μM and 10μM CHIR99021.

(B-F, G) An unpaired Student's t-test was used for statistical analysis, (*, $p<0.05$. **, $p<0.01$. ***, $p<0.001$). Error bars represent mean with SEM. Data shown is technical repeats of one biological replicate. n=2 biological replicates.

The above data shows that over-stimulating canonical Wnt signalling with 10μM CHIR99021 in quiescent AHSPCs, initiates neuronal differentiation. Adult hippocampal neurogenesis *in vivo* begins with the activation and proliferation of quiescent AHSCs before they progress along the neurogenic lineage to generate newborn granule neurons. I next wanted to investigate whether Wnt stimulated quiescent AHSPCs proliferate prior to differentiating towards a neuronal fate. To investigate levels of quiescent AHSPC proliferation upon Wnt stimulation, I used EdU incorporation and Ki67 immunolabelling to mark cells in the cell cycle (Figure 5.3A). I found that the proportion of proliferating AHSPCs remained low in Control, 1μM CHIR99021 and 10μM CHIR99021 treated quiescent AHSPCs (Figure 5.3A, 5.3B and 5.3C). As the expression levels of *Ascl1* and *Sox2* (Figure 5.2C and 5.2D) are similar to Control in 1μM CHIR99021 treated quiescent AHSPCs, this could suggest that Control and 1μM CHIR99021 treated quiescent AHSPCs retain their stemness and remain out of the cell-cycle in quiescence. This could be

further investigated by checking the expression levels of quiescent markers such as *HopX* and *p57*. Conversely, 10μM CHIR99021 treatment of quiescent AHSPCs caused the downregulation of AHSPC genes alongside the upregulation of neuronal differentiation markers (Figure 5.2). This, alongside the low number of proliferating cells, could suggest that 10μM CHIR99021 treatment of quiescent AHSPCs promotes direct neuronal differentiation, without quiescent AHSPC proliferation. This could be further explored by investigating the proliferation changes induced by 10μM CHIR99021 treatment of quiescent AHSPCs over time. However, the proportion of proliferating cells is increased in 5μM CHIR99021 treated quiescent AHSPCs (Figure 5.3). This suggests that a lower stimulation of canonical Wnt signalling in quiescent AHSPCs promotes their activation from quiescence and proliferation. Overall, these data indicate there is a dose-dependent effect of stimulating canonical Wnt signalling in quiescent AHSPCs. Over-stimulation of canonical Wnt signalling could promote direct neuronal differentiation, whereas a lower level of Wnt stimulation also promotes quiescent AHSPC activation and proliferation.

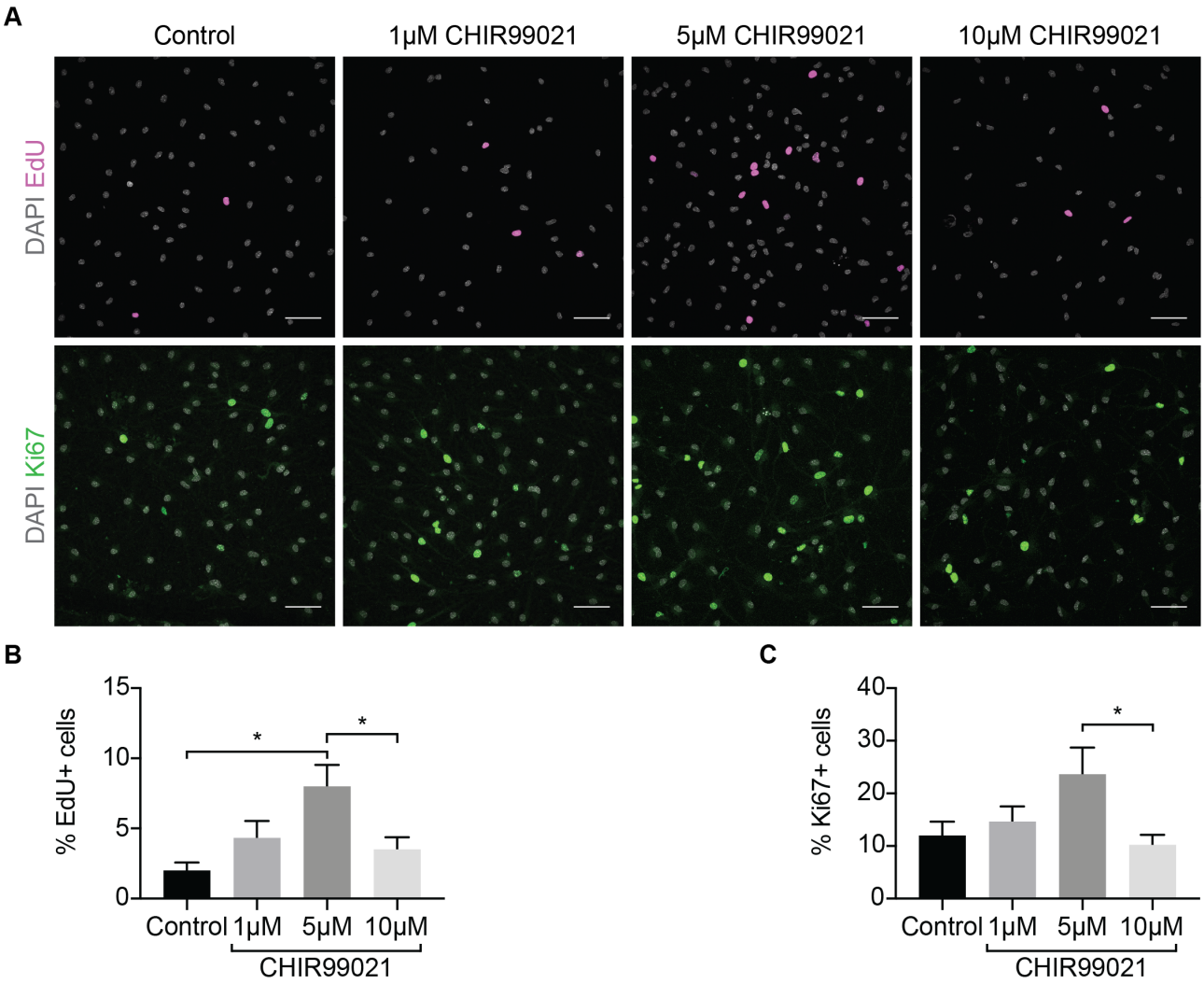


Figure 5.3: Lower Wnt stimulation using 5μM CHIR99021 in quiescent AHSPCs, promotes quiescent AHSPC activation and proliferation.

(A) Immunolabelling of the proliferation markers EdU and Ki67 in quiescent AHSPCs treated with 1μM CHIR99021, 5μM CHIR99021 and 10μM CHIR99021 vs Control. To label cells in S-phase of the cell cycle, cells were pulsed with 10μM EdU for 45min prior to fixation on the last day of treatment and EdU was detected using the Click-iT™ EdU Alexa Fluor® 647 detection kit. Scale bars represent 50μm.

(B, C) Quantification of the data shown in **(A)**. The proportion of EdU+ **(B)** and Ki67+ **(C)** immunolabelled cells increases in quiescent AHSPCs treated with 5μM CHIR99021, indicating that lower stimulation of canonical Wnt signalling could promote quiescent AHSPC activation. An unpaired Student's t-test was used for statistical analysis, (*, $p<0.05$). Error bars represent mean with SEM. Data shown is technical repeats of one biological replicate. n=2 biological replicates.

5.2.2 Wnt Induced Proliferation of Quiescent AHSPCs is Sustained Over Time But Could Promote Lineage Progression Towards a Progenitor Fate

I next wanted to see whether this Wnt induced activation of quiescent AHSPCs is sustained over time, or whether prolonged exposure to a lower level of canonical Wnt stimulation eventually induces neuronal differentiation. I treated quiescent AHSPCs with 5μM CHIR99021 for 24hrs, 48hrs and 72hrs (Figure 5.4A) and confirmed that canonical Wnt signalling was activated by measuring *Axin2* expression levels (Figure 5.4B). *Axin2* is significantly upregulated at 24hrs and is sustained across all time points (Figure 5.4B). This shows that canonical Wnt signalling is activated quite rapidly in quiescent AHSPCs using CHIR99021, and that longer treatments with CHIR99021 do not increase the level of Wnt stimulation. The expression levels of the cell cycle marker *CyclinD1* show a decreasing trend in Control quiescent AHSPCs over time (Figure 5.4C). This suggests that that long-term maintenance of quiescent culture conditions induces a deeper state of quiescence, as has previously been shown in fibroblasts (Augenlicht et al., 1974; Owen et al., 1989; Kwon et al., 2017). This contrasts with the upregulation of *CyclinD1* expression levels in 5μM CHIR99021 treated quiescent AHSPCs at 48hrs and 72hrs (Figure 5.4C). This suggests that sustained canonical Wnt stimulation in quiescent AHSPCs is sufficient to promote quiescent AHSPC activation. However, the increased expression of the quiescent marker *HopX* (Li et al., 2015) following 48hrs and 72hrs Wnt stimulation would seem to contradict this activation phenotype (Figure 5.4D). To confirm that quiescent AHSPCs become activated following sustained canonical Wnt stimulation, I used EdU incorporation (S-phase) and immunolabelling of Ki67 (pan-cell cycle) and CyclinD1 (G1) to identify cells in the cell cycle (Figure 5.4E). I found that the proportion of Ki67 positive and CyclinD1 positive AHSPCs was significantly increased in 5μM CHIR99021 treated quiescent AHSPCs compared to Control at 48hrs and 72hrs (Figure 5.4F and 5.4G). The proportion of EdU positive cells was increased with 5μM CHIR99021 treatment over time, however this was not significant and therefore only represents and trend (Figure 5.4H). Overall, this indicates that prolonged canonical Wnt stimulation in quiescent AHSPCs is sufficient to maintain quiescent AHSPC activation and proliferation.

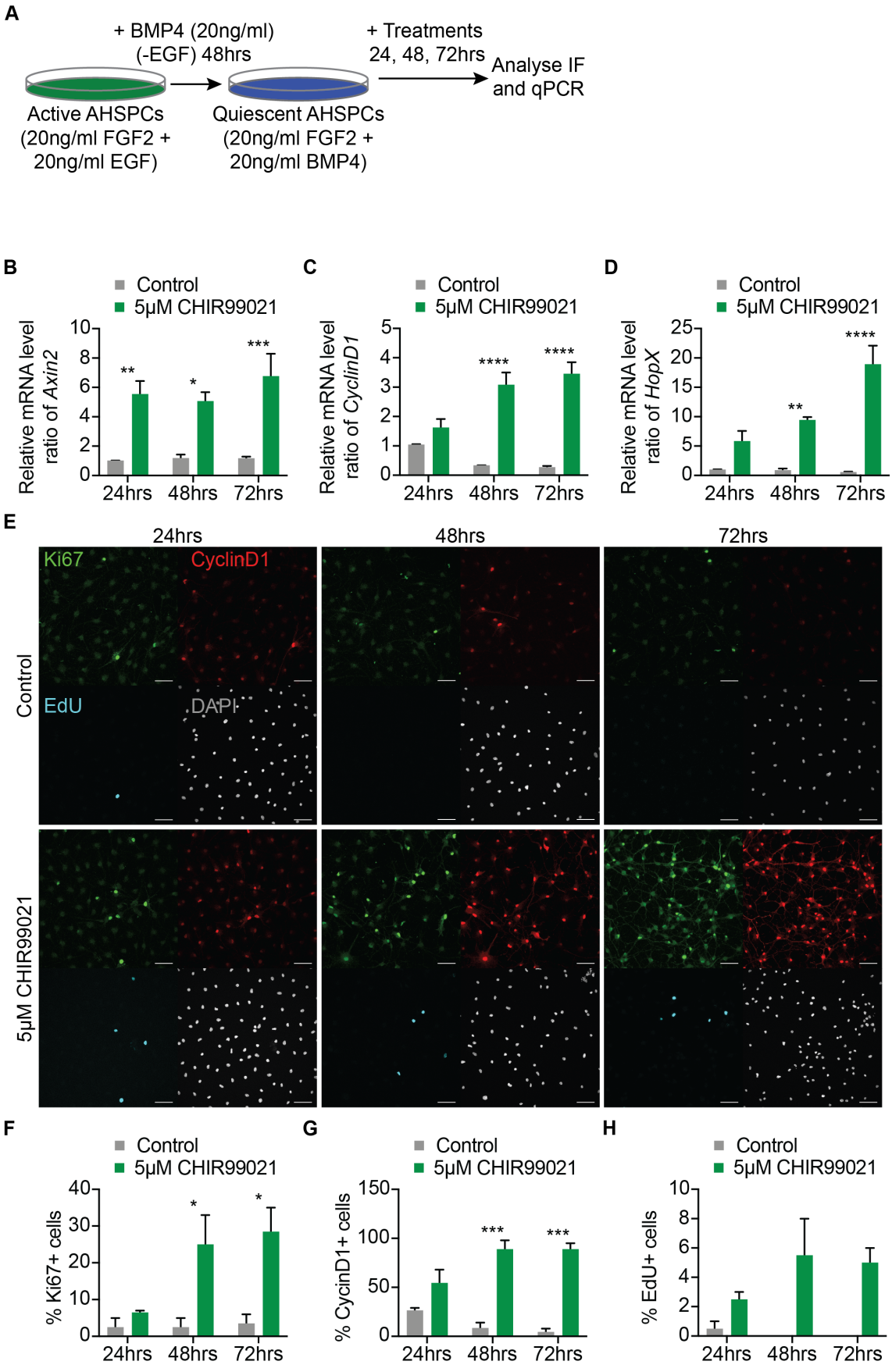


Figure 5.4: 5μM CHIR99021 induced quiescent AHSPC proliferation is sustained over time.

(A) Schematic of experimental design. Quiescent AHSPCs were treated with 5μM CHIR99021 and DMSO vehicle Control for 24hrs, 48hrs and 72hrs.
(B) *Axin2* expression levels increase with 5μM CHIR99021 treatment in quiescent AHSPCs at all time points highlighting an activation of canonical Wnt signalling.
(C) *CyclinD1* expression levels increase in 5μM CHIR99021 treated quiescent AHSPCs suggesting that activation of canonical Wnt signalling promotes quiescent AHSPC activation and proliferation. This contrasts with Control where *CyclinD1* levels decrease over time implying they enter deeper into quiescence.
(D) The expression of the quiescent AHSC marker *HopX* increases in 5μM CHIR99021 treated quiescent AHSPCs over time.
mRNA levels were normalised to *GAPDH* and *ActinB* mRNA and expressed relative to Control at 24hrs. Two-way Anova with Sidak's multiple comparisons test was used for statistical analysis, (*, $p<0.05$. **, $p<0.01$. ***, $p<0.001$. ****, $p<0.0001$). Error bars represent mean with SEM. Data shown is technical repeats of one biological replicate. n=2 biological replicates.
(E) Immunolabelling of proliferation markers Ki67, CyclinD1 and EdU in quiescent AHSPCs treated with 5μM CHIR99021 vs DMSO vehicle control at 24, 48 and 72hrs. Scale bars represent 50μm.
(F, G, H) Quantification of the data shown in **(E)**. The proportion of Ki67+ AHSCs **(F)**, CyclinD1+ AHSPCs **(G)** and EdU+ AHSCs **(H)** increases in quiescent AHSPCs treated with 5μM CHIR99021 vs Control over time, indicating that activation of canonical Wnt signalling in quiescent AHSPCs promotes sustained proliferation. Two-way Anova with Sidak's multiple comparisons test was used for statistical analysis, (*, $p<0.05$. ***, $p<0.001$). Error bars represent mean with SEM. n=2 biological repeats.

Increased proliferation is not the only defining characteristic of quiescent AHSPC activation. Increased mitochondrial activity is also a marker quiescent AHSPC activation (Cottet-Rousselle et al., 2011; Freyer. 1998). I measured mitochondrial activity in quiescent AHSPCs treated with 5μM CHIR99021 over time, using the MitoTracker™ Deep Red fluorescent dye (Cottet-Rousselle et al., 2011; Septinus et al., 1983) (Figure 5.5A). MitoTracker™ Deep Red is a fluorescent dye that diffuses across the plasma membrane of active mitochondria (Cottet-Rousselle et al., 2011; Septinus et al., 1983). The dye intensity within mitochondria is correlated with mitochondrial activity and can therefore be used to distinguish between cells in an active and quiescent state (Cottet-Rousselle et al., 2011; Freyer. 1998) (Figure 5.5A). The trend of decreasing intensity of the MitoTracker™ Deep Red staining in Control quiescent AHSPCs

suggests that they are entering deeper into quiescence with time (Figure 5.5B). This contrasts with the increased MitoTracker™ Deep Red signal intensity I observed in quiescent AHSPCs treated with 5μM CHIR99021 at 48hrs and 72hrs (Figure 5.5B). This suggests that quiescent AHSPCs treated with 5μM CHIR99021 are more active than those maintained in quiescent culture conditions. Overall, these data support the hypothesis that prolonged low stimulation levels of canonical Wnt signalling can sustain quiescent AHSPC activation over time.

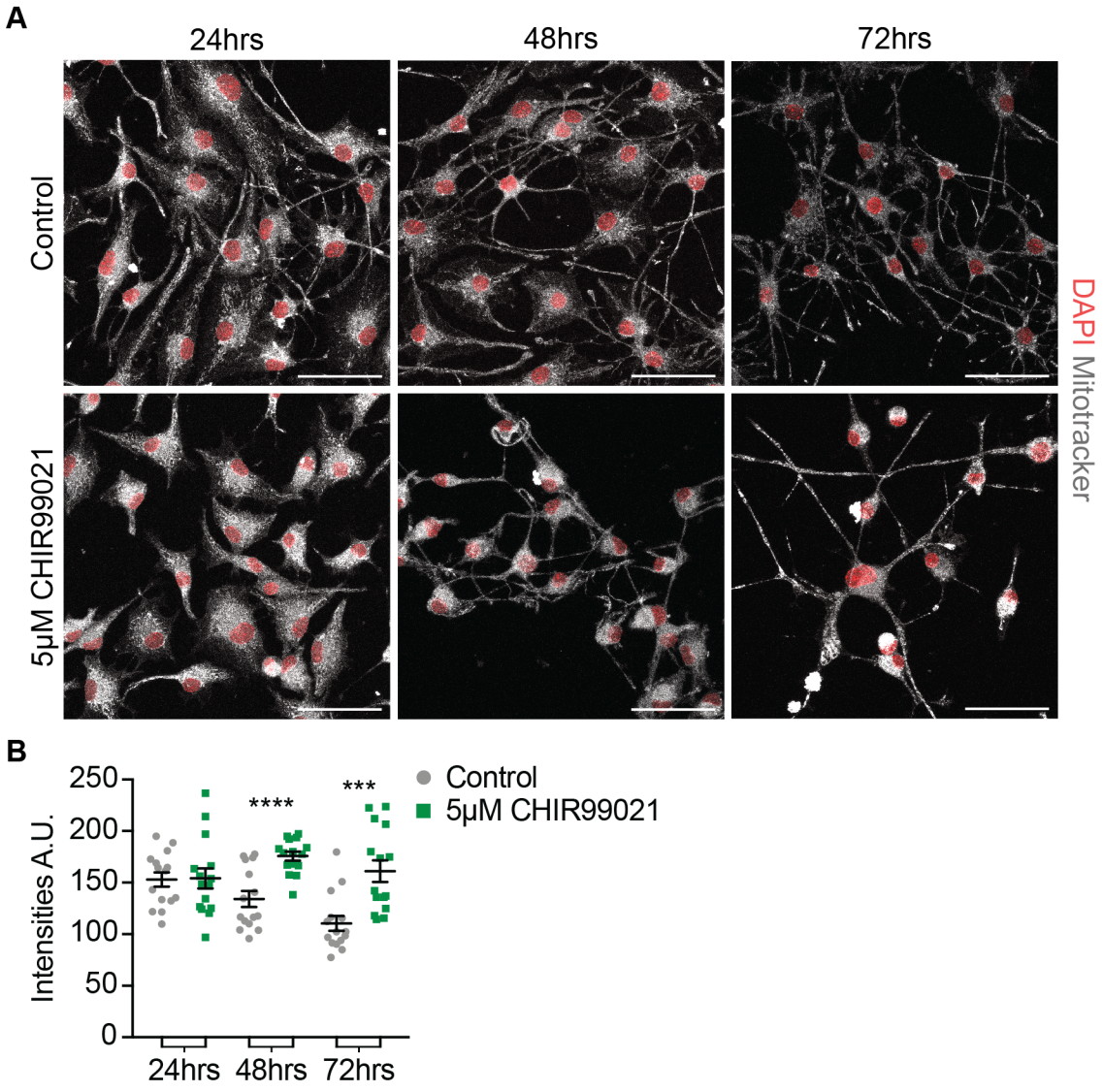


Figure 5.5: MitoTracker™ Deep Red staining in Control quiescent AHSPCs and quiescent AHSPCs treated with 5μM CHIR99021 over time.

(A) MitoTracker™ Deep Red staining in Control vs 5μM CHIR99021 treated quiescent AHSPCs over time. MitoTracker™ Deep Red was used to measure quiescent AHSPC activation. Scale bars represent 20μm.

(B) Quantification of the data shown in **(A)**. The intensity of MitoTracker™ Deep Red staining decreases in control quiescent AHSPCs, as they enter a deeper state of quiescence over time. However, in 5μM CHIR99021 treated quiescent AHSPCs, the intensity MitoTracker™ Deep Red staining increases with time indicating their activation upon prolonged Wnt stimulation. An unpaired Student's test was used for statistical analysis, (***, $p<0.001$. ****, $p<0.0001$). Error bars represent mean with SEM. n=2 biological repeats.

As stated previously, adult hippocampal neurogenesis progresses via a distinct neurogenic lineage that begins with the activation of quiescent AHSPCs. Once activated, AHSPCs proliferate and differentiate through various progenitor stages before terminally differentiating as a mature granule neuron. I next wanted to understand whether the sustained Wnt induced activation of quiescent AHSPCs, maintained AHSPCs in an active state or whether it pushed them further along the neurogenic lineage towards a progenitor fate. To investigate this, I checked the gene expression changes of AHSPC associated genes, in quiescent AHSPCs treated with 5μM CHIR99021 for 24hrs, 48hrs and 72hrs (Figure 5.6). The downregulation of the AHSPC markers *Sox2* (Figure 5.6A), *Ascl1* (Figure 5.6B), *Hes5* (Figure 5.6C) and *GFAP* (Figure 5.6D) suggests that stimulating canonical Wnt signalling in quiescent AHSPCs promotes a loss of stemness, even after 24hrs (Figure 5.6A, 5.6B, 5.6C and 5.6D). However, not all AHSPC marker genes are regulated in this way as *Glast* expression levels are unchanged by stimulating canonical Wnt signalling (Figure 5.6E). *Nestin* is slightly upregulated by 5μM CHIR99021 treatment in quiescent AHSPCs at all time points compared to Control, however this was not statistically significant (Figure 5.6F). As Nestin is highly expressed in IPCs, the increasing trend of *Nestin* expression, could suggest that stimulating canonical Wnt signalling in quiescent AHSPCs drives them towards a progenitor fate whilst also promoting a partial loss of stemness (Figure 5.6A, 5.6B, 5.6C and 5.6D). The trending upregulation of the pro-neuronal marker *Tuj1* in 5μM CHIR99021 treated quiescent AHSPCs suggests that low levels of canonical Wnt stimulation are sufficient to commit quiescent AHSPCs towards a neuronal fate, however this result was no statistically significant (Figure 5.6G). This is further supported by the downregulation of the oligodendrocyte marker *Olig1* at 48hrs and 72hrs (Figure 5.6H) and the trending downregulation of *Olig2* (Figure 5.6I) in Wnt stimulated quiescent AHSPCs, which suggests that oligodendrocyte differentiation is suppressed by stimulation of canonical Wnt signalling. Overall, this suggests that prolonged low levels of stimulated canonical Wnt signalling promotes quiescent AHSPC activation over time and could commit their differentiation towards a neuronal fate.

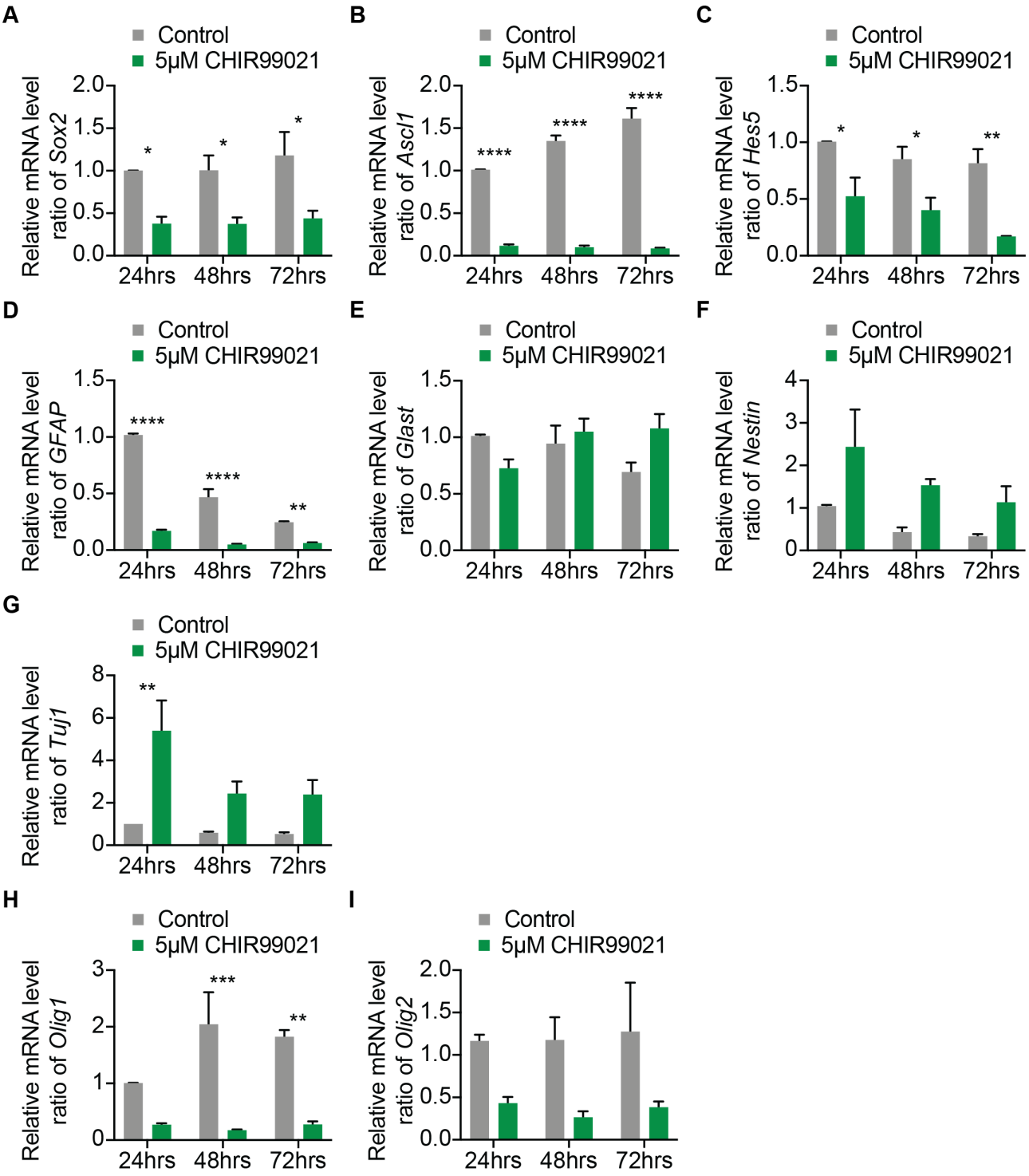


Figure 5.6: qPCR analysis of the gene expression changes induced by 5μM CHIR99021 treatment in quiescent AHSPCs over time.

(A, B, C, D) The decreasing expression levels of the stem cell markers *Sox2* **(A)**, *Ascl1* **(B)**, *Hes5* **(C)** and *GFAP* **(D)** may imply a loss of stemness and progression towards a progenitor-like fate following canonical Wnt stimulation.

(E) *Glast* expression levels are unchanged.

(F) *Nestin* expression levels are upregulated in quiescent AHSPCs treated with 5μM CHIR99021 at all time points.
(G) Upregulation of *Tuj1* expression levels in 5μM CHIR99021 treated quiescent AHSPCs may indicate a preference towards a neuronal fate.
(H, I) Downregulation of *Olig1* **(H)** and *Olig2* **(I)** expression levels suggests that activating canonical Wnt signalling suppresses oligodendrocyte differentiation.
mRNA levels were normalised to *GAPDH* and *ActinB* mRNA and expressed relative to Control at 24hrs. Two-way Anova with Sidak's multiple comparisons test was used for statistical analysis, (*, $p<0.05$. **, $p<0.01$. ***, $p<0.001$. ****, $p<0.0001$). Error bars represent mean with SEM. Data shown is technical repeats of one biological replicate. n=2 biological replicates.

I next wanted to see whether it was possible to activate quiescent AHSPCs by stimulating canonical Wnt signalling, without promoting their progression along the neurogenic lineage. To investigate this, I treated quiescent AHSPCs with even lower concentrations of the Wnt agonist CHIR99021 (1μM, 2.5μM and 5μM CHIR99021) and for shorter treatment times (6hrs, 12hrs and 24hrs) (Figure 5.7A). To look at quiescent AHSPC activation under these conditions, I immunolabelled AHSPCs for the cell cycle markers CyclinD1 and Ki67 (Figure 5.7B). The proportion of CyclinD1+ cells was significantly increased in quiescent AHSPCs treated with CHIR99021 at all time points (Figure 5.7C). However, as CyclinD1 is a direct transcriptional target of canonical Wnt signalling, I wanted to confirm this observation with other proliferation markers. The proportion of Ki67+ (Figure 5.7E) cells was not significantly changed across all CHIR99021 conditions compared to Control, indicating that these experimental conditions were not sufficient for canonical Wnt induced quiescent AHSPC activation. However, as this is preliminary data these observations need to be confirmed with further investigations.

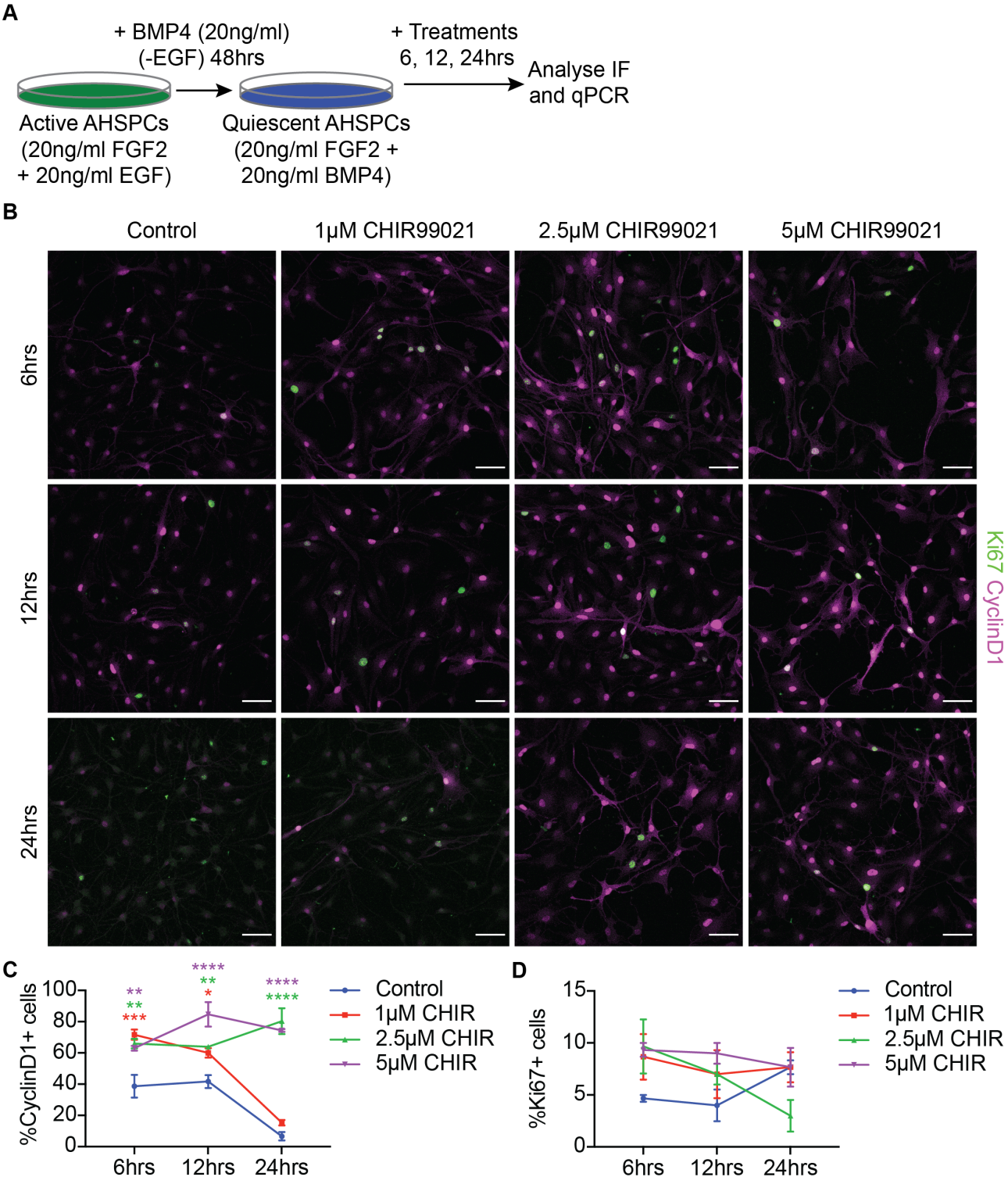


Figure 5.7: Immunostaining of proliferation markers in quiescent AHSPCs treated with 1μM, 2.5μM and 5μM CHIR99021 for 6hrs, 12hrs and 24hrs.

(A) Schematic of experimental design. Quiescent AHSPCs were treated with DMSO vehicle Control, 1μM CHIR99021, 2.5μM CHIR99021 and 5μM CHIR99021 for 6hrs, 12hrs and 24hrs.

(B) Immunolabelling of the proliferation markers CyclinD1 and Ki67 in quiescent AHSPCs treated with 1μM CHIR99021, 2.5μM CHIR99021 and 5μM CHIR99021 vs Control. Scale bars represent 50μM.
(C, D, E) Quantification of the proportion of CyclinD1+ **(C)** and Ki67+ **(D)** AHSPCs shown in **(B)**. Two-way Anova with Tukey's multiple comparisons test was used for statistical analysis, (*, $p<0.05$. **, $p<0.01$. ***, $p<0.001$. ****, $p<0.0001$). Error bars represent mean with SEM. Data shown is technical repeats of one biological replicate.

Previously, I showed that 5μM CHIR99021 treatment in quiescent AHSPCs, drives AHSPCs towards a progenitor fate, as shown by the downregulation of AHSPC associated genes (Figure 5.6). I next wanted to investigate how rapidly these gene expression changes occur following treatment of quiescent AHSPCs with 5μM CHIR99021, and whether lower concentrations of the Wnt agonist also induce these gene expression changes. Firstly, I wanted to confirm the levels of canonical Wnt stimulation induced by 1μM, 2.5μM and 5μM CHIR99021 at 6hrs, 12hrs and 24hrs of treatment. *Axin2* expression levels are unchanged in 1μM CHIR99021 treated quiescent AHSPCs compared to Control (Figure 5.8A), indicating that 1μM CHIR99021 is not sufficient to stimulate canonical Wnt signalling in quiescent AHSPCs at these time points. *Axin2* is significantly upregulated in quiescent AHSPCs treated with 2.5μM CHIR99021 and to a higher extent in 5μM CHIR99021 at all time points (Figure 5.8A), indicating activation of the canonical Wnt signalling pathway. The consistent upregulated level of *Axin2* in 2.5μM and 5μM CHIR99021 treated quiescent AHSPCs across all three time points, suggests that it is the concentration of the Wnt agonist, rather than treatment time, that dictates the level of canonical Wnt stimulation. To investigate whether AHSPC markers were downregulated upon Wnt stimulation under these conditions, I checked the gene expression levels of the AHSPC markers *Ascl1* (Figure 5.8B), *Sox2* (Figure 5.8C) and *GFAP* (Figure 5.8E). *Ascl1* is significantly downregulated in quiescent AHSPCs treated with 1μM, 2.5μM and 5μM CHIR99021 vs Control at all time points (Figure 5.8B), which is consistent with previously observed results. However, *Ascl1* expression levels are downregulated in quiescent AHSPCs treated with 1μM CHIR99021, which failed to robustly activate canonical Wnt signalling at these time points (Figure 5.8A). This suggests that the downregulation of *Ascl1* could be driven by off target effects associated with GSK3β inhibition, rather than direct activation of canonical Wnt signalling. On the other hand, *Sox2* (Figure 5.8C) and *GFAP* (Figure 5.8D) are both downregulated in quiescent AHSPCs treated with 2.5μM and 5μM CHIR99021 at 12hrs and 24hrs, and not in the 1μM CHIR99021 condition. Both 2.5μM and 5μM CHIR99021 induced robust upregulation of *Axin2* and therefore

activated the canonical Wnt signalling pathway (Figure 5.8A). This indicates that stimulating canonical Wnt signalling in quiescent AHSPCs induces a rapid loss of stemness, as AHSPC associated genes start to be downregulated after 12hrs of Wnt stimulation. However, as this is preliminary data, these observations are pending confirmation through further investigations.

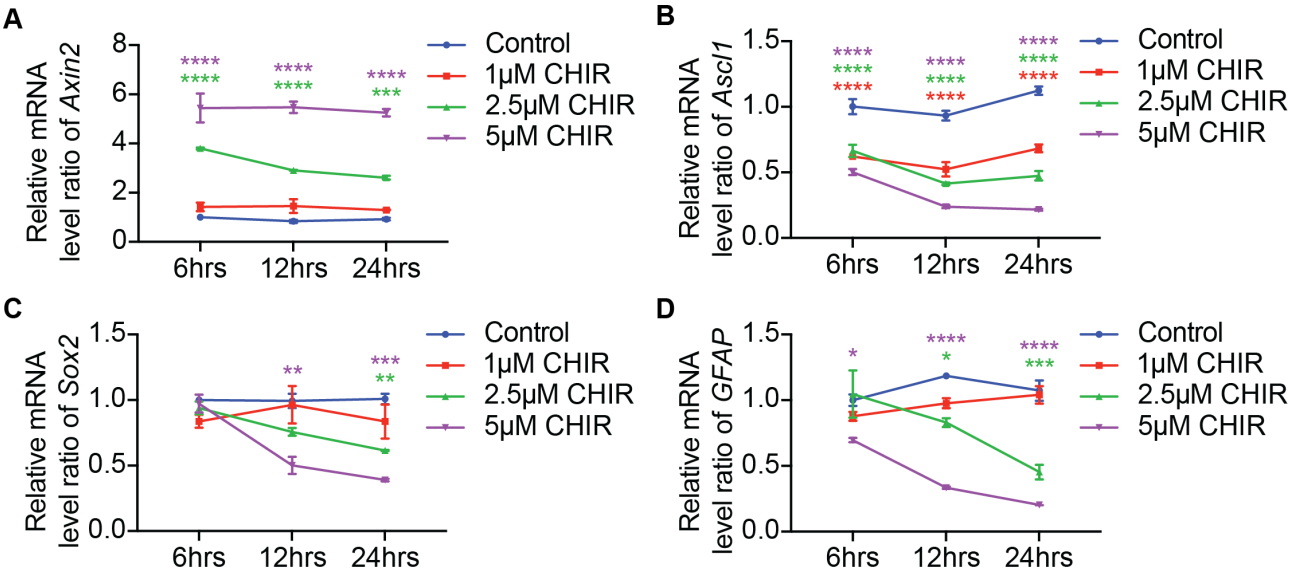


Figure 5.8: qPCR analysis of quiescent AHSPCs treated with 1μM, 2.5μM and 5μM CHIR99021 for 6hrs, 12hrs and 24hrs.

(A) *Axin2* expression levels are upregulated by 2.5μM CHIR99021 and 5μM CHIR99021 treatments, indicating that canonical Wnt signalling is activated. However, *Axin2* levels are unchanged in 1μM CHIR99021, suggesting that 1μM CHIR99021 is not sufficient to significantly activate canonical Wnt signalling.

(B) *Ascl1* expression levels are decreased with all CHIR99021 treatments at all time points. *Ascl1* is downregulated by 1μM CHIR99021 treatment, which failed to induce significant activation of canonical Wnt signalling. This suggests that Ascl1 expression could be regulated by off target effects associated with GSK3β inhibition, rather than stimulation of canonical Wnt signalling.

(C, D) *Sox2* **(C)** and *GFAP* **(D)** expression levels are downregulated in quiescent AHSPCs treated with 2.5μM CHIR99021 and 5μM CHIR99021 for 12hrs and 24hrs. This suggests that these AHSPC marker genes are downregulated by stimulation of canonical Wnt signalling.

mRNA levels were normalised to *GAPDH* and *ActinB* mRNA and expressed relative to Control at 6hrs. Two-way Anova with Tukey's multiple comparisons test was used for statistical analysis, (*, p<0.05. **, p<0.01. ***, p<0.001. ****, p<0.0001). Error bars represent mean with SEM. Data shown is technical repeats of one biological replicate.

5.2.3 Stimulating Canonical Wnt Signalling in Quiescent AHSPCs With Recombinant Wnt3a Also Promotes Proliferation and Activation But With Mechanistic Differences

CHIR99021 stimulates canonical Wnt signalling by inhibiting the activity of GSK3β and therefore preventing the degradation of β-catenin (Ring et al., 2003; Daugherty et al., 2007). However, GSK3β is also responsible for phosphorylating many other proteins involved in a variety of signalling pathways, which would all be affected by GSK3β inhibition (Sutherland. 2011). As such, I wanted to confirm that the activation phenotype and gene expression changes I observed upon CHIR99021 treatment in quiescent AHSPCs, are due to stimulating canonical Wnt signalling and not off target effects induced by GSK3β inhibition. To do this, I titrated recombinant Wnt3a protein (rWnt3a) in quiescent AHSPCs and compared this with quiescent AHSPCs treated with 5μM CHIR99021 for 48hrs (Figure 5.9A). I chose 48hrs for this comparison, as I previously observed that 48hrs of 5μM CHIR99021 treatment in quiescent AHSPCs significantly induced quiescent AHSPC activation and proliferation (Figures 5.3-5.5). To measure quiescent AHSPC activation and proliferation, I labelled proliferating cells using EdU incorporation and immunofluorescence techniques using antibodies against the pan-cell cycle marker Ki67, the G1 cell cycle marker CyclinD1 (Figure 5.9B). Representative images of these proliferation immunostainings show that proliferation is upregulated in quiescent AHSPCs treated with 5μM CHIR99021, 100ng/ml rWnt3a, 250ng/ml rWnt3a and 500ng/ml rWnt3a (Figure 5.9B). This indirectly suggests that the observed activation phenotype, of quiescent AHSPCs, is induced by stimulating canonical Wnt signalling. I quantified the proportion of Ki67 positive, CyclinD1 positive and EdU positive cells in each sample, and normalised this to the proportion of positive cells in the vehicle Control for each Wnt agonist (Figure 5.9C-5.9E). This allowed me to directly compare the fold change of proliferation induced by CHIR99021 and rWnt3a treatments. I found that proliferation was significantly increased in quiescent AHSPCs treated with rWnt3a compared to Control as shown by the fold change of Ki67 and CyclinD1 positive cells (Figure 5.9C and 5.9D). The fold change of EdU positive cells was significantly increased with 500ng/ml rWnt3a treatment compared to Control and was increased with the other treatments, however this was not significant so only illustrates and increasing trend (Figure 5.9E). The fold change of increased proliferation induced by rWnt3a was comparable to that induced by 5μM CHIR99021 treatment of quiescent AHSPCs (Figure 5.9C-5.9E). This indirectly

confirms that stimulating canonical Wnt signalling in quiescent AHSPCs promotes their activation and proliferation.

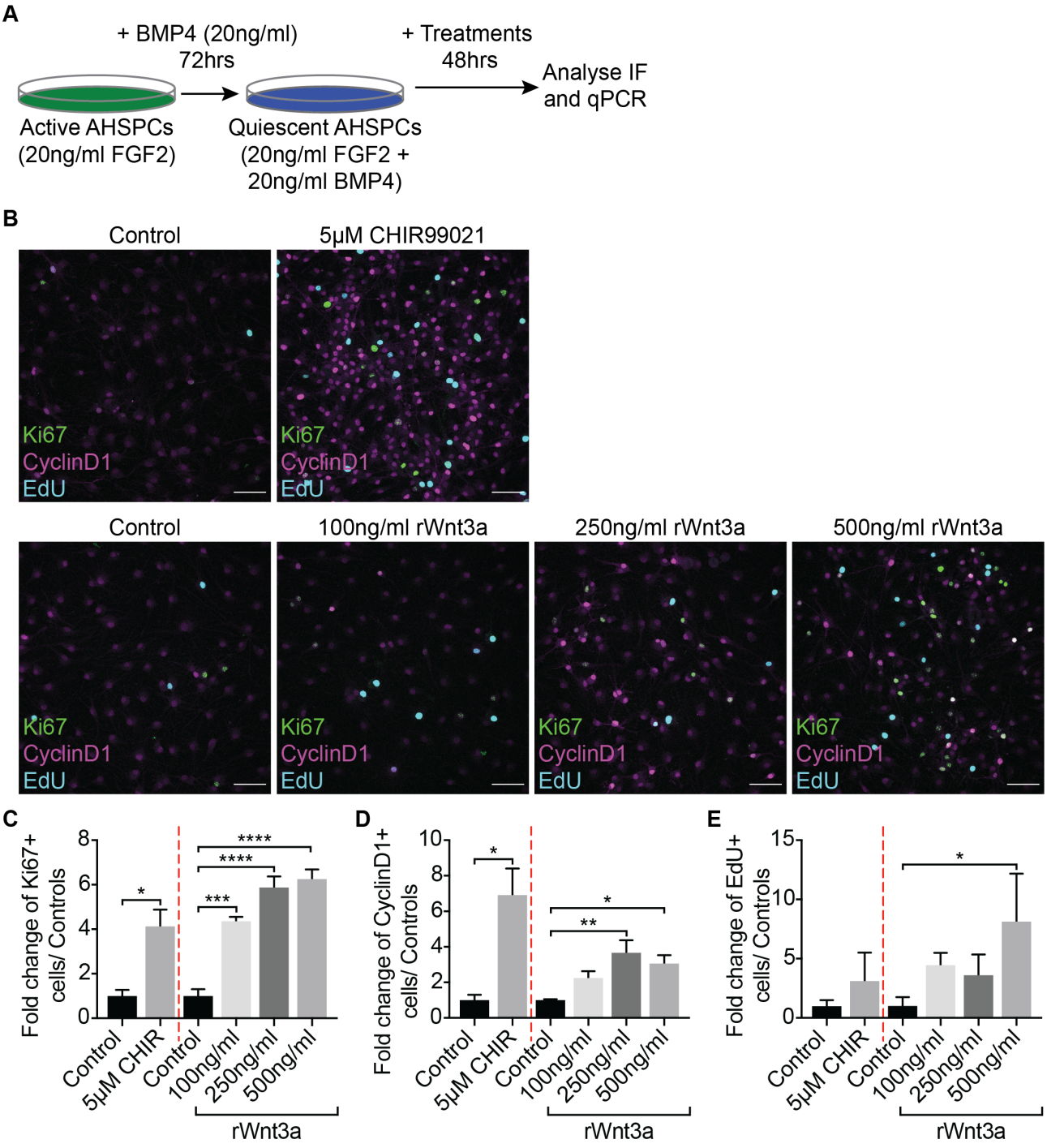


Figure 5.9: Recombinant Wnt3a promotes proliferation of quiescent AHSPCs.

(A) Schematic of experimental design. Quiescent AHSPCs were treated with 0.1% BSA vehicle Control, 100ng/ml rWnt3a, 250ng/ml rWnt3a and 500ng/ml rWnt3a vs DMSO vehicle Control and 5μM CHIR99021 for 48hrs.

(B) Ki67 and CyclinD1 immunolabelling in quiescent AHSPCs treated with Control (0.1%BSA), 100ng/ml rWnt3a, 250ng/ml rWnt3a and 500ng/ml rWnt3a vs Control (DMSO) and 5μM CHIR99021. Scale bars represent 50μM.
(C, D, E) Quantifications of the data shown in **(B)**. Fold change of Ki67+ cells **(C)** CyclinD1+ cells **(D)** and EdU+ cells **(E)** is shown for 5μM CHIR99021 relative to its vehicle Control (DMSO). Likewise, for recombinant Wnt3a, the fold change of proliferating cells is shown relative to its vehicle Control (0.1%BSA). An unpaired Student's t-test and one-way ANOVA with Dunnett's multiple comparisons test was used for statistical analysis, (*, $p<0.05$. **, $p<0.01$. ***, $p<0.001$. ****, $p<0.0001$). Error bars represent mean with SEM. n=3 biological replicates.

To understand the mechanism behind the observed Wnt induced quiescent AHSPC activation, I compared the gene expression changes that occur upon CHIR99021 vs rWnt3a induced quiescent AHSPC activation. I first checked the expression levels of the Wnt target gene *Axin2*, to compare the level of Wnt activation induced by 5μM CHIR99021 vs rWnt3a in quiescent AHSPCs (Figure 5.10A). 5μM CHIR99021 treatment in quiescent AHSPCs approximately induced an eight-fold increase in *Axin2* expression relative to the DMSO vehicle Control (Figure 5.10A). A similar level of *Axin2* upregulation was achieved with 500ng/ml rWnt3a treatment in quiescent AHSPCs (approximately a six-fold increase), whereas 100ng/ml and 250ng/ml rWnt3a significantly upregulated *Axin2* expression but to a lesser extent (Figure 5.10A). Similarly, the canonical Wnt target gene *CyclinD1* is also significantly upregulated in 5μM CHIR99021 treated quiescent AHSPCs and significantly upregulated in a dose-dependent manner with rWnt3a treatments (Figure 5.10B). Overall, this indicates that 500ng/ml rWnt3a stimulates canonical Wnt signalling to a similar level as 5μM CHIR99021 in quiescent AHSPCs under these experimental conditions. Some AHSPC associated genes are similarly regulated by CHIR99021 and rWnt3a treatments in quiescent AHSPCs. For example, the expression level of the AHSPC marker *Hes5* is significantly decreased in quiescent AHSPCs treated with 5μM CHIR99021 and is slightly decreased with 500ng/ml rWnt3a treatment, although this is not statistically significant (Figure 5.10C). In addition, quiescent AHSPCs treated with 5μM CHIR99021 and 500ng/ml rWnt3a show a slight upregulation of *Nestin*, however this is not statistically significant and therefore only represents a slight trend (Figure 5.10D). *HopX* is upregulated by both CHIR99021 and 500ng/ml rWnt3a treatment in quiescent AHSPCs, however CHIR99021 treatment induces *HopX* expression more robustly than rWnt3a treatment (Figure 5.10E). Overall, this shows that some AHSPC genes are similarly regulated by CHIR99021 and rWnt3a treatment in quiescent AHSPCs. However, this is not true for all tested genes. For example, *Glast* expression levels

are relatively unchanged by 5μM CHIR99021 treatment but are significantly increased by 500ng/ml rWnt3a treatment (Figure 5.10F). Similarly, *Sox2* is downregulated by 5μM CHIR99021 but is unaffected by treatment with rWnt3a (Figure 5.10G). *Ascl1* is significantly downregulated by 5μM CHIR99021 treatment and 500ng/ml rWnt3a treatment also significantly reduces *Ascl1* gene expression levels, but this reduction is less robust than the downregulation observed with 5μM CHIR99021 treatment (Figure 5.10H). Overall, these data suggest that stimulating canonical Wnt signalling with either CHIR99021 or rWnt3a promotes quiescent AHSPC activation and proliferation. However, the differences in the gene expression changes induced by these two Wnt agonists suggests that CHIR99021 treatment may be regulating gene expression changes partially independently of canonical Wnt signalling.

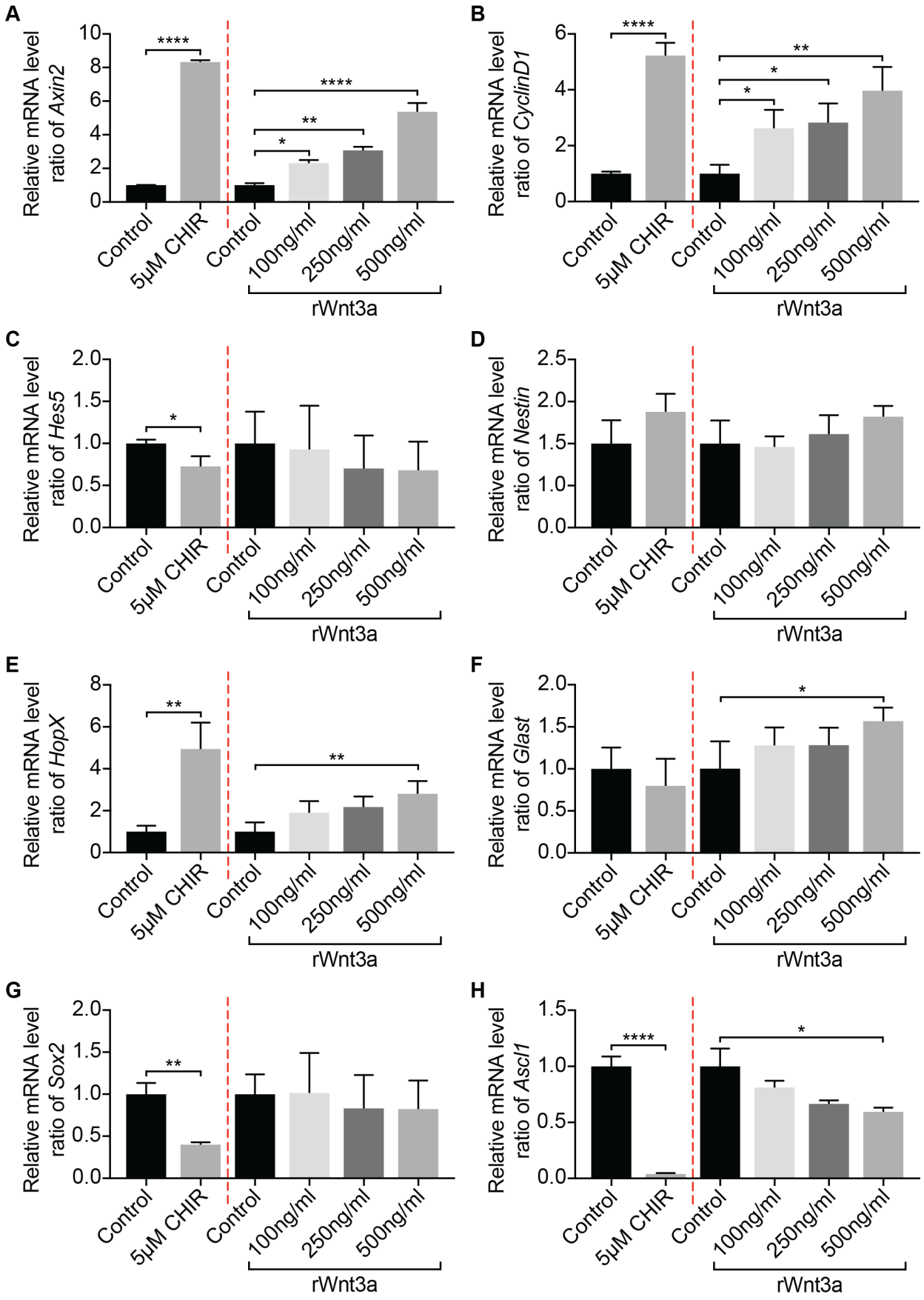


Figure 5.10: Mechanistic differences between recombinant Wnt3a and CHIR99021 induced quiescent AHSPC activation.

(A, B) qPCR analysis of *Axin2* **(A)** and *CyclinD1* **(B)** expression levels. *Axin2* and *CyclinD1* are similarly increased in both 5μM CHIR99021 and 500ng/ml Wnt3a indicating similar activation of canonical Wnt signalling levels. The increase in *CyclinD1* expression levels could also indicate increased quiescent AHSPC activation induced by stimulating canonical Wnt signalling.
(C, D, E, F, G, H) qPCR analysis of *Hes5* **(C)**, *Nestin* **(D)**, *HopX* **(E)**, *Glast* **(F)**, *Sox2* **(G)** and *Ascl1* **(H)** expression levels in quiescent AHSPCs treated with 5μM CHIR99021, 100ng/ml rWnt3a, 250ng/ml rWnt3a and 500ng/ml rWnt3a for 48hrs.
mRNA levels were normalised to *GAPDH* and *ActinB* mRNA and expressed relative to the Vehicle Controls of each Wnt agonist (DMSO and 0.1%BSA for CHIR99021 and recombinant Wnt3a respectively). An unpaired Student's t-test and one-way ANOVA with Dunnett's multiple comparisons test was used for statistical analysis, (*, $p<0.05$. **, $p<0.01$. ****, $p<0.0001$). Error bars represent mean with SEM. n=3 biological replicates.

5.3 Stabilising β-catenin in AHSCs *in vivo* Causes Their Displacement from Their Correct Niche Location

I next wanted to investigate whether stimulating canonical Wnt signalling in AHSCs *in vivo* recapitulated the results obtained when stimulating canonical Wnt signalling in active and quiescent AHSPC cultures. To do this, I generated an inducible transgenic mouse line to stabilise β-catenin and activate canonical Wnt signalling in AHSCs *in vivo*. GlastCreERT2; Cat-ca; RYFP mice were generated as described in Section 2.1.1. The Cat-ca allele contains LoxP sites flanking exon3 of *β-catenin*, which encodes the GSK3β phosphorylation sites S33, S37, T41 and S45 (Harada et al., 1999). Tamoxifen induced recombination causes the deletion of *β-catenin*^{ex3} and generates constitutively active β-catenin, which activates downstream canonical Wnt signalling (Harada et al., 1999). Upon tamoxifen administration in these mice, CreERT2 translocates to the nucleus of Glast+ cells to facilitate recombination of the Cat-ca and RYFP alleles (Feil et al., 1997). The RYFP allele was included to identify the recombined cells (Srinivas et al., 2001).

5.3.1 AHSCs are Lost from the Dentate Gyrus 30 days After β-catenin Stabilisation

2-month-old GlastCreERT2; Cat-ca$^{wt/wt}$; RYFP (Control), GlastCreERT2; Cat-ca$^{fl/wt}$; RYFP (Cat-ca^{Het}), GlastCreERT2; Cat-ca$^{fl/fl}$; RYFP (Cat-ca^{Hom}) mice were administered tamoxifen, by intraperitoneal injection, once daily for 5 consecutive days and were transcardially perfused 30

days after the first tamoxifen injection (30dpi) for analysis (Figure 5.11A). Analysing samples 30 days after the initial tamoxifen injection allowed to me to investigate the effect stabilising β-catenin in AHSCs has on the whole process of adult neurogenesis, including AHSC and intermediate progenitor cell (IPC) proliferation and neuronal differentiation. I used both heterozygous and homozygous mice for the Cat-ca allele to explore the dose-dependent effect of stimulating canonical Wnt signalling in AHSCs *in vivo* that I previously observed *in vitro* (Section 5.2.1).

During this experiment, Cat-ca^{Het} and Cat-ca^{Hom} mice developed an abnormal skin phenotype that first presented approximately 2 weeks after the first tamoxifen injection. Histopathological analysis of this skin phenotype was performed by E. Ross. In her report, she described this skin phenotype as a "*multifocal thickening, lichenification, crusting and alopecia of the skin affecting the limbs, axillae, inguinal area and muzzle. Microscopic examination showed a clear disorganisation of keratinocyte maturation within hair follicles and the accumulation of flaky keratin associated with the distension of the hair follicles. Subsequent rupture of the hair follicles leads to a strong inflammatory response. From a literature search, this phenotype is consistent with the phenotype classically observed when knocking-out β-catenin within hair follicle stem cells* (Huelsken et al., 2001)." Glast has been shown to be expressed in activated stem and progenitor cells in the hair follicle, interfollicular epidermis and sebaceous glands (Reichenbach et al., 2018). This means that in this mouse model, tamoxifen administration promotes the recombination and stabilisation of β-catenin in the Glast+ cells of both the dentate gyrus (DG) and the skin. The similarities of the skin phenotype between these mice and the β-catenin knock out mice from Huelsken et al, 2001 (Huelsken et al., 2001), suggest that stabilising β-catenin in activated stem and progenitor cells of the skin, promotes a dominant negative effect, where the normal function of wild type β-catenin is overridden by the stabilised form of β-catenin. I was able to collect enough samples from the first cohort of mice, looking 30 days after the first tamoxifen injection, to perform relevant immunofluorescence analysis. However, for future experiments and following veterinary advice, Cat-ca mice were sacrificed a maximum of 10 days after the first tamoxifen injection, before the skin phenotype developed.

I performed immunofluorescence staining on coronal sections of the DG of Control, Cat-ca^{Het} and Cat-ca^{Hom} mice 30 days after the first tamoxifen injection at 2 months, to investigate how AHSCs (YFP+ GFAP+ Sox2+ cells with radial morphology) are affected by the stabilisation of β-catenin. To investigate whether proliferation is affected, I immunolabelled cells with an

antibody against the pan cell-cycle marker Ki67 (Figure 5.11B). From the confocal images of this immunofluorescence, I observed fewer YFP+ cells in the DG of Cat-ca^{Het} and Cat-ca^{Hom} mice compared to Control (Figure 5.11B). In addition, many YFP+ cells in the DG of Cat-ca^{Het} and Cat-ca^{Hom} mice did not retain a radial morphology as seen in Control (Figure 5.11B). This suggests that stabilisation of β-catenin negatively affects AHSCs 30 days later. Indeed, the total number of AHSCs normalised to the subgranular zone (SGZ) length is severely reduced in Cat-ca^{Het} and Cat-ca^{Hom} mice (Figure 5.11C). This decrease in total AHSC number was more pronounced in Cat-ca^{Hom} compared to Cat-ca^{Het} mice, indicating there could be a dose-dependent effect to stabilising β-catenin in the AHSCs *in vivo* (Figure 5.11C). The decreased total number of AHSCs in Cat-ca^{Het} and Cat-ca^{Hom} mice could be due to their increased activation, proliferation and progression along the neurogenic lineage. To investigate this, I quantified the proportion of Ki67+ AHSCs in Cat-ca^{Het} and Cat-ca^{Hom} vs Control mice 30 days after stabilising β-catenin in the AHSCs *in vivo* (Figure 5.11D). I found no significant difference in the proportion of Ki67+ AHSCs in Cat-ca^{Het} and Cat-ca^{Hom} mice compared to Control, indicating that the decrease in total number of AHSCs was not due to increased AHSC activation and proliferation (Figure 5.11D). However, as this analysis was performed relatively late after β-catenin stabilisation, I cannot exclude that a proliferation burst may have happened earlier. From the Ki67 immunofluorescence images, there appeared to be an increase in the number of Ki67+ cells in Cat-ca^{Het} mice compared to Control (Figure 5.11B). I quantified the total number of Ki67+ cells in the DG of Control, Cat-ca^{Het} and Cat-ca^{Hom} mice, which includes active AHSCs, IPCs and proliferating neuroblasts (Figure 5.11E). I found that the total number of proliferating cells is increased in Cat-ca^{Het} mice compared to Control 30 days after tamoxifen (Figure 5.11E). The total number of Ki67+ cells in Cat-ca^{Het} mice is also increased compared to Cat-ca^{Hom} mice, indicating there could be a dose-dependent effect to stabilising β-catenin in AHSCs (Figure 5.11E). However, as this is not statistically significant it may only represent a trend (Figure 5.11E). As the proportion of Ki67+ AHSCs is unchanged by β-catenin stabilisation (Figure 5.11D), this suggests that this increase in total proliferation in Cat-ca^{Het} mice originates from IPCs and neuroblasts.

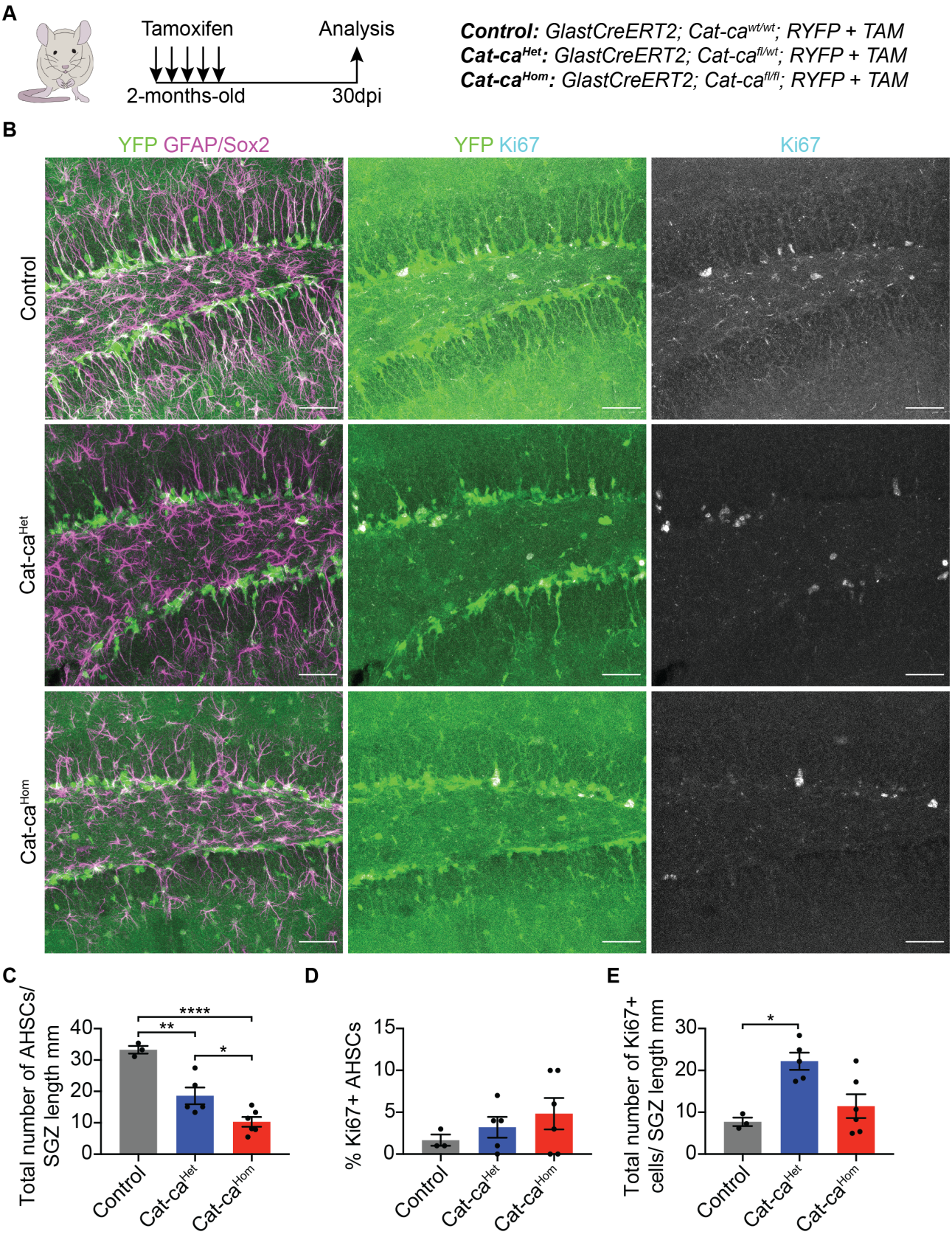


Figure 5.11: AHSCs are lost from the DG 30 days after β-catenin stabilisation in AHSCs.

(A) Schematic of experimental design for the analysis of adult neurogenesis 30 days after β-catenin stabilisation in AHSCs. 2-month-old GlastCreERT2; Cat-ca$^{wt/wt}$; RYFP (Control),

GlastCreERT2; Cat-ca$^{fl/wt}$; RYFP (Cat-ca^{Het}), GlastCreERT2; Cat-ca$^{fl/fl}$; RYFP (Cat-ca^{Hom}) mice were injected once daily with tamoxifen for 5 consecutive days and analysed 30 days after the first injection (30dpi).

(B) Immunolabelling of YFP (GFP antibody), GFAP, Sox2 and Ki67 in the dentate gyrus of Control, Cat-ca^{Het} and Cat-ca^{Hom} adult mice 30 days after tamoxifen administration. YFP is used to identify recombined cells. Recombined AHSCs are identified as YFP+ GFAP+ Sox2+ cells with radial morphology. Ki67 is used to label proliferating cells, which includes active AHSCs, IPCs and neuroblasts. Scale bars represent 50μm.

(C) Quantification of the total number of YFP+ GFAP+ Sox2+ AHSCs normalised to the length of the SGZ (mm) in Control, Cat-ca^{Het} and Cat-ca^{Hom} mice. The total number of AHSCs decreases in Cat-ca^{Het} and Cat-ca^{Hom} vs Control, indicating that β-catenin stabilisation induces a loss of AHSCs from the hippocampal niche 30 days later.

(D) Quantification of the proportion of YFP+ Ki67+ AHSCs in Control, Cat-ca^{Het} and Cat-ca^{Hom} mice 30 days after β-catenin stabilisation. There is no significant difference in the proportion of proliferating AHSCs in Cat-ca^{Het} and Cat-ca^{Hom} mice vs Control.

(E) Quantification of the total number of YFP+ Ki67+ cells normalised to SGZ length (mm) in the dentate gyrus of Control, Cat-ca^{Het} and Cat-ca^{Hom} mice 30 days after β-catenin stabilisation. Cat-ca^{Het} mice display an increase in the total number of proliferating cells compared to both Control and Cat-ca^{Hom} mice 30 days after β-catenin stabilisation.

In all instances n=3 for Control, n=5 for Cat-ca^{Het} and n=6 for Cat-ca^{Hom}. One-way ANOVA with Tukey's multiple comparisons test was used for all statistical analysis, (*, $p<0.05$. **, $p<0.01$. ****, $p<0.0001$). Error bars represent mean with SEM.

5.3.2 AHSC Homeostasis is Unaffected by Short-Term Stabilisation of β-catenin

The data above shows that AHSCs are lost from the DG niche 30 days after stabilising β-catenin in AHSCs. At this time point, AHSC proliferation was unchanged between Control, Cat-ca^{Het} and Cat-ca^{Hom} mice, however an earlier burst in proliferation, which is normally associated with depletion, might explain this loss of AHSCs. To investigate this, I injected 2-month-old GlastCreERT2; Cat-ca$^{wt/wt}$; RYFP (Control), GlastCreERT2; Cat-ca$^{fl/wt}$; RYFP (Cat-ca^{Het}), GlastCreERT2; Cat-ca$^{fl/fl}$; RYFP (Cat-ca^{Hom}) mice with tamoxifen once daily for 4 days and collected samples 6 days after the first tamoxifen injection (Figure 5.12A). This allowed me to investigate the immediate effects stabilising β-catenin has on AHSC homeostasis. I performed immunolabelling for recombined AHSCs (YFP+ GFAP+ Sox2+ cells with radial morphology) and

the proliferation marker Ki67 in brain sections from Control, Cat-ca^{Het} and Cat-ca^{Hom} mice 6 days after the first tamoxifen injection (Figure 5.12B). I found no overall differences in the gross morphologies of YFP+ cells in the DG of Control, Cat-ca^{Het} and Cat-ca^{Hom} animals, however there did appear to be fewer YFP+ cells in Cat-ca^{Hom} images (Figure 5.12B). Quantification of the total number of AHSCs normalised to the SGZ length showed no difference between Control, Cat-ca^{Het} and Cat-ca^{Hom} mice, indicating that short-term stabilisation of β-catenin does not affect AHSC survival or retention within the DG niche (Figure 5.12C). In addition, the proportion of Ki67+ AHSCs is consistent between Control, Cat-ca^{Het} and Cat-ca^{Hom} mice (Figure 5.12D). This suggests that quiescent AHSC activation and proliferation are unaffected by short-term stabilisation of β-catenin and are not responsible for the loss of AHSCs 30 days later. I also quantified the total number of proliferating cells in the DG of Control, Cat-ca^{Het} and Cat-ca^{Hom} mice, which includes active AHSCs, IPCs and neuroblasts (Figure 5.12E). I found that the total number of proliferating cells was slightly increased in Cat-ca^{Het} mice, and to a lesser extent in Cat-ca^{Hom} mice, compared to Control 6 days after the stabilisation of β-catenin (Figure 5.12E). This again suggests that there could be a dose-dependent effect on IPC proliferation when stabilising β-catenin in AHSCs *in vivo*. In addition, this suggests that stabilising β-catenin in AHSCs has a larger effect on the proliferation of their progeny, rather than directly affecting the AHSCs themselves. However, as this is preliminary data, further analysis is required to confirm these observations.

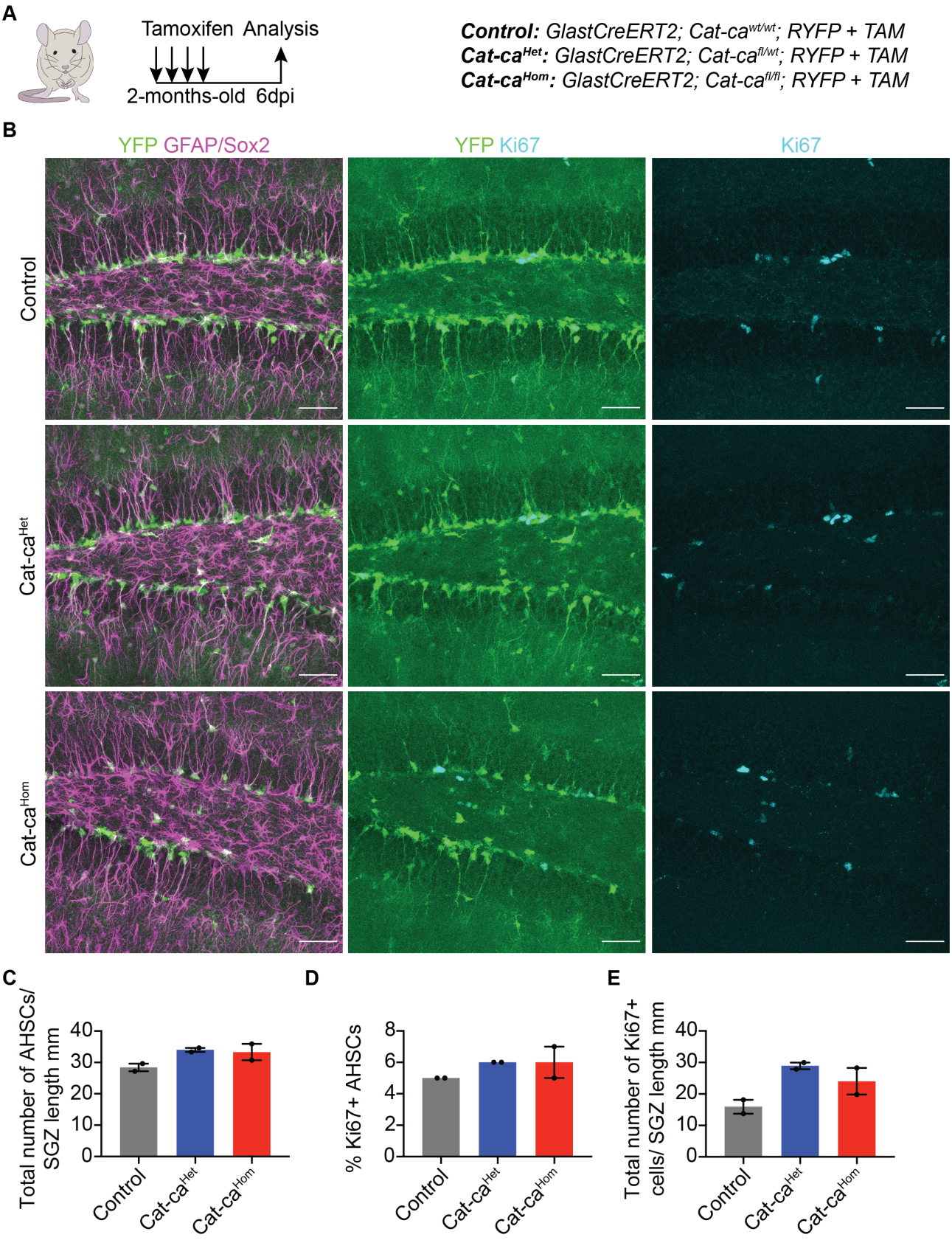


Figure 5.12: AHSCs are unaffected by short-term stabilisation of β-catenin.

(A) Schematic of experimental design for the analysis of AHSCs 6 days after β-catenin stabilisation in AHSCs. 2-month-old GlastCreERT2; Cat-ca$^{wt/wt}$; RYFP (Control), GlastCreERT2;

Cat-ca$^{fl/wt}$; RYFP (Cat-ca^{Het}), GlastCreERT2; Cat-ca$^{fl/fl}$; RYFP (Cat-ca^{Hom}) mice were injected with tamoxifen for 4 consecutive days and analysis was performed 6 days after the first tamoxifen injection.

(B) Immunolabelling of YFP (GFP antibody), GFAP, Sox2 and Ki67 in the dentate gyrus of Control, Cat-ca^{Het} and Cat-ca^{Hom} mice 6 days after tamoxifen administration. YFP is used to identify recombined cells. Recombined AHSCs are identified as YFP+ GFAP+ Sox2+ cells with radial morphology. Ki67 is used to label proliferating cells, which includes active AHSCs, IPCs and neuroblasts. From these images, it appears there are fewer YFP+ cells in the Cat-ca^{Hom} mice. Scale bars represent 50μm.

(C) Quantification of the total number of GFAP+ Sox2+ AHSCs normalised to the length of the SGZ (mm) in Control, Cat-ca^{Het} and Cat-ca^{Hom} 6 days after β-catenin stabilisation.

(D) Quantification of the proportion of Ki67+ AHSCs in Control, Cat-ca^{Het} and Cat-ca^{Hom} mice 6 days after β-catenin stabilisation.

(E) Quantification of the total number of Ki67+ cells normalised to SGZ length (mm) in the dentate gyrus of Control, Cat-ca^{Het} and Cat-ca^{Hom} mice 6 days after β-catenin stabilisation. Cat-ca^{Het}, and to a lesser extent Cat-ca^{Hom}, mice display an increase in the total number of proliferating cells compared to both Control mice 6 days after β-catenin stabilisation.

n=2 for Control, Cat-ca^{Het} and Cat-ca^{Hom} mice. Statistical analysis was not performed for this preliminary data due to insufficient biological replicates. Error bars represent mean with SEM.

One key characteristic of AHSCs is their ability to return to a quiescent state once they have become activated (Urbán et al., 2016). I next wanted to investigate whether AHSCs' ability to return to quiescence was affected by stabilising β-catenin. To do this, I injected 2-month-old GlastCreERT2; Cat-ca$^{wt/wt}$; RYFP (Control), GlastCreERT2; Cat-ca$^{fl/wt}$; RYFP (Cat-ca^{Het}), GlastCreERT2; Cat-ca$^{fl/fl}$; RYFP (Cat-ca^{Hom}) mice with tamoxifen once daily for 4 days (Figure 5.13A). On the 5th day Control, Cat-ca^{Het} and Cat-ca^{Hom} mice were given 3 injections of EdU, spaced throughout the day (Figure 5.13A). These EdU injections were performed to label the AHSCs that are active and proliferating after β-catenin stabilisation (Figure 5.13A). Mice were then sacrificed by perfusion under terminal anaesthesia the day after the EdU injections (Figure 5.13A). I then performed immunofluorescence labelling for AHSCs (GFAP+ Sox2+ cells with radial morphology) and two proliferation markers EdU and Ki67 (Figure 5.13B). As stated above, EdU immunolabelling was used to label the AHSCs that were proliferating after the stabilisation of β-catenin (Figure 5.13B). Co-staining with the pan cell-cycle marker Ki67, allowed me to identify AHSCs that continued to proliferate (EdU+ Ki67+ AHSCs, Figure 5.13B double arrow

heads) and the AHSCs that returned to quiescence following the stabilisation of β-catenin (EdU+ Ki67- AHSCs, Figure 5.13B single arrow heads). I then quantified the proportion of AHSCs that returned to quiescence (EdU+ Ki67- AHSCs) as a fraction of the total number of AHSCs that were proliferating after the stabilisation of β-catenin (EdU+ AHSCs) (Figure 5.13C). I found that there was no difference in the proportion of AHSCs returning to quiescence in Cat-ca^{Het} and Cat-ca^{Hom} vs Control mice (Figure 5.13C), however further analysis is required to confirm this. Overall, these preliminary data suggest that AHSC activation and their ability to return to quiescence, is unaffected by the short-term stabilisation of β-catenin.

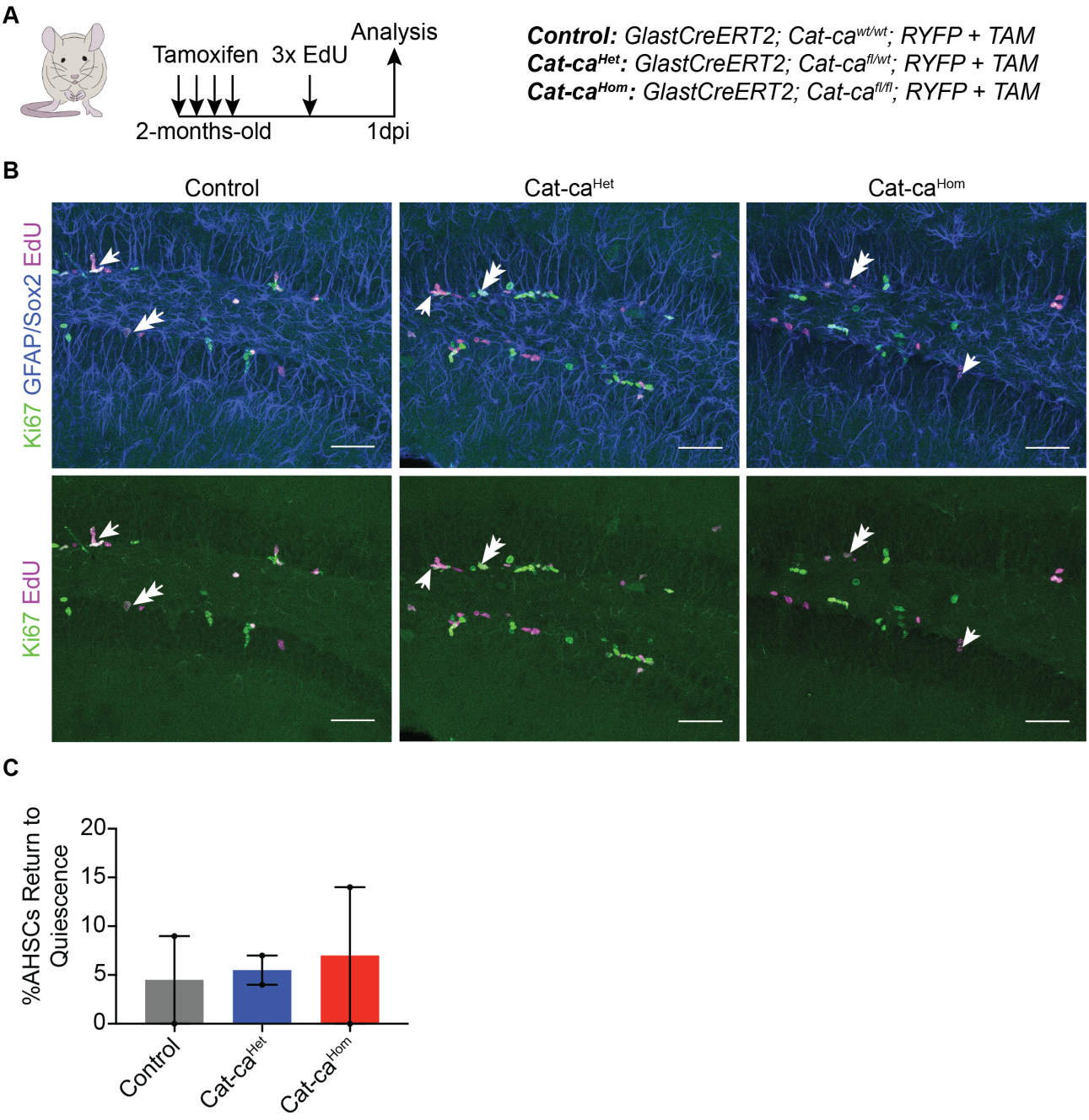


Figure 5.13: β-catenin stabilisation does not affect AHSCs' ability to return to quiescence.

(A) Schematic of experimental design for the analysis of AHSCs ability to return to quiescence following β-catenin stabilisation. 2-month-old GlastCreERT2; Cat-ca$^{wt/wt}$; RYFP (Control), GlastCreERT2; Cat-ca$^{fl/wt}$; RYFP (Cat-ca^{Het}), GlastCreERT2; Cat-ca$^{fl/fl}$; RYFP (Cat-ca^{Hom}) mice were injected with tamoxifen once daily for 4 consecutive days. The day after the final tamoxifen injection, mice were given 3x EdU injections throughout the day to label the cells in S-phase of the cell cycle. Analysis was performed the day after the EdU injections (1dpi).

(B) Immunolabelling of Ki67, GFAP, Sox2 and EdU in the DG of Control, Cat-ca^{Het} and Cat-ca^{Hom} adult mice 1 day after the EdU injections. AHSCs are identified as GFAP+ Sox2+ cells

with radial morphology. EdU is used to label the cells that were in S-phase of cell cycle following the stabilisation of β-catenin in AHSCs. Ki67 is used to label proliferating cells. Single arrow heads represent AHSCs that have returned to quiescence (EdU+ Ki67-). Double arrow heads represent AHSCs that have continued to proliferate (EdU+ Ki67+). Scale bars represent 50μm. **(C)** Quantification of the proportion of AHSCs that have returned to quiescence (%EdU+ Ki67- AHSCs/EdU+ AHSCs) 1 day after the EdU injections. n=2 for Control, Cat-ca^{Het} and Cat-ca^{Hom}. Statistical analysis was not performed for this preliminary data due to insufficient biological replicates. Error bars represent mean with SEM.

5.3.3 β-catenin Stabilisation Causes the Displacement of AHSCs from the SGZ, Which Induces Their Activation

I showed above that AHSCs are unaffected by short-term stabilisation of β-catenin, however AHSCs are lost from the DG niche 30 days after β-catenin stabilisation. To understand how long-term β-catenin stabilisation causes this loss of AHSCs, I analysed the DG of Control, Cat-ca^{Het} and Cat-ca^{Hom} mice at an intermediate time-point of 10 days after the first tamoxifen injection. 2-month-old GlastCreERT2; Cat-ca$^{wt/wt}$; RYFP (Control), GlastCreERT2; Cat-ca$^{fl/wt}$; RYFP (Cat-ca^{Het}), GlastCreERT2; Cat-ca$^{fl/fl}$; RYFP (Cat-ca^{Hom}) mice were administered tamoxifen by intraperitoneal injection once daily for 5 consecutive days and were transcardially perfused 10 days after the first tamoxifen injection (10dpi) for analysis (Figure 5.14A). I then performed immunostainings to identify recombined AHSCs (YFP+ cell with an SGZ located Sox2+ DAPI+ cell body and GFAP+ radial morphology) and to mark proliferating cells (Ki67) (Figure 5.14B). I found that the total number of YFP+ AHSCs was unchanged in the DG of Cat-ca^{Het} and Cat-ca^{Hom} mice vs Control (Figure 5.14C), suggesting that the loss of AHSCs occurs between 10 and 30 days after β-catenin stabilisation. However, the proportion of Ki67+ AHSCs is slightly increased in Cat-ca^{Het} and Cat-ca^{Hom} mice vs Control (Figure 5.14D), as is the total number of proliferating cells (activated AHSCs, IPCs and neuroblasts) although this is not significant and therefore only indicates a trend (Figure 5.14E). This could suggest that the stabilisation of β-catenin in AHSCs enhances AHSC and total proliferation in the DG niche 10 days later (Figure 5.14D), which could explain the loss of AHSCs 30 days later. However, this enhanced AHSC proliferation was not statistically significant and did not seem substantial enough to account for the dramatic loss of AHSCs 30 days after β-catenin stabilisation. When comparing the confocal images of YFP, GFAP, Sox2 and YFP immunolabelling in Control vs Cat-ca^{Het} and Cat-ca^{Hom} mice, I observed that the organisation of the DG niche in Cat-ca^{Het} and

Cat-ca^{Hom} mice was irregular compared to Control (Figure 5.14B). In Control, the majority of YFP+ (recombined) cells are located within the SGZ of the DG and GFAP+ processes are uniformly projected through the granule cell layer (GCL) towards the molecular layer (ML) (Figure 5.14B). In the DG of Cat-ca^{Het} and Cat-ca^{Hom} mice, this uniformity is disrupted. Many YFP+ recombined cells are no longer located in the SGZ but appear to be displaced into the GCL, ML and even the hilus of the DG (Figure 5.14B). The same can be said about the YFP+ Ki67+ cells, which are more dispersed into the GCL, ML and hilus in the DG of Cat-ca^{Het} and Cat-ca^{Hom} mice compared to Control (Figure 5.14B).

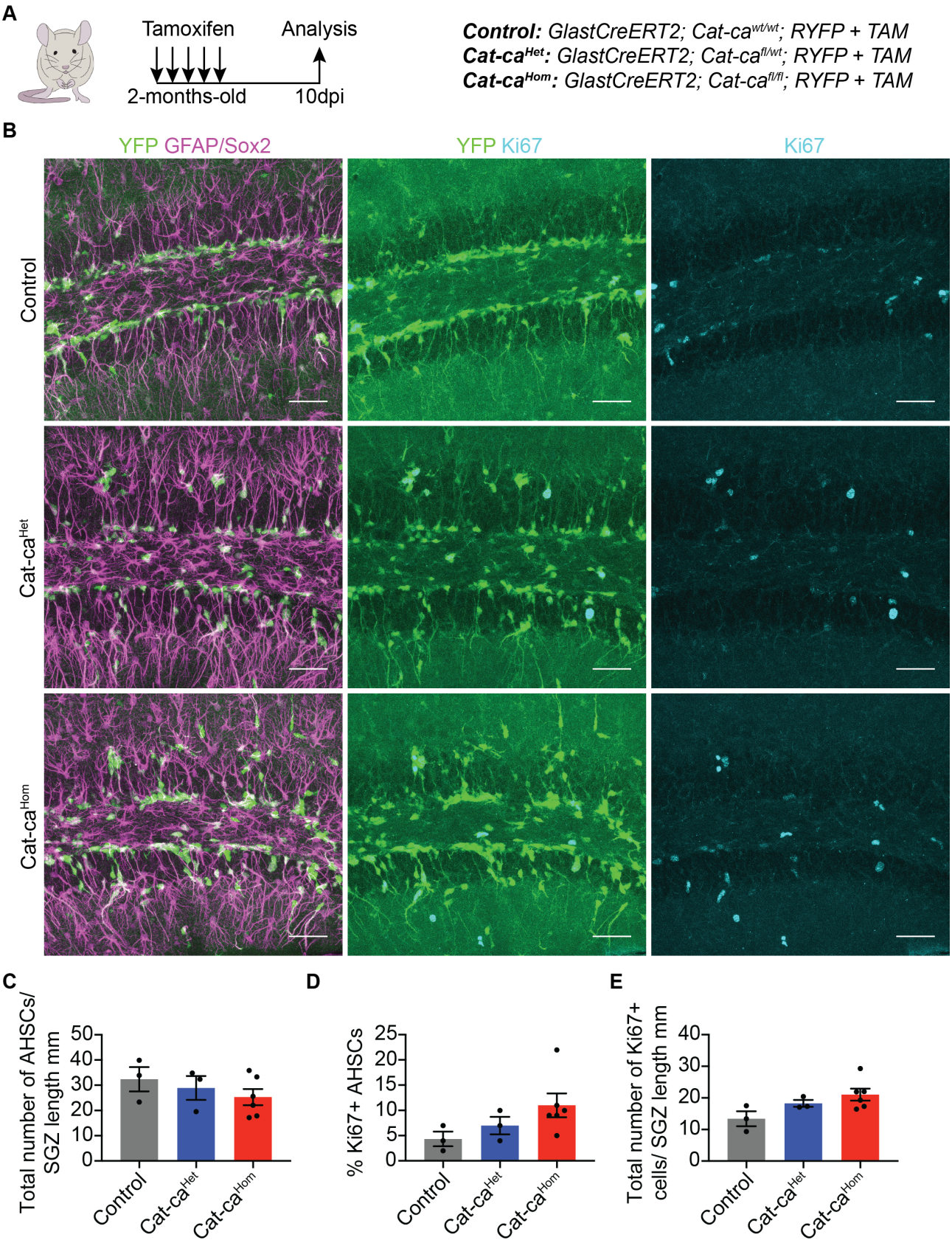


Figure 5.14: Immunofluorescence of AHSCs and proliferation markers in the DG of Control, Cat-ca^{Het} and Cat-ca^{Hom} mice 10 days after β-catenin stabilisation.

(A) Schematic of experimental design for the analysis of adult neurogenesis 10 days after β-catenin stabilisation in AHSCs. 2-month-old GlastCreERT2; Cat-ca$^{wt/wt}$; RYFP (Control), GlastCreERT2; Cat-ca$^{fl/wt}$; RYFP (Cat-ca^{Het}), GlastCreERT2; Cat-ca$^{fl/fl}$; RYFP (Cat-ca^{Hom}) mice were injected with tamoxifen for 5 consecutive days and analysis was performed 10 days after the first tamoxifen injection (10dpi).
(B) Immunolabelling of YFP (GFP antibody), GFAP, Sox2 and Ki67 in the dentate gyrus of Control, Cat-ca^{Het} and Cat-ca^{Hom} mice 10 days after tamoxifen administration. YFP is used to identify recombined cells. Recombined AHSCs are identified as YFP+ GFAP+ Sox2+ cells with RGL morphology and a DAPI+ SGZ located cell body. Ki67 is used to label proliferating cells which includes active AHSCs, IPCs and neuroblasts. Scale bars represent 50μm.
(C) Quantification of the total number of YFP+ GFAP+ Sox2+ AHSCs normalised to the length of the SGZ (mm) in Control, Cat-ca^{Het} and Cat-ca^{Hom} mice 10 days after β-catenin stabilisation. The total number of AHSCs is unchanged in Cat-ca^{Het} and Cat-ca^{Hom} mice vs Control.
(D) Quantification of the proportion of YFP+ Ki67+ AHSCs in Control, Cat-ca^{Het} and Cat-ca^{Hom} mice 10 days after β-catenin stabilisation. There is a modest increase in the proportion of proliferating AHSCs in Cat-ca^{Het} and Cat-ca^{Hom} mice vs Control.
(E) Quantification of the total number of YFP+ Ki67+ cells normalised to SGZ length (mm) in the dentate gyrus of Control, Cat-ca^{Het} and Cat-ca^{Hom} mice 10 days after β-catenin stabilisation. Cat-ca^{Hom} mice display a significant increase in the total number of proliferating cells compared to Control mice 10 days after β-catenin stabilisation.
In all instances n=3 for Control, n=3 for Cat-ca^{Het} and n=6 for Cat-ca^{Hom}. One-way ANOVA with Tukey's multiple comparisons test was used for all statistical analysis, (ns, $p>0.05$). Error bars represent mean with SEM.

Many of these displaced recombined (YFP+) cells in Cat-ca^{Het} and Cat-ca^{Hom} mice retained AHSC characteristics and were YFP+ GFAP+ Sox2+ with a single GFAP+ radial process (Figure 5.15A). I therefore quantified the total number of displaced AHSCs and the proportion of displaced AHSCs as a fraction of the total AHSC population (Figure 5.15B and 5.15C). I classified a displaced AHSCs as being YFP+ GFAP+ Sox2+ with a single GFAP+ radial process, whose cell body was located two or more cell nuclei away from the SGZ (Figure 5.15A). The total number of displaced AHSCs is increased in Cat-ca^{Het} and Cat-ca^{Hom} mice (Figure 15.5B), which approximately amounted to a 3-fold increase in the proportion of displaced AHSCs in Cat-ca^{Het} and Cat-ca^{Hom} mice compared to Control, however this was not statistically significant (Figure 5.15C). This suggests that stabilising β-catenin in AHSCs promotes their displacement

from their correct niche location in the SGZ and could be responsible for the loss of AHSCs 30 days after the stabilisation of β-catenin.

AHSCs in the SGZ are largely maintained in a quiescent state by multiple signalling pathways promoting quiescence, such as Notch and BMP4 signalling, in the SGZ (Bonaguidi et al., 2008; Mira et al., 2010). I next wanted to investigate whether proliferation was enriched in displaced AHSCs, as they have moved away from the quiescent signalling pathways enriched in the SGZ. I could not find any Ki67+ displaced AHSCs in the DG of Control mice (Figure 5.15D). This contrasts with the proportion of Ki67+ displaced AHSCs I observed in the DG of Cat-ca^{Het} and Cat-ca^{Hom} mice (Figure 5.15D). The proportion of proliferating AHSCs is slightly higher in displaced AHSCs compared to AHSCs located within the SGZ of Cat-ca^{Het} and Cat-ca^{Hom} mice, however this was not statistically significant (Figure 5.15D). This could indicate that proliferation is enriched in AHSCs that are displaced from their correct SGZ location and could suggest that AHSCs become activated as they move away from SGZ located quiescent signals. Ascl1 is essential for the activation of quiescent AHSCs *in vivo* (Andersen et al., 2014), and can therefore be used to identify active AHSCs. Ascl1 immunostaining showed a high number of displaced Ascl1+ cells in the DG of Cat-ca^{Het} and Cat-ca^{Hom} mice compared to Control 10 days after β-catenin stabilisation (Figure 5.15E). This supports the hypothesis that the displacement of AHSCs, induced by the stabilisation of β-catenin, promotes the activation of AHSCs possibly due to their migration away from the quiescence signals located within the SGZ. This could be further tested by examining readouts of quiescence signals in the displaced AHSCs of Cat-ca mice.

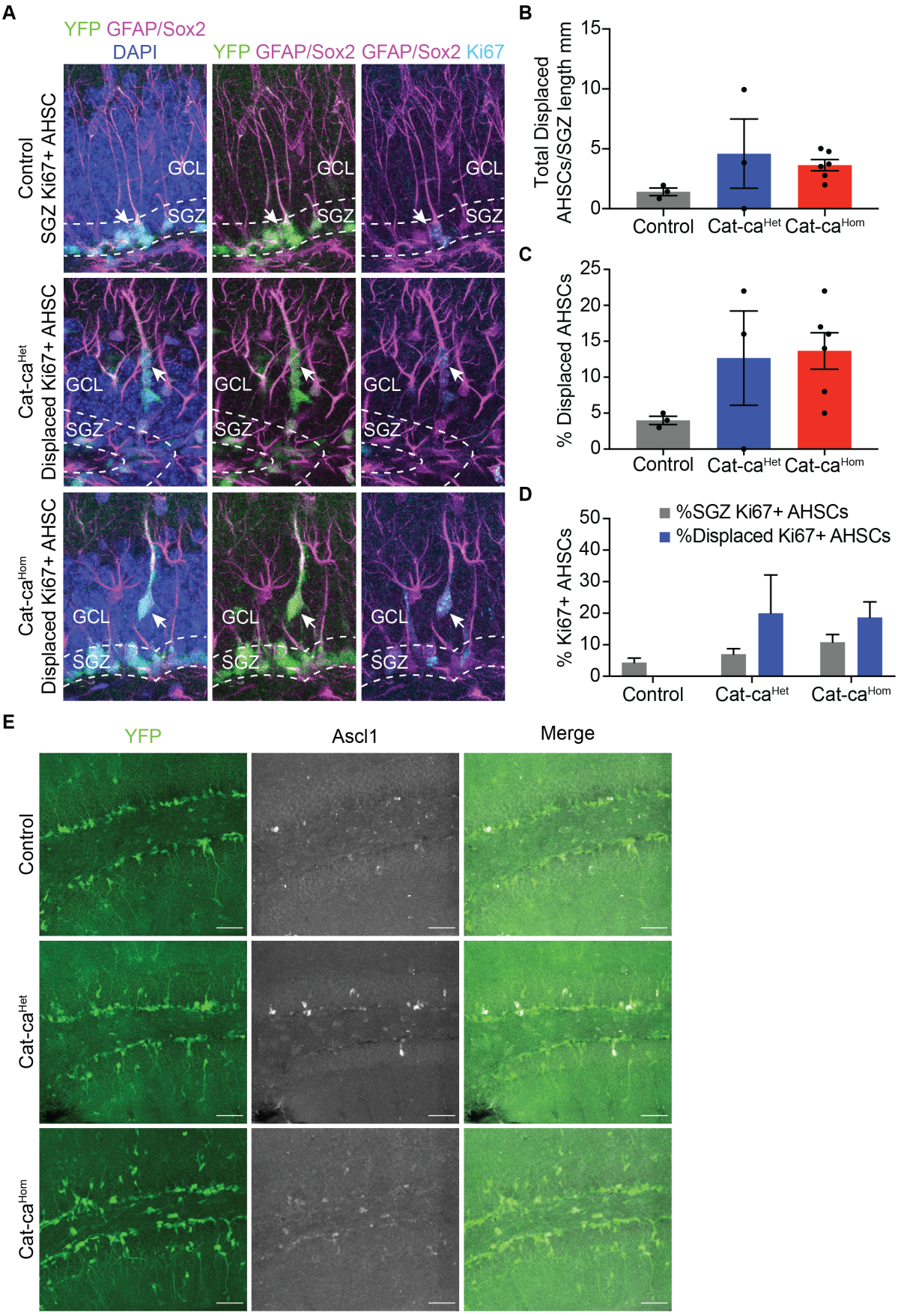


Figure 5.15: AHSCs are displaced from the SGZ 10 days after stabilisation of β-catenin which induces their activation.

(A) Immunolabelling of SGZ located and displaced proliferating AHSCs (YFP+ GFAP/Sox2+ Ki67+ AHSCs) in the DG of Control, Cat-ca^{Het} and Cat-ca^{Hom} mice 10 days after tamoxifen administration. Recombined AHSCs are identified as YFP+ GFAP+ Sox2+ with radial morphology. SGZ located AHSCs (Control) retain their correct location with their cell body located in the SGZ and a radial process through the GCL towards the ML. Displaced AHSCs are identified as YFP+ GFAP+ Sox2+ with radial morphology that are located more than 2 cell nuclei away from the SGZ. Ki67 is used to label proliferating cells. Scale bars represent 50μm.
(B) Quantification of the total number of displaced YFP+ GFAP+ Sox2+ AHSCs normalised to the length of the SGZ (mm) in Control, Cat-ca^{Het} and Cat-ca^{Hom} mice 10 days after β-catenin stabilisation. There is an increase in the number of displaced AHSCs in both Cat-ca^{Het} and Cat-ca^{Hom} mice compared to Control.
(C) Quantification of the proportion of displaced AHSCs in Control, Cat-ca^{Het} and Cat-ca^{Hom} mice 10 days after tamoxifen administration.
(D) Quantification of the proportion of SGZ located and displaced Ki67+ AHSCs. Proliferation is enriched in displaced AHSCs.
(E) Immunolabelling of YFP (GFP antibody) and Ascl1 in the dentate gyrus of Control, Cat-ca^{Het} and Cat-ca^{Hom} mice 10 days after β-catenin stabilisation. Ascl1+ cells are present in the GCL of Cat-ca^{Het} and Cat-ca^{Hom} mice, whereas in Control they are retained in the SGZ.
In all instances n=3 for Control, n=3 for Cat-ca^{Het} and n=6 for Cat-ca^{Hom}. One-way ANOVA with Tukey's multiple comparisons test was used for statistical analysis, (ns, $p>0.05$). Error bars represent mean with SEM.

5.3.4 Adult Neurogenesis is Disrupted by the Displacement of AHSCs Induced by β-catenin Stabilisation

I showed above that stabilising β-catenin in AHSCs promotes their displacement from their SGZ location within the DG neurogenic niche. I next wanted to investigate how this displacement of AHSCs affects the process of adult hippocampal neurogenesis. To do this, I used immunofluorescence techniques to label the progeny of recombined AHSCs, 10 days after the stabilisation of β-catenin. The total number of YFP+ Tbr2+ IPCs, normalised to the SGZ length, is slightly, but not significantly, increased in the DG of Cat-ca^{Het} mice 10 days after β-catenin stabilisation (Figure 5.16B). The total number of YFP+ Tbr2+ IPCs is unchanged between Control and Cat-ca^{Hom} mice (Figure 5.16B). This indicates that stabilising β-catenin in AHSCs does not affect their differentiation into Tbr2+ progenitors. However, from the confocal images

of the Tbr2 immunofluorescence, the YFP+ Tbr2+ IPCs in Cat-ca^{Het} and Cat-ca^{Hom} mice are displaced into the GCL, ML and hilus of the DG away from their correct location near the SGZ as in Control (Figure 5.16A). I quantified the proportion of Tbr2+ cells located within the GCL, ML, and hilus in Control, Cat-ca^{Het} and Cat-ca^{Hom} mice 10 days after β-catenin stabilisation in AHSCs. Approximately 5% of YFP+ Tbr2+ IPCs were located within the GCL in the DG of Control mice, which was increased to 15% in Cat-ca^{Het} and Cat-ca^{Hom} mice (Figure 5.16C). In addition, I found a small proportion of YFP+ Tbr2+ IPCs located in the hilus and ML of Cat-ca^{Het} and Cat-ca^{Hom} mice, which was not observed in Control (Figure 5.16B). This suggests that the correct localisation of Tbr2+ progenitors is dependent on the correct localisation of AHSCs within the DG niche.

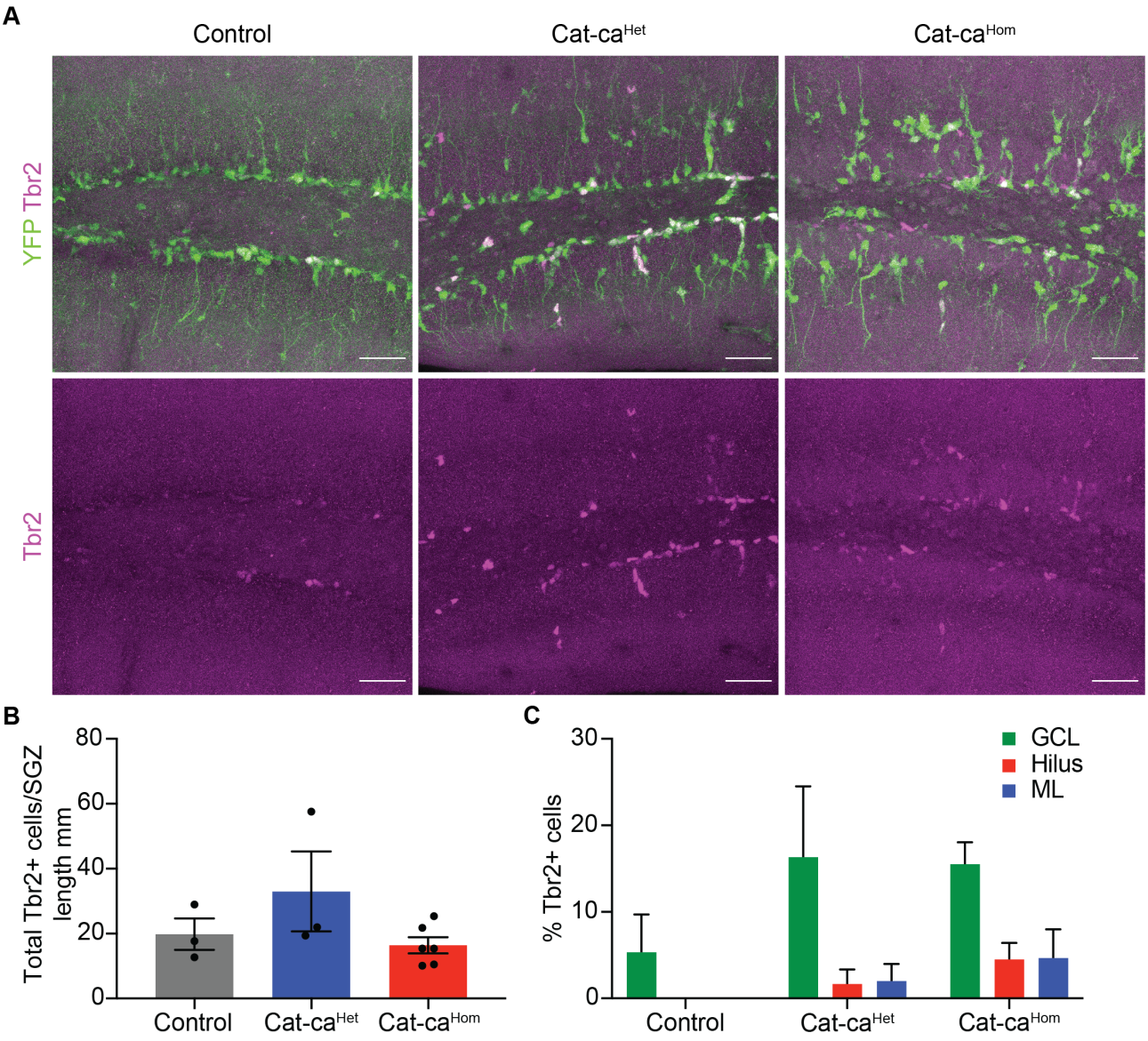


Figure 5.16: Tbr2+ progenitors are displaced in the DG of Cat-ca^{Het} and Cat-ca^{Hom} mice compared to Control.

(A) Immunolabelling of YFP (recombined cells) and Tbr2 (IPCs) in the DG of Control, Cat-ca^{Het} and Cat-ca^{Hom} mice 10 days after tamoxifen administration. YFP+ Tbr2+ IPCs are displaced within the DG of Cat-ca^{Het} and Cat-ca^{Hom} mice compared to Control. Scale bars represent 50μm. **(B)** Quantification of the data shown in **(A)**. The total number of YFP+ Tbr2+ IPCs is shown normalised to the length of the SGZ (mm) in Control, Cat-ca^{Het} and Cat-ca^{Hom} mice 10 days after β-catenin stabilisation. There are no significant differences between Control, Cat-ca^{Het} and Cat-ca^{Hom} mice.

(C) Quantification of the proportion of displaced YFP+ Tbr2+ IPCs shown according to their displaced locations. More YFP+ Tbr2+ IPCs are displaced into the GCL, hilus and ML in Cat-

ca^{Het} and Cat-ca^{Hom} mice compared to Control, indicating that β-catenin stabilisation in AHSCs, affects downstream adult neurogenesis.
GCL, granule cell layer. ML, molecular layer.
In all instances n=3 for Control, n=3 for Cat-ca^{Het}, and n=6 for Cat-ca^{Hom}. One-way ANOVA with Tukey's and Sidak's multiple comparisons tests were used for all statistical analysis, (ns, $p>0.05$). Error bars represent mean with SEM.

To investigate how the later stages of adult hippocampal neurogenesis are affected by AHSCs' displacement, I used immunofluorescence techniques to label the DCX+ neuroblast population in DG sections from Control, Cat-ca^{Het} and Cat-ca^{Hom} mice (Figure 5.17A). The total number of YFP+ DCX+ neuroblasts is not significantly changed between Control, Cat-ca^{Het} and Cat-ca^{Hom} mice 10 days after β-catenin stabilisation in AHSCs, however it is slightly, but not significantly, reduced in Cat-ca^{Hom} mice (Figure 5.17B). This suggests that the neurogenic output of AHSCs is largely unaffected 10 days after the stabilisation of β-catenin in Cat-ca^{Het} and Cat-ca^{Hom} mice, however this may be too short after recombination to examine the consequences in neuroblasts. The morphologies and organisation of YFP+ DCX+ neuroblasts is slightly impaired in the DG of Cat-ca^{Het} mice and is more obviously impaired in Cat-ca^{Hom} mice compared to Control (Figure 5.17A). In Cat-ca^{Het} mice, the YFP+ DCX+ neuroblasts appear slightly more rounded and are displaced deeper into the GCL and hilus (Figure 5.17A). In Cat-ca^{Hom} mice, the YFP+ DCX+ neuroblasts present with stunted and aberrant processes and are displaced in the GCL, ML and hilus (Figure 5.17A). I next quantified the proportion of displaced YFP+ DCX+ neuroblasts according to their displaced location in Cat-ca^{Het} and Cat-ca^{Hom} mice compared to Control (Figure 5.17C). In Control, I found less than 5% of YFP+ DCX+ neuroblasts were located deep within the GCL (Figure 5.17C). This increased to approximately 8% in Cat-ca^{Het} and 13% in Cat-ca^{Hom} mice (Figure 5.17C), highlighting their increased displacement. In addition, I found that approximately 3-6% of YFP+ DCX+ neuroblasts were displaced in the hilus and ML in Cat-ca^{Het} and Cat-ca^{Hom} mice (Figure 5.17C). This contrasts with Control where no YFP+ DCX+ neuroblasts were found in these regions (Figure 5.17C). Overall, this shows that the displacement of AHSCs, induced by the stabilisation of β-catenin, impacts the correct niche locations of their progeny and impairs the maturation of newborn neurons.

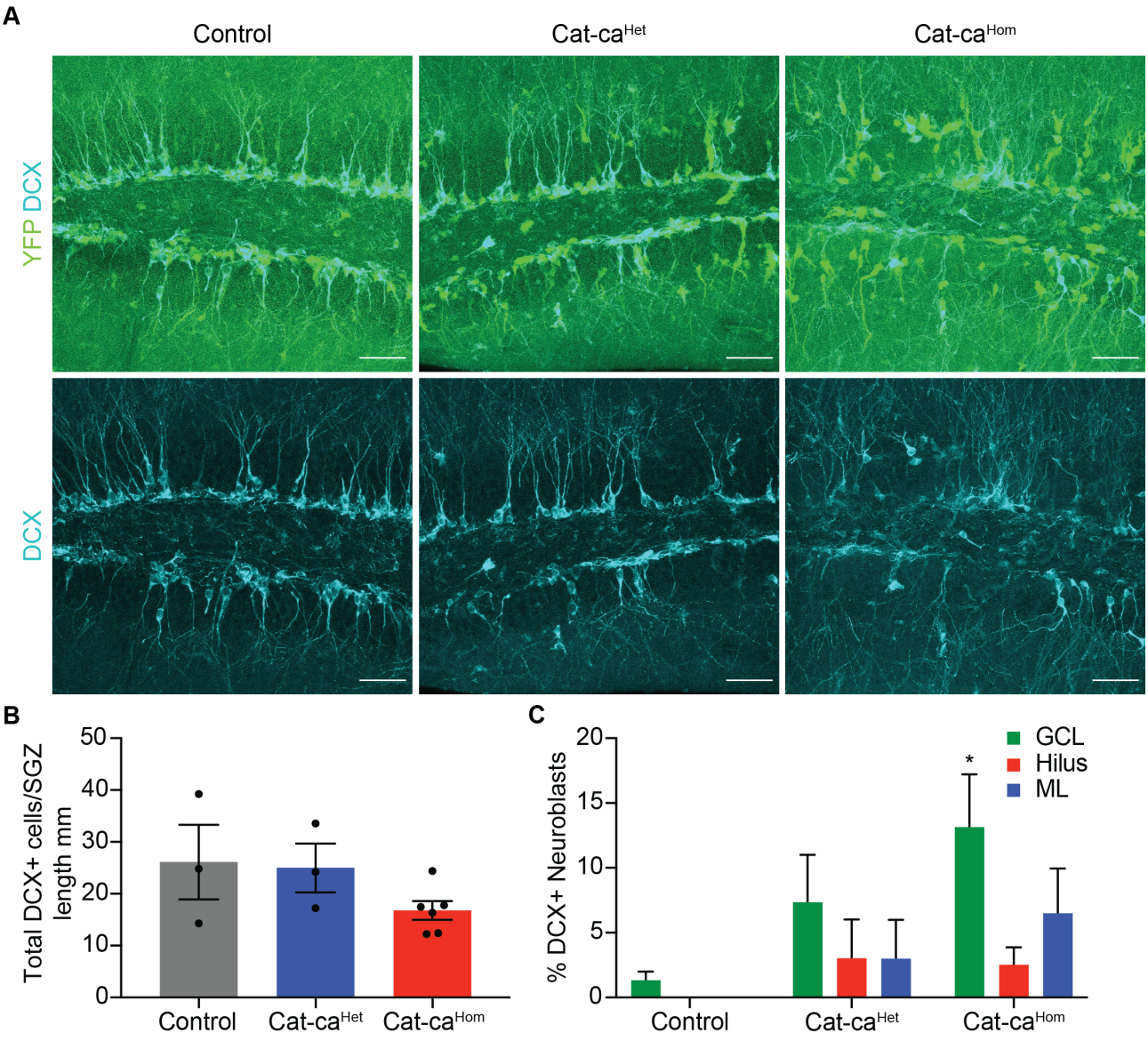


Figure 5.17: DCX+ neuroblasts are disrupted in the DG of Cat-ca^{Het} and Cat-ca^{Hom} mice compared to Control.

(A) Immunolabelling of YFP (recombined cells), DCX (neuroblasts) in the DG of Control, Cat-ca^{Het} and Cat-ca^{Hom} mice 10 days after tamoxifen administration. The morphologies of DCX+ neuroblasts is impaired and their locations are displaced within the DG of Cat-ca^{Het} and Cat-ca^{Hom} mice compared to Control. Scale bars represent 50μm.

(B) Quantification of the data shown in **(A)**. The total number of YFP+ DCX+ neuroblasts is shown normalised to the length of the SGZ (mm) in Control, Cat-ca^{Het} and Cat-ca^{Hom} mice 10 days after β-catenin stabilisation.

(C) Quantification of the proportion of displaced YFP+ DCX+ neuroblasts shown according to their displaced locations. More YFP+ DCX+ neuroblasts are displaced into the GCL, hilus and

ML in Cat-ca^{Het} and Cat-ca^{Hom} mice compared to Control. The %YFP+ DCX+ neuroblasts displaced into the GCL in Cat-ca^{Hom} mice is statistically significant compared to Control.
GCL, granule cell layer. ML, molecular layer.
In all instances n=3 for Control, n=3 for Cat-ca^{Het} and n=6 for Cat-ca^{Hom}. One-way ANOVA with Tukey's and Sidak's multiple comparisons tests were used for all statistical analysis, (ns, $p>0.05$. *, $p<0.05$). Error bars represent mean with SEM.

Chapter 6. Discussion

The work presented in this thesis explores the role of canonical Wnt signalling in regulating AHSC behaviour using both *in vivo* and *in vitro* techniques. I have shown that AHSCs express the necessary machinery to respond to canonical Wnt signalling and that they respond in a heterogeneous manner independent of their activation state under physiological conditions. I also found that active and quiescent AHSPCs display different sensitivities to stimulated canonical Wnt signalling levels despite their similar responses under physiological conditions. In addition, I have shown that AHSCs produce their own Wnt ligands highlighting the possibility of autocrine/paracrine Wnt signalling. Despite this, inhibiting canonical Wnt signalling does not affect AHSPC activation and maintenance under physiological conditions, which is surprising given the current literature indicating a role for canonical Wnt signalling in regulating AHSC behaviour (Qu et al., 2013; Wexler et al., 2009; Jang et al., 2013). However, I found that inhibiting canonical Wnt signalling in AHSCs impairs their correct differentiation along the neurogenic lineage, highlighting the context dependency of canonical Wnt signalling during adult hippocampal neurogenesis. Over-stimulating canonical Wnt signalling in active and quiescent AHSPC cultures initiates neuronal differentiation, however a lower stimulation of canonical Wnt signalling in quiescent AHSPCs promotes their activation. This indicates a dose-dependent role for stimulating canonical Wnt signalling in quiescent AHSPCs, which could reconcile some of the contradictions in the current literature as to the role of canonical Wnt signalling in AHSCs. Finally, I found that stabilising β-catenin in AHSCs *in vivo* promotes their displacement from their correct niche location and impairs correct adult hippocampal neurogenesis. This displacement could be due to the role of β-catenin in cell-cell adhesion rather than canonical Wnt signalling and highlights the importance of maintaining niche organisation and integrity to ensure correct adult hippocampal neurogenesis. A summary of all results evaluating the effects of modulating canonical Wnt signalling levels on various aspects of AHSC behaviour and adult hippocampal neurogenesis is presented in Table 3.

In this chapter, I will discuss the implications of my findings into the role of canonical Wnt signalling in AHSCs framed within the context of the adult neurogenesis field. I will comment on strategies to improve this body of work and propose further experiments to address the questions raised by the data I have presented.

Experiment	AHSC Maintenance	AHSC Activation	Proliferation	Neurogenesis	Niche
LOF in active AHSPCs	No Effect	N/A	No Effect	No Effect	N/A
LOF in quiescent AHSPCs	No Effect	No Effect	No Effect	N/A	N/A
LOF in AHSCs	No Effect	No Effect	No Effect	N.C.	No Effect
GOF in active AHSPCs	-	N/A	-	+	N/A
GOF in quiescent AHSPCs	-	+	+	+	N/A
GOF in AHSCs	-	N.C.	N.C.	N.C.	-

Table 3: Summary Evaluation of Results

LOF, Loss of Function. GOF, Gain of Function. Blue indicates experiments performed *in vitro*. Orange indicates experiments performed *in vivo*. "-" indicates a negative effect. "+" indicates a positive effect. "N.C." indicates a possible effect that was Not Confirmed with these experiments. "N/A" indicates Not Applicable.

Wnt LOF in active AHSPCs *in vitro* has no effect on AHSC maintenance or proliferation. It also has no effect on neurogenesis but may bias differentiation towards a glial fate.

Wnt LOF in quiescent AHSPCs *in vitro* has no effect on AHSC maintenance, activation or proliferation.

Wnt LOF in AHSCs *in vivo* has no effect on AHSC maintenance, activation, proliferation or niche organisation but may impair neurogenesis.

Wnt GOF in active AHSPCs *in vitro* impairs AHSC maintenance and decreases AHSC proliferation as neurogenesis is promoted.

Wnt GOF in quiescent AHSPCs *in vitro* promotes their activation and proliferation from quiescence. At higher stimulation levels, Wnt GOF decreases AHSC maintenance and initiates neurogenesis.

Wnt GOF in AHSCs *in vivo* severely disrupts the niche organisation by displacing AHSCs from their correct niche location resulting in their loss from the neurogenic niche, which impairs AHSC maintenance. This displacement could increase AHSC activation and proliferation as they lose contact with SGZ located quiescent signals. It could also negatively influence neurogenesis.

6.1 AHSCs Respond Heterogeneously to Canonical Wnt Signalling Independent of their Activation State

Using single cell RNA sequencing data from Nestin-GFP+ FAC Sorted dentate gyri, I established that AHSCs *in vivo* express components of the canonical Wnt signalling pathway (Figures 3.1, 3.2 and 3.3). Whilst they don't express all 19 Wnt ligands, all 10 Fzd cell surface receptors, R-spondins, all LGR family members or all Wnt inhibitors, they do express the necessary Wnt pathway transducer molecules to enable their response to canonical Wnt signalling. Similarly, bulk RNA sequencing data generated from active and quiescent AHSPC cultures, showed that the AHSPCs *in vitro* also express components of the canonical Wnt signalling pathway (Figure 3.5). For example, AHSCs *in vivo* and AHSPCs *in vitro* express an array of *Fzd* Wnt receptors and downstream pathway components such as *β-catenin* and *GSK3β* (Figures 3.1, 3.2 and 3.5). However, AHSPCs *in vitro* do not seem to express Wnt inhibitors, such as *Dkk3* and *sFRP1* (data not shown) as AHSCs do *in vivo*, indicating that there are differences between the *in vivo* and *in vitro* systems. Nevertheless, the *in vitro* bulk RNA sequencing dataset largely recapitulates the *in vivo* observations and further validates using this *in vitro* model as a tool for examining the role of canonical Wnt signalling in AHSCs. *Fzd* Wnt receptors are differentially expressed between active and quiescent AHSPCs *in vitro* indicating different demands for Wnt signalling between AHSPC activation states (Figure 3.5A). Using these RNA sequencing datasets, I also showed that AHSCs and AHSPCs express Wnt ligands at the mRNA level *in vivo* and *in vitro* and that this is translated into protein in quiescent AHSPC cultures (Figure 3.3, 3.5C and 3.5D). This highlights the possibility of autocrine/paracrine Wnt signalling in AHSPCs cultures and their ability to self-regulate their own behaviour.

To confirm that AHSCs *in vivo* respond to canonical Wnt signalling, I used the BATGAL Wnt reporter mice. Co-immunolabelling for the β-galactosidase Wnt reporter and AHSC markers showed that 30% of AHSCs in young 2-month-old BATGAL mice were BATGAL+ and responding to canonical Wnt signalling (Figure 3.6C). The proportion of canonical Wnt responding AHSCs decreases in older 7-month-old BATGAL mice, which could be due changes in the niche microenvironment that occur with age (Figure 3.6C). For example, levels of the Wnt inhibitor Dkk1 have been shown to increase in the DG niche with age (Seib et al., 2013), which could explain the global decrease in Wnt responding cells in the DG of 7-month-old mice (Figure 3.6B). Likewise, the β-galactosidase signal intensity in BATGAL+ AHSCs varies substantially, indicating a heterogeneous response to canonical Wnt signalling, which could be due to fluctuations in the levels of Wnt inhibitors or Wnt ligands across different niche locations (Figure

3.6D). Indeed, sFRP3 is expressed in a gradient across the septo-temporal axis of the DG (Sun et al., 2015b) suggesting changing Wnt signalling levels. However, I did not observe a gradient response to canonical Wnt signalling in AHSCs across the septo-temporal axis, which could be because this axis is difficult to define in coronal sections (Sun et al., 2015b) or could be due to the expression of other Wnt ligands and Wnt inhibitors across this axis. I observed that AHSCs respond heterogeneously to canonical Wnt signalling throughout the entire DG irrespective of their location (Figure 3.6A). This highlights the context dependency of canonical Wnt signalling in AHSCs and could reflect a level of heterogeneity within the AHSC pool in their ability to respond to canonical Wnt signalling. It is possible that this observed heterogeneous response is due to oscillating Wnt signalling levels caused by the negative feedback loop (Lustig et al., 2002). Therefore, all AHSCs could respond uniformly to canonical Wnt signalling and the variability in reporter intensities could be due to the timing of their response upon analysis. To determine whether all AHSCs eventually respond to canonical Wnt signalling, or whether only a subset do, it could be interesting to perform long-term conditional labelling of Wnt responding AHSCs using an inducible fluorescent Wnt reporter line such as Axin2-CreERT2; RYFP (Bowman et al., 2013). Long-term tamoxifen administration would allow for more cells to be labelled and allow us to determine whether all AHSCs or only a subset responded to Wnt during the tamoxifen period. The cells across the neurogenic lineage differentially respond to canonical Wnt signalling further highlighting the context dependency of this signalling pathway. AHSCs and granule neurons respond variably to canonical Wnt signalling whereas intermediate progenitor cells (IPCs), neuroblasts and astrocytes are less responsive (Figure 3.7). This indicates a role for canonical Wnt signalling in regulating both early and late stages of adult hippocampal neurogenesis.

To investigate whether AHSPCs *in vitro* respond to canonical Wnt signalling, I nucleofected active and quiescent AHSPCs with the 7TGC canonical Wnt reporter plasmid and found that AHSPCs in both states respond heterogeneously to canonical Wnt signalling (Figure 3.10). As no Wnt agonists were added to these cultures, this supports the presence of autocrine/paracrine canonical Wnt signalling, which was hypothesised based on the RNA sequencing data showing the expression of Wnt ligands and receptors in cultured AHSPCs (Figure 3.5A, 3.5C and 3.5D). The average Wnt reporter activity and *Axin2* expression levels are similar between active and quiescent culture conditions, suggesting that active and quiescent AHSPCs respond similarly to canonical Wnt signalling despite differential expression of cell surface receptors (Figure 3.5A and 3.5B). As Wnt reporter activity and *Axin2* expression was found in both active and quiescent AHSPCs, this suggests that their response to canonical Wnt signalling is independent of their

activation state (Figure 3.5B, 3.10F and 3.10G). This was also observed *in vivo* where AHSC proliferation did not correlate with a response to canonical Wnt signalling (Figure 3.8). Overall, the *in vitro* data recapitulates the *in vivo* observations and validates the *in vitro* model for further investigations.

6.2 Limitations of Canonical Wnt Reporters

Many Wnt reporter models exploit multimerised TCF/LEF response elements to drive reporter gene expression and provide a read-out of canonical Wnt signalling levels in cells (Maretto et al., 2003; DasGupta et al., 1999; Ferrer-Vaquer et al., 2010). However, the current literature cautions against using these models as the sole evidence for identifying novel sites of canonical Wnt signalling (Al Alam et al., 2011; Barolo. 2006). Comparisons between different Wnt reporter models highlights discrepancies in their reporter patterns, which could be due to different integration sites or the use of different minimal promoters (Barolo. 2006). In addition, multimerised TCF/LEF Wnt reporters could falsely represent certain modes of canonical Wnt signalling. For example, β-catenin has been shown to activate gene transcription independent of TCF (Filali et al., 2002), which could lead to some Wnt responding cells being missed by multimerised TCF/LEF Wnt reporters. Also, TCF/LEF can activate gene transcription of Wnt target genes in the absence of a Wnt signal (Hsu et al., 1998; Labbé et al., 2000), which would generate false positives in multimerised TCF/LEF Wnt reporters. Therefore, it is important to validate results obtained using multimerised TCF/LEF Wnt reporter models, with reporters designed to provide a read out of expression levels of known canonical Wnt target genes, such as *Axin2* (Al Alam et al., 2011). Using the single cell RNA sequencing dataset, I found that *Axin2* is expressed in relatively few AHSCs *in vivo* (Figure 3.2G), which is likely due to the limitations of single cell RNA sequencing in detecting lowly expressed genes (Haque et al., 2017). Nevertheless, the presence of some detectable levels of *Axin2* transcripts in AHSCs confirms their potential to respond to canonical Wnt signalling.

Given the limitations of multimerised TCF/LEF Wnt reporter models, it would be beneficial to further validate these results using another Wnt reporter mouse line that reports on the expression levels of a native Wnt target gene. To do this, I started using the Axin2-mTurQ mouse model, however the mTurQ reporter activity was difficult to detect due to the high level of background observed with GFP immunolabelling (Figure 3.9B). More work is needed, either to optimise the immunostaining in the Axin2-mTurQ Wnt reporter mouse line, or to use another

Axin2 Wnt reporter model to fully validate these results. However, in spite of these described difficulties, I did observe some Axin2-mTurQ+ AHSCs (Figure 3.9B), which supports the BATGAL data that some AHSCs respond to canonical Wnt signalling *in vivo*.

6.3 Baseline Canonical Wnt Signalling Persists in AHSCs Despite Various Attempts to Inhibit Canonical Wnt Signalling

To understand the role of endogenous canonical Wnt signalling in AHSCs, I designed experiments to inhibit AHSCs' response to canonical Wnt signalling both *in vitro* and *in vivo* (Chapter 4). To inhibit canonical Wnt signalling in AHSPCs cultures, I used a variety of different small molecule Wnt antagonists that targeted different points along the pathway (Figure 4.1A). This was to ensure that any observed phenotypes were due to inhibiting canonical Wnt signalling and not off target effects. However, I failed to observe a decrease in the expression level of the Wnt target gene *Axin2*, across all experimental conditions used (Figure 4.1). This suggests that treatments with these small molecule Wnt antagonists was insufficient to inhibit baseline canonical Wnt signalling in active AHSPC cultures. It also raises the possibility that *Axin2* is not a reliable read out of decreased canonical Wnt signalling levels in this system. For these experiments, I treated active AHSPCs with one Wnt antagonist at a time. It is possible that using a combination of Wnt antagonists may inhibit baseline canonical Wnt signalling levels, however this approach could also prove to be toxic to AHSPCs (reviewed by (Tran et al., 2017)).

As small molecule Wnt inhibitors were ineffective, I used an AHSPC line derived from a mouse model designed to inhibit canonical Wnt signalling by conditionally deleting β-catenin in the AHSCs *in vivo*. β-catenin is the key mediator of the canonical Wnt signalling pathway, therefore deleting β-catenin in AHSPC cultures should inhibit their response to canonical Wnt signalling (Papkoff et al., 1996; Peifer et al., 1994b). I showed that β-catenin is robustly deleted in β-cat$^{del\ ex3\text{-}6}$ AHSPCs, following Cre adenovirus mediated recombination (Figure 4.2), and in β-cat$^{del\ ex2\text{-}6}$ mice following tamoxifen administration (Figure 4.13D and 4.14B). However, deletion of β-catenin did not downregulate *Axin2* expression levels (Figure 4.2G and 4.13E). This suggests that baseline levels of canonical Wnt signalling in AHSCs are not affected by the deletion of the key canonical Wnt signalling mediator, β-catenin, or that *Axin2* is not a reliable read-out of decreased Wnt signalling levels in these cells. However, β-cat$^{del\ ex3\text{-}6}$ AHSPCs are unable to respond to a canonical Wnt agonist (Figure 4.2H), indicating that their response to a canonical Wnt stimulus is impaired by the loss of β-catenin.

It has been reported that the difficulty in detecting autocrine/paracrine Wnt signalling in AHSPC cultures, is due to low levels of canonical Wnt signalling (Wexler et al., 2009). Therefore, the failure to detect the downregulation *Axin2*, could be because the levels of endogenous canonical Wnt signalling are overall quite low across these culture conditions. The results with the 7TGC Wnt reporter plasmid showed that AHSPCs responded variably to endogenous canonical Wnt signalling levels, with only a few cells responding highly (Figure 3.10G). Therefore, it is possible that the vast majority of AHSPCs in these culture conditions are lowly responsive to canonical Wnt signalling, making it difficult to detect gene expression changes induced by further inhibition of canonical Wnt signalling.

The lack of *Axin2* downregulation following deletion of β-catenin and application of Wnt inhibitors, could also suggest that *Axin2* is not a reliable read out of decreased canonical Wnt signalling levels in these cells. *Axin2* is a direct transcriptional target of canonical Wnt signalling and its expression is restricted to selective tissues in a canonical Wnt dependent manner (Behrens et al., 1998; Lustig et al., 2002; Jho et al., 2002). This contrasts with the expression its ortholog *Axin*, which is ubiquitously expressed throughout mouse development (Zeng et al., 1997; Yan et al., 2001a). The promoter region of *Axin2* contains a series of eight TCF/LEF binding sites indicating that its expression is directly regulated TCF/LEF transcription factors, which are downstream of canonical Wnt signalling (Jho et al., 2002). However, TCF/LEF transcription factors have been shown to activate transcription in the absence of a Wnt signal suggesting that the persistence of *Axin2* expression following inhibition of canonical Wnt signalling could be due to β-catenin or Wnt independent TCF/LEF signalling (Hsu et al., 1998; Labbé et al., 2000). Indeed, TGFβ signalling has been shown to regulate TCF/LEF target genes independently of canonical Wnt signalling (Labbé et al., 2000). This highlights the possibility that *Axin2* expression could be regulated by other signalling pathways in a canonical Wnt/β-catenin-independent manner, which may explain the persistence of *Axin2* expression upon inhibition of canonical Wnt signalling.

6.4 Different Efficiencies of Deleting β-catenin in AHSCs *in vitro* and *in vivo*

As previously stated, I confirmed that β-cat$^{fl/fl\ ex3-6}$ AHSPCs *in vitro* undergo successful recombination of the *β-cat$^{fl/fl\ ex3-6}$* allele resulting in the robust deletion of β-catenin protein (Figure

4.2). However, the same *β-cat*$^{fl/fl\ ex3-6}$ allele failed to recombine *in vivo* following tamoxifen administration in 2-month-old GlastCreERT2; β-cat$^{fl/fl\ ex3-6}$; RYFP mice (Figure 4.9, 4.10 and 4.11). This discrepancy between *in vitro* and *in vivo*, could be due to the different methods used to induce recombination of the *β-cat*$^{fl/fl\ ex3-6}$ allele. *In vitro* recombination is induced via the application of a Cre adenovirus to β-cat$^{fl/fl\ ex3-6}$ AHSPC cultures, whereas *in vivo* recombination is induced by the administration of tamoxifen, which facilitates the translocation of Cre recombinase to the nucleus of Glast+ cells. Tamoxifen inducible Cre could be less active than the non-inducible Cre adenovirus. Also, recombination of the *β-cat*$^{fl/fl\ ex3-6}$ allele *in vitro* may be more effective as the Cre adenovirus is applied to β-cat$^{fl/fl\ ex3-6}$ AHSPCs in excess indicating that successful recombination *in vitro* is due to higher levels of Cre. Using a higher concentration of tamoxifen also failed to induce recombination of the *β-cat*$^{fl/fl\ ex3-6}$ allele *in vivo* (data not shown). qPCR analysis of the floxed region of β-catenin in FAC Sorted YFP+ cells from *β-cat*$^{del\ ex3-6}$ mice showed that recombination between these LoxP sites *in vivo* is inefficient (Figure 4.11D). This inefficiency could be due to the local chromatin landscape and flanking sequences affecting the accessibility of these LoxP sites in Glast+ cells *in vivo*.

The second conditional β-catenin floxed mouse model, GlastCreERT2; β-cat$^{fl/fl\ ex2-6}$; RYFP mice, was more successful in deleting β-catenin in Glast+ cells *in vivo* (Figure 4.13). These mice contained the *β-cat*$^{fl/fl\ ex2-6}$ allele, where the LoxP sites flank exons 2-6 (Figure 4.13A). The previous mouse model, that failed to delete β-catenin, contained the *β-cat*$^{fl/fl\ ex3-6}$ allele, where the LoxP sites flank exons 3-6 (Figure 4.11B). It is possible that the LoxP site located before exon2 in β-cat$^{fl/fl\ ex2-6}$ mice, is more accessible than the one located before exon3 in β-cat$^{fl/fl\ ex3-6}$ mice. This increased accessibility could explain why β-catenin is deleted in β-cat$^{fl/fl\ ex2-6}$ mice and not β-cat$^{fl/fl\ ex3-6}$ mice.

6.5 AHSC Homeostasis is Unaffected by Inhibition of Canonical Wnt Signalling

Using β-cat$^{del\ ex2-6}$ mice and β-cat$^{del\ ex3-6}$ AHSPCs, I found that AHSCs are unaffected by the loss of β-catenin signalling *in vivo* and *in vitro* (Section 4.2 and Figure 4.15). This could be because other signals within the niche or the culture microenvironment could compensate for the lack of intact canonical Wnt signalling in AHSCs. For example, the AHSPCs *in vitro* are exposed to high concentrations of mitogens such as FGF2, and in some cases EGF, which could override the

need for canonical Wnt signalling to maintain active AHSPC proliferation or promote quiescent AHSPC activation (Sun et al., 2011; Palmer et al., 1995). Alternatively, the fact that AHSC behaviour is unaffected by loss of β-catenin *in vivo* and *in vitro* could suggest that intact canonical Wnt/β-catenin signalling is not required to maintain their homeostasis, which is surprising given the current literature. Indeed, inhibiting canonical Wnt signalling in adult rat hippocampal progenitors *in vitro* has been shown to impair proliferation and induce a loss of multipotent precursors (Wexler et al., 2009). Similarly, neural progenitors isolated from adult Wnt7a knock out mouse brains exhibited decreased proliferation and self-renewal capacity compared to wild type (Qu et al., 2013). In addition, Qu and colleagues show that Wnt7a knock out mice have a reduced hippocampal neural stem and progenitor cell population compared to wild type (Qu et al., 2013). However, this phenotype could be due to the loss of Wnt7a expression throughout development and therefore the reduced size of the adult hippocampal progenitor pool could be due to their impaired development rather than their dysregulation during adulthood (Qu et al., 2013). In addition, these papers do not clearly make the distinction between AHSCs with radial morphology and IPCs in the hippocampus, therefore it is difficult to establish which cell type is directly responsible for this impaired proliferation phenotype caused by decreased Wnt signalling levels. It is also possible that other niche cells are affected in these models due to the global decrease of Wnt signalling levels. Conditionally deleting β-catenin in Glast+ cells during adulthood restricts the inhibition of canonical Wnt signalling to AHSCs and astrocytes making it a cleaner approach to investigate the role of canonical Wnt signalling in the AHSC population.

6.6 Neurogenic Lineage Progression is Affected by Loss of β-catenin signalling *in vivo*

Even though deleting β-catenin did not have an effect in AHSCs *in vivo*, I found that it affected their progeny further along the neurogenic lineage (Figure 4.16). I found that the number of proliferating Sox2+ IPCs was increased in β-cat$^{del\ ex2\text{-}6}$ mice (Figure 4.15D) and that there are fewer Tbr2+ IPCs and DCX+ neuroblasts in the DG of β-cat$^{del\ ex2\text{-}6}$ mice (Figure 4.16). This suggests that the loss of β-catenin signalling increases the number of proliferating progenitors whilst also impairing the differentiation of newborn neurons *in vivo*. Canonical Wnt signalling has been shown to play a role in promoting neuronal lineage commitment and differentiation (Lie et al., 2005; Jang et al., 2013; Seib et al., 2013). By deleting β-catenin in AHSCs, their progeny will also lack β-catenin and will therefore be unable to respond to a canonical Wnt stimulus. This

could mean that the progeny of β-cat$^{del\ ex2-6}$ AHSCs are unable to differentiate correctly, in response to a canonical Wnt stimulus, resulting in the impaired neuronal differentiation observed in β-cat$^{del\ ex2-6}$ mice (Figure 4.16). The increased number of proliferating Sox2+ IPCs in of β-cat$^{del\ ex2-6}$ mice (Figure 4.15D), could result from their inability to differentiate along the neurogenic lineage in response to a canonical Wnt stimulus promoting neuronal differentiation. A possible mechanism driving this phenotype could be the dual regulation of the pro-neuronal transcription factor *NeuroD1* by Sox2 and canonical Wnt signalling (Kuwabara et al., 2009). Sox2 represses the expression of *NeuroD1* in progenitors, whereas canonical Wnt signalling induces *NeuroD1* expression to promote neuronal differentiation (Kuwabara et al., 2009). By deleting β-catenin, cells are unable to respond to canonical Wnt signalling, therefore the Sox2 mediated repression of *NeuroD1* is maintained resulting in more Sox2+ progenitors and impaired neuronal differentiation. Conversely, β-cat$^{del\ ex3-6}$ AHSPC cultures were still able to differentiate into both neurons and glia when growth factors were withdrawn and media supplemented with B27 or FBS to promote neuronal or astrocytic differentiation respectively (Figure 4.8). This difference in the ability of AHSCs to differentiate upon loss of canonical Wnt/β-catenin signalling could reflect the differences between *in vitro* and *in vivo* experimental conditions, as *in vitro* treatments could stimulate cells more compared to the local signals they are exposed to *in vivo*. This highlights the importance of verifying results from *in vitro* model systems in an *in vivo* context.

6.7 Levels of Stimulating Canonical Wnt Signalling Are Important for Determining a Proliferative vs Neuronal Differentiation Response in Quiescent AHSPCs

6.7.1 Active and Quiescent AHSPCs Display Different Sensitivities to Levels of Canonical Wnt Stimulation

Stimulating Canonical Wnt signalling in active AHSPCs, using 5μM CHIR9921, initiated neuronal differentiation (Figure 5.1). Neuronal differentiation was also promoted by stimulating canonical Wnt signalling in quiescent AHSPCs, however a higher concentration of CHIR99021 (10μM) was required to achieve this (Figure 5.2). 10μM CHIR99021 treatment in active AHSPCs caused robust cell death, which could be caused by active AHSPCs displaying a higher sensitivity to global inhibition of GSK3β. To determine whether this cell death was caused by stimulation of the canonical Wnt pathway, I could treat active β-cat$^{del\ ex3-6}$ AHSPCs with 10μM

CHIR99021 to investigate whether these cells undergo cell death in the absence of intact canonical Wnt signalling. The cell death observed in active AHSPCs treated with 10μM CHIR99021 could also suggest that they are more sensitive to levels of canonical Wnt stimulation than quiescent AHSPCs. This difference in sensitivity to canonical Wnt signalling levels could be mediated at the level of the Frizzled receptors, as bulk RNA sequencing data shows that *Frizzled* receptors are differentially expressed in active and quiescent AHSPCs (Figure 3.5A). This could suggest that active and quiescent AHSPCs have different requirements for the levels of canonical Wnt signalling.

6.7.2 Potential Mechanisms Responsible for Inducing the Dose-Dependent Effects of Canonical Wnt Signalling in Quiescent AHSPCs

A low level of canonical Wnt stimulation in quiescent AHSPCs promotes proliferation (Figure 5.3). This suggests that stimulating canonical Wnt signalling is able to override BMP4 induced quiescence (Blomfield et al., 2019) to promote quiescent AHSPC activation. Crosstalk between these two pathways has been shown to regulate various biological processes in a context dependent manner (reviewed by (Itasaki et al., 2010). For example, in the developing neural tube Wnt and BMP signalling have been shown to work antagonistically to balance proliferation and neuronal differentiation along the dorsal-ventral axis (Ille et al., 2007). However, in embryonic stem cells Wnt and BMP signalling work synergistically to maintain pluripotency and prevent neuronal differentiation (Ying et al., 2003; Sato et al., 2004). Caution must be applied when looking to other biological systems to delineate the crosstalk between Wnt and BMP signalling in the context of quiescent AHSPC activation. However, it would be interesting in future work to investigate how AHSPCs co-ordinate these two signalling pathways to regulate their behaviour. This could initially be achieved by examining the expression of BMP4 target genes, such as *Id1-4*, in quiescent AHSPCs treated with a Wnt agonist to explore whether canonical Wnt signalling directly antagonises BMP4 signalling in this context.

Work from the Guillemot lab has shown that BMP4 treatment in AHSPC cultures induces quiescence, in part through the upregulation of Id4 (Blomfield et al., 2019). Id4 sequesters the Ascl1 heterodimerisation partner E47, which promotes Ascl1 degradation and induces a quiescent state (Blomfield et al., 2019). Ascl1 was shown to be essential for the activation of quiescent AHSCs *in vivo* (Andersen et al., 2014). However, rWnt3a treatment induced the activation of quiescent AHSPCs alongside a slight decrease in *Ascl1* expression (Figure 5.10H). This could suggest that canonical Wnt signalling promotes quiescent AHSPC activation

independently of Ascl1. CyclinD1 is an important regulator of G1 to S phase progression of the cell cycle and is a direct transcriptional target of both Ascl1 and canonical Wnt signalling (Andersen et al., 2014; Shtutman et al., 1999). Therefore, it is possible that stimulated canonical Wnt signalling promotes quiescent AHSPC activation by directly inducing the expression of *CyclinD1*, and bypassing the need for Ascl1. This could suggest that quiescent AHSPC activation is independently regulated by both canonical Wnt signalling and Ascl1, perhaps in response to different extrinsic factors. It will be interesting in future studies to decipher the molecular mechanisms driving this canonical Wnt induced activation of quiescent AHSPCs, perhaps in the context of an Ascl1 knock out to determine the presence of independent regulatory mechanisms. This could initially be done by first characterising whether quiescent Ascl1-knock-out AHPSCs activate in response to stimulating canonical Wnt signalling. It would then be possible to examine the gene expression changes that occur to determine whether canonical Wnt signalling promotes quiescent AHSPC activation independently of Ascl1.

The homeodomain-only protein HopX is highly expressed in quiescent AHSPCs and is downregulated upon their activation, therefore it is considered to be a quiescent AHSPC marker (Li et al., 2015; Shin et al., 2015). However, I found that Wnt stimulation in quiescent AHSPCs promotes the upregulation of *HopX* alongside an activation phenotype (Figures 5.4D and 5.10E). The close correlation between canonical Wnt stimulation and *HopX* upregulation could indicate that *HopX* is a direct transcriptional target of canonical Wnt signalling, however I did not find any TCF/LEF binding sites within the *HopX* sequence (not shown). This does not exclude the possibility that *HopX* is regulated by secondary effects of stimulating canonical Wnt signalling. HopX is involved in the repression of gene transcription and has been shown to repress the expression of Wnt ligands in cardiomyoblasts during cardiogenesis in cooperation with BMP signalling (Jain et al., 2015). As such the upregulation of *HopX* expression in quiescent AHSPCs upon Wnt stimulation could be a negative feedback mechanism designed to repress canonical Wnt signalling levels. Therefore, it may not be appropriate to use *HopX* as a quiescence marker in this context and other quiescence associated genes, such as the tumour suppressor genes *p53* and *p57* (Meletis et al., 2006; Liu et al., 2009; Furutachi et al., 2013), should be examined in future investigations. It could be interesting to examine the gene expression levels of Wnt ligands in quiescent AHSPCs following Wnt agonist treatment to understand whether they are downregulated by increased *HopX* expression.

Over-stimulating canonical Wnt signalling in active and quiescent AHSPCs promotes neuronal differentiation even in the presence of FGF2 (Figures 5.1 and 5.2). Canonical Wnt signalling has

previously been shown to play a role in promoting neuronal differentiation and neuronal lineage specification in adult hippocampal progenitors but these experiments were performed under differentiating conditions *in vitro* following the transduction of growth factors (Lie et al., 2005). The results presented here suggest that canonical Wnt signalling can override the pro-proliferative effects of FGF2 signalling to directly induce neuronal differentiation of active and quiescent AHSPCs. Canonical Wnt signalling has previously been shown to instruct neurogenesis over astrogliogenesis (Lie et al., 2005; Seib et al., 2013), which is corroborated by the results presented here of over-stimulating canonical Wnt signalling in quiescent AHSPCs (Figure 5.6). However, I did not investigate astrocytic differentiation in active AHSPCs following Wnt stimulation, which should be explored further given the contradictory evidence in the literature showing that the loss of sFPR3 promotes both astrocytic and neurogenic differentiation (Jang et al., 2013).

Over-stimulating canonical Wnt signalling in quiescent AHSPCs directly promotes neuronal differentiation, whereas a lower canonical Wnt stimulation induces proliferation (Section 5.2). This suggests that the level of canonical Wnt stimulation is important in determining the activation or neuronal differentiation of quiescent AHSPCs. Wnt induced quiescent AHSPC proliferation and activation occurs alongside a loss of stemness and progression towards a progenitor fate. Key characteristics of AHSCs include their ability to return to quiescence and their ability to self-renew. Therefore, it would be interesting to investigate whether canonical Wnt activated quiescent AHSPCs retain the ability to return to quiescence and whether they divide through self-renewing or consuming divisions. It would also be interesting to determine how AHSPCs measure different canonical Wnt signalling levels and how this is transduced to promote these different canonical Wnt induced responses in quiescent AHSPCs. One possible mechanism mediating these dose-dependent effects could be via the dual regulation of *NeuroD1* by both Sox2 and canonical Wnt signalling (Kuwabara et al., 2009). A higher level of canonical Wnt stimulation could override the Sox2 dependent repression of *NeuroD1* (Kuwabara et al., 2009) to directly induce neuronal differentiation, whereas a lower level of Wnt stimulation may not be sufficient. This could be examined by qPCR analysis of *NeuroD1* expression levels in quiescent AHSPCs treated with different concentrations of Wnt agonist (Figure 5.2A). Canonical Wnt signalling has been shown to have dose-dependent effects during nervous system development (Machon et al., 2007) and in other adult somatic stem cells (Hirata et al., 2013; Luis et al., 2011). For example, over-activating canonical Wnt signalling in intestinal stem cells promotes their differentiation but a lower dose of canonical Wnt stimulation promotes their proliferation in cooperation with Notch signalling (Hirata et al., 2013). Notch signalling is active

in quiescent AHSPCs and has been shown to be important in maintaining their quiescent state (Lavado et al., 2014; Ables et al., 2010; Lugert et al., 2010; Breunig et al., 2007; Ehm et al., 2010; Imayoshi et al., 2010). The interplay between canonical Wnt and Notch signalling in quiescent AHSPCs could play a role in regulating the dose-dependent effects of stimulating canonical Wnt signalling in quiescent AHSPCs. These two signalling pathways have been shown to cooperatively regulate many developmental processes (Muñoz Descalzo et al., 2012) and it would be interesting in future studies to investigate how these pathways interact to regulate AHSPC behaviour. To further investigate the mechanisms behind these dose-dependent effects of stimulating canonical Wnt signalling, it could be interesting to perform RNA sequencing, ChIP-Seq and assay for transposase-accessible chromatin sequencing (ATAC-Seq) in quiescent AHSPCs stimulated with different concentrations of Wnt agonists. This would allow us to determine whether the dose-dependent effects of stimulating canonical Wnt signalling are driven by the same or independent molecular mechanisms. If they are driven by independent molecular mechanisms one could expect to see distinct transcriptional profiles determined by the level of canonical Wnt stimulation rather than a gradient response if the dose-dependent effects regulate the same molecular mechanisms. Overall, the dose-dependent effect of stimulating canonical Wnt signalling in quiescent AHSPCs, could explain how canonical Wnt signalling is able to induce both proliferation and neuronal differentiation of neural progenitors

6.8 Dose-Dependent Effects of Stimulating Canonical Wnt Signalling in AHSPCs Could Reconcile Current Contradictions in the Literature

In the current literature, stimulating canonical Wnt signalling in neural progenitors during adult hippocampal neurogenesis has been shown to promote proliferation and instruct a neuronal fate (Lie et al., 2005; Seib et al., 2013; Jang et al., 2013; Wexler et al., 2009; Qu et al., 2010; Shi et al., 2004). However, not much is known about how canonical Wnt signalling is able to induce both of these outcomes. The results presented here highlight that the levels of canonical Wnt stimulation are important in determining a proliferation or neuronal differentiation phenotype in quiescent AHSPCs. Different techniques have been used to stimulate canonical Wnt signalling *in vitro* and *in vivo* to investigate the role of canonical Wnt signalling in neural progenitors in the adult hippocampus (Lie et al., 2005; Seib et al., 2013; Jang et al., 2013). The differences in the methodologies used across these studies could stimulate canonical Wnt signalling levels to varying degrees. For example, Lie and colleagues stimulate canonical Wnt signalling in cultured

neural progenitors by overexpressing Wnt3a and observe increased neuronal differentiation (Lie et al., 2005). In contrast, Seib and colleagues saw increased self-renewal in neural progenitors derived from Nestin-Dkk1 knock-out mice (Seib et al., 2013). It can be argued that stimulating canonical Wnt signalling by overexpression a Wnt ligand could produce a higher level of Wnt stimulation compared to knocking out a Wnt inhibitor, however these two scenarios have not been directly compared in this context. As such, the contradictions in the current literature, as to the role of stimulating canonical Wnt signalling in hippocampal neural progenitors, are compatible with the dose-dependent effects of stimulating canonical Wnt signalling in quiescent AHSCs presented here.

6.9 Adult Hippocampal Neurogenesis is Impaired by AHSC Displacement Induced by Stabilised β-catenin

6.9.1 Displacement of AHSCs Promotes their Loss from the Hippocampal Neurogenic Niche

To investigate the effect of stimulating canonical Wnt signalling in AHSCs *in vivo*, I generated an inducible transgenic mouse line to stabilise β-catenin and activate canonical Wnt signalling in AHSCs (Section 5.3). I used mice that were heterozygous (Cat-ca^{Het}) and homozygous (Cat-ca^{Hom}) for the Cat-ca allele with the hope to investigate the *in vitro* observed dose-dependent effects of stimulating canonical Wnt signalling in AHSCs *in vivo*. I observed proliferation differences between Cat-ca^{Het} and Cat-ca^{Hom} mice (Figure 5.11E), however this could be due to the lack of WT β-catenin protein in Cat-ca^{Hom} mice rather than a dose-dependent effect of stimulating canonical Wnt signalling. To show that Cat-cat^{Het} and Cat-ca^{Hom} mice stimulate canonical Wnt signalling to different levels, I have crossed them to the BATGAL Wnt reporter mice. I will use these mice to compare the intensities of the β-galactosidase Wnt reporter immunostaining in YFP+ cells of Cat-ca^{Het} vs Cat-ca^{Hom} mice to provide a read out of stimulated canonical Wnt signalling levels. Another more quantitative way of measuring the level of Wnt stimulation in Cat-ca^{Het} and Cat-ca^{Hom} mice would be to FAC Sort the YFP+ cells from dissected dentate gyri of Cat-ca^{Het} and Cat-ca^{Hom} mice and perform qPCR analysis for the Wnt target gene *Axin2*.

I found that AHSCs are lost from the DG niche 30 days after inducing the stabilisation of β-catenin (Figure 5.11C). This loss of AHSCs could be a direct consequence of the displacement

of AHSCs observed 10 days after β-catenin stabilisation (Figure 5.15). I found that approximately 13% of AHSCs are displaced in Cat-ca^{Het} and Cat-ca^{Hom} mice 10 days after the stabilisation of β-catenin (Figure 5.15B). This displacement promotes AHSC activation (Figure 5.15C and 5.15D), which is possibly due to displaced AHSCs losing exposure to SGZ-located quiescent signals, such as Notch and BMP4 (Ables et al., 2010; Mira et al., 2010). This could be tested by examining readouts of quiescent signal activity in displaced AHSCs *in vivo* such as the presence of the Notch intracellular domain (NICD) or genetic reporters of Hes1 and Hes5 to examine Notch signalling levels (Breunig et al., 2007; Ehm et al., 2010; Imayoshi et al., 2010; Lugert et al., 2010) or testing for phospho-SMAD1 immunoreactivity to investigate the levels of BMP signalling (Mira et al., 2010). However, the small proportion of displaced AHSCs in the DG of Cat-ca^{Het} and Cat-ca^{Hom} (Figure 5.15B), may not account for the 50-60% loss of AHSCs 30 days after β-catenin stabilisation (Figure 5.11C). Recombination of the Cat-ca allele excises exon 3 of β-catenin, which encodes the N-terminal domain and houses the GSK3β phosphorylation sites, thus preventing β-catenin being phosphorylated for degradation (Harada et al., 1999). The accumulation of stabilised β-catenin protein could be toxic to recombined cells and could promote cell death (Bence et al., 2001). The contribution of cell death towards the loss of AHSCs, could be investigated by performing immunolabelling of the apoptosis marker cleaved caspase-3 or counting pyknotic nuclei (reviewed by (Elmore. 2007)) in brain sections of Control, Cat-ca^{Het} and Cat-ca^{Hom} mice 10 days after tamoxifen administration.

6.9.2 Correct Niche organisation Influences Adult Hippocampal Neurogenesis

The displacement of AHSCs, induced by the stabilisation of β-catenin, also affects the generation of newborn neurons. Whilst the total number of Tbr2+ IPCs and DCX+ neuroblasts was similar between Control, Cat-ca^{Het} and Cat-ca^{Hom} mice (Figures 5.16B and 5.17B), their organisation, niche locations and morphologies were impaired (Figures 5.16 and 5.17). The displacement of AHSCs would result in their progeny also being displaced within the DG niche. This would account for the increased proportion of Tbr2+ IPCs and DCX+ neuroblasts located outside their normal niche location in Cat-ca^{Het} and Cat-ca^{Hom} mice (Figures 5.16C and 5.17C). The adult hippocampal neurogenic niche is a highly organised structure and signals from this microenvironment impact on the correct progression of the adult hippocampal neurogenic lineage (reviewed by (Ming et al., 2011; Urbán et al., 2014)). It is therefore possible that the displaced progeny of Cat-ca AHSCs receive inappropriate signals for their differentiation stage because they are mis-located within the hippocampal neurogenic niche. Indeed, using the

BATGAL Wnt reporter mice I showed that the response to canonical Wnt signalling decreased in IPCs and neuroblasts compared to AHSCs and granule neurons (Figure 3.7). This suggests that the context dependency and temporal response to canonical Wnt signalling across the cells of the neurogenic lineage, is important for regulating the maturation of newborn neurons. Progenitors and neuroblasts generated from recombined AHSCs would not be able to stop responding to canonical Wnt signalling due to the stabilisation of β-catenin (Harada et al., 1999). Therefore, the aberrant neuronal differentiation observed in Cat-ca^{Het} and Cat-ca^{Hom} mice could be due to the dysregulated timing of canonical Wnt signalling in the progeny of recombined AHSCs.

Not all of the displaced Tbr2+ IPCs and DCX+ neuroblasts were YFP+ indicating that they were either derived from Cat-ca recombined AHSCs that failed to recombine the RYFP locus (Dause et al., 2020) or that they were derived from non-recombined AHSCs (Figures 5.16A and 5.17A). This could suggest that the displacement of AHSCs not only directly affects their progeny, but also affects the maturation of other lineage cells derived from non-recombined AHSCs, in a non-cell autonomous fashion. This could be due to the severity of the niche disorganisation in Cat-ca mice. Given the level of dysregulated adult neurogenesis in Cat-ca mice, it would be interesting to investigate how they respond to hippocampal dependent behavioural tests such as the Morris Water Maze, that assesses spatial learning and memory (Vorhees et al., 2006). This could highlight the importance of the niche organisation in regulating adult hippocampal neurogenesis and its associated cognitive functions, which could have implications for neurodegenerative disease.

6.9.3 Role of β-catenin at Adherens Junctions Could Mediate the Displacement Phenotype

β-catenin plays a role in cell adhesion at cell-cell junctions by forming a complex with cadherin and the actin cytoskeleton (Bienz. 2005). β-catenin binds to cadherins via its Armadillo repeats (Huber et al., 1997) and binds to α-catenin via its N-terminal domain, which then facilitates the binding to the actin cytoskeleton (Figure 1.9) (Hur et al., 2013). In Cat-ca mice, exon 3 of β-catenin is deleted, which encodes the N-terminal domain containing the GSK3β phosphorylation sites, thus generating stabilised β-catenin (Yost et al., 1996; Harada et al., 1999). As the N-terminal domain of β-catenin also houses the α-catenin binding site (Figure 1.9) (Huber et al., 2001), the interaction between α- and β-catenin could be disrupted in recombined cells (Dar et

al., 2016). In the original paper where these mice are first described, the authors state that the Cat-ca allele does not affect adherence junctions in the intestine, however they do acknowledge that changes in cell adhesion could contribute to their observed phenotype (Harada et al., 1999). This suggests that loss of exon 3 of β-catenin could disrupt AHSC adhesion properties, which could be responsible for the displacement of AHSCs observed in Cat-ca mice (Figure 5.15A and 5.15B). Indeed, conditional deletion of N-cadherin in the developing cortex, causes severe disorganisation of intra-cortical structures due to the disruption of adherens junctions located at the apical end of neuroepithelial cells (Kadowaki et al., 2007). Downregulation of E-cadherin and loss of cell-cell contacts is also associated with increased proliferation and invasiveness of epithelial derived tumours (Berx et al., 2001; Conacci-Sorrell et al., 2002). Furthermore, cadherin signalling has been shown to play a role in regulating the migration of pre-cerebellar neurons in the hindbrain (Taniguchi et al., 2006) as well as enhancing the migration of SVZ neural precursors in response to injury (Klingener et al., 2014). This highlights the importance of cadherin signalling and cell-cell adhesion in regulating tissue organisation and cell migration in a variety of contexts and suggests that changes in these processes could influence the displacement of AHSCs in Cat-ca mice, rather than the direct activation of canonical Wnt signalling. Future work is needed to investigate how stabilising β-catenin in AHSCs affects cadherin signalling and cell adhesion.

Interestingly the displacement of AHSCs was not observed in β-cat$^{ex2\text{-}6\ del}$ mice (Figure 4.15), where the entire β-catenin protein is lost. This could indicate a dominant negative effect of the stabilised form, as it is still able to bind to cadherins despite its disrupted interaction with the actin cytoskeleton, which could have consequences on cadherin signalling. It could also suggest that the loss of cell adhesion could work synergistically with the activation of canonical Wnt signalling in Cat-ca mice to induce AHSC displacement. Indeed, Machon and colleagues show that the organisation of the developing cortex is disrupted at E13.5 onwards in D6-Cre; Cat-ca mice due to the synergistic activation of canonical Wnt signalling and disruption of adherens junctions (Machon et al., 2007).Canonical Wnt signalling has been shown to activate the transcription of genes that promote migration and motility in various cancers and during development (Qi et al., 2016). For example, canonical Wnt signalling has been shown to upregulate a variety of matrix metalloproteinases (MMPs) which are required to remodel the extracellular matrix to facilitate cell migration in both development and cancer (Wu et al., 2007; Ingraham et al., 2011; Lyu et al., 2005; Kamino et al., 2011; Lee et al., 2014; Takahashi et al., 2002; Lowy et al., 2006). This could suggest that the activation of canonical Wnt signalling alongside the disrupted of cell adhesion in Cat-ca recombined cells, could be responsible for

driving the displacement of AHSCs from their correct niche location. It would be interesting to investigate how canonical Wnt signalling and/or cell adhesion contribute to this AHSC displacement phenotype. To do this I could examine the transcriptional profile of Cat-ca cells for the upregulation of Wnt target genes associated with cell migration. Also, immunofluorescence techniques could be employed to examine any changes in the organisation of adherens junctions and the cytoskeleton. Not much is known about the role of cell adhesion in regulating adult hippocampal neurogenesis, however it has been shown to play an important role in maintaining the niche location and quiescent state of SVZ NSCs (Kokovay et al., 2012; Shen et al., 2008; Porlan et al., 2014). The level of hippocampal niche disorganisation and impaired neurogenesis in Cat-ca mice, suggests that the maintenance of cell adhesion properties is integral to ensure the correct progression of adult hippocampal neurogenesis and warrants further investigation.

6.9.4 Different Models are Required to Fine Tune the Activation of Canonical Wnt Signalling in AHSCs *in vivo*

Due to β-catenin's dual role in both canonical Wnt signalling and cell adhesion, it is difficult to determine whether the phenotypes observed by stabilising β-catenin are caused by activating canonical Wnt signalling or off target effects on cell adhesion. In addition, deleting exon 3 of β-catenin generates stabilised β-catenin which could act in a dominant negative fashion making it difficult to adjust the level of canonical Wnt stimulation. Therefore, alternative models and approaches are needed to fine tune the level of canonical Wnt stimulation in AHSCs *in vivo* to investigate the dose-dependent effects I observed when stimulating Wnt to different levels *in vitro* (Section 5.2). Adenomatous polyposis coli (APC) is a component of the β-catenin destruction complex and negatively regulates canonical Wnt signalling (Rubinfeld et al., 1993; Behrens et al., 1998). Mutations within the *APC* gene result in the upregulation of canonical Wnt signalling levels and is a major cause of colon cancer (reviewed by (Zhang et al., 2017). Different mutations within the *APC* gene have been shown to activate canonical Wnt signalling to different levels *in vivo* (Luis et al., 2011). These *APC* mutations have been used to create a gradient of stimulated Wnt signalling levels in the hematopoietic lineage to show that different doses of Wnt signalling regulate various stages of haematopoiesis (Luis et al., 2011). A similar approach could be applied to create a gradient of stimulated canonical Wnt signalling levels in AHSCs *in vivo* to investigate the dose-dependent effects of canonical Wnt signalling. However, this approach

would require five different mouse lines and would not be clean as the APC mutations are not conditional meaning they could not be restricted to AHSCs.

An alternative approach would be to treat wild type mice with a Wnt agonist such as lithium chloride (Clément-Lacroix et al., 2005). Lithium chloride is a potent mood stabiliser that promotes neurogenesis and activates canonical Wnt signalling by inhibiting the activity of GSK3β (Clément-Lacroix et al., 2005; Wexler et al., 2007; Zanni et al., 2017; Chen et al., 2000). This treatment can be administered to mice in their chow or via intraperitoneal injections to examine the chronic and acute effects of stimulating canonical Wnt signalling (Chen et al., 2000; Can et al., 2011). However, this approach would lead to the systemic activation of canonical Wnt signalling, which would make it difficult to determine the direct effects of stimulating canonical Wnt signalling specifically in the AHSCs.

6.10 Canonical Wnt Signalling in AHSCs Could be Required to Facilitate their Response to External Stimuli

I found that inhibiting AHSCs' response to canonical Wnt signalling does not affect their behaviour or homeostasis *in vitro* or *in vivo* (Section 4.2 and Figure 4.15). This suggests that canonical Wnt signalling does not play a role in regulating AHSC behaviour under homeostasis. However, I also found that deleting β-catenin impaired AHSPCs' response to a Wnt agonist (Figure 4.2H), meaning they are unable to respond to increased canonical Wnt signalling levels. Wnt signalling levels have been shown increase in the DG following exercise and direct stimulation of granule neurons, by upregulation of Wnt ligands and downregulation of Wnt inhibitors (Okamoto et al., 2011; Jang et al., 2013). The upregulation of canonical Wnt signalling levels, following exercise and electroconvulsive stimulation, promotes adult hippocampal neurogenesis and this positive effect is abrogated by the direct infusion of sFRP3 into the DG (Jang et al., 2013). This suggests that the pro-neurogenic effects of external stimuli are mediated by increased canonical Wnt signalling levels in the DG. Therefore, canonical Wnt signalling in the DG may not be essential for baseline adult hippocampal neurogenesis, but may be required to regulate adult hippocampal neurogenesis in response to an external stimulus. To investigate this hypothesis, it would be interesting to compare the levels of adult hippocampal neurogenesis, by quantifying total proliferation or number of neuroblasts/ newborn neurons, between β-cat$^{ex2\text{-}6\ del}$ and Control mice following exposure to an enriched environment or voluntary running, which both positively effect adult hippocampal neurogenesis (Kempermann et al., 1997; Aimone et al.,

2014; Kronenberg et al., 2003; van Praag et al., 1999). This could be followed up with hippocampal dependent behavioural assays to determine the functional consequences of activity induced canonical Wnt dependent adult hippocampal neurogenesis.

6.11 Conclusions and Future Perspectives

Adult hippocampal neurogenesis progresses along a distinct neurogenic lineage, which is tightly regulated at each stage by a variety of niche-derived factors. The first key regulatory step of adult neurogenesis begins with the decision of quiescent AHSCs to activate, which must balance the neurogenic demands of the hippocampus whilst also ensuring the long-term maintenance of the AHSC pool. Indeed, the rate of quiescent AHSC activation declines with age, stress and depression (Encinas et al., 2011; Seib et al., 2013; Kempermann. 2011a), therefore understanding how this process is regulated could provide insights into the development of potential therapeutic strategies. Canonical Wnt signalling represents a niche-derived signalling pathway that has been shown to regulate various stages of adult hippocampal neurogenesis (Lie et al., 2005; Seib et al., 2013; Jang et al., 2013; Wexler et al., 2009; Qu et al., 2013). However, the contradictory reports in the current literature do not reconcile how canonical Wnt signalling can play a role in promoting progenitor proliferation whilst also instructing neuronal differentiation. The work presented in this thesis partly explains this dual role by finding that quiescent AHSPCs respond to canonical Wnt signalling in a dose-dependent manner. Over-activation of canonical Wnt signalling promotes neuronal differentiation, whereas a lower Wnt stimulation promotes quiescent AHSPC activation, thus reconciling how one signalling pathway can regulate different cellular responses. More work is needed to understand how AHSCs measure the levels of canonical Wnt signalling within the hippocampal neurogenic niche and to interrogate the downstream mechanisms that mediate these two different responses.

Canonical Wnt signalling levels have been shown to decrease in the dentate gyrus with age and this has been implicated to play a role in mediating the age-associated decline in the levels of adult hippocampal neurogenesis (Seib et al., 2013; Okamoto et al., 2011; Miranda et al., 2012; Jessberger et al., 2009). The work presented here shows that AHSC homeostasis and behaviour is unaffected by inhibition of canonical Wnt signalling under physiological conditions, however progression along the neurogenic lineage is impaired. This suggests that under physiological conditions canonical Wnt signalling regulates the later stages of adult hippocampal neurogenesis and could provide a therapeutic target for ameliorating age-associated cognitive

decline by promoting the maturation of newborn neurons. Conversely, the levels of canonical Wnt signalling increase in the hippocampal neurogenic niche following environmental stimulation or exercise, which promotes adult hippocampal neurogenesis (Okamoto et al., 2011; Kronenberg et al., 2003; Kempermann et al., 1997; van Praag et al., 1999). This suggests that changing canonical Wnt signalling levels within the niche could mediate the pro-neurogenic effects of external stimuli. Quiescent AHSPCs respond differentially to the level of canonical Wnt stimulation but are unaffected by inhibition of canonical Wnt signalling under physiological conditions. This could imply a role for canonical Wnt signalling in regulating AHSC behaviour in response to an external stimulus. Canonical Wnt signalling could promote quiescent AHSPC activation independently of the key activation transcription factor Ascl1, suggesting that quiescent AHSPC activation could be regulated by different mechanisms under baseline conditions and following external stimulation. More work is needed to determine whether canonical Wnt signalling could act as a sensor of external factors to modulate adult hippocampal neurogenesis independently of Ascl1.

Understanding the regulatory mechanisms mediating AHSC behaviour has vast implications for human health and disease in developing therapies to combat hippocampal dependent age-associated cognitive decline and other neuropsychiatric disorders. Changing canonical Wnt signalling levels has been shown to both promote and impair adult neurogenesis in response to external stimulation and ageing. Further understanding the mechanisms behind the dose-dependent effects of canonical Wnt signalling in AHSCs could allow for the development of targeted therapies to promote quiescent AHSC activation or neuronal differentiation to ameliorate the progression of neuropsychiatric and neurodegenerative disease.

Reference List

Åberg, M.A.I., Åberg, N.D., Palmer, T.D., Alborn, A.-M., Carlsson-Skwirut, C., Bang, P., Rosengren, L.E., Olsson, T., Gage, F.H. & Eriksson, P.S. 2003. IGF-I has a direct proliferative effect in adult hippocampal progenitor cells. *Molecular and Cellular Neuroscience,* 24**,** 23-40.

Aberle, H., Bauer, A., Stappert, J., Kispert, A. & Kemler, R. 1997. β-catenin is a target for the ubiquitin-proteasome pathway. *The EMBO Journal,* 16**,** 3797-3804.

Ables, J.L., DeCarolis, N.A., Johnson, M.A., Rivera, P.D., Gao, Z., Cooper, D.C., Radtke, F., Hsieh, J. & Eisch, A.J. 2010. Notch1 is required for maintenance of the reservoir of adult hippocampal stem cells. *The Journal of neuroscience : the official journal of the Society for Neuroscience,* 30**,** 10484-10492.

Adler, P.N. 2002. Planar Signaling and Morphogenesis in Drosophila. *Developmental Cell,* 2**,** 525-535.

Agostino, M. & Pohl, S.O. 2019. Wnt Binding Affinity Prediction for Putative Frizzled-Type Cysteine-Rich Domains. *Int J Mol Sci,* 20.

Agostino, M., Pohl, S.Ö.-G. & Dharmarajan, A. 2017. Structure-based prediction of Wnt binding affinities for Frizzled-type cysteine-rich domains. *The Journal of biological chemistry,* 292**,** 11218-11229.

Ahn, S. & Joyner, A.L. 2005. *In vivo* analysis of quiescent adult neural stem cells responding to Sonic hedgehog. *Nature,* 437**,** 894-897.

Aimone, J.B., Deng, W. & Gage, F.H. 2010. Adult neurogenesis: integrating theories and separating functions. *Trends in Cognitive Sciences,* 14**,** 325-337.

Aimone, J.B., Li, Y., Lee, S.W., Clemenson, G.D., Deng, W. & Gage, F.H. 2014. Regulation and function of adult neurogenesis: from genes to cognition. *Physiological reviews,* 94**,** 991-1026.

Airan, R.D., Meltzer, L.A., Roy, M., Gong, Y., Chen, H. & Deisseroth, K. 2007. High-Speed Imaging Reveals Neurophysiological Links to Behavior in an Animal Model of Depression. *Science,* 317**,** 819.

Al Alam, D., Green, M., Tabatabai Irani, R., Parsa, S., Danopoulos, S., Sala, F.G., Branch, J., El Agha, E., Tiozzo, C., Voswinckel, R., Jesudason, E.C., Warburton, D. & Bellusci, S. 2011. Contrasting Expression of Canonical Wnt Signaling Reporters TOPGAL, BATGAL and Axin2LacZ during Murine Lung Development and Repair. *PLOS ONE,* 6**,** e23139.

Alexandre, C., Baena-Lopez, A. & Vincent, J.-P. 2014. Patterning and growth control by membrane-tethered Wingless. *Nature,* 505**,** 180-185.

Alfonso, J., Le Magueresse, C., Zuccotti, A., Khodosevich, K. & Monyer, H. 2012. Diazepam Binding Inhibitor Promotes Progenitor Proliferation in the Postnatal SVZ by Reducing GABA Signaling. *Cell Stem Cell,* 10**,** 76-87.

Altman, J. 1963. Autoradiographic investigation of cell proliferation in the brains of rats and cats. *The Anatomical Record,* 145**,** 573-591.

Altman, J. 1966. Autoradiographic and histological studies of postnatal neurogenesis. II. A longitudinal investigation of the kinetics, migration and transformation of cells incorporating tritiated

thymidine in infant rats, with special reference to postnatal neurogenesis in some brain regions. *Journal of Comparative Neurology,* 128**,** 431-473.

Altman, J. 1969. Autoradiographic and histological studies of postnatal neurogenesis. IV. Cell proliferation and migration in the anterior forebrain, with special reference to persisting neurogenesis in the olfactory bulb. *Journal of Comparative Neurology,* 137**,** 433-457.

Altman, J. & Das, G.D. 1965. Autoradiographic and histological evidence of postnatal hippocampal neurogenesis in rats. *The Journal of Comparative Neurology,* 124**,** 319-335.

Alvarez-Buylla, A., García-Verdugo, J.M. & Tramontin, A.D. 2001. A unified hypothesis on the lineage of neural stem cells. *Nature Reviews Neuroscience,* 2**,** 287-293.

Amador-Arjona, A., Elliott, J., Miller, A., Ginbey, A., Pazour, G.J., Enikolopov, G., Roberts, A.J. & Terskikh, A.V. 2011. Primary cilia regulate proliferation of amplifying progenitors in adult hippocampus: implications for learning and memory. *The Journal of neuroscience : the official journal of the Society for Neuroscience,* 31**,** 9933-9944.

Ambrogini, P., Lattanzi, D., Ciuffoli, S., Agostini, D., Bertini, L., Stocchi, V., Santi, S. & Cuppini, R. 2004. Morpho-functional characterization of neuronal cells at different stages of maturation in granule cell layer of adult rat dentate gyrus. *Brain Research,* 1017**,** 21-31.

Amit, S., Hatzubai, A., Birman, Y., Andersen, J.S., Ben-Shushan, E., Mann, M., Ben-Neriah, Y. & Alkalay, I. 2002. Axin-mediated CKI phosphorylation of β-catenin at Ser 45: a molecular switch for the Wnt pathway. *Genes & development,* 16**,** 1066-1076.

Anders, S., Pyl, P.T. & Huber, W. 2015. HTSeq--a Python framework to work with high-throughput sequencing data. *Bioinformatics (Oxford, England),* 31**,** 166-169.

Andersen, J., Urbán, N., Achimastou, A., Ito, A., Simic, M., Ullom, K., Martynoga, B., Lebel, M., Göritz, C., Frisén, J., Nakafuku, M. & Guillemot, F. 2014. A Transcriptional Mechanism Integrating Inputs from Extracellular Signals to Activate Hippocampal Stem Cells. *Neuron,* 83**,** 1085-1097.

Andrews, S. 2010. FastQC: a quality control tool for high throughput sequence data.
. *Babraham Bioinformatics*.

Arredondo, S.B., Guerrero, F.G., Herrera-Soto, A., Jensen-Flores, J., Bustamante, D.B., Oñate-Ponce, A., Henny, P., Varas-Godoy, M., Inestrosa, N.C. & Varela-Nallar, L. 2019. Wnt5a promotes differentiation and development of adult-born neurons in the hippocampus by noncanonical Wnt signaling. *STEM CELLS,* n/a.

Artegiani, B., Lyubimova, A., Muraro, M., van Es, J.H., van Oudenaarden, A. & Clevers, H. 2017. A Single-Cell RNA Sequencing Study Reveals Cellular and Molecular Dynamics of the Hippocampal Neurogenic Niche. *Cell Reports,* 21**,** 3271-3284.

Augenlicht, L.H. & Baserga, R. 1974. Changes in the G0 state of WI-38 fibroblasts at different times after confluence. *Experimental Cell Research,* 89**,** 255-262.

Backman, M., Machon, O., Mygland, L., van den Bout, C.J., Zhong, W., Taketo, M.M. & Krauss, S. 2005. Effects of canonical Wnt signaling on dorso-ventral specification of the mouse telencephalon. *Developmental Biology,* 279**,** 155-168.

Bafico, A., Liu, G., Yaniv, A., Gazit, A. & Aaronson, S.A. 2001. Novel mechanism of Wnt signalling inhibition mediated by Dickkopf-1 interaction with LRP6/Arrow. *Nat Cell Biol,* 3**,** 683-6.

Bai, G., Sheng, N., Xie, Z., Bian, W., Yokota, Y., Benezra, R., Kageyama, R., Guillemot, F. & Jing, N. 2007. Id Sustains Hes1 Expression to Inhibit Precocious Neurogenesis by Releasing Negative Autoregulation of Hes1. *Developmental Cell,* 13**,** 283-297.

Bänziger, C., Soldini, D., Schütt, C., Zipperlen, P., Hausmann, G. & Basler, K. 2006. Wntless, a Conserved Membrane Protein Dedicated to the Secretion of Wnt Proteins from Signaling Cells. *Cell,* 125**,** 509-522.

Barker, N., van Es, J.H., Kuipers, J., Kujala, P., van den Born, M., Cozijnsen, M., Haegebarth, A., Korving, J., Begthel, H., Peters, P.J. & Clevers, H. 2007. Identification of stem cells in small intestine and colon by marker gene Lgr5. *Nature,* 449**,** 1003-1007.

Barolo, S. 2006. Transgenic Wnt/TCF pathway reporters: all you need is Lef? *Oncogene,* 25**,** 7505-11.

Bartscherer, K., Pelte, N., Ingelfinger, D. & Boutros, M. 2006. Secretion of Wnt Ligands Requires Evi, a Conserved Transmembrane Protein. *Cell,* 125**,** 523-533.

Basak, O., Giachino, C., Fiorini, E., MacDonald, H.R. & Taylor, V. 2012. Neurogenic Subventricular Zone Stem/Progenitor Cells Are Notch1-Dependent in Their Active But Not Quiescent State. *The Journal of Neuroscience,* 32**,** 5654.

Basak, O., Krieger, T.G., Muraro, M.J., Wiebrands, K., Stange, D.E., Frias-Aldeguer, J., Rivron, N.C., van de Wetering, M., van Es, J.H., van Oudenaarden, A., Simons, B.D. & Clevers, H. 2018. Troy+ brain stem cells cycle through quiescence and regulate their number by sensing niche occupancy. *Proceedings of the National Academy of Sciences,* 115**,** E610.

Baserga, R. 1968. BIOCHEMISTRY OF THE CELL CYCLE: A REVIEW. *Cell Proliferation,* 1**,** 167-191.

Becht, E., McInnes, L., Healy, J., Dutertre, C.-A., Kwok, I.W.H., Ng, L.G., Ginhoux, F. & Newell, E.W. 2019. Dimensionality reduction for visualizing single-cell data using UMAP. *Nature Biotechnology,* 37**,** 38-44.

Beckervordersandforth, R., Ebert, B., Schäffner, I., Moss, J., Fiebig, C., Shin, J., Moore, D.L., Ghosh, L., Trinchero, M.F., Stockburger, C., Friedland, K., Steib, K., von Wittgenstein, J., Keiner, S., Redecker, C., Hölter, S.M., Xiang, W., Wurst, W., Jagasia, R., Schinder, A.F., Ming, G.-l., Toni, N., Jessberger, S., Song, H. & Lie, D.C. 2017. Role of Mitochondrial Metabolism in the Control of Early Lineage Progression and Aging Phenotypes in Adult Hippocampal Neurogenesis. *Neuron,* 93**,** 1518.

Behrens, J., Jerchow, B.-A., Würtele, M., Grimm, J., Asbrand, C., Wirtz, R., Kühl, M., Wedlich, D. & Birchmeier, W. 1998. Functional Interaction of an Axin Homolog, Conductin, with β-Catenin, APC, and GSK3β. *Science,* 280**,** 596-599.

Behrens, J., von Kries, J.P., Kühl, M., Bruhn, L., Wedlich, D., Grosschedl, R. & Birchmeier, W. 1996. Functional interaction of β-catenin with the transcription factor LEF-1. *Nature,* 382**,** 638-642.

Bence, N.F., Sampat, R.M. & Kopito, R.R. 2001. Impairment of the Ubiquitin-Proteasome System by Protein Aggregation. *Science,* 292**,** 1552.

Berg, D.A., Belnoue, L., Song, H. & Simon, A. 2013. Neurotransmitter-mediated control of neurogenesis in the adult vertebrate brain. *Development,* 140**,** 2548.

Berg, D.A., Su, Y., Jimenez-Cyrus, D., Patel, A., Huang, N., Morizet, D., Lee, S., Shah, R., Ringeling, F.R., Jain, R., Epstein, J.A., Wu, Q.-F., Canzar, S., Ming, G.-L., Song, H. & Bond, A.M. 2019. A

Common Embryonic Origin of Stem Cells Drives Developmental and Adult Neurogenesis. *Cell,* 177**,** 654-668.e15.

Bergami, M., Rimondini, R., Santi, S., Blum, R., Götz, M. & Canossa, M. 2008. Deletion of TrkB in adult progenitors alters newborn neuron integration into hippocampal circuits and increases anxiety-like behavior. *Proceedings of the National Academy of Sciences,* 105**,** 15570.

Bertrand, N., Castro, D.S. & Guillemot, F. 2002. Proneural genes and the specification of neural cell types. *Nat Rev Neurosci,* 3**,** 517-530.

Berx, G. & Van Roy, F. 2001. The E-cadherin/catenin complex: an important gatekeeper in breast cancer tumorigenesis and malignant progression. *Breast cancer research : BCR,* 3**,** 289-293.

Bhanot, P., Brink, M., Samos, C.H., Hsieh, J.-C., Wang, Y., Macke, J.P., Andrew, D., Nathans, J. & Nusse, R. 1996. A new member of the frizzled family from Drosophila functions as a Wingless receptor. *Nature,* 382**,** 225-230.

Bienz, M. 2005. β-Catenin: A Pivot between Cell Adhesion and Wnt Signalling. *Current Biology,* 15**,** R64-R67.

Blomfield, I.M., Rocamonde, B., Masdeu, M.D.M., Mulugeta, E., Vaga, S., van den Berg, D.L., Huillard, E., Guillemot, F. & Urbán, N. 2019. Id4 promotes the elimination of the pro-activation factor Ascl1 to maintain quiescence of adult hippocampal stem cells. *eLife,* 8**,** e48561.

Boareto, M., Iber, D. & Taylor, V. 2017. Differential interactions between Notch and ID factors control neurogenesis by modulating Hes factor autoregulation. *Development (Cambridge, England),* 144**,** 3465-3474.

Boldrini, M., Fulmore, C.A., Tartt, A.N., Simeon, L.R., Pavlova, I., Poposka, V., Rosoklija, G.B., Stankov, A., Arango, V., Dwork, A.J., Hen, R. & Mann, J.J. 2018. Human Hippocampal Neurogenesis Persists throughout Aging. *Cell stem cell,* 22**,** 589-599.e5.

Bolger, A.M., Lohse, M. & Usadel, B. 2014. Trimmomatic: a flexible trimmer for Illumina sequence data. *Bioinformatics (Oxford, England),* 30**,** 2114-2120.

Bonaguidi, M.A., McGuire, T., Hu, M., Kan, L., Samanta, J. & Kessler, J.A. 2005. LIF and BMP signaling generate separate and discrete types of GFAP-expressing cells. *Development,* 132**,** 5503.

Bonaguidi, M.A., Peng, C.-Y., McGuire, T., Falciglia, G., Gobeske, K.T., Czeisler, C. & Kessler, J.A. 2008. Noggin expands neural stem cells in the adult hippocampus. *The Journal of neuroscience : the official journal of the Society for Neuroscience,* 28**,** 9194-204.

Bonaguidi, M.A., Song, J., Ming, G.-l. & Song, H. 2012. A unifying hypothesis on mammalian neural stem cell properties in the adult hippocampus. *Current opinion in neurobiology,* 22**,** 754-61.

Bonaguidi, M.A., Wheeler, M.A., Shapiro, J.S., Stadel, R.P., Sun, G.J., Ming, G.-l. & Song, H. 2011. *In vivo* clonal analysis reveals self-renewing and multipotent adult neural stem cell characteristics. *Cell,* 145**,** 1142-55.

Bond, A.M., Ming, G.-L. & Song, H. 2015. Adult Mammalian Neural Stem Cells and Neurogenesis: Five Decades Later. *Cell stem cell,* 17**,** 385-395.

Bond, A.M., Peng, C.-Y., Meyers, E.A., McGuire, T., Ewaleifoh, O. & Kessler, J.A. 2014. BMP Signaling Regulates the Tempo of Adult Hippocampal Progenitor Maturation at Multiple Stages of the Lineage. *STEM CELLS,* 32**,** 2201-2214.

Bovolenta, P., Esteve, P., Ruiz, J.M., Cisneros, E. & Lopez-Rios, J. 2008. Beyond Wnt inhibition: new functions of secreted Frizzled-related proteins in development and disease. *Journal of Cell Science,* 121**,** 737-746.

Bowman, A.N., van Amerongen, R., Palmer, T.D. & Nusse, R. 2013. Lineage tracing with Axin2 reveals distinct developmental and adult populations of Wnt/β-catenin-responsive neural stem cells. *Proceedings of the National Academy of Sciences of the United States of America,* 110**,** 7324-9.

Bracko, O., Singer, T., Aigner, S., Knobloch, M., Winner, B., Ray, J., Clemenson, G.D., Suh, H., Couillard-Despres, S., Aigner, L., Gage, F.H. & Jessberger, S. 2012. Gene Expression Profiling of Neural Stem Cells and Their Neuronal Progeny Reveals IGF2 as a Regulator of Adult Hippocampal Neurogenesis. *Journal of Neuroscience,* 32**,** 3376-3387.

Bragdon, B., Moseychuk, O., Saldanha, S., King, D., Julian, J. & Nohe, A. 2011. Bone Morphogenetic Proteins: A critical review. *Cellular Signalling,* 23**,** 609-620.

Brault, V., Moore, R., Kutsch, S., Ishibashi, M., Rowitch, D.H., McMahon, A.P., Sommer, L., Boussadia, O. & Kemler, R. 2001. Inactivation of the β-catenin gene by Wnt1-Cre-mediated deletion results in dramatic brain malformation and failure of craniofacial development. *Development,* 128**,** 1253.

Breunig, J.J., Sarkisian, M.R., Arellano, J.I., Morozov, Y.M., Ayoub, A.E., Sojitra, S., Wang, B., Flavell, R.A., Rakic, P. & Town, T. 2008. Primary cilia regulate hippocampal neurogenesis by mediating sonic hedgehog signaling. *Proceedings of the National Academy of Sciences of the United States of America,* 105**,** 13127-13132.

Breunig, J.J., Silbereis, J., Vaccarino, F.M., Sestan, N. & Rakic, P. 2007. Notch regulates cell fate and dendrite morphology of newborn neurons in the postnatal dentate gyrus. *Proceedings of the National Academy of Sciences of the United States of America,* 104**,** 20558-20563.

Brown, J.P., Couillard-Després, S., Cooper-Kuhn, C.M., Winkler, J., Aigner, L. & Kuhn, H.G. 2003. Transient expression of doublecortin during adult neurogenesis. *Journal of Comparative Neurology,* 467**,** 1-10.

Bruel-Jungerman, E., Laroche, S. & Rampon, C. 2005. New neurons in the dentate gyrus are involved in the expression of enhanced long-term memory following environmental enrichment. *European Journal of Neuroscience,* 21**,** 513-521.

Brunne, B., Zhao, S., Derouiche, A., Herz, J., May, P., Frotscher, M. & Bock, H.H. 2010. Origin, maturation, and astroglial transformation of secondary radial glial cells in the developing dentate gyrus. *Glia,* 58**,** 1553-1569.

Burd, G.D. & Nottebohm, F. 1985. Ultrastructural characterization of synaptic terminals formed on newly generated neurons in a song control nucleus of the adult canary forebrain. *Journal of Comparative Neurology,* 240**,** 143-152.

Cadigan, K.M. & Liu, Y.I. 2006. Wnt signaling: complexity at the surface. *Journal of Cell Science,* 119**,** 395.

Calnan, D.R. & Brunet, A. 2008. The FoxO code. *Oncogene,* 27**,** 2276-2288.

Cameron, H.A. & Gould, E. 1994. Adult neurogenesis is regulated by adrenal steroids in the dentate gyrus. *Neuroscience,* 61**,** 203-209.

Can, A., Blackwell, R.A., Piantadosi, S.C., Dao, D.T., O'Donnell, K.C. & Gould, T.D. 2011. Antidepressant-like responses to lithium in genetically diverse mouse strains. *Genes, brain, and behavior,* 10**,** 434-443.

Carmon, K.S., Gong, X., Lin, Q., Thomas, A. & Liu, Q. 2011. R-spondins function as ligands of the orphan receptors LGR4 and LGR5 to regulate Wnt/β-catenin signaling. *Proceedings of the National Academy of Sciences,* 108**,** 11452.

Castellano, J.M., Kirby, E.D. & Wyss-Coray, T. 2015. Blood-Borne Revitalization of the Aged Brain. *JAMA Neurology,* 72**,** 1191-1194.

Cavallo, R.A., Cox, R.T., Moline, M.M., Roose, J., Polevoy, G.A., Clevers, H., Peifer, M. & Bejsovec, A. 1998. Drosophila Tcf and Groucho interact to repress Wingless signalling activity. *Nature,* 395**,** 604-608.

Cerpa, W., Gambrill, A., Inestrosa, N.C. & Barria, A. 2011. Regulation of NMDA-Receptor Synaptic Transmission by Wnt Signaling. *The Journal of Neuroscience,* 31**,** 9466.

Chavali, M., Klingener, M., Kokkosis, A.G., Garkun, Y., Felong, S., Maffei, A. & Aguirre, A. 2018. Non-canonical Wnt signaling regulates neural stem cell quiescence during homeostasis and after demyelination. *Nature Communications,* 9**,** 36.

Chen, B., Dodge, M.E., Tang, W., Lu, J., Ma, Z., Fan, C.-W., Wei, S., Hao, W., Kilgore, J., Williams, N.S., Roth, M.G., Amatruda, J.F., Chen, C. & Lum, L. 2009. Small molecule-mediated disruption of Wnt-dependent signaling in tissue regeneration and cancer. *Nature chemical biology,* 5**,** 100-7.

Chen, G., Rajkowska, G., Du, F., Seraji-Bozorgzad, N. & Manji, H.K. 2000. Enhancement of Hippocampal Neurogenesis by Lithium. *Journal of Neurochemistry,* 75**,** 1729-1734.

Chen, J., Park, C.S. & Tang, S.-J. 2006. Activity-dependent Synaptic Wnt Release Regulates Hippocampal Long Term Potentiation. *Journal of Biological Chemistry,* 281**,** 11910-11916.

Chenn, A. & Walsh, C.A. 2002. Regulation of Cerebral Cortical Size by Control of Cell Cycle Exit in Neural Precursors. *Science,* 297**,** 365.

Cheung, T.H. & Rando, T.A. 2013. Molecular regulation of stem cell quiescence. *Nature reviews. Molecular cell biology,* 14**,** 10.1038/nrm3591.

Choe, Y., Pleasure, S.J. & Mira, H. 2015. Control of Adult Neurogenesis by Short-Range Morphogenic-Signaling Molecules. *Cold Spring Harbor perspectives in biology,* 8**,** a018887-a018887.

Choubey, L., Collette, J.C. & Smith, K.M. 2017. Quantitative assessment of fibroblast growth factor receptor 1 expression in neurons and glia. *PeerJ,* 5**,** e3173-e3173.

Ciani, L., Boyle, K.A., Dickins, E., Sahores, M., Anane, D., Lopes, D.M., Gibb, A.J. & Salinas, P.C. 2011. Wnt7a signaling promotes dendritic spine growth and synaptic strength through Ca2+/Calmodulin-dependent protein kinase II. *Proceedings of the National Academy of Sciences,* 108**,** 10732.

Clark, P.J., Brzezinska, W.J., Puchalski, E.K., Krone, D.A. & Rhodes, J.S. 2009. Functional analysis of neurovascular adaptations to exercise in the dentate gyrus of young adult mice associated with cognitive gain. *Hippocampus,* 19**,** 937-950.

Clelland, C.D., Choi, M., Romberg, C., Clemenson, G.D., Jr., Fragniere, A., Tyers, P., Jessberger, S., Saksida, L.M., Barker, R.A., Gage, F.H. & Bussey, T.J. 2009. A functional role for adult hippocampal neurogenesis in spatial pattern separation. *Science (New York, N.Y.),* 325**,** 210-213.

Clément-Lacroix, P., Ai, M., Morvan, F., Roman-Roman, S., Vayssière, B., Belleville, C., Estrera, K., Warman, M.L., Baron, R. & Rawadi, G. 2005. Lrp5-independent activation of Wnt signaling by lithium chloride increases bone formation and bone mass in mice. *Proceedings of the National Academy of Sciences of the United States of America,* 102**,** 17406-17411.

Clevers, H. 2006. Wnt/β-catenin signaling in development and disease. *Cell,* 127.

Clevers, H. & Nusse, R. 2012. Wnt/β-catenin signaling and disease. *Cell,* 149**,** 1192-205.

Codega, P., Silva-Vargas, V., Paul, A., Maldonado-Soto, Angel R., DeLeo, Annina M., Pastrana, E. & Doetsch, F. 2014. Prospective Identification and Purification of Quiescent Adult Neural Stem Cells from Their In Vivo Niche. *Neuron,* 82**,** 545-559.

Colak, D., Mori, T., Brill, M.S., Pfeifer, A., Falk, S., Deng, C., Monteiro, R., Mummery, C., Sommer, L. & Götz, M. 2008. Adult neurogenesis requires Smad4-mediated bone morphogenic protein signaling in stem cells. *The Journal of neuroscience : the official journal of the Society for Neuroscience,* 28**,** 434-446.

Conacci-Sorrell, M., Zhurinsky, J. & Ben-Ze'ev, A. 2002. The cadherin-catenin adhesion system in signaling and cancer. *The Journal of clinical investigation,* 109**,** 987-991.

Cong, F. & Varmus, H. 2004. Nuclear-cytoplasmic shuttling of Axin regulates subcellular localization of β-catenin. *Proceedings of the National Academy of Sciences of the United States of America,* 101**,** 2882-2887.

Cotson, S., Holt, S.J. & Dodds, E.C. 1958. IV. Kinetics of aerial oxidation of indoxyl and some of its halogen derivatives. *Proceedings of the Royal Society of London. Series B - Biological Sciences,* 148**,** 506-519.

Cottet-Rousselle, C., Ronot, X., Leverve, X. & Mayol, J.-F. 2011. Cytometric assessment of mitochondria using fluorescent probes. *Cytometry Part A,* 79A**,** 405-425.

Cruciat, C.-M. & Niehrs, C. 2013. Secreted and Transmembrane Wnt Inhibitors and Activators. *Cold Spring Harbor Perspectives in Biology,* 5.

Cuitino, L., Godoy, J.A., Farías, G.G., Couve, A., Bonansco, C., Fuenzalida, M. & Inestrosa, N.C. 2010. Wnt-5a Modulates Recycling of Functional GABAA Receptors on Hippocampal Neurons. *The Journal of Neuroscience,* 30**,** 8411-8420.

Dahlstrand, J., Lardelli, M. & Lendahl, U. 1995. Nestin mRNA expression correlates with the central nervous system progenitor cell state in many, but not all, regions of developing central nervous system. *Developmental Brain Research,* 84**,** 109-129.

Daniels, D.L. & Weis, W.I. 2005. β-catenin directly displaces Groucho/TLE repressors from Tcf/Lef in Wnt-mediated transcription activation. *Nature Structural & Molecular Biology,* 12**,** 364-371.

Danielson, Nathan B., Kaifosh, P., Zaremba, Jeffrey D., Lovett-Barron, M., Tsai, J., Denny, Christine A., Balough, Elizabeth M., Goldberg, Alexander R., Drew, Liam J., Hen, R., Losonczy, A. & Kheirbek, Mazen A. 2016. Distinct Contribution of Adult-Born Hippocampal Granule Cells to Context Encoding. *Neuron,* 90**,** 101-112.

Dann, C.E., Hsieh, J.-C., Rattner, A., Sharma, D., Nathans, J. & Leahy, D.J. 2001. Insights into Wnt binding and signalling from the structures of two Frizzled cysteine-rich domains. *Nature,* 412**,** 86-90.

Dar, M.S., Singh, P., Singh, G., Jamwal, G., Hussain, S.S., Rana, A., Akhter, Y., Monga, S.P. & Dar, M.J. 2016. Terminal regions of β-catenin are critical for regulating its adhesion and transcription functions. *Biochimica et Biophysica Acta (BBA) - Molecular Cell Research,* 1863**,** 2345-2357.

DasGupta, R. & Fuchs, E. 1999. Multiple roles for activated LEF/TCF transcription complexes during hair follicle development and differentiation. *Development,* 126**,** 4557.

Daugherty, R.L. & Gottardi, C.J. 2007. Phospho-regulation of β-Catenin Adhesion and Signaling Functions. *Physiology (Bethesda, Md.),* 22**,** 303-309.

Dause, T.J. & Kirby, E.D. 2020. Poor concordance of floxed sequence recombination in single neural stem cells: Implications for cell autonomous studies. *eneuro***,** ENEURO.0470-19.2020.

Davidson, G., Wu, W., Shen, J., Bilic, J., Fenger, U., Stannek, P., Glinka, A. & Niehrs, C. 2005. Casein kinase 1 gamma couples Wnt receptor activation to cytoplasmic signal transduction. *Nature,* 438**,** 867-72.

Daynac, M., Tirou, L., Faure, H., Mouthon, M.-A., Gauthier, L.R., Hahn, H., Boussin, F.D. & Ruat, M. 2016. Hedgehog Controls Quiescence and Activation of Neural Stem Cells in the Adult Ventricular-Subventricular Zone. *Stem cell reports,* 7**,** 735-748.

De, A. 2011. Wnt/Ca2+ signaling pathway: a brief overview. *Acta Biochimica et Biophysica Sinica,* 43**,** 745-756.

de Lau, W., Barker, N., Low, T.Y., Koo, B.-K., Li, V.S.W., Teunissen, H., Kujala, P., Haegebarth, A., Peters, P.J., van de Wetering, M., Stange, D.E., van Es, J., Guardavaccaro, D., Schasfoort, R.B.M., Mohri, Y., Nishimori, K., Mohammed, S., Heck, A.J.R. & Clevers, H. 2011. Lgr5 homologues associate with Wnt receptors and mediate R-spondin signalling. *Nature,* 476**,** 293-297.

de Lau, W., Peng, W.C., Gros, P. & Clevers, H. 2014. The R-spondin/Lgr5/Rnf43 module: regulator of Wnt signal strength. *Genes & Development,* 28**,** 305-316.

de Roo, J.J.D., Breukel, C., Chhatta, A.R., Linssen, M.M., Vloemans, S.A., Salvatori, D., Mikkers, H.M.M., Verbeek, S.J. & Staal, F.J.T. 2017. Axin2-mTurquoise2: A novel reporter mouse model for the detection of canonical Wnt signalling. *genesis,* 55**,** e23068-n/a.

DeCarolis, N.A., Mechanic, M., Petrik, D., Carlton, A., Ables, J.L., Malhotra, S., Bachoo, R., Götz, M., Lagace, D.C. & Eisch, A.J. 2013. *In vivo* contribution of nestin- and GLAST-lineage cells to adult hippocampal neurogenesis. *Hippocampus,* 23**,** 708-719.

Deisseroth, K., Singla, S., Toda, H., Monje, M., Palmer, T.D. & Malenka, R.C. 2004. Excitation-Neurogenesis Coupling in Adult Neural Stem/Progenitor Cells. *Neuron,* 42**,** 535-552.

Delgado, Ana C., Ferrón, Sacri R., Vicente, D., Porlan, E., Perez-Villalba, A., Trujillo, Carmen M., D′ Ocón, P. & Fariñas, I. 2014. Endothelial NT-3 Delivered by Vasculature and CSF Promotes Quiescence of Subependymal Neural Stem Cells through Nitric Oxide Induction. *Neuron,* 83**,** 572-585.

Deng, W., Aimone, J.B. & Gage, F.H. 2010. New neurons and new memories: how does adult hippocampal neurogenesis affect learning and memory? *Nature reviews. Neuroscience,* 11**,** 339-350.

Dennis, C.V., Suh, L.S., Rodriguez, M.L., Kril, J.J. & Sutherland, G.T. 2016. Human adult neurogenesis across the ages: An immunohistochemical study. *Neuropathology and applied neurobiology,* 42**,** 621-638.

Dhaliwal, J. & Lagace, D.C. 2011. Visualization and genetic manipulation of adult neurogenesis using transgenic mice. *European Journal of Neuroscience,* 33**,** 1025-1036.

Dieni, C.V., Nietz, A.K., Panichi, R., Wadiche, J.I. & Overstreet-Wadiche, L. 2013. Distinct Determinants of Sparse Activation during Granule Cell Maturation. *The Journal of Neuroscience,* 33**,** 19131.

Dijke, P.t., Miyazono, K. & Heldin, C.-H. 1996. Signaling via hetero-oligomeric complexes of type I and type II serine/threonine kinase receptors. *Current Opinion in Cell Biology,* 8**,** 139-145.

Doetsch, F. & Alvarez-Buylla, A. 1996. Network of tangential pathways for neuronal migration in adult mammalian brain. *Proceedings of the National Academy of Sciences,* 93**,** 14895.

Doetsch, F., Caillé, I., Lim, D.A., García-Verdugo, J.M. & Alvarez-Buylla, A. 1999. Subventricular Zone Astrocytes Are Neural Stem Cells in the Adult Mammalian Brain. *Cell,* 97**,** 703-716.

Donovan, M.H., Yamaguchi, M. & Eisch, A.J. 2008. Dynamic expression of TrkB receptor protein on proliferating and maturing cells in the adult mouse dentate gyrus. *Hippocampus,* 18**,** 435-439.

Douet, V., Arikawa-Hirasawa, E. & Mercier, F. 2012. Fractone-heparan sulfates mediate BMP-7 inhibition of cell proliferation in the adult subventricular zone. *Neuroscience Letters,* 528**,** 120-125.

Driscoll, I., Howard, S.R., Stone, J.C., Monfils, M.H., Tomanek, B., Brooks, W.M. & Sutherland, R.J. 2006. The aging hippocampus: A multi-level analysis in the rat. *Neuroscience,* 139**,** 1173-1185.

Dulken, B.W., Leeman, D.S., Boutet, S.C., Hebestreit, K. & Brunet, A. 2017. Single-Cell Transcriptomic Analysis Defines Heterogeneity and Transcriptional Dynamics in the Adult Neural Stem Cell Lineage. *Cell reports,* 18**,** 777-790.

Dumitru, I., Neitz, A., Alfonso, J. & Monyer, H. 2017. Diazepam Binding Inhibitor Promotes Stem Cell Expansion Controlling Environment-Dependent Neurogenesis. *Neuron,* 94**,** 125-137.e5.

Dupret, D., Revest, J.-M., Koehl, M., Ichas, F., De Giorgi, F., Costet, P., Abrous, D.N. & Piazza, P.V. 2008. Spatial relational memory requires hippocampal adult neurogenesis. *PloS one,* 3**,** e1959-e1959.

Eaton, S., Wepf, R. & Simons, K. 1996. Roles for Rac1 and Cdc42 in planar polarization and hair outgrowth in the wing of Drosophila. *The Journal of Cell Biology,* 135**,** 1277-1289.

Eckenhoff, M.F. & Rakic, P. 1984. Radial organization of the hippocampal dentate gyrus: A Golgi, ultrastructural, and immunocytochemical analysis in the developing rhesus monkey. *Journal of Comparative Neurology,* 223**,** 1-21.

Eckenhoff, M.F. & Rakic, P. 1988. Nature and fate of proliferative cells in the hippocampal dentate gyrus during the life span of the rhesus monkey. *The Journal of neuroscience : the official journal of the Society for Neuroscience,* 8**,** 2729-2747.

Ehm, O., Göritz, C., Covic, M., Schäffner, I., Schwarz, T.J., Karaca, E., Kempkes, B., Kremmer, E., Pfrieger, F.W., Espinosa, L., Bigas, A., Giachino, C., Taylor, V., Frisén, J. & Lie, D.C. 2010. RBPJκ-Dependent Signaling Is Essential for Long-Term Maintenance of Neural Stem Cells in the Adult Hippocampus. *The Journal of Neuroscience,* 30**,** 13794.

Ekdahl, C.T., Claasen, J.-H., Bonde, S., Kokaia, Z. & Lindvall, O. 2003. Inflammation is detrimental for neurogenesis in adult brain. *Proceedings of the National Academy of Sciences,* 100**,** 13632.

Ellwanger, K., Saito, H., Clément-Lacroix, P., Maltry, N., Niedermeyer, J., Lee, W.K., Baron, R., Rawadi, G., Westphal, H. & Niehrs, C. 2008. Targeted Disruption of the Wnt Regulator Kremen Induces Limb Defects and High Bone Density. *Molecular and Cellular Biology,* 28**,** 4875.

Elmi, M., Matsumoto, Y., Zeng, Z.-j., Lakshminarasimhan, P., Yang, W., Uemura, A., Nishikawa, S.-i., Moshiri, A., Tajima, N., Ågren, H. & Funa, K. 2010. TLX activates MASH1 for induction of neuronal lineage commitment of adult hippocampal neuroprogenitors. *Molecular and Cellular Neuroscience,* 45**,** 121-131.

Elmore, S. 2007. Apoptosis: a review of programmed cell death. *Toxicologic pathology,* 35**,** 495-516.

Encinas, J.M., Michurina, T.V., Peunova, N., Park, J.-H., Tordo, J., Peterson, D.A., Fishell, G., Koulakov, A. & Enikolopov, G. 2011. Division-coupled astrocytic differentiation and age-related depletion of neural stem cells in the adult hippocampus. *Cell stem cell,* 8**,** 566-79.

Erickson, M.A., Morofuji, Y., Owen, J.B. & Banks, W.A. 2014. Rapid transport of CCL11 across the blood-brain barrier: regional variation and importance of blood cells. *The Journal of pharmacology and experimental therapeutics,* 349**,** 497-507.

Eriksson, P.S., Perfilieva, E., Bjork-Eriksson, T., Alborn, A.-M., Nordborg, C., Peterson, D.A. & Gage, F.H. 1998. Neurogenesis in the adult human hippocampus. *Nat Med,* 4**,** 1313-1317.

Ernst, A., Alkass, K., Bernard, S., Salehpour, M., Perl, S., Tisdale, J., Possnert, G., Druid, H. & Frisén, J. 2014. Neurogenesis in the Striatum of the Adult Human Brain. *Cell,* 156**,** 1072-1083.

Espósito, M.S., Piatti, V.C., Laplagne, D.A., Morgenstern, N.A., Ferrari, C.C., Pitossi, F.J. & Schinder, A.F. 2005. Neuronal differentiation in the adult hippocampus recapitulates embryonic development. *The Journal of neuroscience : the official journal of the Society for Neuroscience,* 25**,** 10074-10086.

Fabel, K., Fabel, K., Tam, B., Kaufer, D., Baiker, A., Simmons, N., Kuo, C.J. & Palmer, T.D. 2003. VEGF is necessary for exercise-induced adult hippocampal neurogenesis. *European Journal of Neuroscience,* 18**,** 2803-2812.

Fabel, K., Wolf, S.A., Ehninger, D., Babu, H., Leal-Galicia, P. & Kempermann, G. 2009. Additive effects of physical exercise and environmental enrichment on adult hippocampal neurogenesis in mice. *Frontiers in neuroscience,* 3**,** 50-50.

Fagotto, F., Glück, U. & Gumbiner, B.M. 1998. Nuclear localization signal-independent and importin/karyopherin-independent nuclear import of β-catenin. *Current Biology,* 8**,** 181-190.

Faigle, R. & Song, H. 2013. Signaling mechanisms regulating adult neural stem cells and neurogenesis. *Biochimica et biophysica acta,* 1830**,** 2435-2448.

Fan, X., Xu, H., Cai, W., Yang, Z. & Zhang, J. 2003. Spatial and temporal patterns of expression of Noggin and BMP4 in embryonic and postnatal rat hippocampus. *Developmental Brain Research,* 146**,** 51-58.

Fang, L., Zhu, Q., Neuenschwander, M., Specker, E., Wulf-Goldenberg, A., Weis, W.I., von Kries, J.P. & Birchmeier, W. 2016. A Small-Molecule Antagonist of the β-Catenin/TCF4 Interaction Blocks the Self-Renewal of Cancer Stem Cells and Suppresses Tumorigenesis. *Cancer Research,* 76**,** 891.

Fanto, M., Weber, U., Strutt, D.I. & Mlodzik, M. 2000. Nuclear signaling by Rac and Rho GTPases is required in the establishment of epithelial planar polarity in the Drosophila eye. *Current Biology,* 10**,** 979-S1.

Farías, G.G., Alfaro, I.E., Cerpa, W., Grabowski, C.P., Godoy, J.A., Bonansco, C. & Inestrosa, N.C. 2009. Wnt-5a/JNK Signaling Promotes the Clustering of PSD-95 in Hippocampal Neurons. *Journal of Biological Chemistry,* 284**,** 15857-15866.

Feil, R., Wagner, J., Metzger, D. & Chambon, P. 1997. Regulation of Cre Recombinase Activity by Mutated Estrogen Receptor Ligand-Binding Domains. *Biochemical and Biophysical Research Communications,* 237**,** 752-757.

Ferraro, F., Celso, C.L. & Scadden, D. 2010. Adult stem cells and their niches. *Advances in experimental medicine and biology,* 695**,** 155-168.

Ferrer-Vaquer, A., Piliszek, A., Tian, G., Aho, R.J., Dufort, D. & Hadjantonakis, A.-K. 2010. A sensitive and bright single-cell resolution live imaging reporter of Wnt/ß-catenin signaling in the mouse. *BMC developmental biology,* 10**,** 121-121.

Feske, S., Okamura, H., Hogan, P.G. & Rao, A. 2003. Ca2+/calcineurin signalling in cells of the immune system. *Biochemical and Biophysical Research Communications,* 311**,** 1117-1132.

Fiedler, M., Mendoza-Topaz, C., Rutherford, T.J., Mieszczanek, J. & Bienz, M. 2011. Dishevelled interacts with the DIX domain polymerization interface of Axin to interfere with its function in down-regulating β-catenin. *Proceedings of the National Academy of Sciences,* 108**,** 1937.

Filali, M., Cheng, N., Abbott, D., Leontiev, V. & Engelhardt, J.F. 2002. Wnt-3A/β-catenin signaling induces transcription from the LEF-1 promoter. *J Biol Chem,* 277**,** 33398-410.

Filippov, V., Kronenberg, G., Pivneva, T., Reuter, K., Steiner, B., Wang, L.-P., Yamaguchi, M., Kettenmann, H. & Kempermann, G. 2003. Subpopulation of nestin-expressing progenitor cells in the adult murine hippocampus shows electrophysiological and morphological characteristics of astrocytes. *Molecular and Cellular Neuroscience,* 23**,** 373-382.

Finch, P.W., He, X., Kelley, M.J., Üren, A., Schaudies, R.P., Popescu, N.C., Rudikoff, S., Aaronson, S.A., Varmus, H.E. & Rubin, J.S. 1997. Purification and molecular cloning of a secreted, Frizzled-related antagonist of Wnt action. *Proceedings of the National Academy of Sciences of the United States of America,* 94**,** 6770-6775.

Fiorentini, A., Rosi, M.C., Grossi, C., Luccarini, I. & Casamenti, F. 2010. Lithium Improves Hippocampal Neurogenesis, Neuropathology and Cognitive Functions in APP Mutant Mice. *PLOS ONE,* 5**,** e14382.

Font, E., Desfilis, E., Pérez-Cañellas, M.M. & García-Verdugo, J.M. 2001. Neurogenesis and Neuronal Regeneration in the Adult Reptilian Brain. *Brain, Behavior and Evolution,* 58**,** 276-295.

Frederiksen, K. & McKay, R.D. 1988. Proliferation and differentiation of rat neuroepithelial precursor cells in vivo. *The Journal of neuroscience : the official journal of the Society for Neuroscience,* 8**,** 1144-1151.

Freyer, J.P. 1998. Decreased mitochondrial function in quiescent cells isolated from multicellular tumor spheroids. *Journal of Cellular Physiology,* 176**,** 138-149.

Fuentealba, L.C., Obernier, K. & Alvarez-Buylla, A. 2012. Adult neural stem cells bridge their niche. *Cell stem cell,* 10**,** 698-708.

Fuentealba, Luis C., Rompani, Santiago B., Parraguez, Jose I., Obernier, K., Romero, R., Cepko, Constance L. & Alvarez-Buylla, A. 2015. Embryonic Origin of Postnatal Neural Stem Cells. *Cell,* 161**,** 1644-1655.

Fuerer, C. & Nusse, R. 2010. Lentiviral Vectors to Probe and Manipulate the Wnt Signaling Pathway. *PLoS ONE,* 5**,** e9370.

Fukuda, S., Kato, F., Tozuka, Y., Yamaguchi, M., Miyamoto, Y. & Hisatsune, T. 2003. Two distinct subpopulations of nestin-positive cells in adult mouse dentate gyrus. *The Journal of neuroscience : the official journal of the Society for Neuroscience,* 23**,** 9357-9366.

Füllgrabe, A., Joost, S., Are, A., Jacob, T., Sivan, U., Haegebarth, A., Linnarsson, S., Simons, B.D., Clevers, H., Toftgård, R. & Kasper, M. 2015. Dynamics of Lgr6+ Progenitor Cells in the Hair Follicle, Sebaceous Gland, and Interfollicular Epidermis. *Stem Cell Reports,* 5**,** 843-855.

Furutachi, S., Matsumoto, A., Nakayama, K.I. & Gotoh, Y. 2013. p57 controls adult neural stem cell quiescence and modulates the pace of lifelong neurogenesis. *The EMBO Journal,* 32**,** 970-981.

Gage, F.H., Coates, P.W., Palmer, T.D., Kuhn, H.G., Fisher, L.J., Suhonen, J.O., Peterson, D.A., Suhr, S.T. & Ray, J. 1995. Survival and differentiation of adult neuronal progenitor cells transplanted to the adult brain. *Proceedings of the National Academy of Sciences of the United States of America,* 92**,** 11879-11883.

Galceran, J., Miyashita-Lin, E.M., Devaney, E., Rubenstein, J.L. & Grosschedl, R. 2000. Hippocampus development and generation of dentate gyrus granule cells is regulated by LEF1. *Development,* 127**,** 469.

Galichet, C., Guillemot, F. & Parras, C.M. 2008. Neurogenin 2 has an essential role in development of the dentate gyrus. *Development,* 135**,** 2031.

Gao, Z., Ure, K., Ables, J.L., Lagace, D.C., Nave, K.-A., Goebbels, S., Eisch, A.J. & Hsieh, J. 2009. Neurod1 is essential for the survival and maturation of adult-born neurons. *Nature neuroscience,* 12**,** 1090-1092.

Garbe, D.S. & Ring, R.H. 2012. Investigating Tonic Wnt Signaling Throughout the Adult CNS and in the Hippocampal Neurogenic Niche of BatGal and Ins-TopGal Mice. *Cellular and Molecular Neurobiology,* 32**,** 1159-1174.

Garcia, A.D.R., Petrova, R., Eng, L. & Joyner, A.L. 2010. Sonic Hedgehog Regulates Discrete Populations of Astrocytes in the Adult Mouse Forebrain. *The Journal of Neuroscience,* 30**,** 13597.

Ge, S., Goh, E.L.K., Sailor, K.A., Kitabatake, Y., Ming, G.-l. & Song, H. 2006. GABA regulates synaptic integration of newly generated neurons in the adult brain. *Nature,* 439**,** 589-593.

Ge, S., Yang, C.-h., Hsu, K.-s., Ming, G.-l. & Song, H. 2007. A Critical Period for Enhanced Synaptic Plasticity in Newly Generated Neurons of the Adult Brain. *Neuron,* 54**,** 559-566.

Gebara, E., Bonaguidi, M.A., Beckervordersandforth, R., Sultan, S., Udry, F., Gijs, P.-J., Lie, D.C., Ming, G.-L., Song, H. & Toni, N. 2016. Heterogeneity of Radial Glia-Like Cells in the Adult Hippocampus. *Stem cells (Dayton, Ohio),* 34**,** 997-1010.

Giachino, C., Barz, M., Tchorz, J.S., Tome, M., Gassmann, M., Bischofberger, J., Bettler, B. & Taylor, V. 2014. GABA suppresses neurogenesis in the adult hippocampus through GABAB receptors. *Development,* 141**,** 83.

Gil-Mohapel, J., Simpson, J.M., Ghilan, M. & Christie, B.R. 2011. Neurogenesis in Huntington's disease: Can studying adult neurogenesis lead to the development of new therapeutic strategies? *Brain Research,* 1406**,** 84-105.

Glinka, A., Dolde, C., Kirsch, N., Huang, Y.-L., Kazanskaya, O., Ingelfinger, D., Boutros, M., Cruciat, C.-M. & Niehrs, C. 2011. LGR4 and LGR5 are R-spondin receptors mediating Wnt/β-catenin and Wnt/PCP signalling. *EMBO reports,* 12**,** 1055-1061.

Glinka, A., Wu, W., Delius, H., Monaghan, A.P., Blumenstock, C. & Niehrs, C. 1998. Dickkopf-1 is a member of a new family of secreted proteins and functions in head induction. *Nature,* 391**,** 357-362.

Gobeske, K.T., Das, S., Bonaguidi, M.A., Weiss, C., Radulovic, J., Disterhoft, J.F. & Kessler, J.A. 2009. BMP signaling mediates effects of exercise on hippocampal neurogenesis and cognition in mice. *PloS one,* 4**,** e7506-e7506.

Goldman, S.A. & Nottebohm, F. 1983. Neuronal production, migration, and differentiation in a vocal control nucleus of the adult female canary brain. *Proceedings of the National Academy of Sciences of the United States of America,* 80**,** 2390-2394.

Gonzalez-Reyes, L.E., Chiang, C.-C., Zhang, M., Johnson, J., Arrillaga-Tamez, M., Couturier, N.H., Reddy, N., Starikov, L., Capadona, J.R., Kottmann, A.H. & Durand, D.M. 2019. Sonic Hedgehog is expressed by hilar mossy cells and regulates cellular survival and neurogenesis in the adult hippocampus. *Scientific Reports,* 9**,** 17402.

Gooding, J.M., Yap, K.L. & Ikura, M. 2004. The cadherin–catenin complex as a focal point of cell adhesion and signalling: new insights from three-dimensional structures. *BioEssays,* 26**,** 497-511.

Goodrich, L.V. 2008. The plane facts of PCP in the CNS. *Neuron,* 60**,** 9-16.

Gould, E. 2007. How widespread is adult neurogenesis in mammals? *Nature Reviews Neuroscience,* 8**,** 481-488.

Gould, E., Cameron, H.A., Daniels, D.C., Woolley, C.S. & McEwen, B.S. 1992. Adrenal hormones suppress cell division in the adult rat dentate gyrus. *The Journal of neuroscience : the official journal of the Society for Neuroscience,* 12**,** 3642-3650.

Gould, E., McEwen, B.S., Tanapat, P., Galea, L.A. & Fuchs, E. 1997. Neurogenesis in the dentate gyrus of the adult tree shrew is regulated by psychosocial stress and NMDA receptor activation. *The Journal of neuroscience : the official journal of the Society for Neuroscience,* 17**,** 2492-2498.

Gould, E., Reeves, A.J., Fallah, M., Tanapat, P., Gross, C.G. & Fuchs, E. 1999. Hippocampal neurogenesis in adult Old World primates. *Proceedings of the National Academy of Sciences of the United States of America,* 96**,** 5263-5267.

Gould, E., Tanapat, P., McEwen, B.S., Flügge, G. & Fuchs, E. 1998. Proliferation of granule cell precursors in the dentate gyrus of adult monkeys is diminished by stress. *Proceedings of the National Academy of Sciences of the United States of America,* 95**,** 3168-3171.

Groisman, A.I., Yang, S.M. & Schinder, A.F. 2020. Differential Coupling of Adult-Born Granule Cells to Parvalbumin and Somatostatin Interneurons. *Cell Rep,* 30**,** 202-214 e4.

Gross, C.G. 2000. Neurogenesis in the adult brain: death of a dogma. *Nature Reviews Neuroscience,* 1**,** 67-73.

Gross, J.C., Chaudhary, V., Bartscherer, K. & Boutros, M. 2012. Active Wnt proteins are secreted on exosomes. *Nat Cell Biol,* 14**,** 1036-1045.

Groszer, M., Erickson, R., Scripture-Adams, D.D., Dougherty, J.D., Le Belle, J., Zack, J.A., Geschwind, D.H., Liu, X., Kornblum, H.I. & Wu, H. 2006. PTEN negatively regulates neural stem cell self-renewal by modulating G0-G1 cell cycle entry. *Proceedings of the National Academy of Sciences of the United States of America,* 103**,** 111-116.

Grove, E.A., Tole, S., Limon, J., Yip, L. & Ragsdale, C.W. 1998. The hem of the embryonic cerebral cortex is defined by the expression of multiple Wnt genes and is compromised in Gli3-deficient mice. *Development,* 125**,** 2315.

Grumolato, L., Liu, G., Mong, P., Mudbhary, R., Biswas, R., Arroyave, R., Vijayakumar, S., Economides, A.N. & Aaronson, S.A. 2010. Canonical and noncanonical Wnts use a common mechanism to activate completely unrelated coreceptors. *Genes & Development,* 24**,** 2517-2530.

Gu, Y., Arruda-Carvalho, M., Wang, J., Janoschka, S.R., Josselyn, S.A., Frankland, P.W. & Ge, S. 2012. Optical controlling reveals time-dependent roles for adult-born dentate granule cells. *Nature Neuroscience,* 15**,** 1700-1706.

Guan, K.-L. & Rao, Y. 2003. Signalling mechanisms mediating neuronal responses to guidance cues. *Nature Reviews Neuroscience,* 4**,** 941-956.

Guidi, S., Ciani, E., Severi, S., Contestabile, A. & Bartesaghi, R. 2005. Postnatal neurogenesis in the dentate gyrus of the guinea pig. *Hippocampus,* 15**,** 285-301.

Habas, R., Dawid, I.B. & He, X. 2003. Coactivation of Rac and Rho by Wnt/Frizzled signaling is required for vertebrate gastrulation. *Genes & Development,* 17**,** 295-309.

Habas, R., Kato, Y. & He, X. 2001. Wnt/Frizzled Activation of Rho Regulates Vertebrate Gastrulation and Requires a Novel Formin Homology Protein Daam1. *Cell,* 107**,** 843-854.

Halbleib, J.M. & Nelson, W.J. 2006. Cadherins in development: cell adhesion, sorting, and tissue morphogenesis. *Genes & Development,* 20**,** 3199-3214.

Hall, A.C., Lucas, F.R. & Salinas, P.C. 2000. Axonal Remodeling and Synaptic Differentiation in the Cerebellum Is Regulated by WNT-7a Signaling. *Cell,* 100**,** 525-535.

Hall, A.K. & Miller, R.H. 2004. Emerging roles for bone morphogenetic proteins in central nervous system glial biology. *Journal of Neuroscience Research,* 76**,** 1-8.

Hamblet, N.S., Lijam, N., Ruiz-Lozano, P., Wang, J., Yang, Y., Luo, Z., Mei, L., Chien, K.R., Sussman, D.J. & Wynshaw-Boris, A. 2002. Dishevelled 2 is essential for cardiac outflow tract development, somite segmentation and neural tube closure. *Development,* 129**,** 5827.

Han, K. & Kim, E. 2008a. Synaptic adhesion molecules and PSD-95. *Progress in Neurobiology,* 84**,** 263-283.

Han, Y.-G., Spassky, N., Romaguera-Ros, M., Garcia-Verdugo, J.-M., Aguilar, A., Schneider-Maunoury, S. & Alvarez-Buylla, A. 2008b. Hedgehog signaling and primary cilia are required for the formation of adult neural stem cells. *Nature Neuroscience,* 11**,** 277-284.

Hao, H.-X., Xie, Y., Zhang, Y., Charlat, O., Oster, E., Avello, M., Lei, H., Mickanin, C., Liu, D., Ruffner, H., Mao, X., Ma, Q., Zamponi, R., Bouwmeester, T., Finan, P.M., Kirschner, M.W., Porter, J.A.,

Serluca, F.C. & Cong, F. 2012. ZNRF3 promotes Wnt receptor turnover in an R-spondin-sensitive manner. *Nature,* 485**,** 195-200.

Haque, A., Engel, J., Teichmann, S.A. & Lönnberg, T. 2017. A practical guide to single-cell RNA-sequencing for biomedical research and clinical applications. *Genome Medicine,* 9**,** 75.

Harada, N., Tamai, Y., Ishikawa, T., Sauer, B., Takaku, K., Oshima, M. & Taketo, M.M. 1999. Intestinal polyposis in mice with a dominant stable mutation of the β-catenin gene. *The EMBO Journal,* 18**,** 5931-5942.

Harris, L., Rigo, P., Stiehl, T., Gaber, Z., Austin, S.H.L., del Mar Masdeu, M., Edwards, A., Urbán, N., Marciniak-Czochra, A. & Guillemot, F. 2020. Progressive changes in hippocampal stem cell properties ensure lifelong neurogenesis. *bioRxiv***,** 2020.03.12.987107.

Harrison-Uy, S.J. & Pleasure, S.J. 2012. Wnt signaling and forebrain development. *Cold Spring Harbor perspectives in biology,* 4**,** a008094-a008094.

Hartsock, A. & Nelson, W.J. 2008. Adherens and tight junctions: structure, function and connections to the actin cytoskeleton. *Biochimica et biophysica acta,* 1778**,** 660-669.

Hastings, N.B. & Gould, E. 1999. Rapid extension of axons into the CA3 region by adult-generated granule cells. *Journal of Comparative Neurology,* 413**,** 146-154.

Haubensak, W., Attardo, A., Denk, W. & Huttner, W.B. 2004. Neurons arise in the basal neuroepithelium of the early mammalian telencephalon: a major site of neurogenesis. *Proceedings of the National Academy of Sciences of the United States of America,* 101**,** 3196-3201.

He, X., Semenov, M., Tamai, K. & Zeng, X. 2004. LDL receptor-related proteins 5 and 6 in Wnt/β-catenin signaling: Arrows point the way. *Development,* 131**,** 1663.

Heldin, C.-H., Miyazono, K. & ten Dijke, P. 1997. TGF-β signalling from cell membrane to nucleus through SMAD proteins. *Nature,* 390**,** 465-471.

Herr, P. & Basler, K. 2012. Porcupine-mediated lipidation is required for Wnt recognition by Wls. *Developmental Biology,* 361**,** 392-402.

Herrera, D.G., Garcia-Verdugo, J.M. & Alvarez-Buylla, A. 1999. Adult-derived neural precursors transplanted into multiple regions in the adult brain. *Annals of Neurology,* 46**,** 867-877.

Hikasa, H., Ezan, J., Itoh, K., Li, X., Klymkowsky, M.W. & Sokol, S.Y. 2010. Regulation of TCF3 by Wnt-Dependent Phosphorylation during Vertebrate Axis Specification. *Developmental Cell,* 19**,** 521-532.

Hinck, L., Näthke, I.S., Papkoff, J. & Nelson, W.J. 1994. Dynamics of cadherin/catenin complex formation: novel protein interactions and pathways of complex assembly. *The Journal of cell biology,* 125**,** 1327-1340.

Hirabayashi, Y., Itoh, Y., Tabata, H., Nakajima, K., Akiyama, T., Masuyama, N. & Gotoh, Y. 2004. The Wnt/β-catenin pathway directs neuronal differentiation of cortical neural precursor cells. *Development,* 131**,** 2791-2801.

Hirata, A., Utikal, J., Yamashita, S., Aoki, H., Watanabe, A., Yamamoto, T., Okano, H., Bardeesy, N., Kunisada, T., Ushijima, T., Hara, A., Jaenisch, R., Hochedlinger, K. & Yamada, Y. 2013. Dose-dependent roles for canonical Wnt signalling in de novo crypt formation and cell cycle properties of the colonic epithelium. *Development (Cambridge, England),* 140**,** 66-75.

Hochgerner, H., Zeisel, A., Lönnerberg, P. & Linnarsson, S. 2018. Conserved properties of dentate gyrus neurogenesis across postnatal development revealed by single-cell RNA sequencing. *Nature Neuroscience,* 21**,** 290-299.

Hodge, R.D., Kowalczyk, T.D., Wolf, S.A., Encinas, J.M., Rippey, C., Enikolopov, G., Kempermann, G. & Hevner, R.F. 2008. Intermediate progenitors in adult hippocampal neurogenesis: Tbr2 expression and coordinate regulation of neuronal output. *The Journal of neuroscience : the official journal of the Society for Neuroscience,* 28**,** 3707-3717.

Hodge, R.D., Nelson, B.R., Kahoud, R.J., Yang, R., Mussar, K.E., Reiner, S.L. & Hevner, R.F. 2012. Tbr2 is essential for hippocampal lineage progression from neural stem cells to intermediate progenitors and neurons. *The Journal of Neuroscience,* 32**,** 6275-6287.

Hofmann, K. 2000. A superfamily of membrane-bound O-acyltransferases with implications for Wnt signaling. *Trends in Biochemical Sciences,* 25**,** 111-112.

Hogan, P.G., Chen, L., Nardone, J. & Rao, A. 2003. Transcriptional regulation by calcium, calcineurin, and NFAT. *Genes & Development,* 17**,** 2205-2232.

Hsieh, J.-C., Kodjabachian, L., Rebbert, M.L., Rattner, A., Smallwood, P.M., Samos, C.H., Nusse, R., Dawid, I.B. & Nathans, J. 1999. A new secreted protein that binds to Wnt proteins and inhibits their activites. *Nature,* 398**,** 431-436.

Hsu, S.C., Galceran, J. & Grosschedl, R. 1998. Modulation of transcriptional regulation by LEF-1 in response to Wnt-1 signaling and association with β-catenin. *Molecular and cellular biology,* 18**,** 4807-4818.

Huang, S.-M.A., Mishina, Y.M., Liu, S., Cheung, A., Stegmeier, F., Michaud, G.A., Charlat, O., Wiellette, E., Zhang, Y., Wiessner, S., Hild, M., Shi, X., Wilson, C.J., Mickanin, C., Myer, V., Fazal, A., Tomlinson, R., Serluca, F., Shao, W., Cheng, H., Shultz, M., Rau, C., Schirle, M., Schlegl, J., Ghidelli, S., Fawell, S., Lu, C., Curtis, D., Kirschner, M.W., Lengauer, C., Finan, P.M., Tallarico, J.A., Bouwmeester, T., Porter, J.A., Bauer, A. & Cong, F. 2009. Tankyrase inhibition stabilizes axin and antagonizes Wnt signalling. *Nature,* 461**,** 614-20.

Huber, A.H., Nelson, W.J. & Weis, W.I. 1997. Three-Dimensional Structure of the Armadillo Repeat Region of β-Catenin. *Cell,* 90**,** 871-882.

Huber, A.H. & Weis, W.I. 2001. The Structure of the β-Catenin/E-Cadherin Complex and the Molecular Basis of Diverse Ligand Recognition by β-Catenin. *Cell,* 105**,** 391-402.

Huelsken, J., Vogel, R., Erdmann, B., Cotsarelis, G. & Birchmeier, W. 2001. β-Catenin Controls Hair Follicle Morphogenesis and Stem Cell Differentiation in the Skin. *Cell,* 105**,** 533-545.

Hur, J. & Jeong, S. 2013. Multitasking β-catenin: from adhesion and transcription to RNA regulation. *Animal Cells and Systems,* 17**,** 299-305.

Hussaini, S.M.Q., Choi, C.-I., Cho, C.H., Kim, H.J., Jun, H. & Jang, M.-H. 2014. Wnt signaling in neuropsychiatric disorders: ties with adult hippocampal neurogenesis and behavior. *Neuroscience and biobehavioral reviews,* 47**,** 369-383.

Ikeda, S., Kishida, S., Yamamoto, H., Murai, H., Koyama, S. & Kikuchi, A. 1998. Axin, a negative regulator of the Wnt signaling pathway, forms a complex with GSK-3β and β-catenin and promotes GSK-3β-dependent phosphorylation of β-catenin. *The EMBO journal,* 17**,** 1371-1384.

Ille, F., Atanasoski, S., Falk, S., Ittner, L.M., Märki, D., Büchmann-Møller, S., Wurdak, H., Suter, U., Taketo, M.M. & Sommer, L. 2007. Wnt/BMP signal integration regulates the balance between proliferation and differentiation of neuroepithelial cells in the dorsal spinal cord. *Developmental Biology,* 304**,** 394-408.

Imayoshi, I. & Kageyama, R. 2011. The Role of Notch Signaling in Adult Neurogenesis. *Molecular neurobiology,* 44**,** 7-12.

Imayoshi, I. & Kageyama, R. 2014. bHLH Factors in Self-Renewal, Multipotency, and Fate Choice of Neural Progenitor Cells. *Neuron,* 82**,** 9-23.

Imayoshi, I., Sakamoto, M., Yamaguchi, M., Mori, K. & Kageyama, R. 2010. Essential roles of Notch signaling in maintenance of neural stem cells in developing and adult brains. *The Journal of neuroscience : the official journal of the Society for Neuroscience,* 30**,** 3489-3498.

Ingraham, C.A., Park, G.C., Makarenkova, H.P. & Crossin, K.L. 2011. Matrix metalloproteinase (MMP)-9 induced by Wnt signaling increases the proliferation and migration of embryonic neural stem cells at low O2 levels. *The Journal of biological chemistry,* 286**,** 17649-17657.

Ishitani, T., Ninomiya-Tsuji, J., Nagai, S.I., Nishita, M., Meneghini, M., Barker, N., Waterman, M., Bowerman, B., Clevers, H., Shibuya, H. & Matsumoto, K. 1999. The TAK1-NLK-MAPK-related pathway antagonizes signaling between β-catenin and transcription factor TCF. *Nature,* 399**,** 798-802.

Israsena, N., Hu, M., Fu, W., Kan, L. & Kessler, J.A. 2004. The presence of FGF2 signaling determines whether β-catenin exerts effects on proliferation or neuronal differentiation of neural stem cells. *Developmental biology,* 268**,** 220-31.

Itasaki, N. & Hoppler, S. 2010. Crosstalk between Wnt and bone morphogenic protein signaling: A turbulent relationship. *Developmental Dynamics,* 239**,** 16-33.

Jacobs, B.L., van Praag, H. & Gage, F.H. 2000. Adult brain neurogenesis and psychiatry: a novel theory of depression. *Molecular Psychiatry,* 5**,** 262-269.

Jain, R., Li, D., Gupta, M., Manderfield, L.J., Ifkovits, J.L., Wang, Q., Liu, F., Liu, Y., Poleshko, A., Padmanabhan, A., Raum, J.C., Li, L., Morrisey, E.E., Lu, M.M., Won, K.J. & Epstein, J.A. 2015. HEART DEVELOPMENT. Integration of Bmp and Wnt signaling by Hopx specifies commitment of cardiomyoblasts. *Science,* 348**,** aaa6071.

Janda, C.Y., Dang, L.T., You, C., Chang, J., de Lau, W., Zhong, Z.A., Yan, K.S., Marecic, O., Siepe, D., Li, X., Moody, J.D., Williams, B.O., Clevers, H., Piehler, J., Baker, D., Kuo, C.J. & Garcia, K.C. 2017. Surrogate Wnt agonists that phenocopy canonical Wnt and β-catenin signalling. *Nature,* 545**,** 234-237.

Janda, C.Y., Waghray, D., Levin, A.M., Thomas, C. & Garcia, K.C. 2012. Structural Basis of Wnt Recognition by Frizzled. *Science,* 337**,** 59.

Jang, M.-H., Bonaguidi, M.A., Kitabatake, Y., Sun, J., Song, J., Kang, E., Jun, H., Zhong, C., Su, Y., Guo, J.U., Wang, M.X., Sailor, K.A., Kim, J.-Y., Gao, Y., Christian, K.M., Ming, G.-l. & Song, H. 2013. Secreted frizzled-related protein 3 regulates activity-dependent adult hippocampal neurogenesis. *Cell stem cell,* 12**,** 215-23.

Jessberger, S., Clark, R.E., Broadbent, N.J., Clemenson, G.D., Consiglio, A., Lie, D.C., Squire, L.R. & Gage, F.H. 2009. Dentate gyrus-specific knockdown of adult neurogenesis impairs spatial and object recognition memory in adult rats. *Learning & memory (Cold Spring Harbor, N.Y.),* 16**,** 147-54.

Jessberger, S. & Kempermann, G. 2003. Adult-born hippocampal neurons mature into activity-dependent responsiveness. *European Journal of Neuroscience,* 18**,** 2707-2712.

Jessberger, S. & Parent, J.M. 2015. Epilepsy and Adult Neurogenesis. *Cold Spring Harbor Perspectives in Biology*.

Jessberger, S., Zhao, C., Toni, N., Clemenson, G.D., Li, Y. & Gage, F.H. 2007. Seizure-Associated, Aberrant Neurogenesis in Adult Rats Characterized with Retrovirus-Mediated Cell Labeling. *The Journal of Neuroscience,* 27**,** 9400.

Jho, E.-h., Zhang, T., Domon, C., Joo, C.-K., Freund, J.-N. & Costantini, F. 2002. Wnt/β-Catenin/Tcf Signaling Induces the Transcription of Axin2, a Negative Regulator of the Signaling Pathway. *Molecular and Cellular Biology,* 22**,** 1172-1183.

Jin, K., Sun, Y., Xie, L., Batteur, S., Mao, X.O., Smelick, C., Logvinova, A. & Greenberg, D.A. 2003. Neurogenesis and aging: FGF-2 and HB-EGF restore neurogenesis in hippocampus and subventricular zone of aged mice. *Aging Cell,* 2**,** 175-183.

Jin, K., Zhu, Y., Sun, Y., Mao, X.O., Xie, L. & Greenberg, D.A. 2002. Vascular endothelial growth factor (VEGF) stimulates neurogenesis in vitro and in vivo. *Proceedings of the National Academy of Sciences of the United States of America,* 99**,** 11946-11950.

Jun-ya Kato, H.M., Scott W. Hiebert, Mark E. Ewen, Charles J. Sherr 1993. Direct binding of cyclin D to the retinoblastoma gene product (pRb) and pRb phosphorylation by the cyclin D-dependent kinase CDK4. *Genes & Development,* 7**,** 331-342.

Kadowaki, M., Nakamura, S., Machon, O., Krauss, S., Radice, G.L. & Takeichi, M. 2007. N-cadherin mediates cortical organization in the mouse brain. *Developmental Biology,* 304**,** 22-33.

Kadowaki, T., Wilder, E., Klingensmith, J., Zachary, K. & Perrimon, N. 1996. The segment polarity gene porcupine encodes a putative multitransmembrane protein involved in Wingless processing. *Genes & Development,* 10**,** 3116-3128.

Kageyama, R., Ohtsuka, T., Shimojo, H. & Imayoshi, I. 2008. Dynamic Notch signaling in neural progenitor cells and a revised view of lateral inhibition. *Nature Neuroscience,* 11**,** 1247-1251.

Kakugawa, S., Langton, P.F., Zebisch, M., Howell, S.A., Chang, T.-H., Liu, Y., Feizi, T., Bineva, G., O'Reilly, N., Snijders, A.P., Jones, E.Y. & Vincent, J.-P. 2015. Notum deacylates Wnt proteins to suppress signalling activity. *Nature,* 519**,** 187-192.

Kalamakis, G., Brüne, D., Ravichandran, S., Bolz, J., Fan, W., Ziebell, F., Stiehl, T., Catalá-Martinez, F., Kupke, J., Zhao, S., Llorens-Bobadilla, E., Bauer, K., Limpert, S., Berger, B., Christen, U., Schmezer, P., Mallm, J.P., Berninger, B., Anders, S., del Sol, A., Marciniak-Czochra, A. & Martin-Villalba, A. 2019. Quiescence Modulates Stem Cell Maintenance and Regenerative Capacity in the Aging Brain. *Cell,* 176**,** 1407-1419.e14.

Kamino, M., Kishida, M., Kibe, T., Ikoma, K., Iijima, M., Hirano, H., Tokudome, M., Chen, L., Koriyama, C., Yamada, K., Arita, K. & Kishida, S. 2011. Wnt-5a signaling is correlated with infiltrative activity in human glioma by inducing cellular migration and MMP-2. *Cancer Science,* 102**,** 540-548.

Kang, E., Wen, Z., Song, H., Christian, K.M. & Ming, G.-L. 2016. Adult Neurogenesis and Psychiatric Disorders. *Cold Spring Harbor perspectives in biology,* 8**,** a019026.

Kang, W. & Hebert, J.M. 2015. FGF Signaling Is Necessary for Neurogenesis in Young Mice and Sufficient to Reverse Its Decline in Old Mice. *J Neurosci,* 35**,** 10217-23.

Kaplan, M.S. & Bell, D.H. 1984. Mitotic neuroblasts in the 9-day-old and 11-month-old rodent hippocampus. *The Journal of neuroscience : the official journal of the Society for Neuroscience,* 4**,** 1429-1441.

Kaplan, M.S. & Hinds, J.W. 1977. Neurogenesis in the adult rat: electron microscopic analysis of light radioautographs. *Science,* 197**,** 1092.

Karalay, Ö., Doberauer, K., Vadodaria, K.C., Knobloch, M., Berti, L., Miquelajauregui, A., Schwark, M., Jagasia, R., Taketo, M.M., Tarabykin, V., Lie, D.C. & Jessberger, S. 2011. Prospero-related homeobox 1 gene (Prox1) is regulated by canonical Wnt signaling and has a stage-specific role in adult hippocampal neurogenesis. *Proceedings of the National Academy of Sciences of the United States of America,* 108**,** 5807-5812.

Kaslin, J., Ganz, J. & Brand, M. 2008. Proliferation, neurogenesis and regeneration in the non-mammalian vertebrate brain. *Philosophical transactions of the Royal Society of London. Series B, Biological sciences,* 363**,** 101-122.

Kawaguchi, D., Furutachi, S., Kawai, H., Hozumi, K. & Gotoh, Y. 2013. Dll1 maintains quiescence of adult neural stem cells and segregates asymmetrically during mitosis. *Nature communications,* 4**,** 1880-1880.

Kawai, H., Kawaguchi, D., Kuebrich, B.D., Kitamoto, T., Yamaguchi, M., Gotoh, Y. & Furutachi, S. 2017. Area-Specific Regulation of Quiescent Neural Stem Cells by Notch3 in the Adult Mouse Subependymal Zone. *The Journal of Neuroscience,* 37**,** 11867.

Kazanskaya, O., Glinka, A., del Barco Barrantes, I., Stannek, P., Niehrs, C. & Wu, W. 2004. R-Spondin 2 Is a Secreted Activator of Wnt/β-Catenin Signaling and Is Required for Xenopus Myogenesis. *Developmental Cell,* 7**,** 525-534.

Kazanskaya, O., Glinka, A. & Niehrs, C. 2000. The role of Xenopus dickkopf1 in prechordal plate specification and neural patterning. *Development,* 127**,** 4981.

Kempermann, G. 2011a. The pessimist's and optimist's views of adult neurogenesis. *Cell,* 145**,** 1009-11.

Kempermann, G. 2011b. Seven principles in the regulation of adult neurogenesis. *European Journal of Neuroscience,* 33**,** 1018-1024.

Kempermann, G. 2012. New neurons for 'survival of the fittest'. *Nature Reviews Neuroscience,* 13**,** 727-736.

Kempermann, G., Gage, F.H., Aigner, L., Song, H., Curtis, M.A., Thuret, S., Kuhn, H.G., Jessberger, S., Frankland, P.W., Cameron, H.A., Gould, E., Hen, R., Abrous, D.N., Toni, N., Schinder, A.F., Zhao, X., Lucassen, P.J. & Frisén, J. 2018. Human Adult Neurogenesis: Evidence and Remaining Questions. *Cell stem cell,* 23**,** 25-30.

Kempermann, G., Gast, D. & Gage, F.H. 2002. Neuroplasticity in old age: Sustained fivefold induction of hippocampal neurogenesis by long-term environmental enrichment. *Annals of Neurology,* 52**,** 135-143.

Kempermann, G., Jessberger, S., Steiner, B. & Kronenberg, G. 2004. Milestones of neuronal development in the adult hippocampus. *Trends in Neurosciences,* 27**,** 447-452.

Kempermann, G., Kuhn, H.G. & Gage, F.H. 1997. More hippocampal neurons in adult mice living in an enriched environment. *Nature,* 386**,** 493-495.

Kempermann, G., Kuhn, H.G. & Gage, F.H. 1998. Experience-induced neurogenesis in the senescent dentate gyrus. *The Journal of neuroscience : the official journal of the Society for Neuroscience,* 18**,** 3206-3212.

Kempermann, G., Song, H. & Gage, F.H. 2015. Neurogenesis in the Adult Hippocampus. *Cold Spring Harbor perspectives in biology,* 7**,** a018812-.

Kiecker, C. & Niehrs, C. 2001. A morphogen gradient of Wnt/β-catenin signalling regulates anteroposterior neural patterning in *Xenopus*. *Development,* 128**,** 4189.

Kim, D., Pertea, G., Trapnell, C., Pimentel, H., Kelley, R. & Salzberg, S.L. 2013. TopHat2: accurate alignment of transcriptomes in the presence of insertions, deletions and gene fusions. *Genome Biology,* 14**,** R36.

Kim, E.J., Leung, C.T., Reed, R.R. & Johnson, J.E. 2007. *In vivo* Analysis of Ascl1 Defined Progenitors Reveals Distinct Developmental Dynamics during Adult Neurogenesis and Gliogenesis. *The Journal of Neuroscience,* 27**,** 12764.

Kim, K.-A., Kakitani, M., Zhao, J., Oshima, T., Tang, T., Binnerts, M., Liu, Y., Boyle, B., Park, E., Emtage, P., Funk, W.D. & Tomizuka, K. 2005. Mitogenic Influence of Human R-Spondin1 on the Intestinal Epithelium. *Science,* 309**,** 1256.

Kimble, J.E. & White, J.G. 1981. On the control of germ cell development in Caenorhabditis elegans. *Developmental Biology,* 81**,** 208-219.

Kitagawa, M., Hatakeyama, S., Shirane, M., Matsumoto, M., Ishida, N., Hattori, K., Nakamichi, I., Kikuchi, A., Nakayama, K.-i. & Nakayama, K. 1999. An F-box protein, FWD1, mediates ubiquitin-dependent proteolysis of β-catenin. *The EMBO Journal,* 18**,** 2401-2410.

Kjell, J., Fischer-Sternjak, J., Thompson, A.J., Friess, C., Sticco, M.J., Salinas, F., Cox, J., Martinelli, D.C., Ninkovic, J., Franze, K., Schiller, H.B. & Götz, M. 2020. Defining the Adult Neural Stem Cell Niche Proteome Identifies Key Regulators of Adult Neurogenesis. *Cell stem cell,* 26**,** 277-293.e8.

Klingener, M., Chavali, M., Singh, J., McMillan, N., Coomes, A., Dempsey, P.J., Chen, E.I. & Aguirre, A. 2014. N-cadherin promotes recruitment and migration of neural progenitor cells from the SVZ neural stem cell niche into demyelinated lesions. *The Journal of neuroscience : the official journal of the Society for Neuroscience,* 34**,** 9590-9606.

Knobloch, M., Braun, S.M.G., Zurkirchen, L., von Schoultz, C., Zamboni, N., Arauzo-Bravo, M.J., Kovacs, W.J., Karalay, O., Suter, U., Machado, R.A.C., Roccio, M., Lutolf, M.P., Semenkovich, C.F. & Jessberger, S. 2013. Metabolic control of adult neural stem cell activity by Fasn-dependent lipogenesis. *Nature,* 493**,** 226-230.

Knobloch, M., Pilz, G.-A., Ghesquière, B., Kovacs, W.J., Wegleiter, T., Moore, D.L., Hruzova, M., Zamboni, N., Carmeliet, P. & Jessberger, S. 2017. A Fatty Acid Oxidation-Dependent Metabolic Shift Regulates Adult Neural Stem Cell Activity. *Cell Reports,* 20**,** 2144-2155.

Knoth, R., Singec, I., Ditter, M., Pantazis, G., Capetian, P., Meyer, R.P., Horvat, V., Volk, B. & Kempermann, G. 2010. Murine Features of Neurogenesis in the Human Hippocampus across the Lifespan from 0 to 100 Years. *PLOS ONE,* 5**,** e8809.

Knudsen, K.A., Soler, A.P., Johnson, K.R. & Wheelock, M.J. 1995. Interaction of alpha-actinin with the cadherin/catenin cell-cell adhesion complex via alpha-catenin. *The Journal of Cell Biology,* 130**,** 67-77.

Kohn, A.D. & Moon, R.T. 2005. Wnt and calcium signaling: β-Catenin-independent pathways. *Cell Calcium,* 38**,** 439-446.

Kokovay, E., Wang, Y., Kusek, G., Wurster, R., Lederman, P., Lowry, N., Shen, Q. & Temple, S. 2012. VCAM1 Is Essential to Maintain the Structure of the SVZ Niche and Acts as an Environmental Sensor to Regulate SVZ Lineage Progression. *Cell Stem Cell,* 11**,** 220-230.

Komiya, Y. & Habas, R. 2008. Wnt signal transduction pathways. *Organogenesis,* 4**,** 68-75.

Koo, B.-K., Spit, M., Jordens, I., Low, T.Y., Stange, D.E., van de Wetering, M., van Es, J.H., Mohammed, S., Heck, A.J.R., Maurice, M.M. & Clevers, H. 2012. Tumour suppressor RNF43 is a stem-cell E3 ligase that induces endocytosis of Wnt receptors. *Nature,* 488**,** 665-669.

Koo, J.W. & Duman, R.S. 2008. IL-1β is an essential mediator of the antineurogenic and anhedonic effects of stress. *Proceedings of the National Academy of Sciences,* 105**,** 751.

Korinek, V., Barker, N., Morin, P.J., van Wichen, D., de Weger, R., Kinzler, K.W., Vogelstein, B. & Clevers, H. 1997. Constitutive Transcriptional Activation by a β-Catenin-Tcf Complex in APC−/− Colon Carcinoma. *Science,* 275**,** 1784.

Korkut, C., Ataman, B., Ramachandran, P., Ashley, J., Barria, R., Gherbesi, N. & Budnik, V. 2009. Trans-Synaptic Transmission of Vesicular Wnt Signals through Evi/Wntless. *Cell,* 139**,** 393-404.

Kornack, D.R. & Rakic, P. 1999. Continuation of neurogenesis in the hippocampus of the adult macaque monkey. *Proceedings of the National Academy of Sciences of the United States of America,* 96**,** 5768-5773.

Kronenberg, G., Reuter, K., Steiner, B., Brandt, M.D., Jessberger, S., Yamaguchi, M. & Kempermann, G. 2003. Subpopulations of proliferating cells of the adult hippocampus respond differently to physiologic neurogenic stimuli. *Journal of Comparative Neurology,* 467**,** 455-463.

Kühl, M., Sheldahl, L.C., Malbon, C.C. & Moon, R.T. 2000. Ca2+/Calmodulin-dependent Protein Kinase II Is Stimulated by Wnt and Frizzled Homologs and Promotes Ventral Cell Fates in Xenopus. *Journal of Biological Chemistry,* 275**,** 12701-12711.

Kuhn, H.G., Dickinson-Anson, H. & Gage, F.H. 1996. Neurogenesis in the dentate gyrus of the adult rat: age-related decrease of neuronal progenitor proliferation. *The Journal of neuroscience : the official journal of the Society for Neuroscience,* 16**,** 2027-2033.

Kukekov, V.G., Laywell, E.D., Suslov, O., Davies, K., Scheffler, B., Thomas, L.B., O'Brien, T.F., Kusakabe, M. & Steindler, D.A. 1999. Multipotent Stem/Progenitor Cells with Similar Properties Arise from Two Neurogenic Regions of Adult Human Brain. *Experimental Neurology,* 156**,** 333-344.

Kuwabara, T., Hsieh, J., Muotri, A., Yeo, G., Warashina, M., Lie, D.C., Moore, L., Nakashima, K., Asashima, M. & Gage, F.H. 2009. Wnt-mediated activation of NeuroD1 and retro-elements during adult neurogenesis. *Nature Neuroscience,* 12**,** 1097.

Kuwahara, A., Hirabayashi, Y., Knoepfler, P.S., Taketo, M.M., Sakai, J., Kodama, T. & Gotoh, Y. 2010. Wnt signaling and its downstream target N-myc regulate basal progenitors in the developing neocortex. *Development,* 137**,** 1035.

Kwon, J.S., Everetts, N.J., Wang, X., Wang, W., Della Croce, K., Xing, J. & Yao, G. 2017. Controlling Depth of Cellular Quiescence by an Rb-E2F Network Switch. *Cell reports,* 20**,** 3223-3235.

Kwong, L.N. & Dove, W.F. 2009. APC and its modifiers in colon cancer. *Advances in experimental medicine and biology,* 656**,** 85-106.

Labbé, E., Letamendia, A. & Attisano, L. 2000. Association of Smads with lymphoid enhancer binding factor 1/T cell-specific factor mediates cooperative signaling by the transforming growth factor-beta and wnt pathways. *Proceedings of the National Academy of Sciences of the United States of America,* 97**,** 8358-8363.

Lai, K., Kaspar, B.K., Gage, F.H. & Schaffer, D.V. 2003. Sonic hedgehog regulates adult neural progenitor proliferation in vitro and in vivo. *Nature Neuroscience,* 6**,** 21-27.

Langmead, B. & Salzberg, S.L. 2012. Fast gapped-read alignment with Bowtie 2. *Nature methods,* 9**,** 357-359.

Lavado, A., Lagutin, O.V., Chow, L.M.L., Baker, S.J. & Oliver, G. 2010. Prox1 Is Required for Granule Cell Maturation and Intermediate Progenitor Maintenance During Brain Neurogenesis. *PLOS Biology,* 8**,** e1000460.

Lavado, A. & Oliver, G. 2014. Jagged1 is necessary for postnatal and adult neurogenesis in the dentate gyrus. *Developmental Biology,* 388**,** 11-21.

Lazarov, O. & Marr, R.A. 2010. Neurogenesis and Alzheimer's disease: at the crossroads. *Experimental neurology,* 223**,** 267-281.

Lazarov, O. & Marr, R.A. 2013. Of mice and men: neurogenesis, cognition and Alzheimer's disease. *Frontiers in aging neuroscience,* 5**,** 43-43.

Lee, F.S., Kim, A.H., Khursigara, G. & Chao, M.V. 2001. The uniqueness of being a neurotrophin receptor. *Current Opinion in Neurobiology,* 11**,** 281-286.

Lee, M.A., Park, J.-H., Rhyu, S.Y., Oh, S.-T., Kang, W.-K. & Kim, H.-N. 2014. Wnt3a expression is associated with MMP-9 expression in primary tumor and metastatic site in recurrent or stage IV colorectal cancer. *BMC cancer,* 14**,** 125-125.

Lee, S., Tole, S., Grove, E. & McMahon, A. 2000. A local Wnt-3a signal is required for development of the mammalian hippocampus. *Development,* 127**,** 457-467.

Lee, W., Swarup, S., Chen, J., Ishitani, T. & Verheyen, E.M. 2009. Homeodomain-interacting protein kinases (Hipks) promote Wnt/Wg signaling through stabilization of β-catenin/Arm and stimulation of target gene expression. *Development,* 136**,** 241.

Lendahl, U., Zimmerman, L.B. & McKay, R.D.G. 1990. CNS stem cells express a new class of intermediate filament protein. *Cell,* 60**,** 585-595.

Li, D., Takeda, N., Jain, R., Manderfield, L.J., Liu, F., Li, L., Anderson, S.A. & Epstein, J.A. 2015. Hopx distinguishes hippocampal from lateral ventricle neural stem cells. *Stem cell research,* 15**,** 522-529.

Li, G., Fang, L., Fernández, G. & Pleasure, S.J. 2013. The ventral hippocampus is the embryonic origin for adult neural stem cells in the dentate gyrus. *Neuron,* 78**,** 658-72.

Li, L. & Xie, T. 2005. STEM CELL NICHE: Structure and Function. *Annual Review of Cell and Developmental Biology,* 21**,** 605-631.

Li, Vivian S.W., Ng, Ser S., Boersema, Paul J., Low, Teck Y., Karthaus, Wouter R., Gerlach, Jan P., Mohammed, S., Heck, Albert J.R., Maurice, Madelon M., Mahmoudi, T. & Clevers, H. 2012. Wnt Signaling through Inhibition of β-Catenin Degradation in an Intact Axin1 Complex. *Cell,* 149**,** 1245-1256.

Li, Y., Luikart, B.W., Birnbaum, S., Chen, J., Kwon, C.-H., Kernie, S.G., Bassel-Duby, R. & Parada, L.F. 2008. TrkB Regulates Hippocampal Neurogenesis and Governs Sensitivity to Antidepressive Treatment. *Neuron,* 59**,** 399-412.

Li, Y., Mu, Y. & Gage, F.H. 2009. Chapter 5 Development of Neural Circuits in the Adult Hippocampus. *Current Topics in Developmental Biology.* Academic Press.

Li, Z. & Sheng, M. 2003. Some assembly required: the development of neuronal synapses. *Nature Reviews Molecular Cell Biology,* 4**,** 833-841.

Licht, T., Rothe, G., Kreisel, T., Wolf, B., Benny, O., Rooney, A.G., ffrench-Constant, C., Enikolopov, G. & Keshet, E. 2016. VEGF preconditioning leads to stem cell remodeling and attenuates age-related decay of adult hippocampal neurogenesis. *Proceedings of the National Academy of Sciences,* 113**,** E7828.

Lichtenwalner, R.J., Forbes, M.E., Bennett, S.A., Lynch, C.D., Sonntag, W.E. & Riddle, D.R. 2001. Intracerebroventricular infusion of insulin-like growth factor-I ameliorates the age-related decline in hippocampal neurogenesis. *Neuroscience,* 107**,** 603-613.

Lie, D.-C., Colamarino, S.A., Song, H.-J., Désiré, L., Mira, H., Consiglio, A., Lein, E.S., Jessberger, S., Lansford, H., Dearie, A.R. & Gage, F.H. 2005. Wnt signalling regulates adult hippocampal neurogenesis. *Nature,* 437**,** 1370-5.

Lieberwirth, C. & Wang, Z. 2012. The social environment and neurogenesis in the adult Mammalian brain. *Frontiers in human neuroscience,* 6**,** 118-118.

Lim, D.A., Tramontin, A.D., Trevejo, J.M., Herrera, D.G., García-Verdugo, J.M. & Alvarez-Buylla, A. 2000. Noggin Antagonizes BMP Signaling to Create a Niche for Adult Neurogenesis. *Neuron,* 28**,** 713-726.

Lindsey, B.W. & Tropepe, V. 2006. A comparative framework for understanding the biological principles of adult neurogenesis. *Progress in Neurobiology,* 80**,** 281-307.

Liu, C., Li, Y., Semenov, M., Han, C., Baeg, G.-H., Tan, Y., Zhang, Z., Lin, X. & He, X. 2002. Control of β-Catenin Phosphorylation/Degradation by a Dual-Kinase Mechanism. *Cell,* 108**,** 837-847.

Liu, J., Pan, S., Hsieh, M.H., Ng, N., Sun, F., Wang, T., Kasibhatla, S., Schuller, A.G., Li, A.G., Cheng, D., Li, J., Tompkins, C., Pferdekamper, A., Steffy, A., Cheng, J., Kowal, C., Phung, V., Guo, G., Wang, Y., Graham, M.P., Flynn, S., Brenner, J.C., Li, C., Villarroel, M.C., Schultz, P.G., Wu, X., McNamara, P., Sellers, W.R., Petruzzelli, L., Boral, A.L., Seidel, H.M., McLaughlin, M.E., Che, J., Carey, T.E., Vanasse, G. & Harris, J.L. 2013. Targeting Wnt-driven cancer through the inhibition of Porcupine by LGK974. *Proceedings of the National Academy of Sciences of the United States of America,* 110**,** 20224-20229.

Liu, X., Wang, Q., Haydar, T.F. & Bordey, A. 2005. Nonsynaptic GABA signaling in postnatal subventricular zone controls proliferation of GFAP-expressing progenitors. *Nature Neuroscience,* 8**,** 1179-1187.

Liu, Y., Elf, S.E., Miyata, Y., Sashida, G., Liu, Y., Huang, G., Di Giandomenico, S., Lee, J.M., Deblasio, A., Menendez, S., Antipin, J., Reva, B., Koff, A. & Nimer, S.D. 2009. p53 regulates hematopoietic stem cell quiescence. *Cell stem cell,* 4**,** 37-48.

Lledo, P.-M., Alonso, M. & Grubb, M.S. 2006. Adult neurogenesis and functional plasticity in neuronal circuits. *Nat Rev Neurosci,* 7**,** 179-193.

Llorens-Bobadilla, E., Zhao, S., Baser, A., Saiz-Castro, G., Zwadlo, K. & Martin-Villalba, A. 2015. Single-Cell Transcriptomics Reveals a Population of Dormant Neural Stem Cells that Become Activated upon Brain Injury. *Cell Stem Cell,* 17**,** 329-340.

Llorens-Martín, M., Torres-Alemán, I. & Trejo, J.L. 2010. Exercise modulates insulin-like growth factor 1-dependent and -independent effects on adult hippocampal neurogenesis and behaviour. *Molecular and Cellular Neuroscience,* 44**,** 109-117.

Loftis, J.M., Huckans, M. & Morasco, B.J. 2010. Neuroimmune mechanisms of cytokine-induced depression: Current theories and novel treatment strategies. *Neurobiology of Disease,* 37**,** 519-533.

Logan, C.Y. & Nusse, R. 2004. The Wnt signalling pathway in development and disease. *Annual Review of Cell and Developmental Biology,* 20**,** 781-810.

Lois, C. & Alvarez-Buylla, A. 1994. Long-distance neuronal migration in the adult mammalian brain. *Science,* 264**,** 1145.

Lois, C., García-Verdugo, J.-M. & Alvarez-Buylla, A. 1996. Chain Migration of Neuronal Precursors. *Science,* 271**,** 978.

Lowy, A.M., Clements, W.M., Bishop, J., Kong, L., Bonney, T., Sisco, K., Aronow, B., Fenoglio-Preiser, C. & Groden, J. 2006. β-Catenin/Wnt Signaling Regulates Expression of the Membrane Type 3 Matrix Metalloproteinase in Gastric Cancer. *Cancer Research,* 66**,** 4734.

Lu, B., Pang, P.T. & Woo, N.H. 2005. The yin and yang of neurotrophin action. *Nature Reviews Neuroscience,* 6**,** 603-614.

Lu, L., Bao, G., Chen, H., Xia, P., Fan, X., Zhang, J., Pei, G. & Ma, L. 2003. Modification of hippocampal neurogenesis and neuroplasticity by social environments. *Experimental Neurology,* 183**,** 600-609.

Lu, W., Yamamoto, V., Ortega, B. & Baltimore, D. 2004a. Mammalian Ryk Is a Wnt Coreceptor Required for Stimulation of Neurite Outgrowth. *Cell,* 119**,** 97-108.

Lu, X., Borchers, A.G.M., Jolicoeur, C., Rayburn, H., Baker, J.C. & Tessier-Lavigne, M. 2004b. PTK7/CCK-4 is a novel regulator of planar cell polarity in vertebrates. *Nature,* 430**,** 93-98.

Lucas, F.R., Goold, R.G., Gordon-Weeks, P.R. & Salinas, P.C. 1998. Inhibition of GSK-3β leading to the loss of phosphorylated MAP-1B is an early event in axonal remodelling induced by WNT-7a or lithium. *Journal of Cell Science,* 111**,** 1351.

Lucas, F.R. & Salinas, P.C. 1997. WNT-7a Induces Axonal Remodeling and Increases Synapsin I Levels in Cerebellar Neurons. *Developmental Biology,* 192**,** 31-44.

Lugert, S., Basak, O., Knuckles, P., Haussler, U., Fabel, K., Götz, M., Haas, C.A., Kempermann, G., Taylor, V. & Giachino, C. 2010. Quiescent and Active Hippocampal Neural Stem Cells with Distinct Morphologies Respond Selectively to Physiological and Pathological Stimuli and Aging. *Cell Stem Cell,* 6**,** 445-456.

Luis, Tiago C., Naber, Brigitta A.E., Roozen, Paul P.C., Brugman, Martijn H., de Haas, Edwin F.E., Ghazvini, M., Fibbe, Willem E., van Dongen, Jacques J.M., Fodde, R. & Staal, Frank J.T. 2011. Canonical Wnt Signaling Regulates Hematopoiesis in a Dosage-Dependent Fashion. *Cell Stem Cell,* 9**,** 345-356.

Luskin, M.B. 1993. Restricted proliferation and migration of postnatally generated neurons derived from the forebrain subventricular zone. *Neuron,* 11**,** 173-189.

Lustig, B., Jerchow, B., Sachs, M., Weiler, S., Pietsch, T., Karsten, U., van de Wetering, M., Clevers, H., Schlag, P.M., Birchmeier, W. & Behrens, J. 2002. Negative Feedback Loop of Wnt Signaling through Upregulation of Conductin/Axin2 in Colorectal and Liver Tumors. *Molecular and Cellular Biology,* 22**,** 1184-1193.

Lyu, J. & Joo, C.-K. 2005. Wnt-7a Up-regulates Matrix Metalloproteinase-12 Expression and Promotes Cell Proliferation in Corneal Epithelial Cells during Wound Healing. *Journal of Biological Chemistry,* 280**,** 21653-21660.

Machon, O., Backman, M., Machonova, O., Kozmik, Z., Vacik, T., Andersen, L. & Krauss, S. 2007. A dynamic gradient of Wnt signaling controls initiation of neurogenesis in the mammalian cortex and cellular specification in the hippocampus. *Developmental Biology,* 311**,** 223-237.

Machon, O., van den Bout, C.J., Backman, M., Kemler, R. & Krauss, S. 2003. Role of β-catenin in the developing cortical and hippocampal neuroepithelium. *Neuroscience,* 122**,** 129-143.

Mao, B., Wu, W., Li, Y., Hoppe, D., Stannek, P., Glinka, A. & Niehrs, C. 2001. LDL-receptor-related protein 6 is a receptor for Dickkopf proteins. *Nature,* 411**,** 321-5.

Mao, Y., Ge, X., Frank, C.L., Madison, J.M., Koehler, A.N., Doud, M.K., Tassa, C., Berry, E.M., Soda, T., Singh, K.K., Biechele, T., Petryshen, T.L., Moon, R.T., Haggarty, S.J. & Tsai, L.-H. 2009. DISC1 regulates neural progenitor proliferation via modulation of GSK3β/β-catenin signaling. *Cell,* 136**,** 1017-1031.

Mardones, M.D., Andaur, G.A., Varas-Godoy, M., Henriquez, J.F., Salech, F., Behrens, M.I., Couve, A., Inestrosa, N.C. & Varela-Nallar, L. 2016. Frizzled-1 receptor regulates adult hippocampal neurogenesis. *Molecular Brain,* 9**,** 29.

Maretto, S., Cordenonsi, M., Dupont, S., Braghetta, P., Broccoli, V., Hassan, A.B., Volpin, D., Bressan, G.M. & Piccolo, S. 2003. Mapping Wnt/β-catenin signaling during mouse development and in colorectal tumors. *Proceedings of the National Academy of Sciences of the United States of America,* 100**,** 3299-3304.

Marín-Burgin, A., Mongiat, L.A., Pardi, M.B. & Schinder, A.F. 2012. Unique Processing During a Period of High Excitation/Inhibition Balance in Adult-Born Neurons. *Science,* 335**,** 1238.

Marlow, F., Topczewski, J., Sepich, D. & Solnica-Krezel, L. 2002. Zebrafish Rho Kinase 2 Acts Downstream of Wnt11 to Mediate Cell Polarity and Effective Convergence and Extension Movements. *Current Biology,* 12**,** 876-884.

Marr, D. & Brindley, G.S. 1971. Simple memory: a theory for archicortex. *Philosophical Transactions of the Royal Society of London. B, Biological Sciences,* 262**,** 23-81.

Martynoga, B., Mateo, J.L., Zhou, B., Andersen, J., Achimastou, A., Urbán, N., van den Berg, D., Georgopoulou, D., Hadjur, S., Wittbrodt, J., Ettwiller, L., Piper, M., Gronostajski, R.M. & Guillemot, F. 2013. Epigenomic enhancer annotation reveals a key role for NFIX in neural stem cell quiescence. *Genes & development,* 27**,** 1769-86.

Mathews, K.J., Allen, K.M., Boerrigter, D., Ball, H., Shannon Weickert, C. & Double, K.L. 2017. Evidence for reduced neurogenesis in the aging human hippocampus despite stable stem cell markers. *Aging cell,* 16**,** 1195-1199.

Maurer, M.H., Tripps, W.K.C., Feldmann, R.E. & Kuschinsky, W. 2003. Expression of vascular endothelial growth factor and its receptors in rat neural stem cells. *Neuroscience Letters,* 344**,** 165-168.

McGough, I.J. & Vincent, J.-P. 2016. Exosomes in developmental signalling. *Development,* 143**,** 2482.

McGrew, L.L., Lai, C.-J. & Moon, R.T. 1995. Specification of the Anteroposterior Neural Axis through Synergistic Interaction of the Wnt Signaling Cascade withnogginandfollistatin. *Developmental Biology,* 172**,** 337-342.

McMahon, A.P. & Bradley, A. 1990. The Wnt-1 (int-1) proto-oncogene is required for development of a large region of the mouse brain. *Cell,* 62**,** 1073-1085.

McMahon, A.P. & Moon, R.T. 1989. Ectopic expression of the proto-oncogene int-1 in Xenopus embryos leads to duplication of the embryonic axis. *Cell,* 58**,** 1075-1084.

McQuate, A., Latorre-Esteves, E. & Barria, A. 2017. A Wnt/Calcium Signaling Cascade Regulates Neuronal Excitability and Trafficking of NMDARs. *Cell Rep,* 21**,** 60-69.

Megason, S.G. & McMahon, A.P. 2002. A mitogen gradient of dorsal midline Wnts organizes growth in the CNS. *Development,* 129**,** 2087.

Meletis, K., Wirta, V., Hede, S.-M., Nistér, M., Lundeberg, J. & Frisén, J. 2006. p53 suppresses the self-renewal of adult neural stem cells. *Development,* 133**,** 363.

Mercier, F. & Douet, V. 2014. Bone morphogenetic protein-4 inhibits adult neurogenesis and is regulated by fractone-associated heparan sulfates in the subventricular zone. *Journal of Chemical Neuroanatomy,* 57-58**,** 54-61.

Merkle, F.T., Mirzadeh, Z. & Alvarez-Buylla, A. 2007. Mosaic Organization of Neural Stem Cells in the Adult Brain. *Science,* 317**,** 381.

Metzis, V., Steinhauser, S., Pakanavicius, E., Gouti, M., Stamataki, D., Ivanovitch, K., Watson, T., Rayon, T., Mousavy Gharavy, S.N., Lovell-Badge, R., Luscombe, N.M. & Briscoe, J. 2018. Nervous System Regionalization Entails Axial Allocation before Neural Differentiation. *Cell,* 175**,** 1105-1118.e17.

Mignone, J.L., Kukekov, V., Chiang, A.-S., Steindler, D. & Enikolopov, G. 2004. Neural stem and progenitor cells in nestin-GFP transgenic mice. *Journal of Comparative Neurology,* 469**,** 311-324.

Miller, B.R. & Hen, R. 2015. The current state of the neurogenic theory of depression and anxiety. *Current opinion in neurobiology,* 30**,** 51-58.

Miller, F.D. & Kaplan, D.R. 2001. Neurotrophin signalling pathways regulating neuronal apoptosis. *Cellular and Molecular Life Sciences CMLS,* 58**,** 1045-1053.

Mineur, Y.S., Belzung, C. & Crusio, W.E. 2007. Functional implications of decreases in neurogenesis following chronic mild stress in mice. *Neuroscience,* 150**,** 251-259.

Ming, G.-L. & Song, H. 2011. Adult neurogenesis in the mammalian brain: significant answers and significant questions. *Neuron,* 70**,** 687-702.

Mira, H., Andreu, Z., Suh, H., Lie, D.C., Jessberger, S., Consiglio, A., San Emeterio, J., Hortigüela, R., Marqués-Torrejón, M.Á., Nakashima, K., Colak, D., Götz, M., Fariñas, I. & Gage, F.H. 2010. Signaling through BMPR-IA Regulates Quiescence and Long-Term Activity of Neural Stem Cells in the Adult Hippocampus. *Cell Stem Cell,* 7**,** 78-89.

Miranda, C.J., Braun, L., Jiang, Y., Hester, M.E., Zhang, L., Riolo, M., Wang, H., Rao, M., Altura, R.A. & Kaspar, B.K. 2012. Aging brain microenvironment decreases hippocampal neurogenesis through Wnt-mediated survivin signaling. *Aging cell,* 11**,** 542-52.

Mirzadeh, Z., Merkle, F.T., Soriano-Navarro, M., Garcia-Verdugo, J.M. & Alvarez-Buylla, A. 2008. Neural stem cells confer unique pinwheel architecture to the ventricular surface in neurogenic regions of the adult brain. *Cell stem cell,* 3**,** 265-278.

Miyata, T., Kawaguchi, A., Saito, K., Kawano, M., Muto, T. & Ogawa, M. 2004. Asymmetric production of surface-dividing and non-surface-dividing cortical progenitor cells. *Development,* 131**,** 3133.

Mizrak, D., Levitin, H.M., Delgado, A.C., Crotet, V., Yuan, J., Chaker, Z., Silva-Vargas, V., Sims, P.A. & Doetsch, F. 2019. Single-Cell Analysis of Regional Differences in Adult V-SVZ Neural Stem Cell Lineages. *Cell reports,* 26**,** 394-406.e5.

Molenaar, M., van de Wetering, M., Oosterwegel, M., Peterson-Maduro, J., Godsave, S., Korinek, V., Roose, J., Destrée, O. & Clevers, H. 1996. XTcf-3 Transcription Factor Mediates β-Catenin-Induced Axis Formation in Xenopus Embryos. *Cell,* 86**,** 391-399.

Mongiat, L.A., Espósito, M.S., Lombardi, G. & Schinder, A.F. 2009. Reliable Activation of Immature Neurons in the Adult Hippocampus. *PLOS ONE,* 4**,** e5320.

Moreno-Jiménez, E.P., Flor-García, M., Terreros-Roncal, J., Rábano, A., Cafini, F., Pallas-Bazarra, N., Ávila, J. & Llorens-Martín, M. 2019. Adult hippocampal neurogenesis is abundant in neurologically healthy subjects and drops sharply in patients with Alzheimer's disease. *Nature Medicine*.

Mori, T., Tanaka, K., Buffo, A., Wurst, W., Kühn, R. & Götz, M. 2006. Inducible gene deletion in astroglia and radial glia—A valuable tool for functional and lineage analysis. *Glia,* 54**,** 21-34.

Morrison, S.J. & Spradling, A.C. 2008. Stem cells and niches: mechanisms that promote stem cell maintenance throughout life. *Cell,* 132**,** 598-611.

Morshead, C.M., Reynolds, B.A., Craig, C.G., McBurney, M.W., Staines, W.A., Morassutti, D., Weiss, S. & van der Kooy, D. 1994. Neural stem cells in the adult mammalian forebrain: A relatively quiescent subpopulation of subependymal cells. *Neuron,* 13**,** 1071-1082.

Moss, J., Gebara, E., Bushong, E.A., Sánchez-Pascual, I., O'Laoi, R., El M'Ghari, I., Kocher-Braissant, J., Ellisman, M.H. & Toni, N. 2016. Fine processes of Nestin-GFP-positive radial glia-like stem cells in the adult dentate gyrus ensheathe local synapses and vasculature. *Proceedings of the National Academy of Sciences of the United States of America,* 113**,** E2536-E2545.

Mulligan, K.A. & Cheyette, B.N.R. 2012. Wnt signaling in vertebrate neural development and function. *Journal of neuroimmune pharmacology : the official journal of the Society on NeuroImmune Pharmacology,* 7**,** 774-787.

Muñoz Descalzo, S. & Martinez Arias, A. 2012. The structure of Wntch signalling and the resolution of transition states in development. *Seminars in Cell & Developmental Biology,* 23**,** 443-449.

Murai, K., Qu, Q., Sun, G., Ye, P., Li, W., Asuelime, G., Sun, E., Tsai, G.E. & Shi, Y. 2014. Nuclear receptor TLX stimulates hippocampal neurogenesis and enhances learning and memory in a transgenic mouse model. *Proceedings of the National Academy of Sciences,* 111**,** 9115.

Nácher, J., Varea, E., Miguel Blasco-Ibáñez, J., Gómez-Climent, M.Á., Castillo-Gómez, E., Crespo, C., Martínez-Guijarro, F.J. & McEwen, B.S. 2007. N-methyl-d-aspartate receptor expression during adult neurogenesis in the rat dentate gyrus. *Neuroscience,* 144**,** 855-864.

Najdi, R., Proffitt, K., Sprowl, S., Kaur, S., Yu, J., Covey, T.M., Virshup, D.M. & Waterman, M.L. 2012. A uniform human Wnt expression library reveals a shared secretory pathway and unique signaling activities. *Differentiation,* 84**,** 203-213.

Namba, T., Mochizuki, H., Onodera, M., Mizuno, Y., Namiki, H. & Seki, T. 2005. The fate of neural progenitor cells expressing astrocytic and radial glial markers in the postnatal rat dentate gyrus. *European Journal of Neuroscience,* 22**,** 1928-1941.

Nishita, M., Yoo, S.K., Nomachi, A., Kani, S., Sougawa, N., Ohta, Y., Takada, S., Kikuchi, A. & Minami, Y. 2006. Filopodia formation mediated by receptor tyrosine kinase Ror2 is required for Wnt5a-induced cell migration. *The Journal of cell biology,* 175**,** 555-562.

Noctor, S.C., Flint, A.C., Weissman, T.A., Dammerman, R.S. & Kriegstein, A.R. 2001. Neurons derived from radial glial cells establish radial units in neocortex. *Nature,* 409**,** 714-720.

Noctor, S.C., Martínez-Cerdeño, V., Ivic, L. & Kriegstein, A.R. 2004. Cortical neurons arise in symmetric and asymmetric division zones and migrate through specific phases. *Nature Neuroscience,* 7**,** 136-144.

Noordermeer, J., Klingensmith, J., Perrimon, N. & Nusse, R. 1994. Dishevelled and armadillo act in the Wingless signalling pathway in Drosophila. *Nature,* 367**,** 80-83.

Nowakowski, R.S., Lewin, S.B. & Miller, M.W. 1989. Bromodeoxyuridine immunohistochemical determination of the lengths of the cell cycle and the DNA-synthetic phase for an anatomically defined population. *Journal of Neurocytology,* 18**,** 311-318.

Nusse, R. & Clevers, H. 2017. Wnt/β-Catenin Signaling, Disease, and Emerging Therapeutic Modalities. *Cell,* 169**,** 985-999.

Nusse, R. & Varmus, H.E. 1982. Many tumors induced by the mouse mammary tumor virus contain a provirus integrated in the same region of the host genome. *Cell,* 31**,** 99-109.

Nüsslein-Volhard, C. & Wieschaus, E. 1980. Mutations affecting segment number and polarity in Drosophila. *Nature,* 287**,** 795-801.

Obernier, K. & Alvarez-Buylla, A. 2019. Neural stem cells: origin, heterogeneity and regulation in the adult mammalian brain. *Development,* 146**,** dev156059.

Obernier, K., Cebrian-Silla, A., Thomson, M., Parraguez, J.I., Anderson, R., Guinto, C., Rodas Rodriguez, J., Garcia-Verdugo, J.-M. & Alvarez-Buylla, A. 2018. Adult Neurogenesis Is Sustained by Symmetric Self-Renewal and Differentiation. *Cell Stem Cell,* 22**,** 221-234.e8.

Okamoto, M., Inoue, K., Iwamura, H., Terashima, K., Soya, H., Asashima, M. & Kuwabara, T. 2011. Reduction in paracrine Wnt3 factors during aging causes impaired adult neurogenesis. *The FASEB Journal,* 25**,** 3570-3582.

Olson, A.K., Eadie, B.D., Ernst, C. & Christie, B.R. 2006. Environmental enrichment and voluntary exercise massively increase neurogenesis in the adult hippocampus via dissociable pathways. *Hippocampus,* 16**,** 250-260.

Ottone, C., Krusche, B., Whitby, A., Clements, M., Quadrato, G., Pitulescu, M.E., Adams, R.H. & Parrinello, S. 2014. Direct cell-cell contact with the vascular niche maintains quiescent neural stem cells. *Nature cell biology,* 16**,** 1045-1056.

Owen, T.A., Soprano, D.R. & Soprano, K.J. 1989. Analysis of the growth factor requirements for stimulation of WI-38 cells after extended periods of density-dependent growth arrest. *Journal of Cellular Physiology,* 139**,** 424-431.

Paik, J.-h., Ding, Z., Narurkar, R., Ramkissoon, S., Muller, F., Kamoun, W.S., Chae, S.-S., Zheng, H., Ying, H., Mahoney, J., Hiller, D., Jiang, S., Protopopov, A., Wong, W.H., Chin, L., Ligon, K.L. & DePinho, R.A. 2009. FoxOs Cooperatively Regulate Diverse Pathways Governing Neural Stem Cell Homeostasis. *Cell Stem Cell,* 5**,** 540-553.

Palma, V., Lim, D.A., Dahmane, N., Sánchez, P., Brionne, T.C., Herzberg, C.D., Gitton, Y., Carleton, A., Alvarez-Buylla, A. & Ruiz i Altaba, A. 2005. Sonic hedgehog controls stem cell behavior in the postnatal and adult brain. *Development (Cambridge, England),* 132**,** 335-344.

Palmer, T.D., Ray, J. & Gage, F.H. 1995. FGF-2-Responsive Neuronal Progenitors Reside in Proliferative and Quiescent Regions of the Adult Rodent Brain. *Molecular and Cellular Neuroscience,* 6**,** 474-486.

Palmer, T.D., Takahashi, J. & Gage, F.H. 1997. The Adult Rat Hippocampus Contains Primordial Neural Stem Cells. *Molecular and Cellular Neuroscience,* 8**,** 389-404.

Palmer, T.D., Willhoite, A.R. & Gage, F.H. 2000. Vascular niche for adult hippocampal neurogenesis. *Journal of Comparative Neurology,* 425**,** 479-494.

Papkoff, J., Rubinfeld, B., Schryver, B. & Polakis, P. 1996. Wnt-1 regulates free pools of catenins and stabilizes APC-catenin complexes. *Mol Cell Biol,* 16.

Pardee, A.B. 1974. A restriction point for control of normal animal cell proliferation. *Proceedings of the National Academy of Sciences of the United States of America,* 71**,** 1286-1290.

Parr, B.A., Shea, M.J., Vassileva, G. & McMahon, A.P. 1993. Mouse Wnt genes exhibit discrete domains of expression in the early embryonic CNS and limb buds. *Development,* 119**,** 247.

Patel, D., Morton, D.J., Carey, J., Havrda, M.C. & Chaudhary, J. 2015. Inhibitor of differentiation 4 (ID4): From development to cancer. *Biochimica et biophysica acta,* 1855**,** 92-103.

Paton, J.A. & Nottebohm, F.N. 1984. Neurons generated in the adult brain are recruited into functional circuits. *Science,* 225**,** 1046.

Peifer, M., Pai, L.-M. & Casey, M. 1994a. Phosphorylation of the Drosophila Adherens Junction Protein Armadillo: Roles for Wingless Signal and Zeste-white 3 Kinase. *Developmental Biology,* 166**,** 543-556.

Peifer, M., Sweeton, D., Casey, M. & Wieschaus, E. 1994b. Wingless signal and Zeste-white 3 kinase trigger opposing changes in the intracellular distribution of Armadillo. *Development,* 120**,** 369.

Pereira, A.C., Huddleston, D.E., Brickman, A.M., Sosunov, A.A., Hen, R., McKhann, G.M., Sloan, R., Gage, F.H., Brown, T.R. & Small, S.A. 2007. An *in vivo* correlate of exercise-induced neurogenesis in the adult dentate gyrus. *Proceedings of the National Academy of Sciences of the United States of America,* 104**,** 5638-5643.

Pérez-Cañellas, M.M., Font, E. & García-Verdugo, J.M. 1997. Postnatal neurogenesis in the telencephalon of turtles: evidence for nonradial migration of new neurons from distant proliferative ventricular zones to the olfactory bulbs. *Developmental Brain Research,* 101**,** 125-137.

Persad, A., Venkateswaran, G., Hao, L., Garcia, M.E., Yoon, J., Sidhu, J. & Persad, S. 2016. Active β-catenin is regulated by the PTEN/PI3 kinase pathway: a role for protein phosphatase PP2A. *Genes & cancer,* 7**,** 368-382.

Petrova, R., Garcia, A.D.R. & Joyner, A.L. 2013. Titration of GLI3 repressor activity by sonic hedgehog signaling is critical for maintaining multiple adult neural stem cell and astrocyte functions. *The Journal of neuroscience : the official journal of the Society for Neuroscience,* 33**,** 17490-17505.

Philipp, M. & Caron, M.G. 2009. Hedgehog Signaling: Is Smo a G Protein-Coupled Receptor? *Current Biology,* 19**,** R125-R127.

Pilz, G.-A., Bottes, S., Betizeau, M., Jörg, D.J., Carta, S., Simons, B.D., Helmchen, F. & Jessberger, S. 2018. Live imaging of neurogenesis in the adult mouse hippocampus. *Science,* 359**,** 658.

Pleasure, S.J., Collins, A.E. & Lowenstein, D.H. 2000. Unique expression patterns of cell fate molecules delineate sequential stages of dentate gyrus development. *The Journal of neuroscience : the official journal of the Society for Neuroscience,* 20**,** 6095-6105.

Porlan, E., Martí-Prado, B., Morante-Redolat, J.M., Consiglio, A., Delgado, A.C., Kypta, R., López-Otín, C., Kirstein, M. & Fariñas, I. 2014. MT5-MMP regulates adult neural stem cell functional quiescence through the cleavage of N-cadherin. *Nature Cell Biology,* 16**,** 629-638.

Proffitt, K.D., Madan, B., Ke, Z., Pendharkar, V., Ding, L., Lee, M.A., Hannoush, R.N. & Virshup, D.M. 2013. Pharmacological Inhibition of the Wnt Acyltransferase PORCN Prevents Growth of WNT-Driven Mammary Cancer. *Cancer Research,* 73**,** 502.

Qi, J., Yu, Y., Akilli Öztürk, Ö., Holland, J.D., Besser, D., Fritzmann, J., Wulf-Goldenberg, A., Eckert, K., Fichtner, I. & Birchmeier, W. 2016. New Wnt/β-catenin target genes promote experimental metastasis and migration of colorectal cancer cells through different signals. *Gut,* 65**,** 1690.

Qu, Q., Sun, G., Li, W., Yang, S., Ye, P., Zhao, C., Yu, R.T., Gage, F.H., Evans, R.M. & Shi, Y. 2010. Orphan nuclear receptor TLX activates Wnt/β-catenin signalling to stimulate neural stem cell proliferation and self-renewal. *Nature cell biology,* 12**,** 31-9.

Qu, Q., Sun, G., Murai, K., Ye, P., Li, W., Asuelime, G., Cheung, Y.-T. & Shi, Y. 2013. Wnt7a regulates multiple steps of neurogenesis. *Molecular and cellular biology,* 33**,** 2551-9.

Rai, K.S., Hattiangady, B. & Shetty, A.K. 2007. Enhanced production and dendritic growth of new dentate granule cells in the middle-aged hippocampus following intracerebroventricular FGF-2 infusions. *European Journal of Neuroscience,* 26**,** 1765-1779.

Rakic, P. 1985a. DNA Synthesis and Cell Division in the Adult Primate Braina. *Annals of the New York Academy of Sciences,* 457**,** 193-211.

Rakic, P. 1985b. Limits of neurogenesis in primates. *Science,* 227**,** 1054.

Rakic, P. 2004. Immigration denied. *Nature,* 427**,** 685-686.

Ramón y Cajal, S. 1928. *Degeneration and Regeneration of the Nervous System,* New York, USA, Haffner Publishing Co.
.

Rebo, J., Mehdipour, M., Gathwala, R., Causey, K., Liu, Y., Conboy, M.J. & Conboy, I.M. 2016. A single heterochronic blood exchange reveals rapid inhibition of multiple tissues by old blood. *Nature Communications,* 7**,** 13363.

Regensburger, M., Prots, I. & Winner, B. 2014. Adult hippocampal neurogenesis in Parkinson's disease: impact on neuronal survival and plasticity. *Neural Plast,* 2014**,** 454696.

Reichenbach, B., Classon, J., Aida, T., Tanaka, K., Genander, M. & Göritz, C. 2018. Glutamate transporter Slc1a3 mediates inter‐niche stem cell activation during skin growth. *The EMBO Journal*.

Renault, V.M., Rafalski, V.A., Morgan, A.A., Salih, D.A.M., Brett, J.O., Webb, A.E., Villeda, S.A., Thekkat, P.U., Guillerey, C., Denko, N.C., Palmer, T.D., Butte, A.J. & Brunet, A. 2009. FoxO3 Regulates Neural Stem Cell Homeostasis. *Cell Stem Cell,* 5**,** 527-539.

Reynolds, B.A. & Weiss, S. 1992. Generation of neurons and astrocytes from isolated cells of the adult mammalian central nervous system. *Science,* 255**,** 1707.

Richards, L.J., Kilpatrick, T.J. & Bartlett, P.F. 1992. De novo generation of neuronal cells from the adult mouse brain. *Proceedings of the National Academy of Sciences of the United States of America,* 89**,** 8591-8595.

Rijsewijk, F., Schuermann, M., Wagenaar, E., Parren, P., Weigel, D. & Nusse, R. 1987. The Drosophila homology of the mouse mammary oncogene int-1 is identical to the segment polarity gene wingless. *Cell,* 50**,** 649-657.

Ring, D.B., Johnson, K.W., Henriksen, E.J., Nuss, J.M., Goff, D., Kinnick, T.R., Ma, S.T., Reeder, J.W., Samuels, I., Slabiak, T., Wagman, A.S., Hammond, M.-E.W. & Harrison, S.D. 2003. Selective Glycogen Synthase Kinase 3 Inhibitors Potentiate Insulin Activation of Glucose Transport and Utilization In Vitro and In Vivo. *Diabetes,* 52**,** 588-595.

Rios-Esteves, J., Haugen, B. & Resh, M.D. 2014. Identification of Key Residues and Regions Important for Porcupine-mediated Wnt Acylation. *Journal of Biological Chemistry,* 289**,** 17009-17019.

Rios-Esteves, J. & Resh, Marilyn D. 2013. Stearoyl CoA Desaturase Is Required to Produce Active, Lipid-Modified Wnt Proteins. *Cell Reports,* 4**,** 1072-1081.

Risso, D., Ngai, J., Speed, T.P. & Dudoit, S. 2014. Normalization of RNA-seq data using factor analysis of control genes or samples. *Nature biotechnology,* 32**,** 896-902.

Risso, D., Schwartz, K., Sherlock, G. & Dudoit, S. 2011. GC-content normalization for RNA-Seq data. *BMC bioinformatics,* 12**,** 480-480.

Rodriguez-Iglesias, N., Sierra, A. & Valero, J. 2019. Rewiring of Memory Circuits: Connecting Adult Newborn Neurons With the Help of Microglia. *Front Cell Dev Biol,* 7**,** 24.

Rohatgi, R., Milenkovic, L. & Scott, M.P. 2007. Patched1 Regulates Hedgehog Signaling at the Primary Cilium. *Science,* 317**,** 372.

Roose, J., Molenaar, M., Peterson, J., Hurenkamp, J., Brantjes, H., Moerer, P., van de Wetering, M., Destrée, O. & Clevers, H. 1998. The Xenopus Wnt effector XTcf-3 interacts with Groucho-related transcriptional repressors. *Nature,* 395**,** 608-612.

Rosin-Arbesfeld, R., Townsley, F. & Bienz, M. 2000. The APC tumour suppressor has a nuclear export function. *Nature,* 406**,** 1009-1012.

Rossi, C., Angelucci, A., Costantin, L., Braschi, C., Mazzantini, M., Babbini, F., Fabbri, M.E., Tessarollo, L., Maffei, L., Berardi, N. & Caleo, M. 2006. Brain-derived neurotrophic factor (BDNF) is required for the enhancement of hippocampal neurogenesis following environmental enrichment. *European Journal of Neuroscience,* 24**,** 1850-1856.

Rosso, S.B., Sussman, D., Wynshaw-Boris, A. & Salinas, P.C. 2005. Wnt signaling through Dishevelled, Rac and JNK regulates dendritic development. *Nature Neuroscience,* 8**,** 34-42.

Roy, N.S., Wang, S., Jiang, L., Kang, J., Benraiss, A., Harrison-Restelli, C., Fraser, R.A.R., Couldwell, W.T., Kawaguchi, A., Okano, H., Nedergaard, M. & Goldman, S.A. 2000. *In vitro* neurogenesis by progenitor cells isolated from the adult human hippocampus. *Nature Medicine,* 6**,** 271-277.

Roybon, L., Hjalt, T., Stott, S., Guillemot, F., Li, J.-Y. & Brundin, P. 2009. Neurogenin 2 Directs Granule Neuroblast Production and Amplification while NeuroD1 Specifies Neuronal Fate during Hippocampal Neurogenesis. *PLOS ONE,* 4**,** e4779.

Rubinfeld, B., Souza, B., Albert, I., Müller, O., Chamberlain, S.H., Masiarz, F.R., Munemitsu, S. & Polakis, P. 1993. Association of the APC gene product with β-catenin. *Science,* 262**,** 1731-1734.

Ryan, S.M., O'Keeffe, G.W., O'Connor, C., Keeshan, K. & Nolan, Y.M. 2013. Negative regulation of TLX by IL-1β correlates with an inhibition of adult hippocampal neural precursor cell proliferation. *Brain, Behavior, and Immunity,* 33**,** 7-13.

Saha, K., Keung, A.J., Irwin, E.F., Li, Y., Little, L., Schaffer, D.V. & Healy, K.E. 2008. Substrate modulus directs neural stem cell behavior. *Biophysical journal,* 95**,** 4426-4438.

Sahay, A., Drew, M.R. & Hen, R. 2007. Dentate gyrus neurogenesis and depression. *In:* SCHARFMAN, H. E. (ed.) *Progress in Brain Research.* Elsevier.

Sahay, A., Scobie, K.N., Hill, A.S., O'Carroll, C.M., Kheirbek, M.A., Burghardt, N.S., Fenton, A.A., Dranovsky, A. & Hen, R. 2011a. Increasing adult hippocampal neurogenesis is sufficient to improve pattern separation. *Nature,* 472**,** 466-470.

Sahay, A., Wilson, Donald A. & Hen, R. 2011b. Pattern Separation: A Common Function for New Neurons in Hippocampus and Olfactory Bulb. *Neuron,* 70**,** 582-588.

Sakanaka, C. 2002. Phosphorylation and Regulation of β-Catenin by Casein Kinase Iε. *The Journal of Biochemistry,* 132**,** 697-703.

Sakanaka, C., Weiss, J.B. & Williams, L.T. 1998. Bridging of β-catenin and glycogen synthase kinase-3β by axin and inhibition of β-catenin-mediated transcription. *Proceedings of the National Academy of Sciences of the United States of America,* 95**,** 3020-3023.

Salic, A. & Mitchison, T.J. 2008. A chemical method for fast and sensitive detection of DNA synthesis in vivo. *Proceedings of the National Academy of Sciences,* 105**,** 2415-2420.

Sanai, N., Nguyen, T., Ihrie, R.A., Mirzadeh, Z., Tsai, H.-H., Wong, M., Gupta, N., Berger, M.S., Huang, E., Garcia-Verdugo, J.-M., Rowitch, D.H. & Alvarez-Buylla, A. 2011. Corridors of migrating neurons in the human brain and their decline during infancy. *Nature,* 478**,** 382-386.

Sanai, N., Tramontin, A.D., Quiñones-Hinojosa, A., Barbaro, N.M., Gupta, N., Kunwar, S., Lawton, M.T., McDermott, M.W., Parsa, A.T., Manuel-García Verdugo, J., Berger, M.S. & Alvarez-Buylla, A. 2004. Unique astrocyte ribbon in adult human brain contains neural stem cells but lacks chain migration. *Nature,* 427**,** 740-744.

Sato, N., Meijer, L., Skaltsounis, L., Greengard, P. & Brivanlou, A.H. 2004. Maintenance of pluripotency in human and mouse embryonic stem cells through activation of Wnt signaling by a pharmacological GSK-3-specific inhibitor. *Nature medicine,* 10**,** 55-63.

Sato, T., Vries, R.G., Snippert, H.J., van de Wetering, M., Barker, N., Stange, D.E., van Es, J.H., Abo, A., Kujala, P., Peters, P.J. & Clevers, H. 2009. Single Lgr5 stem cells build crypt-villus structures in vitro without a mesenchymal niche. *Nature,* 459**,** 262-265.

Schafer, S.T., Han, J., Pena, M., von Bohlen Und Halbach, O., Peters, J. & Gage, F.H. 2015. The Wnt adaptor protein ATP6AP2 regulates multiple stages of adult hippocampal neurogenesis. *The Journal of neuroscience : the official journal of the Society for Neuroscience,* 35**,** 4983-98.

Schänzer, A., Wachs, F.-P., Wilhelm, D., Acker, T., Cooper-Kuhn, C., Beck, H., Winkler, J., Aigner, L., Plate, K.H. & Kuhn, H.G. 2004. Direct Stimulation of Adult Neural Stem Cells In Vitro and Neurogenesis In Vivo by Vascular Endothelial Growth Factor. *Brain Pathology,* 14**,** 237-248.

Scharfman, H., Goodman, J., Macleod, A., Phani, S., Antonelli, C. & Croll, S. 2005. Increased neurogenesis and the ectopic granule cells after intrahippocampal BDNF infusion in adult rats. *Experimental Neurology,* 192**,** 348-356.

Schindelin, J., Arganda-Carreras, I., Frise, E., Kaynig, V., Longair, M., Pietzsch, T., Preibisch, S., Rueden, C., Saalfeld, S., Schmid, B., Tinevez, J.-Y., White, D.J., Hartenstein, V., Eliceiri, K., Tomancak, P. & Cardona, A. 2012. Fiji - an Open Source platform for biological image analysis. *Nature methods,* 9**,** 10.1038/nmeth.2019.

Schmidt-Hieber, C., Jonas, P. & Bischofberger, J. 2004. Enhanced synaptic plasticity in newly generated granule cells of the adult hippocampus. *Nature,* 429**,** 184-187.

Schofield, R. 1978. The relationship between the spleen colony-forming cell and the haemopoietic stem cell. *Blood cells,* 4**,** 7-25.

Schouten, M., Bielefeld, P., Garcia-Corzo, L., Passchier, E.M.J., Gradari, S., Jungenitz, T., Pons-Espinal, M., Gebara, E., Martín-Suárez, S., Lucassen, P.J., De Vries, H.E., Trejo, J.L., Schwarzacher, S.W., De Pietri Tonelli, D., Toni, N., Mira, H., Encinas, J.M. & Fitzsimons, C.P. 2019. Circadian glucocorticoid oscillations preserve a population of adult hippocampal neural stem cells in the aging brain. *Molecular Psychiatry*.

Schwarz-Romond, T., Fiedler, M., Shibata, N., Butler, P.J.G., Kikuchi, A., Higuchi, Y. & Bienz, M. 2007. The DIX domain of Dishevelled confers Wnt signaling by dynamic polymerization. *Nature Structural & Molecular Biology,* 14**,** 484-492.

Scott, I.C., Steiglitz, B.M., Clark, T.G., Pappano, W.N. & Greenspan, D.S. 2000. Spatiotemporal expression patterns of mammalian chordin during postgastrulation embryogenesis and in postnatal brain. *Developmental Dynamics,* 217**,** 449-456.

Seib, D.R.M., Corsini, N.S., Ellwanger, K., Plaas, C., Mateos, A., Pitzer, C., Niehrs, C., Celikel, T. & Martin-Villalba, A. 2013. Loss of Dickkopf-1 restores neurogenesis in old age and counteracts cognitive decline. *Cell stem cell,* 12**,** 204-14.

Seki, T. 2002. Expression patterns of immature neuronal markers PSA-NCAM, CRMP-4 and NeuroD in the hippocampus of young adult and aged rodents. *Journal of Neuroscience Research,* 70**,** 327-334.

Semënov, M., Tamai, K. & He, X. 2005. SOST Is a Ligand for LRP5/LRP6 and a Wnt Signaling Inhibitor. *Journal of Biological Chemistry,* 280**,** 26770-26775.

Semënov, M.V., Tamai, K., Brott, B.K., Kühl, M., Sokol, S. & He, X. 2001. Head inducer Dickkopf-1 is a ligand for Wnt coreceptor LRP6. *Curr Biol,* 11**,** 951-61.

Semënov, M.V., Zhang, X. & He, X. 2008. DKK1 Antagonizes Wnt Signaling without Promotion of LRP6 Internalization and Degradation. *Journal of Biological Chemistry,* 283**,** 21427-21432.

Septinus, M., Seiffert, W. & Zimmermann, H.W. 1983. Hydrophobic acridine dyes for fluorescence staining of mitochondria in living cells. *Histochemistry,* 79**,** 443-456.

Seri, B., García-Verdugo, J.M., Collado-Morente, L., McEwen, B.S. & Alvarez-Buylla, A. 2004. Cell types, lineage, and architecture of the germinal zone in the adult dentate gyrus. *Journal of Comparative Neurology,* 478**,** 359-378.

Seri, B., García-Verdugo, J.M., McEwen, B.S. & Alvarez-Buylla, A. 2001. Astrocytes Give Rise to New Neurons in the Adult Mammalian Hippocampus. *The Journal of Neuroscience,* 21**,** 7153.

Sharma, P., Chinaranagari, S. & Chaudhary, J. 2015. Inhibitor of differentiation 4 (ID4) acts as an inhibitor of ID-1, -2 and -3 and promotes basic helix loop helix (bHLH) E47 DNA binding and transcriptional activity. *Biochimie,* 112**,** 139-150.

Sheldahl, L.C., Slusarski, D.C., Pandur, P., Miller, J.R., Kühl, M. & Moon, R.T. 2003. Dishevelled activates Ca2+ flux, PKC, and CamKII in vertebrate embryos. *The Journal of cell biology,* 161**,** 769-777.

Shen, Q., Goderie, S.K., Jin, L., Karanth, N., Sun, Y., Abramova, N., Vincent, P., Pumiglia, K. & Temple, S. 2004. Endothelial Cells Stimulate Self-Renewal and Expand Neurogenesis of Neural Stem Cells. *Science,* 304**,** 1338.

Shen, Q., Wang, Y., Kokovay, E., Lin, G., Chuang, S.-M., Goderie, S.K., Roysam, B. & Temple, S. 2008. Adult SVZ stem cells lie in a vascular niche: a quantitative analysis of niche cell-cell interactions. *Cell stem cell,* 3**,** 289-300.

Shi, Y., Chichung Lie, D., Taupin, P., Nakashima, K., Ray, J., Yu, R.T., Gage, F.H. & Evans, R.M. 2004. Expression and function of orphan nuclear receptor TLX in adult neural stem cells. *Nature,* 427**,** 78-83.

Shimizu, K., Chiba, S., Saito, T., Kumano, K., Hamada, Y. & Hirai, H. 2002. Functional Diversity among Notch1, Notch2, and Notch3 Receptors. *Biochemical and Biophysical Research Communications,* 291**,** 775-779.

Shin, J., Berg, Daniel A., Zhu, Y., Shin, Joseph Y., Song, J., Bonaguidi, Michael A., Enikolopov, G., Nauen, David W., Christian, Kimberly M., Ming, G.-l. & Song, H. 2015. Single-Cell RNA-Seq with Waterfall Reveals Molecular Cascades underlying Adult Neurogenesis. *Cell Stem Cell,* 17**,** 360-372.

Shors, T.J., Miesegaes, G., Beylin, A., Zhao, M., Rydel, T. & Gould, E. 2001. Neurogenesis in the adult is involved in the formation of trace memories. *Nature,* 410**,** 372-376.

Shors, T.J., Townsend, D.A., Zhao, M., Kozorovitskiy, Y. & Gould, E. 2002. Neurogenesis may relate to some but not all types of hippocampal-dependent learning. *Hippocampus,* 12**,** 578-584.

Shtutman, M., Zhurinsky, J., Simcha, I., Albanese, C., D'Amico, M., Pestell, R. & Ben-Ze'ev, A. 1999. The cyclin D1 gene is a target of the β-catenin/LEF-1 pathway. *Proceedings of the National Academy of Sciences,* 96**,** 5522-5527.

Siegfried, E., Chou, T.-B. & Perrimon, N. 1992. Wingless signaling acts through zeste-white 3, the drosophila homolog of glycogen synthase kinase-3, to regulate engrailed and establish cell fate. *Cell,* 71**,** 1167-1179.

Sierra, A., Encinas, J.M., Deudero, J.J.P., Chancey, J.H., Enikolopov, G., Overstreet-Wadiche, L.S., Tsirka, S.E. & Maletic-Savatic, M. 2010. Microglia shape adult hippocampal neurogenesis through apoptosis-coupled phagocytosis. *Cell stem cell,* 7**,** 483-495.

Sierra, A., Martín-Suárez, S., Valcárcel-Martín, R., Pascual-Brazo, J., Aelvoet, S.-A., Abiega, O., Deudero, J.J., Brewster, A.L., Bernales, I., Anderson, A.E., Baekelandt, V., Maletić-Savatić, M. & Encinas, J.M. 2015. Neuronal hyperactivity accelerates depletion of neural stem cells and impairs hippocampal neurogenesis. *Cell stem cell,* 16**,** 488-503.

Slusarski, D.C., Yang-Snyder, J., Busa, W.B. & Moon, R.T. 1997. Modulation of Embryonic Intracellular Ca2+ Signaling by Wnt-5A. *Developmental Biology,* 182**,** 114-120.

Smith, L.K., White, C.W., 3rd & Villeda, S.A. 2018a. The systemic environment: at the interface of aging and adult neurogenesis. *Cell and tissue research,* 371**,** 105-113.

Smith, L.R., Cho, S. & Discher, D.E. 2018b. Stem Cell Differentiation is Regulated by Extracellular Matrix Mechanics. *Physiology (Bethesda, Md.),* 33**,** 16-25.

Snippert, H.J., Haegebarth, A., Kasper, M., Jaks, V., van Es, J.H., Barker, N., van de Wetering, M., van den Born, M., Begthel, H., Vries, R.G., Stange, D.E., Toftgård, R. & Clevers, H. 2010. *Lgr6* Marks Stem Cells in the Hair Follicle That Generate All Cell Lineages of the Skin. *Science,* 327**,** 1385.

Solanas, G., Miravet, S., Casagolda, D., Castaño, J., Raurell, I., Corrionero, A., de Herreros, A.G. & Duñach, M. 2004. β-Catenin and Plakoglobin N- and C-tails Determine Ligand Specificity. *Journal of Biological Chemistry,* 279**,** 49849-49856.

Song, H., Stevens, C.F. & Gage, F.H. 2002. Astroglia induce neurogenesis from adult neural stem cells. *Nature,* 417**,** 39-44.

Song, J., Zhong, C., Bonaguidi, M.A., Sun, G.J., Hsu, D., Gu, Y., Meletis, K., Huang, Z.J., Ge, S., Enikolopov, G., Deisseroth, K., Luscher, B., Christian, K.M., Ming, G.-l. & Song, H. 2012. Neuronal circuitry mechanism regulating adult quiescent neural stem-cell fate decision. *Nature,* 489**,** 150-154.

Sorrells, S.F., Paredes, M.F., Cebrian-Silla, A., Sandoval, K., Qi, D., Kelley, K.W., James, D., Mayer, S., Chang, J., Auguste, K.I., Chang, E.F., Gutierrez, A.J., Kriegstein, A.R., Mathern, G.W., Oldham, M.C., Huang, E.J., Garcia-Verdugo, J.M., Yang, Z. & Alvarez-Buylla, A. 2018. Human hippocampal neurogenesis drops sharply in children to undetectable levels in adults. *Nature,* 555**,** 377-381.

Spalding, K.L., Bergmann, O., Alkass, K., Bernard, S., Salehpour, M., Huttner, H.B., Boström, E., Westerlund, I., Vial, C., Buchholz, B.A., Possnert, G., Mash, D.C., Druid, H. & Frisén, J. 2013. Dynamics of hippocampal neurogenesis in adult humans. *Cell,* 153**,** 1219-1227.

Spalding, K.L., Bhardwaj, R.D., Buchholz, B.A., Druid, H. & Frisén, J. 2005. Retrospective Birth Dating of Cells in Humans. *Cell,* 122**,** 133-143.

Srinivas, S., Watanabe, T., Lin, C.-S., William, C.M., Tanabe, Y., Jessell, T.M. & Costantini, F. 2001. Cre reporter strains produced by targeted insertion of EYFP and ECFP into the ROSA26 locus. *BMC Developmental Biology,* 1**,** 4-4.

Städeli, R., Hoffmans, R. & Basler, K. 2006. Transcription under the Control of Nuclear Arm/β-Catenin. *Current Biology,* 16**,** R378-R385.

Stamos, J.L., Chu, M.L.-H., Enos, M.D., Shah, N. & Weis, W.I. 2014. Structural basis of GSK-3 inhibition by N-terminal phosphorylation and by the Wnt receptor LRP6. *eLife,* 3**,** e01998.

Steiner, B., Kronenberg, G., Jessberger, S., Brandt, M.D., Reuter, K. & Kempermann, G. 2004. Differential regulation of gliogenesis in the context of adult hippocampal neurogenesis in mice. *Glia,* 46**,** 41-52.

Steiner, B., Zurborg, S., Hörster, H., Fabel, K. & Kempermann, G. 2008. Differential 24 h responsiveness of Prox1–expressing precursor cells in adult hippocampal neurogenesis to physical activity, environmental enrichment, and kainic acid–induced seizures. *Neuroscience,* 154**,** 521-529.

Strutt, D.I., Weber, U. & Mlodzik, M. 1997. The role of RhoA in tissue polarity and Frizzled signalling. *Nature,* 387**,** 292-295.

Stuart, T., Butler, A., Hoffman, P., Hafemeister, C., Papalexi, E., Mauck, W.M., Hao, Y., Stoeckius, M., Smibert, P. & Satija, R. 2019. Comprehensive Integration of Single-Cell Data. *Cell,* 177**,** 1888-1902.e21.

Sueda, R., Imayoshi, I., Harima, Y. & Kageyama, R. 2019. High Hes1 expression and resultant Ascl1 suppression regulate quiescent vs. active neural stem cells in the adult mouse brain. *Genes & Development,* 33**,** 511-523.

Suh, H., Consiglio, A., Ray, J., Sawai, T., D'Amour, K.A. & Gage, Fred H. 2007. *In vivo* Fate Analysis Reveals the Multipotent and Self-Renewal Capacities of Sox2+ Neural Stem Cells in the Adult Hippocampus. *Cell Stem Cell,* 1**,** 515-528.

Suhonen, J.O., Peterson, D.A., Ray, J. & Gage, F.H. 1996. Differentiation of adult hippocampus-derived progenitors into olfactory neurons in vivo. *Nature,* 383**,** 624-627.

Sun, G., Yu, R.T., Evans, R.M. & Shi, Y. 2007. Orphan nuclear receptor TLX recruits histone deacetylases to repress transcription and regulate neural stem cell proliferation. *Proceedings of the National Academy of Sciences of the United States of America,* 104**,** 15282-15287.

Sun, G.J., Zhou, Y., Stadel, R.P., Moss, J., Yong, J.H.A., Ito, S., Kawasaki, N.K., Phan, A.T., Oh, J.H., Modak, N., Reed, R.R., Toni, N., Song, H. & Ming, G.-l. 2015a. Tangential migration of neuronal precursors of glutamatergic neurons in the adult mammalian brain. *Proceedings of the National Academy of Sciences,* 112**,** 9484.

Sun, J., Bonaguidi, M.A., Jun, H., Guo, J.U., Sun, G.J., Will, B., Yang, Z., Jang, M.-H., Song, H., Ming, G.-L. & Christian, K.M. 2015b. A septo-temporal molecular gradient of sfrp3 in the dentate

gyrus differentially regulates quiescent adult hippocampal neural stem cell activation. *Molecular brain,* 8**,** 52.

Sun, Y., Hu, J., Zhou, L., Pollard, S.M. & Smith, A. 2011. Interplay between FGF2 and BMP controls the self-renewal, dormancy and differentiation of rat neural stem cells. *Journal of Cell Science,* 124**,** 1867.

Sutherland, C. 2011. What Are the bona fide GSK3 Substrates? *International Journal of Alzheimer’s Disease,* 2011**,** 23.

Tabatadze, N., Tomas, C., McGonigal, R., Lin, B., Schook, A. & Routtenberg, A. 2012. Wnt transmembrane signaling and long-term spatial memory. *Hippocampus,* 22**,** 1228-1241.

Tahinci, E. & Symes, K. 2003. Distinct functions of Rho and Rac are required for convergent extension during Xenopus gastrulation. *Developmental Biology,* 259**,** 318-335.

Takada, R., Satomi, Y., Kurata, T., Ueno, N., Norioka, S., Kondoh, H., Takao, T. & Takada, S. 2006. Monounsaturated Fatty Acid Modification of Wnt Protein: Its Role in Wnt Secretion. *Developmental Cell,* 11**,** 791-801.

Takahashi, M., Tsunoda, T., Seiki, M., Nakamura, Y. & Furukawa, Y. 2002. Identification of membrane-type matrix metalloproteinase-1 as a target of the β-catenin/Tcf4 complex in human colorectal cancers. *Oncogene,* 21**,** 5861-5867.

Takahashi, T., Nowakowski, R.S. & Caviness, V.S., Jr. 1996. The leaving or Q fraction of the murine cerebral proliferative epithelium: a general model of neocortical neuronogenesis. *The Journal of neuroscience : the official journal of the Society for Neuroscience,* 16**,** 6183-6196.

Tanaka, K., Kitagawa, Y. & Kadowaki, T. 2002. Drosophila Segment Polarity Gene Product Porcupine Stimulates the Posttranslational N-Glycosylation of Wingless in the Endoplasmic Reticulum. *Journal of Biological Chemistry,* 277**,** 12816-12823.

Tanegashima, K., Zhao, H. & Dawid, I.B. 2008. WGEF activates Rho in the Wnt-PCP pathway and controls convergent extension in Xenopus gastrulation. *The EMBO journal,* 27**,** 606-617.

Taniguchi, H., Kawauchi, D., Nishida, K. & Murakami, F. 2006. Classic cadherins regulate tangential migration of precerebellar neurons in the caudal hindbrain. *Development,* 133**,** 1923.

Tao, Q., Yokota, C., Puck, H., Kofron, M., Birsoy, B., Yan, D., Asashima, M., Wylie, C.C., Lin, X. & Heasman, J. 2005. Maternal Wnt11 Activates the Canonical Wnt Signaling Pathway Required for Axis Formation in Xenopus Embryos. *Cell,* 120**,** 857-871.

Tauriello, D.V.F., Jordens, I., Kirchner, K., Slootstra, J.W., Kruitwagen, T., Bouwman, B.A.M., Noutsou, M., Rüdiger, S.G.D., Schwamborn, K., Schambony, A. & Maurice, M.M. 2012. Wnt/β-catenin signaling requires interaction of the Dishevelled DEP domain and C terminus with a discontinuous motif in Frizzled. *Proceedings of the National Academy of Sciences,* 109**,** E812.

Theil, T., Alvarez-Bolado, G., Walter, A. & Ruther, U. 1999. Gli3 is required for Emx gene expression during dorsal telencephalon development. *Development,* 126**,** 3561.

Thomas, R.M., Hotsenpiller, G. & Peterson, D.A. 2007. Acute psychosocial stress reduces cell survival in adult hippocampal neurogenesis without altering proliferation. *The Journal of neuroscience : the official journal of the Society for Neuroscience,* 27**,** 2734-2743.

Tian, Y., Cohen, E.D. & Morrisey, E.E. 2010. The importance of Wnt signaling in cardiovascular development. *Pediatric cardiology,* 31**,** 342-348.

Tole, S., Ragsdale, C.W. & Grove, E.A. 2000. Dorsoventral Patterning of the Telencephalon Is Disrupted in the Mouse Mutant extra-toesJ. *Developmental Biology,* 217**,** 254-265.

Torban, E., Patenaude, A.-M., Leclerc, S., Rakowiecki, S., Gauthier, S., Andelfinger, G., Epstein, D.J. & Gros, P. 2008. Genetic interaction between members of the Vangl family causes neural tube defects in mice. *Proceedings of the National Academy of Sciences of the United States of America,* 105**,** 3449-3454.

Traiffort, E., Charytoniuk, D., Watroba, L., Faure, H., Sales, N. & Ruat, M. 1999. Discrete localizations of hedgehog signalling components in the developing and adult rat nervous system. *European Journal of Neuroscience,* 11**,** 3199-3214.

Tran, F.H. & Zheng, J.J. 2017. Modulating the wnt signaling pathway with small molecules. *Protein science : a publication of the Protein Society,* 26**,** 650-661.

Trapnell, C., Williams, B.A., Pertea, G., Mortazavi, A., Kwan, G., van Baren, M.J., Salzberg, S.L., Wold, B.J. & Pachter, L. 2010. Transcript assembly and quantification by RNA-Seq reveals unannotated transcripts and isoform switching during cell differentiation. *Nature biotechnology,* 28**,** 511-515.

Trejo, J.L., Carro, E. & Torres-Aleman, I. 2001. Circulating insulin-like growth factor I mediates exercise-induced increases in the number of new neurons in the adult hippocampus. *The Journal of neuroscience : the official journal of the Society for Neuroscience,* 21**,** 1628-1634.

Trejo, J.L., Llorens-Martín, M.V. & Torres-Alemán, I. 2008. The effects of exercise on spatial learning and anxiety-like behavior are mediated by an IGF-I-dependent mechanism related to hippocampal neurogenesis. *Molecular and Cellular Neuroscience,* 37**,** 402-411.

Trifonov, S., Yamashita, Y., Kase, M., Maruyama, M. & Sugimoto, T. 2016. Overview and assessment of the histochemical methods and reagents for the detection of β-galactosidase activity in transgenic animals. *Anatomical science international,* 91**,** 56-67.

Urbán, N., Blomfield, I.M. & Guillemot, F. 2019. Quiescence of Adult Mammalian Neural Stem Cells: A Highly Regulated Rest. *Neuron,* 104**,** 834-848.

Urbán, N. & Guillemot, F. 2014. Neurogenesis in the embryonic and adult brain: same regulators, different roles. *Frontiers in Cellular Neuroscience,* 8**,** 396.

Urbán, N., van den Berg, D.L.C., Forget, A., Andersen, J., Demmers, J.A.A., Hunt, C., Ayrault, O. & Guillemot, F. 2016. Return to quiescence of mouse neural stem cells by degradation of a proactivation protein. *Science,* 353**,** 292.

Valenta, T., Gay, M., Steiner, S., Draganova, K., Zemke, M., Hoffmans, R., Cinelli, P., Aguet, M., Sommer, L. & Basler, K. 2011. Probing transcription-specific outputs of β-catenin in vivo. *Genes & development,* 25**,** 2631-2643.

Valenta, T., Hausmann, G. & Basler, K. 2012. The many faces and functions of β-catenin. *The EMBO journal,* 31**,** 2714-2736.

van de Wetering, M., Cavallo, R., Dooijes, D., van Beest, M., van Es, J., Loureiro, J., Ypma, A., Hursh, D., Jones, T., Bejsovec, A., Peifer, M., Mortin, M. & Clevers, H. 1997. Armadillo Coactivates

Transcription Driven by the Product of the Drosophila Segment Polarity Gene dTCF. *Cell,* 88**,** 789-799.

Van der Borght, K., Kóbor-Nyakas, D.É., Klauke, K., Eggen, B.J.L., Nyakas, C., Van der Zee, E.A. & Meerlo, P. 2009. Physical exercise leads to rapid adaptations in hippocampal vasculature: Temporal dynamics and relationship to cell proliferation and neurogenesis. *Hippocampus,* 19**,** 928-936.

van Praag, H., Kempermann, G. & Gage, F.H. 1999. Running increases cell proliferation and neurogenesis in the adult mouse dentate gyrus. *Nat Neurosci,* 2**,** 266-270.

van Praag, H., Schinder, A.F., Christie, B.R., Toni, N., Palmer, T.D. & Gage, F.H. 2002. Functional neurogenesis in the adult hippocampus. *Nature,* 415**,** 1030-1034.

Varela-Nallar, L., Alfaro, I.E., Serrano, F.G., Parodi, J. & Inestrosa, N.C. 2010. Wingless-type family member 5A (Wnt-5a) stimulates synaptic differentiation and function of glutamatergic synapses. *Proceedings of the National Academy of Sciences of the United States of America,* 107**,** 21164-21169.

Varela-Nallar, L. & Inestrosa, N.C. 2013. Wnt signaling in the regulation of adult hippocampal neurogenesis. *Frontiers in Cellular Neuroscience,* 7**,** 100.

Varela-Nallar, L., Parodi, J., Farias, G.G. & Inestrosa, N.C. 2012. Wnt-5a is a synaptogenic factor with neuroprotective properties against Abeta toxicity. *Neurodegener Dis,* 10**,** 23-6.

Veeman, M.T., Axelrod, J.D. & Moon, R.T. 2003. A Second Canon: Functions and Mechanisms of β-Catenin-Independent Wnt Signaling. *Developmental Cell,* 5**,** 367-377.

Villeda, S.A., Luo, J., Mosher, K.I., Zou, B., Britschgi, M., Bieri, G., Stan, T.M., Fainberg, N., Ding, Z., Eggel, A., Lucin, K.M., Czirr, E., Park, J.-S., Couillard-Després, S., Aigner, L., Li, G., Peskind, E.R., Kaye, J.A., Quinn, J.F., Galasko, D.R., Xie, X.S., Rando, T.A. & Wyss-Coray, T. 2011. The ageing systemic milieu negatively regulates neurogenesis and cognitive function. *Nature,* 477**,** 90-94.

Vorhees, C.V. & Williams, M.T. 2006. Morris water maze: procedures for assessing spatial and related forms of learning and memory. *Nature protocols,* 1**,** 848-858.

Walker, T.L. & Kempermann, G. 2014. One mouse, two cultures: isolation and culture of adult neural stem cells from the two neurogenic zones of individual mice. *Journal of visualized experiments : JoVE***,** e51225-e51225.

Wang, C., Liu, F., Liu, Y.-Y., Zhao, C.-H., You, Y., Wang, L., Zhang, J., Wei, B., Ma, T., Zhang, Q., Zhang, Y., Chen, R., Song, H. & Yang, Z. 2011. Identification and characterization of neuroblasts in the subventricular zone and rostral migratory stream of the adult human brain. *Cell research,* 21**,** 1534-1550.

Webb, A.E., Pollina, E.A., Vierbuchen, T., Urbán, N., Ucar, D., Leeman, D.S., Martynoga, B., Sewak, M., Rando, T.A., Guillemot, F., Wernig, M. & Brunet, A. 2013. FOXO3 shares common targets with ASCL1 genome-wide and inhibits ASCL1-dependent neurogenesis. *Cell reports,* 4**,** 10.1016/j.celrep.2013.06.035.

Weiser, D.C., Pyati, U.J. & Kimelman, D. 2007. Gravin regulates mesodermal cell behavior changes required for axis elongation during zebrafish gastrulation. *Genes & development,* 21**,** 1559-1571.

Westfall , T.A., Brimeyer , R., Twedt , J., Gladon , J., Olberding , A., Furutani-Seiki , M. & Slusarski , D.C. 2003. Wnt-5/pipetail functions in vertebrate axis formation as a negative regulator of Wnt/β-catenin activity. *The Journal of Cell Biology,* 162**,** 889-898.

Wexler, E.M., Geschwind, D.H. & Palmer, T.D. 2007. Lithium regulates adult hippocampal progenitor development through canonical Wnt pathway activation. *Mol Psychiatry,* 13**,** 285-292.

Wexler, E.M., Paucer, A., Kornblum, H.I., Palmer, T.D. & Geschwind, D.H. 2009. Endogenous Wnt Signaling Maintains Neural Progenitor Cell Potency. *Stem cells (Dayton, Ohio),* 27**,** 1130-1141.

Wilkinson, G., Dennis, D. & Schuurmans, C. 2013. Proneural genes in neocortical development. *Neuroscience,* 253**,** 256-273.

Willert, K., Brown, J.D., Danenberg, E., Duncan, A.W., Weissman, I.L., Reya, T., Yates, J.R. & Nusse, R. 2003. Wnt proteins are lipid-modified and can act as stem cell growth factors. *Nature,* 423**,** 448-452.

Winner, B. & Winkler, J. 2015. Adult Neurogenesis in Neurodegenerative Diseases. *Cold Spring Harbor Perspectives in Biology,* 7.

Wiskott, L., Rasch, M.J. & Kempermann, G. 2006. A functional hypothesis for adult hippocampal neurogenesis: Avoidance of catastrophic interference in the dentate gyrus. *Hippocampus,* 16**,** 329-343.

Woodhead, G.J., Mutch, C.A., Olson, E.C. & Chenn, A. 2006. Cell-autonomous β-catenin signaling regulates cortical precursor proliferation. *The Journal of neuroscience : the official journal of the Society for Neuroscience,* 26**,** 12620-12630.

Wrobel, C.N., Mutch, C.A., Swaminathan, S., Taketo, M.M. & Chenn, A. 2007. Persistent expression of stabilized β-catenin delays maturation of radial glial cells into intermediate progenitors. *Developmental biology,* 309**,** 285-297.

Wu, B., Crampton, S.P. & Hughes, C.C.W. 2007. Wnt signaling induces matrix metalloproteinase expression and regulates T cell transmigration. *Immunity,* 26**,** 227-239.

Wyss-Coray, T. & Rogers, J. 2012. Inflammation in Alzheimer Disease—A Brief Review of the Basic Science and Clinical Literature. *Cold Spring Harbor Perspectives in Medicine,* 2.

Xie, T. & Spradling, A.C. 1998. decapentaplegic Is Essential for the Maintenance and Division of Germline Stem Cells in the Drosophila Ovary. *Cell,* 94**,** 251-260.

Xing, Y., Takemaru, K.-I., Liu, J., Berndt, J.D., Zheng, J.J., Moon, R.T. & Xu, W. 2008. Crystal structure of a full-length β-catenin. *Structure (London, England : 1993),* 16**,** 478-487.

Yan, D., Wallingford, J.B., Sun, T.Q., Nelson, A.M., Sakanaka, C., Reinhard, C., Harland, R.M., Fantl, W.J. & Williams, L.T. 2001a. Cell autonomous regulation of multiple Dishevelled-dependent pathways by mammalian Nkd. *Proceedings of the National Academy of Sciences of the United States of America,* 98**,** 3802-3807.

Yan, D., Wiesmann, M., Rohan, M., Chan, V., Jefferson, A.B., Guo, L., Sakamoto, D., Caothien, R.H., Fuller, J.H., Reinhard, C., Garcia, P.D., Randazzo, F.M., Escobedo, J., Fantl, W.J. & Williams, L.T. 2001b. Elevated expression of axin2 and hnkd mRNA provides evidence that Wnt/β-catenin signaling is activated in human colon tumors. *Proceedings of the National Academy of Sciences of the United States of America,* 98**,** 14973-14978.

Yan, K.S., Janda, C.Y., Chang, J., Zheng, G.X.Y., Larkin, K.A., Luca, V.C., Chia, L.A., Mah, A.T., Han, A., Terry, J.M., Ootani, A., Roelf, K., Lee, M., Yuan, J., Li, X., Bolen, C.R., Wilhelmy, J., Davies, P.S., Ueno, H., von Furstenberg, R.J., Belgrader, P., Ziraldo, S.B., Ordonez, H., Henning, S.J., Wong, M.H., Snyder, M.P., Weissman, I.L., Hsueh, A.J., Mikkelsen, T.S., Garcia, K.C. & Kuo, C.J. 2017. Non-equivalence of Wnt and R-spondin ligands during Lgr5+ intestinal stem-cell self-renewal. *Nature,* 545**,** 238-242.

Yanagawa, S.-i., Matsuda, Y., Lee, J.-S., Matsubayashi, H., Sese, S., Kadowaki, T. & Ishimoto, A. 2002. Casein kinase I phosphorylates the Armadillo protein and induces its degradation in Drosophila. *The EMBO journal,* 21**,** 1733-1742.

Yang, S.-Z., Zhang, L.-M., Huang, Y.-L. & Sun, F.-Y. 2003. Distribution of Flk-1 and Flt-1 receptors in neonatal and adult rat brains. *The Anatomical Record Part A: Discoveries in Molecular, Cellular, and Evolutionary Biology,* 274A**,** 851-856.

Yeh, C.-Y., Asrican, B., Moss, J., Quintanilla, L.J., He, T., Mao, X., Cassé, F., Gebara, E., Bao, H., Lu, W., Toni, N. & Song, J. 2018. Mossy Cells Control Adult Neural Stem Cell Quiescence and Maintenance through a Dynamic Balance between Direct and Indirect Pathways. *Neuron,* 99**,** 493-510.e4.

Ying, Q.-L., Nichols, J., Chambers, I. & Smith, A. 2003. BMP Induction of Id Proteins Suppresses Differentiation and Sustains Embryonic Stem Cell Self-Renewal in Collaboration with STAT3. *Cell,* 115**,** 281-292.

Yost, C., Torres, M., Miller, J.R., Huang, E., Kimelman, D. & Moon, R.T. 1996. The axis-inducing activity, stability, and subcellular distribution of β-catenin is regulated in Xenopus embryos by glycogen synthase kinase 3. *Genes & Development,* 10**,** 1443-1454.

Yousef, H., Morgenthaler, A., Schlesinger, C., Bugaj, L., Conboy, I.M. & Schaffer, D.V. 2015. Age-Associated Increase in BMP Signaling Inhibits Hippocampal Neurogenesis. *Stem cells (Dayton, Ohio),* 33**,** 1577-1588.

Yu, J., Chia, J., Canning, Claire A., Jones, C.M., Bard, Frédéric A. & Virshup, David M. 2014. WLS Retrograde Transport to the Endoplasmic Reticulum during Wnt Secretion. *Developmental Cell,* 29**,** 277-291.

Yu, X. & Malenka, R.C. 2003. β-catenin is critical for dendritic morphogenesis. *Nature Neuroscience,* 6**,** 1169-1177.

Zanni, G., Michno, W., Di Martino, E., Tjärnlund-Wolf, A., Pettersson, J., Mason, C.E., Hellspong, G., Blomgren, K. & Hanrieder, J. 2017. Lithium Accumulates in Neurogenic Brain Regions as Revealed by High Resolution Ion Imaging. *Scientific Reports,* 7**,** 40726.

Zechner, D., Müller, T., Wende, H., Walther, I., Taketo, M.M., Crenshaw, E.B., Treier, M., Birchmeier, W. & Birchmeier, C. 2007. Bmp and Wnt/β-catenin signals control expression of the transcription factor Olig3 and the specification of spinal cord neurons. *Developmental Biology,* 303**,** 181-190.

Zeng, L., Fagotto, F., Zhang, T., Hsu, W., Vasicek, T.J., Perry, W.L.I., Lee, J.J., Tilghman, S.M., Gumbiner, B.M. & Costantini, F. 1997. The Mouse *Fused* Locus Encodes Axin, an Inhibitor of the Wnt Signaling Pathway That Regulates Embryonic Axis Formation. *Cell,* 90**,** 181-192.

Zeng, X., Tamai, K., Doble, B., Li, S., Huang, H., Habas, R., Okamura, H., Woodgett, J. & He, X. 2005. A dual-kinase mechanism for Wnt co-receptor phosphorylation and activation. *Nature,* 438**,** 873-877.

Zhang, C.-L., Zou, Y., He, W., Gage, F.H. & Evans, R.M. 2008. A role for adult TLX-positive neural stem cells in learning and behaviour. *Nature,* 451**,** 1004-1007.

Zhang, L. & Shay, J.W. 2017. Multiple Roles of APC and its Therapeutic Implications in Colorectal Cancer. *Journal of the National Cancer Institute,* 109**,** djw332.

Zhang, X., Cheong, S.-M., Amado, Nathalia G., Reis, Alice H., MacDonald, Bryan T., Zebisch, M., Jones, E.Y., Abreu, Jose G. & He, X. 2015. Notum Is Required for Neural and Head Induction via Wnt Deacylation, Oxidation, and Inactivation. *Developmental Cell,* 32**,** 719-730.

Zhang, Z., Ma, Z., Zou, W., Guo, H., Liu, M., Ma, Y. & Zhang, L. 2019. The Appropriate Marker for Astrocytes: Comparing the Distribution and Expression of Three Astrocytic Markers in Different Mouse Cerebral Regions. *BioMed Research International,* 2019**,** 15.

Zhao, C., Sun, G., Li, S. & Shi, Y. 2009. A feedback regulatory loop involving microRNA-9 and nuclear receptor TLX in neural stem cell fate determination. *Nature Structural & Molecular Biology,* 16**,** 365-371.

Zhao, M., Li, D., Shimazu, K., Zhou, Y.-X., Lu, B. & Deng, C.-X. 2007. Fibroblast Growth Factor Receptor-1 is Required for Long-Term Potentiation, Memory Consolidation, and Neurogenesis. *Biological Psychiatry,* 62**,** 381-390.

Ziebell, F., Dehler, S., Martin-Villalba, A. & Marciniak-Czochra, A. 2018. Revealing age-related changes of adult hippocampal neurogenesis using mathematical models. *Development,* 145**,** dev153544.

Zupanc, G.K.H. & Horschke, I. 1995. Proliferation zones in the brain of adult gymnotiform fish: A quantitative mapping study. *Journal of Comparative Neurology,* 353**,** 213-233.

Appendix

Page No.	Type of work	Name of work	Source of work	Copyright holder and contact	Permission requested on	I have permission Yes/No	Permission note
26	Figure	Figure 3. The SVZ and DG niches	Urbán, N., Blomfield, I.M. & Guillemot, F. 2019. Quiescence of Adult Mammalian Neural Stem Cells: A Highly Regulated Rest. *Neuron,* 104, 834-848.	Elsevier permissions@elsevier.com	04/03/2020	Yes	Licensed by Elsevier through the Copyright Clearance Center RightsLink® - License Number: 4781830734495
28	Figure	Figure 3. The SVZ and DG niches	Urbán, N., Blomfield, I.M. & Guillemot, F. 2019. Quiescence of Adult Mammalian Neural Stem Cells: A Highly Regulated Rest. *Neuron,* 104, 834-848	Elsevier permissions@elsevier.com	04/03/2020	Yes	Licensed by Elsevier through the Copyright Clearance Center RightsLink® - License Number: 4781830734495
30	Figure	Figure 1. Adult Neurogenesis, from Quiescent NSCs to Neurons	Urbán, N., Blomfield, I.M. & Guillemot, F. 2019. Quiescence of Adult Mammalian Neural Stem Cells: A Highly Regulated Rest. *Neuron,* 104, 834-848	Elsevier permissions@elsevier.com	04/03/2020	Yes	Licensed by Elsevier through the Copyright Clearance Center RightsLink® - License Number: 4781830734495
40	Figure	Figure 1. Adult Neurogenesis, from Quiescent NSCs to Neurons	Urbán, N., Blomfield, I.M. & Guillemot, F. 2019. Quiescence of Adult Mammalian Neural Stem Cells: A Highly Regulated Rest. *Neuron,* 104, 834-848	Elsevier permissions@elsevier.com	04/03/2020	Yes	Licensed by Elsevier through the Copyright Clearance Center RightsLink® - License Number: 4781830734495
56	Figure	Figure 4. Signalling Hubs Controlling Quiescence	Urbán, N., Blomfield, I.M. & Guillemot, F. 2019. Quiescence of Adult Mammalian Neural Stem Cells: A Highly Regulated Rest. *Neuron,* 104, 834-848	Elsevier permissions@elsevier.com	04/03/2020	Yes	Licensed by Elsevier through the Copyright Clearance Center RightsLink® - License Number: 4781830734495
58	Figure	Figure 1. Model of Wnt Secretion	Nusse, R. & Clevers, H. 2017. Wnt/β-Catenin Signaling, Disease, and Emerging Therapeutic Modalities. *Cell,* 169, 985-999.	Elsevier permissions@elsevier.com	04/03/2020	Yes	Licensed by Elsevier through the Copyright Clearance Center RightsLink® - License Number: 4781831089906

Table 4: Permissions summary for third party copyright works.